

Between the Basins: Exploring the Western Mojave and Southern Basin and Range Province

Robert E. Reynolds, Editor
LSA Associates, Inc.

and

Abstracts from the 2002 Desert Symposium

California State University, Desert Studies Consortium
Department of Biological Science
California State University, Fullerton
Fullerton, California 92384

in association with

LSA Associates, Inc.
1650 Spruce Street, Suite 500
Riverside, California 92507

April 2002

Table of Contents

Between the Basins: Field Guide	
Robert E. Reynolds	3
California Dinosaur Tracks: Inventory and Management	
R.E. Reynolds and Ted Weasma	15
Borax Smith and the Tonopah & Tidewater Railroad	
Stephen P. Mulqueen.....	19
Geology and Minerals in the Area of Pisgah Volcanic Cone	
Larry W. Monroe.....	26
The Sulfur Hole, Calico District, San Bernardino County, California	
J.F. Cooper Jr., G.E. Dunning, T.A. Hadley, W.P. Moller, and R.E. Reynolds	29
Fossil Creodont and Carnivore Footprints from California, Nevada, and Wyoming	
W.A.S. Sarjeant, R.E. Reynolds, and M.M. Kissell-Jones	37
Preliminary Report on the Stratigraphic Setting and Microstructure of Avian Eggshell Fragments from the Calico Mountains: Barstow Formation, Mojave Desert, California	
V. Leroy Leggitt	51
Carbonate Phytoherm Mounds in the Middle Miocene Barstow Formation, Mud Hills, California	
Vicki Pedone and Carmen Caceres	58
Mineralogical Survey of the Mount General Area	
R.M. Housley and R.E. Reynolds	61
The Bodfish Layered Basic Intrusive	
Gregg Wilkerson	64
The Goler Formation of California	
Don Lofgren and Malcolm McKenna.....	66
Ag-Cu-Pb-Bi Sulfosalts New to Darwin, Inyo County, California	
G.E. Dunning, Yves Moëlo, A.C. Roberts, and J.E. Cooper, Jr.	69
Abstracts from the 2001 Desert Symposium.....	76

Front Cover. View west of the Trona Pinnacles.
Back Cover. View south across the salt flats of Searles Lake. The Trona Pinnacles are in mid-ground; Pilot Knob is on the skyline.

Between the Basins: Field Guide

Robert E. Reynolds, LSA Associates, 1650 Spruce Street, Ste 500, Riverside, California 92507

Introduction

Baker is located between the dry lakes of Silver (north) and Soda (south), which filled and joined during the late Pleistocene (Reynolds and others, 1990; Brown and others, 1990). To the southeast are the Cowhole Mountains (Ferriz, this volume), which contain the Jurassic Aztec Sandstone (Reynolds and Weasma, this volume). The Halloran Hills are to the northeast (Reynolds, 1997; Reynolds and Calzia, 1996) and the Soda Mountains are to the west (Grose, 1959; Gourley and Brady, 2000). Look south toward Fort Soda and Zzyzx along the Tonopah and Tidewater Railroad grade (Mulqueen, this volume; Flinchum, this volume, Myrick, 1991) which ran north from the Santa Fe Railroad at Ludlow to Death Valley Junction in 1906 and to Rhyolite in 1907. Borax and salts played an important part in the development of transportation routes through the Mojave Desert, and our trip will pass borax mines and saline playas, as well as crossing the routes of the mule teams that carried these ores to railheads at Daggett and Mojave.

Salts and borate minerals were formed in Miocene and Pleistocene lakes. At stops along this trip we will compare “tufa” (calcium carbonate stromatolites precipitated by blue green algae) from Pleistocene lakes with similar deposits formed in 17 million year old Miocene lakes. These tufa deposits can be used as marker horizons that follow shoreline elevations of transgressive lake-filling events.

Day 1

Convene at Baker. Make sure gas tanks are full, tires are inflated, and you’re provisioned with sunscreen, hats, snacks, and water. Proceed southwest to Interstate 15.

0.0 (0.0) Enter Interstate 15, westbound.

6.2 (6.2) Cross under the Zzyzx overpass which leads south to California State University’s Desert Studies Center.

12.0 (5.8) Pass Razor Road.

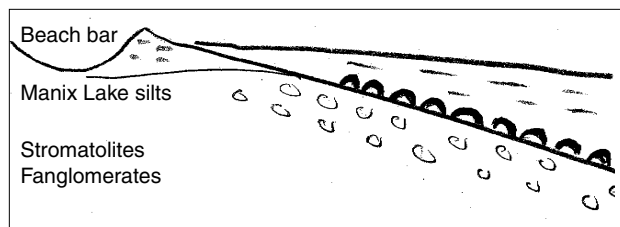
15.7 (3.7) Pass Basin Road.

24.0 (8.3) EXIT RIGHT onto Afton Road.

24.3 (0.3) Stop at the overpass, TURN LEFT (south), and proceed over the freeway.

24.4 (0.1) TURN RIGHT (westerly) on Dunn Road along the south side of the freeway.

25.0 (0.6) PARK and walk to the south side of the frontage road. **STOP 1-1:** Tufa-coated cobbles were deposited as the result of the transgressive lake-filling event in Lake Manix (Awramik and others, 2000). We will examine other localities



Schematic sketch of Manix beach bar, view south.



White stromatolites on cobbles mark the contact between fanglomerates (below) and lacustrine siltstones (above). Stop 1-1., Afton offramp, Manix Lake.

with tufa and stromatolites that mark similar Miocene transgressive lake events at upcoming outcrops. RETRACE to Afton Road.

25.5 (0.5) Afton Road. TURN LEFT (north) and cross over the freeway.

25.7 (0.2) TURN LEFT onto westbound I-15.

33.4 (7.7) Pass Field Road.

40.2 (6.8) EXIT at the Harvard offramp.

40.4 (0.2) Stop, TURN LEFT (south), and proceed over the freeway.

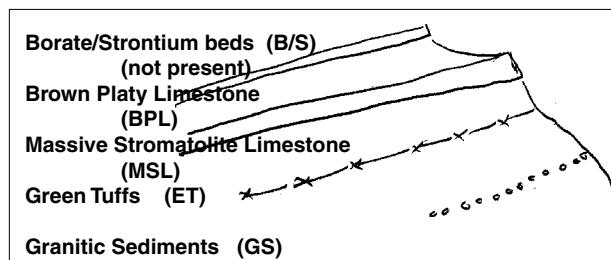
40.7 (0.3) Stop at Yermo Road.

40.8 (0.1) Cross the railroad tracks and immediately TURN RIGHT (west) on the dirt road on the south side of the tracks.

42.5 (1.7) TURN LEFT (south) toward the west side of Harvard Hill.

42.8 (0.3) PARK at north base of Harvard Hill. **STOP 1-2.** The Harvard Hill section contains early Miocene marker beds that can be traced westward through Daggett Ridge and the Calico Mountains to the type section of the Barstow Formation (Reynolds, 2000; Reynolds and Woodburne, this volume). RETRACE to railroad tracks.

43.2 (0.5) Railroad tracks. RETRACE to Harvard Road.



Schematic sketch of section at Harvard.

44.9 (1.7) Harvard Road. RETRACE to the north side of the freeway.

45.0 (0.1) Stop at Yermo Road.

45.3 (0.3) Cross over the freeway.

45.4 (0.1) Enter I-15 and PROCEED WEST.

50.2 (4.8) The freeway road cut exposes the trace of the Manix Fault, where Pliocene (?) gravels are in contact with gray siltstones of Lake Manix. The Manix Fault is west-trending, with movement indicators showing different vertical and lateral aspects (McGill and others, 1988). It is the southerly-most west-trending fault in the Mojave Desert; west-trending faults are more common northward toward the west-trending portion of the Garlock Fault (Jennings and others, 1962).

52.8 (2.6) Exit at Minneola Road. We are heading toward the Calico Mountains and the Borate Mining District, 1892–1907 (Reynolds, 1999). We are crossing combined borax freight routes from the Harmony Borax Works (1881) and the Amargosa Borax Works (1883) that lead from Death Valley (Vredenburg, 1994) to the Union Pacific Railroad at Daggett.

53.1 (0.3) Stop, TURN RIGHT and bear easterly through a small business complex.

53.6 (0.5) TURN LEFT (north) at the sign for the Calico Mountains Archaeological Site (Simpson, 1999). Proceed north.

54.7 (1.1) The Calico Mountain Archaeological Site is to the right; a recycling station is at 12:00, due north. TURN LEFT (west) toward the Calico Mountains.

55.5 (0.8) Pass a right turn to Emerald Basin where sedimentary exposures contain Miocene marker units.

56.3 (0.8) Junction with a north-south pole line road. BEAR RIGHT (north) along the pole line road.

56.5 (0.2) TURN LEFT (west) on Mule Canyon Road.

57.0 (0.5) PARK. STOP 1–3. Walk south to the east end of a hill capped by resistant silicified algal limestone (MSL). The algal mats preserved here are the deep water facies of the MSL marker unit. The brown platy limestone is absent in this area. The view east shows rockhound excavations along the MSL as it trends toward the Calico Mountains Archaeological Site.

57.7 (0.7) The Sulfur Hole (Cooper and others, this volume).

57.9 (0.2) Big Borate Canyon.

58.0 (0.1) Tin Can Alley is to our north.

58.3 (0.3) Pass differential recumbent folds in sediments on the north wall of canyon.

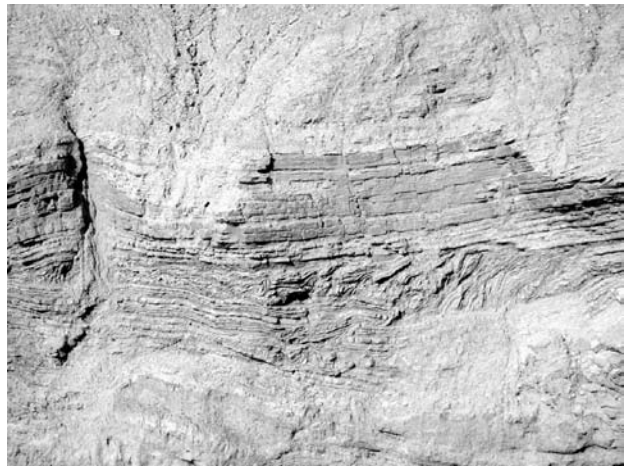
58.5 (0.2) Little Borate Canyon. Happy Hollow (Reynolds, 1999) is to the left (south).

58.6 (0.1) View at 2:00 of andesite domes of the Calico Mountains. Andesite (17.1 Ma) was shed southerly from the domes to cap the 15.5 Ma lacustrine sediments, viewed at 7:00.

59.2 (0.6) Crest of Mule Canyon Road.

60.2 (0.3) East end of Phillips Drive.

60.6 (0.4) Camp Rock. This was a camp site for mule teams and borax freight wagons at the half-way point of the two day trip from Borate to Daggett.



Recumbent folding in north wall of Mule Canyon. Competent shale beds at top and bottom are less folded than the more plastic sediments in between them.

61.4 (0.8) Leave the Calico Mountains.

62.1 (0.7) Stop at paved Calico Road. Watch for oncoming traffic and TURN LEFT (south).

62.9 (0.8) TURN RIGHT on Calico Blvd. before reaching the freeway. Proceed west.

65.5 (2.6) Stop at Ghost Town Road. TURN LEFT and proceed south.

65.9 (0.4) Pass under I-15 and stop at Yermo Road. PROCEED SOUTH on Ghost Town Road, which becomes Daggett Road.

67.2 (1.3) Rattlesnake Rock is to the left.

67.5 (0.3) Waterloo Mill, on the base of Elephant Mountain to the west (right), processed silver ore in the 1880s from the Waterloo mine west of Calico Ghost Town .

67.9 (0.4) Cross the Mojave River and enter the town of Daggett. This railhead was the shipping point for borax from Death Valley via the 1883 Saratoga Springs–Cave Springs–Garlic Spring route (Vredenburg, 1994), and via the Wingate Wash–Pilot Knob route about the same time. Borax freighting from Death Valley moved to a westerly route via Pilot Knob/Blackwater Well to Mojave between 1884 and 1888. The arrival of the Atlantic and Pacific Railroad at Waterman's in 1882 (Myrick, 1991) improved the shipping of colemanite from Borate and Death Valley, offloaded at Daggett, to Alameda.

68.2 (0.3) Alf's blacksmith shop, to the southeast, built wheels and repaired borax wagons hauled by teams of mules from Borate to the railhead at Daggett.

68.4 (0.2) Cross the railroad tracks and Route 66, National Old Trails Highway.

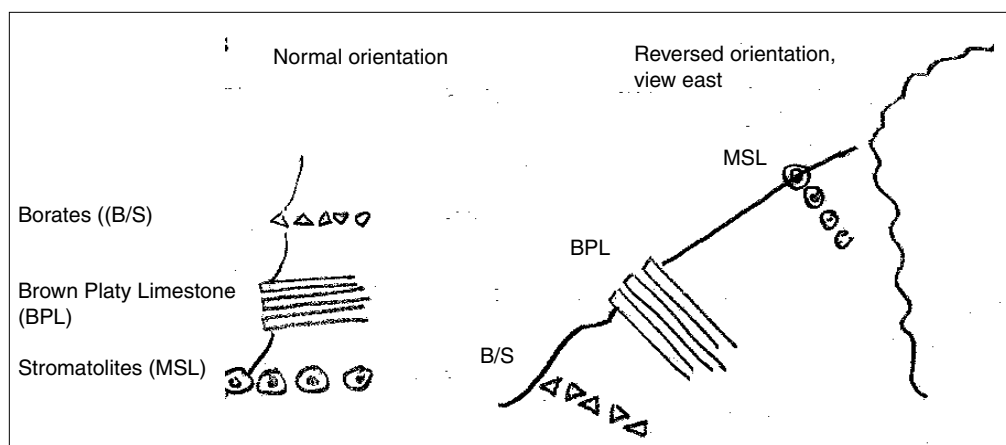
69.0 (0.6) Cross over I-40.

69.2 (0.2) Stop at the frontage road on the south side of I-40 and TURN LEFT (east).

70.1 (0.9) Pavement ends. BEAR RIGHT on Camp Rock Road.

71.2 (1.2) Pass the first powerline road; wooden posts are on the right. Proceed 100 feet and TURN RIGHT at yellow metal posts. Proceed west-southwest along the powerline road.

71.7 (0.5) TURN LEFT (south) at Tower #449.2 (marked on



Schematic sketches of sections at Daggett Ridge Stop 1-4.

southeast leg).

73.3 (1.6) Pass a right turn to the west.

73.7 (0.4) Take right fork.

73.9 (0.2) BEAR LEFT (east) at the Gem (Columbus) mine.

74.1 (0.2) PARK on drill pad. **STOP 1-4.** This overturned section shows, in reverse stratigraphic order, pink tuff, borax-strontium layer, three brown platy limestones, thick granitic fanglomerate, and three strata of massive cylindrical stromatolites, the stratigraphic lowest (now the uppermost) of which is silicified. Farther south, across a branch of the Camp Rock Fault, are aplitic quartz monzonite outcrops that, when uplifted in the Daggett Ridge event, contributed to the granitic debris now found elsewhere in the lower part of the stratigraphic section. RETRACE toward powerline road.

79.9 (0.6) TURN LEFT (west) at intersection.

80.6 (0.9) BEAR RIGHT (west) at "Y" turn.

81.1 (0.5) PARK. **STOP 1-5.** Look northeast at colorful badlands exposures which include the pink tuff that we saw at the last stop. This pink marker tuff is useful in tracing this portion of the stratigraphic section westward. Proceed to powerline road.

81.4 (0.3) TURN RIGHT (north) on the section line road toward the powerline road.

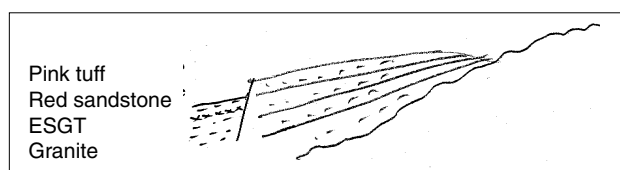
82.4 (1.0) Powerline road. TURN LEFT (southwest).

82.9 (0.5) Proceed over a hill of Quaternary older fanglomerate.

83.3 (0.4) At the bottom of the hill, TURN LEFT (south) on Ord Mountain Road (BLM road OM 4).

9.7 (0.7) Park. **STOP 1-6.** Fine-grained sediments with pink tuff are to the east-northeast. At this locality, red fanglomerates to the east-southeast were shed from sources of granite south of the biotite quartz monzonite to the southeast (Dibblee, 1970). Proceed south on Ord Mountain Road.

84.1 (0.3) Pass quartz monzonite outcrops at the narrows.



Schematic sketch at Daggett Ridge, view east, Stop 1-6.

85.8 (1.7) Pass through red, brecciated granitic rocks and aplite dikes.

86.6 (0.8) On the west are steeply north-dipping volcanic agglomerates.

86.7 (0.1) Pass over a section line cattle guard.

87.1 (0.4) TURN RIGHT (south), uphill, on the road to Stoddard Valley.

87.4 (0.3) At the saddle on Daggett Ridge, TURN RIGHT (westerly) into Stoddard Wash.

89.6 (2.2) Pass two desert willows.

89.7 (0.1) Park. **stop 1-7.** Walk north up the wash to look at cylindrical stromatolites mixed with large blocks of rock from Daggett Ridge. The age of the stromatolites constrains activity on the tectonic activity of Daggett Ridge. Return to vehicles and CONTINUE WEST to the gate.

90.0 (0.3) Open the gate at the San Bernardino Meridian, due north of Mount San Bernardino. Proceed through and close the gate; BEAR LEFT (south) out of Stoddard Wash at the next possible left turn, in about 50 feet.

90.3 (0.3) TURN LEFT (south) around a point extending from a gravel hill.

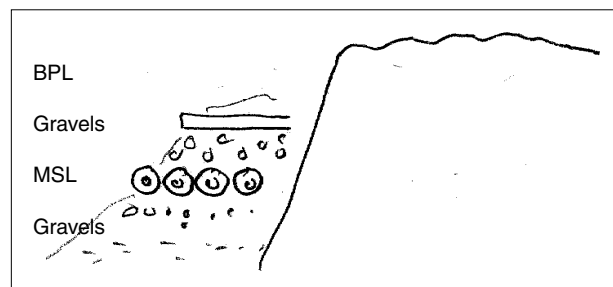
90.5 (0.2) Cross the wash.

91.7 (0.8) Pass a lone hill on the left (east).

92.0 (0.3) Stop, TURN RIGHT (west) on the section line road. A private residence is to the south.

95.4 (3.4) Pass through an intersection.

95.7 (0.3) Stop at Highway 247 (Barstow Road). Watch for traffic and TURN RIGHT (north) onto Highway 247.



Schematic sketch at Daggett Ridge, view west, Stop 1-7.



Cylindrical stromatolites in limey siltstone, south side of Stoddard Valley on the north side of Daggett Ridge.

- 96.5 (0.8) Pass under power lines.
- 96.7 (0.2) Pass the Slash X Ranch café on the left.
- 99.1 (2.4) View northeast at 2:00 toward the Miocene sediments of Daggett Ridge.
- 100.8 (1.7) Proceed up grade.
- 102.2 (1.4) Pass the entrance to a land fill. Highway 247 becomes Barstow Road.
- 104.6 (2.4) BLM offices are on the right; Barstow High School is on the left.
- 104.9 (0.3) Stop light at Rim Rock.
- 105.3 (0.4) Stop light at Armory.
- 105.7 (0.4) Cross over I-15. Stop light.
- 105.8 (0.1) Stop light. Turning left (west) on Virginia Way leads to the Mojave River Valley Museum. On Barstow Road 100 feet past the fire station you can TURN RIGHT into the Community Center parking lot to visit the Desert Discovery Center at 831 Barstow Road. Proceed on Barstow Road.
- 106.3 (0.5) Stop light at Mountain View Street.
- 106.7 (0.4) Stop light at Main Street. TURN LEFT (west) onto Main Street.
- 107.0 (0.3) Stop light at Second Street.
- 107.1 (0.1) Stop light at First Street. TURN RIGHT (north) onto First Street. Cross over the railroad bridge and pass the Harvey House. Proceed on the second bridge over the Mojave River.
- 107.6 (0.5) Buzzard Rock is on the left.
- 107.7 (0.1) TURN LEFT onto Irwin Road and proceed north.
- 108.2 (0.5) Stop at the intersection with Old Highway 58 (westbound). Proceed north on Irwin Road.
- 108.4 (0.2) Stop at the intersection with Old Highway 58 (eastbound). Proceed north on Irwin Road.
- 110.9 (2.5) Slow for curves.
- 112.4 (1.5) Pass a left turn toward the microwave station where the Waterman Hills Detachment Fault (WHDF) is exposed

(Glazner, 1989). In the early Miocene, the WHDF slid eastward from the rising metamorphic core complex of the Waterman Hills/Mitchell Range. The basin that resulted to the east of the Waterman Hills filled with volcanic rocks of the Pickhandle Formation and sediments of the Barstow Formation.

- 113.9 (1.5) TURN LEFT onto Fossil Bed Road.
- 116.8 (2.9) TURN RIGHT onto Rainbow Basin Loop Road toward colorful Miocene sediments (Dibblee, 1968).
- 117.1 (0.3) TURN RIGHT toward Owl Canyon Campground.
- 118.5 (1.4) Owl Canyon Campground.

STOP 1-8. PARK adjacent to camp spot three. Walk west across the wash to look at the marker units of the massive stromatolite layer (MSL) and the brown platy limestone (BPL) (Reynolds, 2000, and this volume). Similar carbonate phytoherm mounds are described to the north from a similar position in the stratigraphy (Pedone and Caceres, this volume; Reynolds, 2000 and this volume).

The first stop introduced us to stromatolites at Pleistocene Lake Manix that transgressed topography and time as the lake filled. At subsequent stops in Miocene sediments of the Barstow Formation, we saw examples of stromatolites deposited in deep and shallow lake environments. Like the Lake Manix deposits, the Miocene marker stromatolites are somewhat time and topography transgressive, and serve to mark the initial filling of the newly formed Barstow Basin in early Miocene time.

End of Day 1

Day 2

- 0.0 (0.0) Leave Owl Canyon Campground and retrace to Fossil Bed Road.
- 1.4 (1.4) At Rainbow Basin Loop Road, watch for traffic and TURN LEFT (south).
- 1.8 (0.4) Fossil Bed Road. Stop, TURN LEFT (southeast) and proceed to Irwin Road.
- 4.6 (2.8) Stop at Irwin Road and TURN RIGHT (south) on Irwin Road.
- 9.7 (5.1) Stop at the intersection with eastbound Highway 58. Proceed on Irwin Road.
- 9.9 (0.2) Stop, TURN RIGHT on westbound Highway 58.
- 10.8 (0.9) Pass on the right (north) the site of Waterman's Mill, roughly south of the Waterman Gold mine in the Waterman Hills to the north. The Atlantic and Pacific Railroad reached Waterman in 1882. We are passing through greenish-gray outcrops of the Waterman Gneiss. Robert Whitney Waterman (b. 1826) developed prosperous mines in this area in 1880. A Republican, he was elected Lt. Governor of California in 1886 and became governor a few months later with the death of Democratic Governor Washington Bartlett. Waterman died in 1891 (Bancroft, 2002)..
- 13.3 (2.5) Pass yellow limestones deposited during pre-Barstovian time (Dibblee, 1970).
- 15.0 (1.7) Mt. General is to the north at 2:00 (Housley and Reynolds, this volume). Mount General is capped by Miocene volcanics which make up the upper plate of the WHDF. The

volcanics sit on early Paleozoic rocks of the lower plate. Fremont Peak is in the distance at 1:30.

15.5 (0.5) Intersection with Lenwood Road. TURN LEFT (south) on Lenwood Road.

15.9 (0.4) Stop at Highway 58. TURN RIGHT (westbound) on Highway 58.

19.9 (4.0) Continue past Hinkley Road. Black Mountain is to the north (Dibblee, 1968; Burke and others, 1982). Opal Mountain, with patches of white tuff and purple welded tuff, is to the left of Black Mountain.

28.0 (8.1) Pass Harper Lake Road.

40.9 (12.9) Stop at Kramer Junction. PROCEED WEST on Highway 58. The Randsburg Railroad grade was built north from Kramer in 1897 as a spur of the Atlantic & Pacific Railroad. It serviced the mines at Randsburg, Johannesburg, and Red Mountain through their productive days, but was dismantled in 1933 (Myrick, 1991)

43.4 (2.5) Cross the railroad tracks.

44.6 (1.2) Highway 58 bears north and westerly.

47.3 (2.7) Pass under Boron Avenue. The 20-Mule Team Museum to the south in central Boron has exhibits of local minerals, mining artifacts, and regional human and natural history.

49.9 (2.6) Exit from Highway 58 on Borax Road.

50.2 (0.3) Stop at Borax Road, TURN RIGHT (north). The view northeast shows mine dumps with round overburden. The view north shows mine dumps that contain borax reserves.

51.6 (1.4) Bear right at the Suckow Road sign and proceed past the US Borax Visitors' Center.

52.2 (0.6) Stop at the guard booth for a guest permit (entry fee \$2 in early 2002).

53.0 (0.8) Park at the Visitors' Center. **STOP 2-1.** The view north into the Boron Open Pit Mine shows black Saddleback Basalt (18.3 Ma, Whistler, 1991) at the base of the section, overlain by the Shale Member, greenish sediments that contain white borate minerals. The overlying Arkose Member contains 17 taxa of mid-Hemingfordian age vertebrates that comprise the Boron Local Fauna (Whistler, 1984). Exhibits and videos can be seen



Boron open pit mine exposes the upper part of the Tropic Group, which includes three members: the black Saddleback Basalt, the Shale Member, greenish with white borates, and the overlying tan Arkose Member.

inside the museum. 20-mule team wagons, a headframe, and mineral stockpiles for young and old collectors are outside. RETRACE to Highway 58.

53.8 (0.8) Exit at guard shack.

55.7 (1.9) TURN LEFT onto the Highway 58 westbound onramp.

56.7 (1.0) Pass a rest stop.

57.8 (1.1) Pass Gephart Road.

59.0 (1.2) Pass the 20 Mule Team overpass.

62.6 (3.6) Stable dunes at 11:00 that surround Rodgers Lake contain small Pleistocene vertebrate fossils (Reynolds and Reynolds, 1991).

63.5 (0.9) Pass Clay Mine Road.

65.8 (2.3) Pass Rosamond Blvd. and the entrance to Edwards Air Force Base.

67.8 (2.0) EXIT right on California City Blvd. Proceed north to California City.

69.7 (1.9) Cross the northwest trending Muroc Fault, which elevates Mesozoic granitic rocks overlain by the early Miocene Tropic Group of sediments.

73.7 (4.0) California City Boulevard bears northwest; the scarp of the Garlock Fault is ahead at 10:30.

74.2 (0.5) South College.

74.9 (0.7) TURN LEFT onto Proctor Blvd (California City Blvd). 20-Mule Team Parkway trends northeast from this intersection to the Desert Tortoise Natural Area and Interpretive Center, a 39.5 square mile reserve of prime habitat for the desert tortoise and more than 200 species of plants and 20 species of reptiles and birds.

75.9 (1.0) Pass Hacienda Blvd.

77.4 (1.5) TURN RIGHT (north) at Neuralia Road in central California City.

82.3 (4.9) Pass Phillips Road. Kohen Lake can be seen to the northeast in Fremont Valley.

88.9 (6.6) Cross the railroad tracks.

89.1 (0.2) TURN LEFT (west) on Rodgers Road.

8915 (0.4) Park before reaching Highway 14. **STOP 2-2.** View west of Jawbone Canyon area and the Bodfish Pluton (Wilkinson, this volume). The name Jawbone Canyon is in reference to its shape (Gudde 1969). Nearby, Cantil (Spanish, "steep rock") was the name of the station along the Nevada and California Railroad when it extended from Mojave to Owens Lake in 1908.

Visible from northeast to northwest is the trace of the left-lateral Garlock Fault. The El Paso Fault is north of the Garlock at the steep base of the El Paso Mountains. The Cantil Valley Fault is south of the Garlock Fault, running along the southeast side of Koehn Dry Lake (Jennings and others, 1962). The Sierra Nevada Frontal Fault (SNFF) runs northerly along the east side of the Sierra Nevada Mountain Range.

At this stop, we are at the junction of three of California's natural provinces: the Mojave Desert, the Sierra Nevada and

the Basin and Range provinces. Our trip has crossed from the eastern portion of the Mojave Desert to this site at the northwest margin of the Mojave. To the northwest we see the southern Sierra Nevada Province, and over the El Paso Mountain Range to the northeast lies the southwestern portion of the Basin and Range Province. These provinces can be viewed as either “natural provinces,” with limits based on biologic communities, topography and drainage, or as “geologic provinces,” called “blocks” (as in the Mojave Block). The margins of the natural provinces don’t always coincide with the limits of the geologic blocks (Baker, 1911; Thompson, 1929; Hewett, 1956; Sharp and Glazner, 1997; Schoenherr, 1994).

The Mojave Block is geologically defined as being bounded on the north and northwest by the left-lateral Garlock Fault, on the southwest by the right-lateral San Andreas Fault (SAF), on the south by the left-lateral Pinto Mountain Fault, and on the east by the Eastern California Shear-zone (Brady, 1992; Brady and Dokka, 1989). The geologic provinces that surround the Mojave Block are, to the northeast, the Basin and Range Province; to the northwest, the Sierra Nevada Block; to the south west, the Transverse Ranges; and to the southeast, the Colorado Desert. Internally, the Mojave Block is characterized as being cut/crossed by northwest-trending faults, roughly parallel to the SAF along the southwest margin. Also of importance are the west-trending faults from the Manix Fault north that parallel the Garlock Fault on the north boundary of the Mojave Block, and which often show left-lateral movement. The western portion of the Mojave Block is an east-draining plane, in part due to the depression forming at the intersection of the left-lateral Garlock Fault and the right-lateral SAF. The central and eastern Mojave Block does not have the significant cover of fill that the western Mojave does, in part due to the activity of faults and drainage systems.

The Transverse Range Province lies to the south, and consists of mountain ranges that trend east-west such as the San Gabriels and the San Bernadinos.

The Sierra Nevada Block to the northwest consists of granitic rocks that are uplifted on the east by the Sierra Nevada Frontal Fault, which tilts the block to the west.

The Basin and Range Province to the northeast east is characterized by fault-bounded, east-tilted, north-south trending mountain ranges with intervening playas or valley fill.

The natural province of the Mojave Desert is defined by the northern limit of the Joshua Tree (Darlington, 1996; Schoenherr, 1994), and is found north of the Mojave Block in the Basin and Range (B & R) geologic province. The B & R province is characterized by Great Basin Sagebrush, which is snow-tolerant. Creosote Bush and many species of cacti are not snow-tolerant, and are restricted to the Mojave Desert natural province.

Return to vehicles. Proceed west to Highway 14.

89.9 (0.4) Stop, watch for cross traffic, and TURN RIGHT (north) onto Highway 14.

90.8 (0.9) Pass Garlock /Randsburg Road.

91.8 (1.0) The colorful sediments ahead lie between the Garlock (south) and El Paso (north) faults, and contain Hemphillian LMA fossils, suggesting that they have been translated left-laterally westward as a shutter ridge 30 miles from Lava



Red Rock Canyon and rocks of the Cudahy Camp Formation including the pink tuff and basalts which date from 18 to 15 Ma. These rocks originated in the Eagle Crags volcanic field, now 30 miles east on the south side of the Garlock Fault.

Mountains to the east.

92.4 (0.6) Enter Red Rock Canyon and the Dove Spring Formation. Low in the section, the pink ash flow tuff is of unknown age, but is overlain by an andesite flow and flow breccia that is 18.5 ± 0.60 Ma. The basalts and basaltic andesites stratigraphically above the pink tuff range in age from 17.90 ± 1.60 Ma to 15.10 ± 0.50 Ma. All of these rocks are units of the Cudahy Camp Formation (Monastero and others, 1997). The granitophyre of the El Paso Mountains is to the left as we pass through Red Rock Gorge (Whistler, 1991). Move to left lane.

92.6 (0.2) TURN LEFT (northwest) onto Abbott Drive and Red Rock Canyon.

93.2 (0.6) Pass black basalt and bear left.

93.5 (0.2) Park before reaching the kiosk. To reach the visitor center, turn left; to reach the campground, turn right. **STOP 2-2.** The Ricardo group was deposited in the El Paso Basin, and consists of the Cudahy Camp Formation (early Miocene) and the conformable Dove Spring Formation (middle and late Miocene, Monastero and others, 1997, 2001; Reynolds and others, 1991; Whistler and Burbank, 1992). This group records deposition of sediments derived from the southeast, and a subsequent change to sources from the northwest, which introduced the first clasts of rock indicating unroofing of the Sierra Nevada batholith at 7.5+ Ma (Reynolds, Whistler and Woodburne, 1991; Whistler, 1991). Deposits of “Dove Spring Lignites” inset in canyons to the north contain a significant Late Pleistocene plant and vertebrate fauna. The relationship of sediments and pediments to fault activity is discussed by Miller (this volume). RETRACE to Highway 14.

94.2 (0.7) TURN LEFT (north) on Highway 14.

96.9 (2.7) The Dove Spring OHV area is west along the powerline road.

97.1 (0.2) Note the buff, resistant silcretes to the east and west. The red beds in the lower Dove Spring Formation are paleosols composed of deeply weathered sediments. The weathering has produced clays, calcite (as diffuse caliche or in kernels), and iron oxides—hence the red or brown color. The paleosols higher in the Dove Spring Formation are rich in silica, as well as calcite, thus the term “silcrete”.

98.0 (0.9) Pass Red Rock/Inyokern Road on the right. The



View east from Trona Road of the Eagle Crags volcanic field and Pilot Knob.

view east shows Black Mountains basalt capping the El Paso Range.

100.8 (2.8) A BLM marker sign for Jawbone (Butterbredt turnout) is on the left (west).

103.1 (2.3) Pass a right turn to the Burro Schmidt Tunnel.

106.1 (3.0) Robbers' Roost is on the left at 10:00. Its name comes from the time when the infamous Californio bandito Tiburcio Vasquez used the rocks as a staging area to prey on passing freight wagons and stage coaches.

109.8 3.7) Pass a memorial on right recognizing the services to the people of Inyo and Mono Counties by Father John J. Crowley. Prepare for a left turn, watching for oncoming traffic.

110.3 (0.5) TURN LEFT on Highway 178 westbound, leading through Freeman Canyon and Walker Pass to Lake Isabella.

110.5 (0.2) The Freeman Junction marker, historic landmark 766. With direction from Indians, Joseph R. Walker pioneered trails through this area south toward Los Angeles. In Walker's first expedition in 1834, he led a party from Monterey to Owens Valley. He followed with trips in 1843 and 1845, the latter with Fremont, Owens and Kit Carson (China Lake-Ridgecrest AAUW, 1996).

111.0 (0.5) TURN LEFT at the LADWP Road marked by a BLM sign for Jawbone (Butterbredt). Proceed south parallel to a concrete cap of the 1911 LADWP Aqueduct. The Los Angeles Owens River Aqueduct stretches 238 miles from the Owens River to Los Angeles. Under the leadership of William Mulholland of the Los Angeles Department of Water, 5000 men worked for five years to complete the project; water was first delivered to Los Angeles through the aqueduct in November, 1913. In 1940, an extension of the system tapped the water of the Mono Basin. Without the water provided from outside sources, Los Angeles could not have exceeded a population of 500,000. The small farmers and ranchers of Owens Valley had anticipated a federal water reclamation project in 1902 to regulate the flow of the Owens River for their own use; the diversion of this water to Los Angeles remains controversial a century later. Bear southwest towards Robbers' Roost.

111.5 (0.5) Park. at the site of the Freeman Stage Station (Coyote Holes). **STOP 2-3**. Freeman Station was established by the ex-stage driver Freeman S. Raymond in 1872. On the last day of February, 1874, the Station was attacked by Tiburcio Vasquez. Although the station occupants had surrendered, "Old Tex" (who was sleeping in the barn) awoke and fired



Granitic rocks of Robbers' Roost from Freeman Station.

at Vasquez, wounding him in the leg. Vasquez returned fire and delivered a leg wound to Tex (Pracchia, 1994). In 1894, Freeman's parcel became the first homestead in Indian Wells Valley. Walk uphill 100 feet west for overview and to look at roof pendants of metamorphosed Paleozoic sediment in granitic pluton. From this overview (Montastero and others, 2001), we see that Indian Wells Valley is bounded on the west by the Sierra Nevada, the Argus Range on the east, the Coso Range on the north, and the Rademacher/ Spangler Hills and El Paso Mountains on the south. The Sierra Nevada Frontal Fault (SNFF) can be distinguished between the craggy pink outcrops of the granitic rock and the low hills immediately to the west. Outcrops of the Ricardo Group and Goler Formation are to the south, but there is no evidence of these formations in Indian Wells Valley to the east. The SNFF exhibits more than 2km of vertical relief on the eastern front of the Sierras. Structural accommodation forces the SNFF to turn sharply southwest in the area west of the El Paso Mountains. The down-to-the-east offset forms a fluid flow barrier. The SNFF truncates the east face of Owens Peak to the north and the Goler Formation and Ricardo Group sediments to the southwest. RETRACE north to Highway 178.

112.0 (0.5) Stop at Highway 178. Watch for traffic. Proceed across the highway (north) on the LADWP road.

112.2 (0.2) PARK off the road at the site of Panamint Station. **STOP 2-4**. As you walk east across the aqueduct for 0.1 mile, you are crossing the historic debris of Panamint Station, active from 1875 to 1882 (Pracchia, 1994), at which time Remi Nadeau's freight line ceased operations. Look west to roof pendants of metamorphosed Paleozoic sediments in a granitic plutonic intrusion. The 60 foot diameter creosote ring to the west is an excellent example of an 11,000 year old plant and shows that flora of the Mojave Desert is trying to invade the natural provinces to the north and west. To the north-northeast at the northwest corner of Indian Wells Valley, Pleistocene basalts (440,000 years old and younger) flowed south from cinder cones through topographic lows, leaving hills such as the White Hills Anticline exposed. The White Hills Anticline to the northeast exposes Plio-Pleistocene sediments of the White Hills Sequence (Montastero and others, 2001). The east-plunging anticline is the result of the left-step on a Holocene strike-fault system passing across the eastern Indian Wells Valley. The western face of the distant Argus Range contains two sets of alluvial fans that prograde westward. The older set interdigitates with the White Hills sequence, and the younger set may have been deposited in late Pleistocene time (Monastero and others,

2001). RETRACE to Highway 178, then go east to Highway 14.

112.7 (0.5) TURN RIGHT (east) at Highway 178.

113.4 (0.7) TURN LEFT (north) at Highway 14.

115.3 (1.9) Granitic outcrops to the west mark the SNFF.

116.0 (2.7) Pass Highway 178 east to Ridgecrest.

118.0 (2.0) Indian Wells Spring, from whence the valley gets its name, is marked by Indian Wells Brewery. Willows and mesquite mark the trace of the SNFF.

119.0 (1.0) Athel Street.

119.9 (0.9) Cross over Highway 395 on the overpass.

120.0 (0.1) The first left turn across Highway 14/395 leads to Short Canyon. Wet winters allow the waterfall to flow, and spring provides a spectacular display of wildflowers. More than 290 species of plants representing a mixture of surrounding habitats have been recorded in this canyon (Lum and Midlemis, this volume)

125.4 (5.4) Pass Brown Road, which leads west to Sand Canyon.

125.9 (0.5) Pearsonville.

128.5 (2.6) Prepare for a left turn.

128.8 (0.3) TURN LEFT onto Nine Mile Canyon Road leading to Kennedy Meadows.

129.7 (0.9) TURN RIGHT (north) onto the power line road.

132.0 (2.3) View east of 440,000 ybp basalt that flowed from base cones through saddles, canyons, and valleys. At the road junction, continue straight (north), down into the canyon.

132.5 (0.5) TURN LEFT, cross the wash, and PARK on the north side of the wash at a complex junction of roads. **STOP 2-5** (Montastero and others, 2001). This stop is immediately east of the SNFF. There are four types of coarse sedimentary deposits proximal to the SNFF: megabreccia, landslide deposits, debris flows, and alluvial fans with soil profiles. The road cut at this stop exhibits debris flows interspersed with soil profiles. The granodiorite boulders are of Sierran origin in a poorly sorted ground-mass of matrix-supported clasts. These debris flows are interbedded with approximately seven buried, half-meter thick, reddish-brown soil profiles that may each represent 20,000 years of time, suggesting that the exposed fanglomerates span a 140,000 year period. Return to vehicles and take the left of

two roads north and uphill to observe loamy paleosols interbedded with coarse debris flows in the road cut. Metamorphism has produced pistachio green epidote associated with pink feldspar of granitic pegmatites.

132.8 (0.3) TURN AROUND at the aqueduct and RETRACE to

Soil horizons developed in coarse fanglomerates on the east side of the SNFF, north of Nine Mile Canyon.



Stop 2-5, at the bottom of the hill.

133.2 (0.4) TURN SHARP LEFT on the second road to the north-northeast.

134.2 (1.0) PARK between LADWP vents 1007+3 and 1007+9. **STOP 2-6** (Montastero and others, 2001). Walk west to the end of a rugged spur. The landslide facies is exposed here as large, coherent blocks of plutonic rocks basinward of megabreccia blocks. Slow movement caused many blocks to be fractured in place, while the surrounding matrix is jumbled, unsorted fragments of the same lithology. The trace of the breakaway fault can be seen to the north. Return to vehicles, PROCEED NORTH.

134.7 (0.5) TURN RIGHT (east) at the small batch plant.

134.8 (0.1) Stop, TURN RIGHT (south) on Highway 395.

136.8 (2.0) Highway 395 bears east.

138.9 (2.1) Exit from Highway 395 at Nine Mile Canyon Road and PARK. **STOP 2-7**. To the northeast, the White Hills anticline of Plio-Pleistocene sediments protrudes as a window through 440,000 year old Pleistocene basalt flows. The measured portion of the White Hills Anticline consists of over 2700 feet of Pliocene sediment that strike northwest and dip up to 20° SW. The sediments consist of white, diatomaceous silts and sands, thin beds of limestone, and occasional arkosic sands and conglomerates. A late-middle Pliocene basalt near the top of the sequence has been dated (40Ar/39Ar) at 3.11±0.21 Ma (Montastero and others, 2001). RETRACE to Highway 395, watch for traffic, and TURN RIGHT (south).

141.8 (2.9) Pass Pearsonville/Sterling, the Hubcap Capitol of the World.

142.3 (0.5) Pass Brown Road.

146.5 (4.2) Pass Leliter Road. Stay in the left lane and prepare to exit Highway 395 (the direction signs point to San Bernardino).

148.6 (2.1) EXIT LEFT (southwest) from Highway 14/395, staying on Highway 395.

150.5 (1.9) Pass Athel Street.

152.0 (1.5) Pass Brown Road.

153.5 (1.5) Pass the exit for Highway 178 east to Ridgecrest.

157.4 (3.9) Pass Bowman Road.

162.2 (4.8) EXIT Highway 395 onto China Lake Boulevard.



White Hills anticline surrounded by 440,000 ybp basalt flows.

SIDE TRIP: China Lake Blvd. leads six miles east to the Maturango Museum at the northeast corner of China Lake Road and Los Flores Avenue.

End Day 2

Day 3

0.0 (0.0) Convene on the east side of Highway 395, at the junction of China Lake Road and Randsburg/Inyokern Road. PROCEED WEST on Randsburg/Inyokern Road.

2.8 (2.8) On the hill to southwest at 10:00 is the roadbed for the Nevada & California (Southern Pacific) Railroad that ran northerly from Mojave to Owenyo through a 4000 foot long tunnel at “Summit” in the El Paso Mountains.

3.4 (0.6) Randsburg/Inyokern Road bears northwesterly.

3.8 (0.4) TURN LEFT (southerly) onto a road that runs toward the El Paso Mountains. We are crossing the Owenyo S. P. railroad grade.

4.4 (0.6) Pass BLM road EP 26.

5.9 (1.5) Bear right to avoid a gravel pit.

6.0 (0.1) TURN LEFT (southeast) around the gravel pit.

6.3 (0.3) TURN RIGHT, south, to Sheep Springs.

8.8 (2.5) Continue past a left turn.

8.9 (0.1) Continue past the left turn to Sheep Tank.

9.1 (0.2) Pass a second left turn to Sheep Tank and proceed downhill, west.

9.2 (0.1) PARK at Sheep Spring. **STOP 3-1.** Sheep Spring is marked by cottonwoods and willows. It is an excellent site to observe migrant birds and is one of the few local sources of water for plants and animals. RETRACE northeast to Sheep Tank.

9.3 (0.1) TURN RIGHT, northeast.

9.4 (0.1) TURN RIGHT (northeast) to Sheep Tank. Take the right branch of a rough road.

9.7 (0.3) PARK at Sheep Tank. **STOP 3-2.** Hike east to the Laudate Site. This is the site of the original discovery of Paleocene mammal fossils from the Goler Formation. With the persistence of Malcolm McKenna, Don Lofgren (this volume), and Steve Walsh, significant new specimens from this section of the Goler Formation have allowed redefinition of the fauna and the age of deposition. RETRACE.

10.1 (0.4) TURN RIGHT onto EP26N.

12.9 (2.8) At a berm on southeast side of the gravel pit, BEAR LEFT (west) around the pit.

15.2 (2.3) Stop at Randsburg/Inyokern Road. TURN RIGHT (east).

19.2 (4.0) Stop at Highway 395. Proceed across Highway 395 onto China Lake Blvd.

23.8 (4.6) Pass the intersection with College Heights Blvd. China Lake Blvd. bears left (north).

24.3 (0.5) Pass Upjohn Street.

24.7 (0.4) Pass California Avenue.

24.8 (0.1) TURN RIGHT (east) at Ridgecrest Blvd. (Highway 178).

28.6 (3.8) Pass a BLM wild horse and burro facility.

28.9 (0.3) Highway 178 bears left (northeast). The granitic outcrops on the ridge to the north are deeply weathered, perhaps due to being covered by saline lake waters during the Tahoe glacial.

32.1(3.2) Pull to the right and PARK. **STOP 3-3.** Deposits of tufa over calcareous beach sand at this elevation (2000') are from the Tioga shoreline, 200 feet lower in elevation than deposits including tufa mounds from the Tahoe shoreline at elevation 2200'. The mid-Pleistocene Tahoe shoreline indicates that Searles Lake was once full, connecting to China Lake. At the following stops, we will see three kinds of tufa formations: the Pinnacles, ridge tops covered with tufa, and shoreline features at elevations 2200' and 2000', which date respectively to the Tahoe Glaciation (75,000 ybp) and the Tioga Glaciation (20,000 ybp). The adjacent elevation sign indicates that we are at the shoreline elevation from the later lake. RETURN TO VEHICLES and proceed east on Highway 178.

33.8 (1.7) TURN RIGHT (south) on Trona–Red Mountain Road.

35.2 (1.4) Prepare to turn left at the yellow “curve” sign.

35.3 (0.1) TURN LEFT on the dirt gas line road, a part of the old Trona–Red Mountain Road.

35.5 (0.2) Pull to the right and PARK in the wash east of the outcrop. **STOP 3-4.** We are at the high stand of the Tahoe glaciation shoreline developed at elevation 2200' when Searles Lake was connected to China Lake basin 70,000 years ago. Looking downhill (northeast) into Salt Wells Valley, we can see tufa marking the shoreline of the late Pleistocene Tioga high stand at elevation 2000'. The Tioga filling of Searles Lake left shoreline features and stromatolite precipitation but did not cause it to connect with China Lake. The lightweight tufa deposits in this area were quarried for use as building stone used in the suburbs of Ridgecrest in the early twentieth century. As a result, many outcrops have degraded. PROCEED SOUTH, up the wash, to the pole line road.

35.8 (0.3) TURN LEFT (east) on the pole line road.

36.4 (0.6) Dip.



Laudate site area, Goler Formation. D. Lofgren photo.



East-northeast trending tufa alignment along a mapped fault, Stop 3-6.

- 37.3 (0.9) TURN RIGHT (south) on BLM Road C1.
- 37.5 (0.2) Cross the gas line road and BEAR LEFT.
- 37.8 (0.3) Drop into the wash and PROCEED SOUTH, up the wash.
- 38.3 (0.5) PARK at the BLM C1 sign. **STOP 3-5.** We are at tufa-cemented outcrops at 2200' elevation, the high stand of the Tahoe shoreline. To the north is an east-northeast trending tufa alignment. PROCEED NORTHEAST to the tufa alignment.
- 38.8 (0.5) TURN LEFT at the C1 road sign, and continue to the west end of the tufa alignment.
- 39.1 (0.3) PARK. **STOP 3-6.** Examine the east-northeast trending tufa pinnacle alignments. We are at elevation 2180' and the top of the pinnacles is 2200'. The geologic map (Jennings and others, 1962) indicates this alignment is along a N50°E-trending fault that cuts Mesozoic granitic rocks and Pleistocene sediments. RETRACE north to C1.
- 39.3 (0.2) Cross C1.
- 39.4 (0.1) Cross the gas line road.
- 39.6 (0.2) Cross the pole line road.
- 40.0 (0.4) Stop, TURN RIGHT onto the pavement of old Trona Road.
- 40.9 (0.9) Stop at "The Y." Watch for fast cross-traffic and TURN RIGHT on Highway 178.
- 41.2 (0.3) To the north, layered lacustrine sediments with local soft sediment deformation contain efflorescences of halite and other salts.
- 41.7 (0.5) Enter Poison Canyon where lacustrine sediments lie on granitic and metamorphic basement rock.
- 43.7 (2.0) Leave Poison Canyon. Note "Fish Rock" graffiti to the left.
- 45.4 (1.7) Shorelines of Pleistocene Searles Lake can be seen on granitic rock at at 9:00 (north).
- 46.0 (0.6) Prepare to turn right. The Pinnacles are visible in the distance at 3:00.
- 46.1 (0.1) TURN RIGHT toward the Trona Pinnacles. We are at the junction of two freight routes used by the Searles brothers to haul borax from Borax (Searles) Lake to Mojave. The southern route ran west of Pinnacles to Garden City (UPRR at Searles



View across Searles Lake, showing shorelines up to 2200' elevation on the west side of the Slate Range.

Station). The western route went through Salt Wells Canyon (Poison Canyon), and then to Garden City where both routes joined, continuing to Garlock and Mojave. The 31-mile Trona Railway (ahead) was completed from Garden City (Nevada & California R. R.) to the potash and borax mines at Trona in 1914 (Myrick, 1991). On a smaller scale, but with grander engineering innovations, the Epsom Salt Monorail was built from Magnesia Siding (ahead) across Searles Lake and the Slate Range, through Panamint Valley to the Epsom Salt works south of Wingate Wash near the Owlshead Mountains. The monorail and mine operated successfully only during 1924–1925 (Myrick, 1991).

- 46.7 (0.6) Pinnacles Road bears south.
- 47.3 (0.6) Cross the railroad tracks.
- 50.0 (2.7) Exposures to the left show a contact of green lacustrine sediments and overlying brown fluvial sediments. Notice the green lacustrine sediments and a shoreline on the granitic hills at 3:00.
- 50.3 (0.3) TURN LEFT, southeast, to the Pinnacles.
- 50.6 (0.3) The road turns right, down hill, southwest, toward the Pinnacles—"The Ultimate Stromatolite."
- 51.0 (0.4) PARK at the BLM sign (restrooms). **STOP 3-7.** Five hundred tufa spires rise to heights of 150 feet. Studies (Scholl, 1960; Rieger, 1952) indicate that the tufa pinnacles were formed during at least the latter two Pleistocene events (Tahoe, 70,000 ybp, and Tioga, 20,000 ybp.). Seven textures of tufa are described (Scholl, 1960). The interior deposits include



View west of three tufa pinnacles south of Trona.



Figure 14. Tunnel in pinnacle exposes dense interior tufa. Dendritic tufa exfoliates from the exterior.

cavernous and stony lithoid tufa from the Tahoe deposition that were probably indurated by subsequent deposition. The nodose, dendritic, and tubular tufa probably formed on the exterior of the Tahoe tufa during the Tioga lake filling. The porous punky exterior has exfoliated, leaving a “debris cone” around the base of each pinnacle, which contains a dense calcium carbonate interior. Walk 200 feet east to the tufa tower with the tunnel and examine the internal and external textures. Shorelines can be seen on hills to northwest. Return to vehicles, circle south, then westerly, then northerly around the pinnacles.

52.1 (1.1) Rejoin the entry road and RETRACE to Highway 178.

56.7 (4.6) Stop, TURN LEFT (west) on Highway 178.

63.0 (6.3) Intersection of Highway 178 and China Lake Blvd.

We have explored portions of the western Mojave Desert that include the Mojave Block, the Sierra Nevada Province and the southwestern Basin and Range Province. The Goler Formation contains California’s oldest fossil mammals (60 Ma). “Stromatolites,” or tufa, are incrustations precipitated by blue-green algae in clear, shallow, lake waters. Similar tufa deposits can be recognized in lake deposits that are 17 million years old and in those that are 70,000 years (Searles Lake) and 20,000 years (Searles and Manix lakes). Fill your gas tank in Ridgecrest, and travel south on Highway 395 to San Bernardino, Highway 14 to Los Angeles, or Highways 178 or 58 to Bakersfield.

End of Trip

Acknowledgements

The author thanks Frank Monastero and Janet Westbrook for contributions to this guide, and for the thoughtful reviews of Monastero, Westbrook, Steve Conkling (supporting papers), and George T. Jefferson (abstracts).

References

- Awramik, S.M., Buchheim, H.P., Leggitt, L. and Woo, K.S., 2000. Oncoids of the late Pleistocene Manix Formation, Mojave Desert Region, CA. San Bernardino County Museum Association Quarterly 47(2):25-31.
- Baker, C.L., 1911. Notes on the later Cenozoic history of the Mojave Desert region in southeastern California. University of California Publications in Geological Sciences, 6:333-383.
- Bancroft Library, 2002. California Views from the R.W. Waterman Family Papers, ca. 1865–1900. <http://www.oac.cdlib.org/dynaweb/>

- ead/calher/waterman/@Generic_BookTextView/129 (accessed 4/12/02).
- Brady, R.H. III, 1992. The eastern California shear zone in the northern Bristol Mountains, southeastern California. San Bernardino County Museum Association Spec. Publ. 92-1:6-10.
- Brady, R.H. III and Dokka, R.K., 1989. The eastern Mojave shear zone: a major tectonic boundary in the southwestern Cordillera: GSA abstracts with programs, vol. 21 no. 5:59.
- Brown, W.J., Wells, S.G., Enzel, Y., Anderson, R.Y. and McFadden, L.D., 1990. The late Quaternary history of pluvial Lake Mojave–Silver Lake and Soda Lake basins, California. San Bernardino County Museum Association Spec. Publ. 90-1:55-72.
- Burke, D.B., Hillhouse, J.W., McKee, E.H., Miller, S.T., and Morton, J.L., 1982. Cenozoic rocks in the Barstow Basin of southern California—stratigraphic relations, radiometric ages, and paleomagnetism: U.S.G.S. Bulletin, 1529:E1-E16.
- China Lake–Ridgecrest branch of the American Association of University Women, 1996. Indian Wells Valley and northern Mojave Desert Handbook: 194 p.
- Cooper and others, 2002. The Sulfur Hole, Calico district, San Bernardino County, California. Desert Studies Center, CSU Fullerton (this volume).
- Darlington, D., 1996. The Mojave: a portrait of the definitive American desert. New York, Henry Holt: 337 p.
- Dibblee, T.W. Jr., 1968. Geology of the Fremont Peak and Opal Mountain quadrangle, California. CDMG Bulletin 188: 64 p.
- _____, 1970. Geologic map of the Daggett quadrangle, San Bernardino County, California. USGS misc. inv. map I-592.
- Ferriz, H., 2002. Geology of the Cowhole Mountains, Mojave Desert, California [abs]. Desert Studies Center, CSU Fullerton (this volume).
- Flinchum, R., 2002. Nona Proctor Rosenberg: her life on the Tonopah and Tidewater Railroad [abs]. Desert Studies Center, CSU Fullerton (this volume).
- Glazner, A.F., Bartley, J.M. and Walker, J.D., 1989. The Waterman Hills detachment fault, central Mojave Desert, California. San Bernardino County Museum Association Spec. Publ. 89-1:52-60.
- Gourley, J.R. and Brady, R.H. III, 2000. Facies analysis of Neogene syntectonic strata in the Soda Mountains, San Bernardino County, Ca: implications for constraint on faulting on the Soda–Avawatz fault zone (abs). Empty Basins, Vanished Lakes, San Bernardino County Museum Association Quarterly 47(2):76.
- Grose, L.T., 1959. Structure and petrology of the northeastern part of the Soda Mountains, San Bernardino County, California. GSA Bulletin, 70(12):1509–1548.
- Gudde, E., 1969. California Place Names. University of California Press: 389 p.
- Hewett, D.F., 1956. Geology and mineral resources of the Ivanpah quadrangle, California and Nevada. USGS Prof. Paper 275:172.
- Housley, R.M. and Reynolds, R.E., 2002. Mineralogical survey of the Mount General area. Desert Studies Center, CSU Fullerton (this volume).
- Jennings, C.W., Burnett, J.L., and Troxel, B. W., 1962. Geologic map of California, Trona sheet, scale 1:250,000. California Division of Mines and Geology.
- Lofgren, D. and McKenna, M., 2002. The Goler Formation of California. Desert Studies Center, CSU Fullerton (this volume).
- Lum, M.A. and Middlemiss, T., 2002. Rare plants of Short Canyon in Kern County, California [abs]. Desert Studies Center, CSU Fullerton (this volume).
- McGill, S.F., Murray, B.C., Maher, K.A., Leiske, J.H., Rowan, L.R. and Budinger, F., 1988. Quaternary history of the Manix Fault, Lake Manix Basin, Mojave Desert, California. San Bernardino County Museum Association Quarterly 35(3,4): 3-20.
- Miller, D.M., 2002. Overview of the surficial geology of Dove Spring area, Kern County, California [abs]. Desert Studies Center, CSU Fullerton (this volume).
- Montastero, F.C., Kamola, D.L. and Walker, J.D., 2001. Late Neogene evolution of the Indian Wells Valley and the Coso Range. Pacific Section SEPM, book 88:55-90.
- Monastero, F.C., Sabin, A.E., and Walker, J.D., 1997. Evidence for

- post-early Miocene initiation of movement on the Garlock Fault from offset of the Cudahy Camp Formation, east-central California. *Geology*, vol. 25, p. 247-250.
- Mulqueen, S.P., 2002. Borax Smith and the Tonopah & Tidewater Railroad. Between the Basins: Exploring the Western Mojave and Southern Basin and Range Province. Desert Studies Center, CSU Fullerton (this volume).
- Myrick, D.F., 1991. Railroads of Nevada and eastern California. Reno: University of Nevada Press: 399 p.
- Pedone, V. and Caceres, C., 2002. Carbonate phytoherm mounds in the middle Miocene Barstow Formation, Mud Hills, California. Desert Studies Center, CSU Fullerton (this volume).
- Pracchia, Lou, 1994. Indian Wells Valley Stage and Freight Stops, 1874-1906. Historical Society of the Upper Mojave Desert, Ridgecrest, 29 p.
- Rieger, Ted, 1952. Calcareous tufa formations, Searles Lake and Mono Lake. *California Geology*, July/August 1992:99-109.
- Reynolds, R.E., 1997. A model for strike-slip overprint on the Halloran detachment terrain. *San Bernardino County Museum Association Quarterly* 44(2):25-28.
- _____, 1999. A walk through Borate: rediscovering a borax mining town in the Calico Mountains. *San Bernardino County Museum Association Quarterly*, 46(1): 31 p.
- _____, 2000. Marker units suggest correlation between the Calico Mountains and the Mud Hills, central Mojave Desert, California. *San Bernardino County Museum Association Quarterly*, 47(2):21-24.
- Reynolds, R.E. and Calzia, J., 1996. Punctuated chaos. *San Bernardino County Museum Association Quarterly* 43(1,2): 131-134.
- Reynolds, R.E. and Reynolds, R.L., 1991. Late Pleistocene faunas of Lake Thompson. *San Bernardino County Museum Association Quarterly* 38(3,4) :114-115.
- Reynolds, R.E. and Weasma, Ted, 2002. California dinosaur tracks: inventory and management. Between the Basins: Exploring the Western Mojave and Southern Basin and Range Province. Desert Studies Center, CSU Fullerton (this volume).
- Reynolds, R.E., Wells, S.G., Brady, R.H. III, 1990. Road log: the end of the Mojave. *San Bernardino County Museum Association Quarterly*, Spec. Pub. 90-1:5-16.
- Reynolds, R.E., Whistler, D.P. and Woodburne, M.O., 1991. Road log: the 1991 SVP field trip to paleontologic localities in inland Southern California. *San Bernardino County Museum Association Quarterly* 38(3,4): 5-36.
- Reynolds, R.E. and Woodburne, M.O., 2002. Marker bed correlations between the Mud Hills, Calico Mountains, and Daggett Ridge, central Mojave Desert, California [abs]. Desert Studies Center, CSU Fullerton (this volume).
- Schoenherr, A.A., 1994. *A Natural History of California*. University of California Press: 772 p.
- Scholl, D.W., 1960. Pleistocene algal pinnacles at Searles Lake, California. *Journal of Sedimentary Petrology*, 30(3):414-431.
- Sharp, R.P. and Glazner, A.F. 1997. *Geology underfoot in Death Valley and Owens Valley*. Mountain Press Publishing Company: 319 p.
- Simpson, R.D., 1999. An introduction to the Calico Early Man Site lithic assemblage. *San Bernardino County Museum Association Quarterly*, (46)4: 48 p.
- Thompson, D.G., 1929. The Mojave Desert Region, California: a geologic and hydrologic reconnaissance. U.S.G.S. Water-supply paper 578.
- Whistler, D.P., 1984. An early Hemingfordian (early Miocene) fossil vertebrate fauna from Boron, western Mojave Desert, California. *Los Angeles County Museum of Natural History Contrib. in Sci.*, 355.
- _____, 1991. Geologic history of the El Paso Mountains region. *San Bernardino County Museum Association Quarterly* 38(3,4) :108-113.
- Whistler, D.P. and Burbank, D.W., 1992. Miocene biostratigraphy and biochronology of the Dove Spring Formation, Mojave Desert, California, and characterization of the Clarendonian land mammal age (late Miocene) in California: *GSA Bull.* 104:644-658.
- Vredenburg, L.M., 1994. Fort Irwin and vicinity: history of mining development. *San Bernardino County Museum Association Spec. Pub.* 94-1:81-20.
- Wilkerson, Gregg, 2002. The Bodfish layered basic intrusive [abs]. Desert Studies Center, CSU Fullerton (this volume).

California Dinosaur Tracks: Inventory and Management

Robert E. Reynolds, LSA Associates, Inc., Riverside CA 92507
Ted Weasma, Mojave National Preserve, Barstow, CA 92311

Abstract

California's only dinosaur tracks are middle Jurassic in age and are located in the Aztec Sandstone of the Mescal Range, Mountain Pass, in the eastern Mojave Desert. The Aztec crops out in the Mojave Block at Ord Mountain, the Soda Mountains, Cow Hole Mountains and in the Mescal Range. The western occurrences are metamorphosed, while the eastern outcrops are orthoquartzites that retain biologic and sedimentary structures.

The popularity of dinosaurs during the late 20th century prompted concern that no detailed inventory existed for California's only tracks. Not only are the tracks unique in the state, but early Jurassic track sites are rare in the western United States. Previous work identified trackways representing three bipedal coeleurosaurs assigned to ichnogenera *Anchisauripus*, *Grallator*, and an unnamed ichnogenus. In addition to coeleurosaurs, tracks and trackways of more than four quadrupedal ichnogenera are represented. The track impressions of both quadrupeds and bipeds produce compression rings that suggest original slope of dune topography. Also preserved are sedimentary structures, cross-bedding, ripples, raindrops, and trails and tracks left by invertebrates.

One hundred sixteen track and structure localities were recorded, including outcrop panels and loose slabs. Of importance, the second of two occurrences of a small (juvenile) bipedal trackway paralleling an adult trackway was located. All loci were photographed and attitudes were taken of outcrops that reflected the local dune surface. Baseline data is now available for further inventory and management of the trackway site. Research questions that can now be quantified include what are the characteristics of the sedimentary facies in which tracks are preserved, and where they are not preserved; and whether there is significance to the bearing of the track maker.

Introduction

The only dinosaur tracks known in California are in the Jurassic Aztec Sandstone of the Mescal Range, at Mountain Pass in the eastern Mojave Desert. The Aztec Sandstone is exposed in many outcrops in the Mojave Block. Western occurrences are metamorphosed, but eastern outcrops retain biological and sedimentary structures. Trackways of coeleurosaurs and of more than four quadrupedal ichnogenera are represented. The track impressions of both quadrupeds and bipeds produce compression rings that suggest original slope of dune topography. Sedimentary structures, cross-bedding, ripples, raindrops, and trails and tracks left by invertebrates are also preserved. Previous work identified trackways representing three bipedal coeleurosaurs assigned to ichnogenera *Anchisauripus*, *Grallator*, and an unnamed ichnogenus. The named ichnogenera are present in the Jurassic Newark Supergroup on the North American continent's eastern margin. Not only are the tracks unique in the state, but early Jurassic track sites are rare throughout the western United States. A recent inventory of tracks using a portable GPS unit recorded one hundred sixteen localities. This exercise added a second occurrence of juvenile tracks paralleling those of a small adult. Baseline data is now available to help quantify research questions and for further inventory and management of the trackway site.

Previous Work

The tracks in the Aztec Sandstone of California were first recognized by Evans (1958; 1971). Descriptions of the three bipedal and four quadrupedal tracks were published by Reynolds (1989), who documented the direction of travel for the quadruped tracks and showed the bipeds had less directional preference. The age of the Aztec and the tracks was reviewed (Fleck and Reynolds, 1996). Review of Jurassic tracks in Utah and Wyoming (Kvale and others, 2001; Breithaupt and others, 2001) as well as field investigations in the Aztec of southern Nevada suggest that the ichnogenera and ichnospecies represented in the Mescal Range section are uncommon west of the Rocky Mountains.

The Aztec Sandstone: Age and Distribution

The Aztec Sandstone is a quartz arenite first mapped by D. F. Hewett (1956) at the type section in Goodsprings, Nevada. Although similar in appearance, it was recognized as distinct from the Navajo Sandstone in the Grand Canyon sequence to the east. The Aztec has since been shown to occur at many localities in the Mojave Block, including the Cowhole Mountains (Barca, 1966; Ferriz, herein; Jennings, 1961), the Soda Mountains (Jennings and others, 1962), the Ord Mountains (Bortugno and Spittler, 1986; Weber, 1963). Geologic studies in the southeastern Mojave-Colorado Desert area suggest that the Palen Formation in the northern Palen Mountains correlates to the Aztec, and was deposited prior to 175 Ma (Le Veque, 1982; Pelka, 1973).

The age of the Aztec Sandstone in the Mescal and Goodsprings Ranges was originally referred to the Jurassic (Hewett, 1956; Evans, 1958). Its position within the Jurassic was questioned (Marzolf, 1980, 1982) because the first tentative dates on the Delfont Volcanics that overlie the Aztec in the Mescal Range were in the 150 Ma range, and two of the dinosaurian ichnogenera were known from the Newark Supergroup of the Connecticut Valley which spans the Triassic and the Jurassic Epochs. Recent work (Busby-Spera and others, 1987; Ferriz, this vol.) presents dates on andesite (173 \pm 4 Ma) interbedded with the Aztec in the Cowhole sequence and a date on the basal ignimbrite (170 \pm 2 Ma) that overlies the sequence. Dates on Unit 2 of the Delfont volcanics are 100.5 \pm 2 Ma (Fleck and others, 1994; Fleck and Reynolds, 1996), indicate this eruptive event is related to the emplacement of the Teutonia Batholith (Beckerman and others, 1982).

Based on the dates from the Cowhole section (Busby-Spera and others, 1987) the age of the dinosaurian trackways would be middle Jurassic, and based on the stratigraphic relationships in the Mescal Range, no younger than mid-Cretaceous. A middle Jurassic age accords well with the relationship of two ichnogenera (*Anchisauripus* and *Grallator*) to the tracks



Left and right: co-author Ted Weasma carrying the Trimble Pro-XRS GPS unit at the dinosaur track locality.

in the Jurassic portion of the Newark Supergroup as well as in the Moenave Formation of northeastern Arizona (Irby, 1993). The unnamed ichnogenus from the Mescal Range is smaller than tracks with similar morphology from the lower Cretaceous of South Dakota (Anderson, 1939) and the Jurassic of China (Zhen and others, 1986), and presumably indicates a pre-Cretaceous age.

Track Utility and Research Questions

Evans (1958) described the Mescal Range tracks as useful for determining the stratigraphically upright position of the sandstone beds. If additional age constraints can be placed on the tracks, they may well be useful in proposing dates for sediments that are otherwise undatable.

Each track, quadruped or biped, leaves more or less distinct impressions. The displacement of the underlying sediment by the weight of the animal leaves a compression ring around the print (Reynolds, 1989). If the substrate is sloping, the compression ring slumps in a down hill direction. Track clarity and the orientation of the compression ring can be used to ascertain degree of paleoslope and moisture content of the substrate.

Preliminary measurement of trackways in the Mescal Range show that individuals changed their length of stride as they left a standing position. The combination of small (juvenile) tracks following parallel to larger tracks of the same morphology suggest that population dynamics can be interpreted from trackway analysis. Other track sites have provided similar information

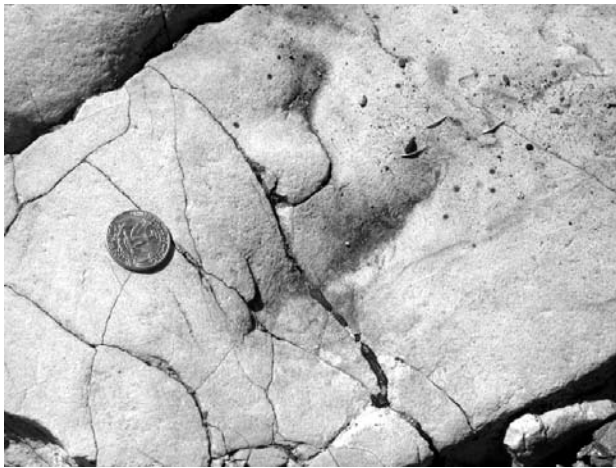
(Ostrom, 1972)

Research Questions

- Do the tracks reflect the population dynamics of each ichnogenus?
- How do the dynamics of quadrupedal ichnogenus relate to those of the bipeds?
- How do the dynamics of all ichnogenus relate to the specific substrate; what were they doing as they crossed dune sand; can feeding habits be speculated upon?
- The size of the foot imprint varies both with maturity of individual and with consistency of substrate. Can parameters for variation by age be distinguished from differentiation due to substrate?
- Will making correctional adjustments for anticlinal folding and block rotation (paleomagnetic data) have an effect upon direction and bearing of bipedal and quadrupedal track makers?
- Tracks apparently are best or only preserved in certain sandstone lithologies. Can environmental parameters be applied to those lithologies?
- Track bearing horizons can now be measured to the lowest overlying volcanoclastic unit. Can this unit be dated to provide time constraints on the local ichnogenus?
- Will detailed measurements of the print sizes of the large sample of one ichnogenus lead to data on population diversity within that genus?



Left, co-author Bob Reynolds pours latex to replicate a dinosaur track. Right, latex mold in situ.



Track of bipedal dinosaur.

- Are invertebrate tracks at this site identifiable to ichnogen-
era?
- Will further morphometric analysis identify other or previ-
ously unnamed ichnogenera at this site?
- Can invertebrate ichnogenera at this site be named and
quantified, and compared to other Mesozoic sites?

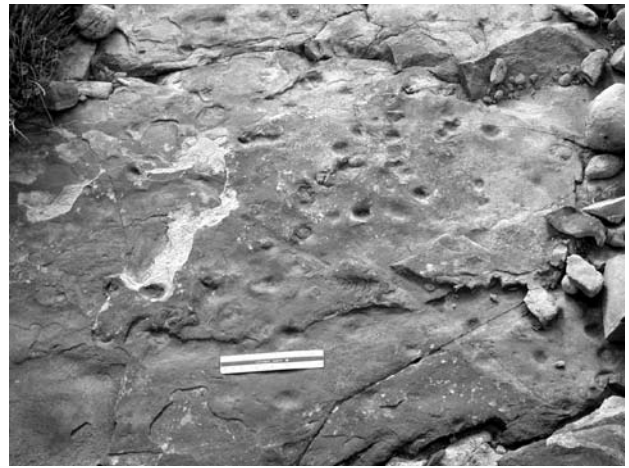
Inventory Methods

The Dinosaur Trackway site is a BLM “area of critical environmental concern” (ACEC) which receives special protection, regular patrol and focused management programs. Consequently, authorization for inventory and replication was conducted under a Bureau of Land Management (BLM) permit. The detailed inventory of the Mescal Range trackways was undertaken in the fall of 2001 by volunteers from the Mojave River Valley Museum through its Desert Discovery Center “Tracks through Time” program. Assistance was received from staff of the BLM, National Park Service and the Mojave Desert Ecosystem Program. The inventory of trackways was designed to determine base line reference data in order to establish rates of attrition and loss of tracks. Each outcrop exposure was examined by teams to locate and flag each locality with tracks. A second team photographed the tracks digitally, and recorded attitudes of the bedding planes containing the tracks. A third team plotted the UTM coordinates of each outcrop or loose slab with the pack-mounted Trimble Pro-XRS GPS unit, with TSC1 data recorded with real time coordinates in the field. The data has been recorded graphically, and UTM coordinates are attached to attitudes and photographs. The GIS data recovered was compiled, analyzed and put into a usable format by James Essex of the Mojave Desert Ecosystem Program.

During the inventory, it was recognized that exposed bedding planes were actually the surface of sand dunes, and did not reflect the overall attitude of the sandstone facies. A plot (Figure 1) of all the track sites does, however, show that the track sites fall within two specific facies which reflect the surface exposure of the anticlinally folded formation.

Selected track sites were replicated during this inventory. The samples included small and large tracks following the same bearing, since these have been interpreted as herd behavior (Reynolds, 1989).

Good examples of the unnamed biped and of a large quadruped trackway were also replicated so that copies could be used by local offices of federal agencies for educational purposes.



Quadruped trackway.

All trackways that were exposed for the purposes of replication were reburied and the landscape restored.

Summary

Recently acquired UTM coordinates record 116 tracks, trackways or structures in the Aztec Sandstone of the Mescal Range in the eastern Mojave Desert. The 2001 inventory identified loose slabs or outcrops which contained 44 panels with bipedal coeleurosaur tracks, 73 panels with quadruped tracks and 19 panels with invertebrate tracks. Five localities were recorded where sedimentary structures might prove useful in interpreting sandstone diagenesis. Plots of the loci suggest that tracks occur in two arenaceous facies of the Aztec Sandstone. Among the more interesting discoveries was a new panel which contained small and large tracks of the unnamed ichnogenus walking in

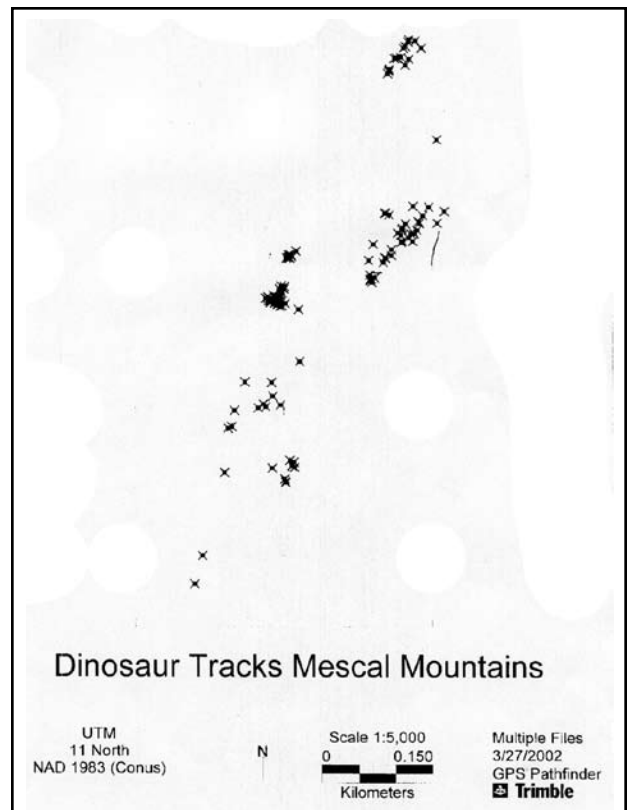


Figure 1.

parallel directions.

The 2001 inventory of the Mescal Range tracks provides base line data for management and further inventory and research in the Aztec Sandstone. The detailed locational data allow resource managers to determine if sandstone blocks and outcrops are subject to movement, degradation or removal. The photographic record will indicate whether outcrops and individual tracks are subject to degradation by weather or vandalism. Further surveys are needed since other outcrops remain to be examined for track impressions, and the existing data only describes sets of conditions where track preservation is most likely to exist. Annual review of changes to California's only dinosaur track site will determine if the current level of resource management is adequate for their long-term preservation for scientific study and educational interpretation.

References

- Anderson, S. M. 1939, *Jour. Paleo.*, Vol. 13, no. 3, p.361-364.
- Barca, Richard A. 1966, Geology of the northern part of the Old Dad Mountain Quadrangle, San Bernardino County, California. C. D. M. G. Map Sheet 7, Scale 1:62,500.
- Beckerman, G. M., Robinson, J. P., and Anderson, J. L., 1982, The Teutonia Batholith: *in* Frost, E. G. and D. L. Martin, Mesozoic-Cenozoic Tectonic Evolution of the Colorado River Region, California, Arizona, and Nevada: Cordilleran Publishers, Geol. Soc. Am. Field Trip Volume pp. 205-220.
- Bortugno, E. J., and T. E. Spittler, 1986. Geologic Map of the San Bernardino Quadrangle, Scale: 1:250,000. California Division of Mines and Geology, regional geologic map series, Map 3A.
- Breithaupt, Brent H., and E. H. Southwell, T. L. Adams, and N. A. Matthews, 2001. Innovative documentation methodologies in the study of the most extensive dinosaur tracksite in Wyoming. p. 113-122. *In* Proceedings of the 6th Fossil Resource Conference. (Eds) Vincent L. Santucci and Lindsay McClelland p. 214.
- Busby-Spera, C.J., Schermer, E. R., Mattinson, J. M., 1987, Lower Mesozoic extensional continental arc, Arizona and California: A depocenter for craton-derived quartz arenites: Geological Society of America Abstracts with Programs, v. 19, no. 7, p.607.
- Evans, J. R., 1958, Geology of the Mescal Range, San Bernardino County, California. Scale 1:24,000. University of Southern California, Unpublished M. A. Thesis.
- Evans, J. R., 1971, Geology and mineral deposits of the Mescal Range quadrangle, San Bernardino County, California: C. D. M. G. Map Sheet 17, SCALE 1:62,500.
- Ferriz, Horacio, 2002, Geology of the Cowhole Mountains, Mojave Desert, California [abs], *in* Abstracts from the 2002 Desert Symposium. California State University, Fullerton, this volume.
- Fleck, R. J., and M. D. Carr, G. A. Davis, and C. B. Burchfiel, 1994, Isotopic Complexities of the Delfont Volcanic Rocks, Eastern Mescal Range, southeastern California. Stratigraphic and Tectonic Implications: *Geol. Soc. Am. Bull.*, v. 106, p. 1242-1253., 1994.
- Fleck, R. J. and R. E. Reynolds, 1996, Mesozoic stratigraphic Units of the Eastern Mescal Range, Southeastern California. *San Bernardino County Museum Association Quarterly*, 43(1): 49-54.
- Hewett, D. F., 1956, Geology and Mineral resources of the Ivanpah Quadrangle, California and Nevada: U. S. Geol. Survey Prof. Paper 275, 172p.
- Irby, G. V., 1993, Early Jurassic dinosaur Track sites, northeastern Arizona, p.15-23, *in* Boaz, D. and Dornan, M., eds. First Annual Symposium, Fossils of Arizona: Mesa Southwest Museum, 91p.
- Jennings, C. W., 1961, Geologic Map of California, Kingman Sheet, C. D. M. G. scale 1:250,000.
- Jennings, C. W., J. L. Burnett and B. W. Troxel, 1962. Geologic Map of California: Trona Sheet. C. D. M. G., Scale 1:250,000.
- Kvale, Erik P., Johnson, G. D., Mickelson, D. L., K. Keller, L. C. Furer and A. W. Archer. 2001, Middle Jurassic (Bajocian and Bathonian) Dinosaur Megatracksites, Bighorn Basin, Wyoming, U. S. A. *Palaio*, V. 16, p.233-254.
- Le Veque, Richard A. 1982, Stratigraphy and Structure of the Palen Formation, Palen mountains, Southeastern California. p. 267-274. *In* Frost, E. G. and D. L. Martin (eds), Mesozoic-Cenozoic Tectonic Evolution of the Colorado River Region, California, Arizona, and Nevada. *Geol. Soc. Am. Field Trip Volume*.
- Marzolf, J. E., 1980. The Aztec Sandstone and Stratigraphically Related rocks in the Mojave Desert: *in* Geology and Mineral Wealth of the California Desert. Fife, D. L. and A. R. Brown, (eds.), Southcoast Geol. Soc., p.215-220.
- Marzolf, J. E., 1982. Paleogeographic Implications of the Early Jurassic (?) Navajo and Aztec Sandstones: p. 493-501. *in* Frost, E. G. and D. L. Martin (eds), Mesozoic-Cenozoic Tectonic Evolution of the Colorado River Region, California, Arizona, and Nevada. *Geol. Soc. Am. Field Trip Volume*.
- Ostrom, J. 1972. Were some Dinosaurs Gregarious? *Paleogeography, Paleoclimatology, Paleoecology* 11: 287-301.
- Pelka, G. J. 1973, Geology of the McCoy and Palen Mountains: southeastern California: Ph. D. thesis, Univ. of Calif. Santa Barbara, 162p.
- Reynolds, R. E., 1989, Dinosaur Trackways in the lower Jurassic Aztec Sandstone of California, p.298-292, *in* Gillette, D. D. and M. G. Lockley, eds. *Dinosaur Tracks and Traces*: Cambridge University Publications, 454p.
- Weber, Harold F., Jr., 1963. Geology and Mineral Deposits of the Ord Mountain District, San Bernardino County, California. C. D. M. G. Special Report 77, p. 45.
- Zhen, S., J. Li, and C. Rao, 1986, Dinosaur Footprints of Jinning, Yunnan: *Mem. Beijing Nat. Hist. Museum*, 33, 18p.

Borax Smith and the Tonopah & Tidewater Railroad

Stephen P. Mulqueen, *Dept of Conservation, Division of Oil, Gas, and Geothermal Resources, Ventura, CA 93303*

Introduction

The Tonopah & Tidewater Railroad operated between 1907 and 1940 servicing mines and communities along a route which extended north from Ludlow, California into western Nevada. What began as one man's challenge to a transportation problem at a borate mine in the Amargosa Desert east of Death Valley resulted in a rail system which benefited all those who lived in the surrounding area.

The history of the Tonopah & Tidewater is a story of success in overcoming formidable obstacles in the desert regions of California and Nevada. These obstacles included steep mountains, dry lakes and washes subject to flooding, and long expanses of uninhabited land devoid of trees and reliable sources of water. The great geologic forces that formed high-grade mineral deposits also created adverse conditions which impeded the economic development of those resources.

William T. Coleman

The occurrence of borate minerals in the Death Valley region of Inyo County attracted early settlers to the area. These minerals included ulexite and colemanite which occurred naturally within lacustrine deposits at locations on the floor of Death Valley and in the hills surrounding the Furnace Creek wash. In 1881, Isadore Daunet became the first to develop borate minerals within Death Valley. Daunet's operations were known as the Eagle Borax Works.

During that same year, Aaron Winters discovered "cottonball" ulexite in the playa mud, a short distance from the northwest edge of the alluvial fan of the Furnace Creek wash. William T. Coleman bought claims from Winters and began developing the deposit. With the help of Chinese laborers, Coleman successfully harvested cottonball ulexite from the mud flats. In 1883, a processing plant was built to convert ulexite into borax, a more desirable commodity that could be marketed.

He called his operations the Harmony Borax Works.

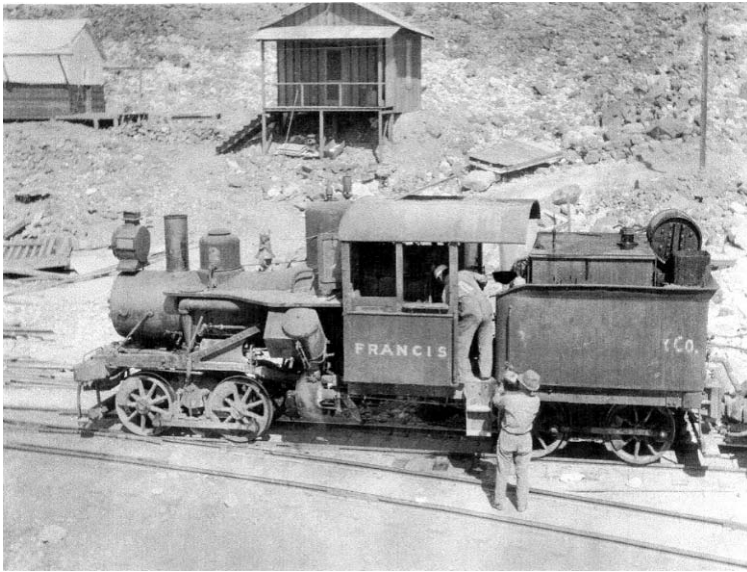
Hauling borax out of Death Valley was a great task for Coleman. He had heard about the use of large wagons pulled by a team of 20 mules which, at that time, were the most efficient means of transporting heavy loads of freight and ore.¹ The 20 mule team wagons were first designed in the early 1870s to haul freight and ore for remote mining camps in California, Nevada and Arizona. John Searles was the first to apply this technology to haul borax. In 1873, Searles and his teamsters transported borax from his mining operations at what was then known as "Slate Range Playa" and later called "Borax Lake" (now Searles dry lake). Before the railroad was built through Mojave, Searles' 20 mule teams and wagons hauled borax 175 miles to the harbor at San Pedro. In 1883, Coleman ordered his own 20 mule team wagons which were built by craftsmen in Mojave, California. Later that year, Coleman and his teamsters began hauling borax out of Death Valley to the Southern Pacific Railroad at Mojave using the 20 mule teams and wagons. (The "20 mule team" actually consisted of 18 mules and 2 horses).

"Borax" Smith

Coleman produced and shipped borax from the Harmony Works for several years. By 1888, his operations met with financial losses. It was during this time that Francis Marion Smith (also known as "Borax" Smith) purchased Coleman's properties and all his holdings. With this acquisition, Smith took possession of all the claims, borate deposits and mines originally held by Coleman. These properties included the borax plant at Harmony, the cottonball ulexite deposit within the Death Valley playa, the colemanite deposit at the Lila C. mine (southwest of the present day Death Valley Junction, at the edge of the Greenwater Range, Amargosa Desert), and the colemanite deposits at Mule Canyon near Calico in the Mojave Desert. Included in the purchase were the successful 20 mule



Twenty Mule Team at the 1949 Death Valley encampment. © William H. Smitheram.



Ryan, narrow-gauge locomotive "Francis, 1915. This locomotive was first used at Borate on the Borate & Daggett railroad. In cab is engineer John Connelly. © W. H. Smitheram.

teams, wagons and rigging. (The Lila C. mine was named after Coleman's daughter Lila.)

Smith was familiar with borate mining from his experience producing borax at Teel's Marsh in Nevada. In 1890, Smith combined the three properties in California and formed the Pacific Coast Borax Company (PCB).

To haul borax from the mill at Borate to the railhead at Daggett, Smith first used the 20 mule teams and wagons. Beginning in 1894, a steam traction engine known as "Old Dinah" pulled borax wagons and hauled freight, traversing the 11 mile trek to the railroad. Old Dinah was not as reliable as the 20 mule teams. The steam engine developed frequent breakdowns, and its heavy wheels would often bog down in mud and soft sand. In 1898, the narrow-gauge Borate & Daggett Railroad was built to transport borax and supplies.

In 1899, Smith formed an organization formally known as Borax Consolidated, Limited, an international organization with headquarters in London, England. By the year 1904, the deposits at Borate were beginning to reach the end of their productive life. Smith began moving the mining equipment and personnel northward to the large colemanite deposit at the Lila C. mine.

Hauling borax from the Lila C. mine proved to be Smith's greatest challenge. At that time, the closest railhead was at Ivanpah, which was over 100 miles from the mine. He first met the challenge by placing Old Dinah back into operation. In April, 1904, Smith put the engine to the test. After traversing only 14 miles, the steam boiler blew out and the machine came to a sudden stop.² The failure of Old Dinah was *the* event which set the stage for the construction of the Tonopah & Tidewater Railroad.

The Tonopah & Tidewater Railroad

Borax Smith was convinced that a railroad was the only answer to his transportation dilemma. He set his sights high and envisioned a standard-gauge railroad which would not only service his mine but also extend to the gold and silver mines around Goldfield and Tonopah in Nevada. Smith also considered extending the route south to the tidewater at San Diego, although this plan was never implemented. On July 19, 1904,

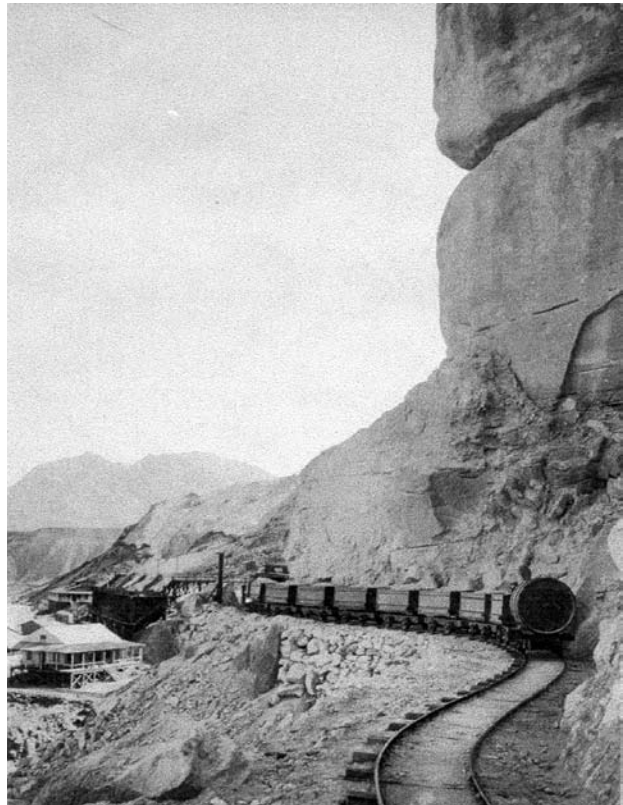
the Tonopah and Tidewater Railroad Company (T & T) was incorporated by Smith and registered in the State of New Jersey. Smith immediately claimed title to the wagon road between Ivanpah and the Lila C. mine and began the task of finding investors for his great project.

Survey crews began charting a route from Ivanpah northward. During that time, a new Southern Pacific Line was reaching completion, known as the San Pedro, Los Angeles & Salt Lake Railroad (SP, LA & SL). With the line open for traffic, survey crews also mapped a possible path for the T & T from the SP, LA & SL line north, through the Kingston Range and on to the Lila C. mine. Survey crews also considered a route from Las Vegas.

By 1905, Smith decided to begin building the railroad at Las Vegas. Smith met with Senator William A. Clark and, with a handshake, was given verbal approval for the railroad. (Clark was a Senator from Montana who had sizable investments and considerable political power within the State of Nevada).

This gave Smith the consent he needed to begin construction of the railroad. On May 29, 1905, groundbreaking ceremonies were performed dedicating the start of grading operations for the new T & T line near Las Vegas.

Shortly after this event, Senator Clark began having second thoughts about letting Smith build the T & T railroad from Las Vegas. Clark wanted to form his own railroad from Las Vegas to the mines at Tonopah. He had large investments in the mines around Goldfield and Tonopah. With a railroad to service those mines, Clark would have more control over those investments and the railroad would add to their success.



Ryan, "baby-gauge" ore train approaching the ore bunker, PCB company store in foreground; superintendent's house just beyond bunkers, 1915. © W. H. Smitheram.



Head frame at Shaft #2, Borate; narrow-gauge tracks of the Borate & Daggett. Mule Canyon, Calico Mountains, 1898. © W. H. Smitheram.

Clark did not make it clear to Smith regarding his change of plans. Instead, he made it difficult for Smith to build his railroad. Without warning, the Southern Pacific Railroad began charging the T & T the prohibitive rate of 45 cents freight for each railroad tie arriving at Las Vegas. This new freight charge would add considerably to the construction costs. Smith tried to gain permission to connect the T & T line to the SP, LA & SL rails. His request was flatly denied. Clark had indirectly put a stop to Smith's plans by exerting his influence on the construction operations. Shortly after this event, Clark announced the formation of the Nevada Transit Company which began planning the construction of the Las Vegas & Tonopah Railroad (LV & T).

This action was a great setback for Smith. Over 12 miles of railroad bed had been graded. It was "a road to nowhere." Smith had no choice but to shift his operations from Las Vegas, Nevada to Ludlow, California.

Smith obtained approval to connect the proposed rail line with the main line of the Santa Fe Railroad near Ludlow. By August, 1905, the transfer of equipment to the new site was completed and a tent city was constructed. The new starting point at Ludlow added 50 miles to the goal of reaching Gold Center, Nevada. (Gold Center was a railroad siding south of Beatty, Nevada). The race between Clark's LV & T and Smith's T & T was in full swing.

In October, 1905, Clark and the Nevada Transit Company purchased the 12 miles of graded railroad bed built by the T & T and began construction of the LV & T. This sale gave Smith and the T & T the money to recover from the setback of relocation. Smith wasted no time. He appointed John Ryan, Clarence Rasor and William (Wash) Cahill to supervise construction operations along its extensive route. By November, 1905, the first rail was laid at the "Big Loop", the term given to the circular rail pattern at the rail yard near Ludlow. (Written accounts of the T & T also refer to the "Big Loop" as the "T & T Loop Line" and/ or the "Balloon Track".) The "Big Loop" enabled trains coming south to easily turn around for the return trip north.

From Ludlow, the railroad crossed the SP, LA & SL line at Crucero (Spanish word for "crossing") and

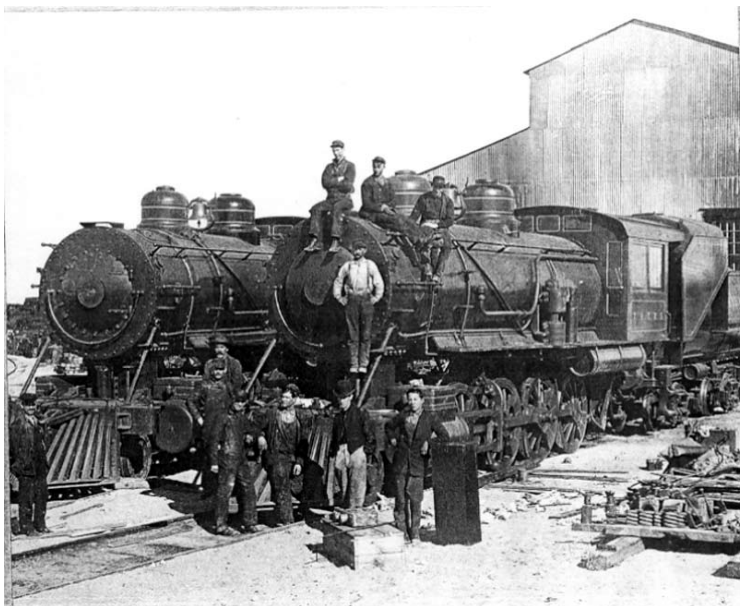
extended over Broadwell and Soda (dry) Lakes. By March, 1906, the T & T completed the crossing of Silver (dry) Lake north of Baker. At that stage of the project, survey crews continued to chart a detailed path for the railroad, in advance of the construction operations. In May of 1906, 75 miles of rail had been completed to a point just beyond Dumont, north of the Dumont dunes in San Bernardino County.

The greatest challenge that the crew faced was the 12 mile ascent through the Alexander Hills north of Dumont by way of the Amargosa River Gorge. These mountains were formed by left-lateral movement along the Garlock Fault. This great obstacle extended east to west for many miles. Going around it was not an option for Smith.³

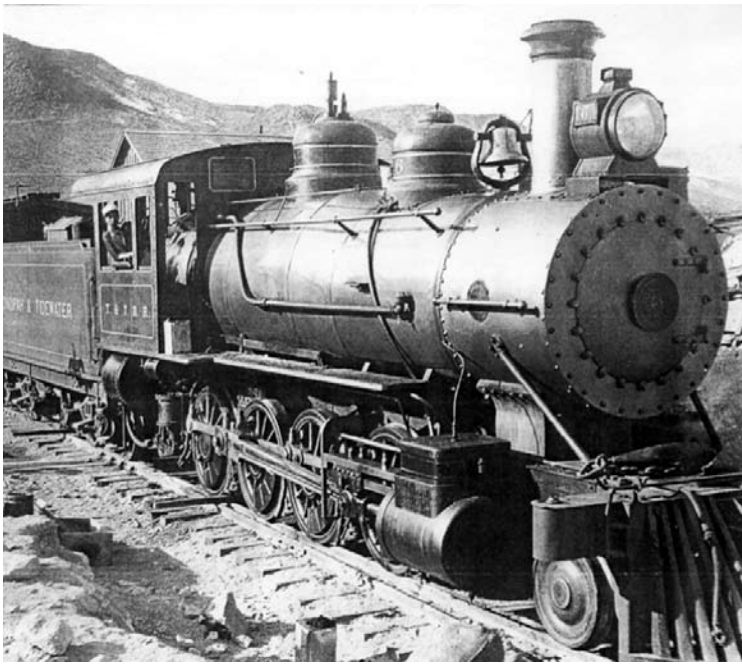
Smith met the challenge by starting at Tecopa and working downhill from north to south. By attacking the problem in this manner, the workmen were able to use gravity to their advantage, a well known factor commonly applied in the mining industry. Supplies and equipment were offloaded at Dumont and hauled by horse-drawn wagons to the construction site.

By this time, the hot weather during the summer of 1906 was paying its toll on the work crew. Construction workers began quitting. By the time Smith was able to attract additional crews to the area, the weather had cooled and the fall season had arrived. By February 10, 1907, the line was completed from Tecopa south to Sperry, a railroad siding just south of China Ranch where the Sperry Wash joins the Amargosa River.

Workmen constructed three trestles, excavated several long cuts and compacted numerous fill-slopes. Many of the cuts were excavated through solid rock which required extensive hand drilling and blasting with dynamite. One of the trestles was over 500 feet long. In order to reduce the steep grade and elevate the tracks above the bed of the Amargosa River, the railroad crossed the canyon several times. In May, 1907, the railroad was completed through the Amargosa Gorge connecting rails at Sperry with those at Dumont. Within days after achieving this great accomplishment, scheduled train service began operating to Tecopa, on the south edge of the Amargosa Valley. Smith had lost several months worth of time from the delays encountered in the Amargosa Gorge.



T & T engines #7 and 8, T & T rail yard at Ludlow, 1910. © W. H. Smitheram.



T & T engine #6 at the Lila C. mine, 1910. © W. H. Smitheram.

By June, 1907, the railroad was completed to Zabriskie, a railroad siding 4 mile north of Tecopa. While construction continued northward, borax from the Lila C. mill was hauled by wagon to the advancing rail line. Shortly after reaching Zabriskie, Smith formed the Tonopah & Greenwater Railroad which was incorporated in 1907. He proposed a railroad spur off of the T & T line at Zabriskie to the mines of the Greenwater District in the area surrounding Greenwater Valley. The Tonopah & Greenwater Railroad was never built as a result of the collapse of the mining industry during the Panic of 1907 and because of rumors of stock swindles common to the mines of the Greenwater District.

On August 16, 1907, the railroad was completed all the way to the Lila C. mine. Borax from the mill was shipped by rail on that same day. By this time over 700 men were working on the railroad. Camps were established at Leeland and at Gold Center, Nevada. Work progressed north from the Lila C. and south from Gold Center. On October 30, 1907 rail lines were joined and rail service arrived at Gold Center. There was no celebration for this great event. By that time, the economy was feeling the full effect of the Panic of 1907. Many mines in the area continued to close. Also, the Las Vegas & Tonopah Railroad reached Gold Center the year before and during October, 1907, was completed all the way to Goldfield, Nevada.

The T & T became known as "The Nevada Short Line." On November 25, 1907 the T & T opened the entire line to scheduled freight service. By December 5 of the same year, the T & T boasted with the opening of passenger service. In the spring of 1908, a new rotary kiln was put into operation at the Lila C. mine. The town which grew around the Lila C. was named Ryan in honor of John Ryan, Smith's right-hand man during the construction phase of the railroad. All remaining equipment, buildings and personnel were moved from Borate to Ryan.

On June 15, 1908, a holding company was formed under the name Tonopah & Tidewater Company, which assumed operations of the Bullfrog Goldfield Railroad. This gave the T & T exclusive trackage rights to Goldfield. With time, the Tonopah & Tidewater Company was absorbed by the T & T.

With this action, the Tonopah & Tidewater Railroad now extended from Ludlow, California all the way to Goldfield, Nevada.

A Full-Service Railroad

The opening of scheduled rail service by the T & T brought progress to all the mines and towns along its route. The great hardship of hauling supplies and ore long distances by wagon had been superceded by the new railroad. Food, supplies, mail, mining equipment, farm equipment and even potable water could now be transported with relative ease. Commodities from surrounding mines, transferred on the T & T, included refined borax, colemanite ore, gold and silver ores, base metal ores, bentonite clay, talc, gypsum, fluorspar and quarried marble. The railroad brought many new industries and jobs to the area to service the mining and farming industries. Prospectors who were waiting for supplies from their grubstakers could arrange for deliveries at any point along the route.

A railroad timetable which was printed in the Spring of 1917 proclaimed that passengers could leave the Santa Fe Depot in Los Angeles on the eastbound Santa Fe Railroad at 8:30 PM, transfer to the T & T line at Ludlow and arrive at Death Valley Junction at 10:50 AM the next morning. From Death Valley Junction, passengers could transfer to the Death Valley Railroad and arrive in Ryan at 12:40 PM or continue on the main line through Beatty and arrive in Goldfield, Nevada at 6:00 PM. The T & T offered this service three times each week. Pullman service was also available for those traveling "first class."

Smith's Final Challenge

During the year 1913, Borax Smith began having his own financial troubles. His shares of Pacific Coast Borax Company stock were sold on the London Stock Market. With the sale of stock, he lost his controlling interest in the company. On July 17, 1914, Smith resigned. What began as an American-owned organization under the name Pacific Coast Borax Company, was now British-owned. The borax mining company and the railroad which Smith struggled to create continued to prosper. After Smith stepped down, Wash Cahill managed the T & T railroad while Richard Baker took over the affairs of PCB.

With time, Smith again entered into the borax business by



Greenwater Valley in 1916 (Cadillac is model year 1912). Bob Tubbs (left), Barney Minor (right), William Smitheram in car. © William H. Smitheram.



Death Valley Railroad, Brill car #5, a gasoline-powered, narrow-gauge passenger car, 1927. © W. H. Smitheram.

developing a colemanite deposit at the Anniversary mine in the Muddy Mountains northeast of Las Vegas, Nevada. Smith also developed borax and other products from the brines of Searles Lake at the Westend plant, operated by West End Chemical, located south of Trona in San Bernardino county, Ca. In 1928, Smith officially retired. His health was failing rapidly with complications from minor strokes. On August 27, 1931 Francis Marion Smith died. He had achieved a legendary 60-year career in the borax industry. The borax empire he created under the name Borax Consolidated, Limited and the Pacific Coast Borax Co. is still operating as Rio Tinto Corp. PLC and its subsidiary U. S. Borax Inc.

The Tecopa Railroad

In May, 1909, the Tecopa Railroad Company was incorporated in California and funded by private investments. By 1910, a railroad spur from the T & T main line at Tecopa was extended southeast to the Gunsight and Noonday mines in the Nopah Range.

The Death Valley Railroad

After ore deposits at the Lila C. were exhausted in 1914, mining operations were moved to the Bidley McCarty mine at the northwest edge of the Greenwater Range near Furnace Creek Wash on the east side of Death Valley. In January, 1914 the Death Valley Railroad (DVRR) was incorporated. New construction of the narrow-gauge DVRR began at Horton, a railroad siding halfway between Death Valley Junction and the Lila C. mine. From this point, construction continued west 17 miles to the Bidley McCarty mine. On December 1, 1914, the DVRR was formally dedicated. The new town that grew around the mine was also named "Ryan". The term "Old" Ryan was later used in reference to the abandoned site at the Lila C. mine.

Several borate mines which were operated by PCB from Ryan included the Upper Bidley McCarty, Lower Bidley McCarty, the Played Out, Grand View, Oakley and Widow Mines. The Monte Blanco Mine operated several miles northwest from Ryan.

Geologic Hazards

The T & T continued to face great challenges throughout its life. Flashfloods, flooded "dry" lakes, landslides, debris flows, erosion of the railroad bed, train

derailments and mechanical problems were all too common on the T & T. Much of this was the result of the construction, operation and maintenance of a railroad in the harsh desert environment. Many of the conditions that resulted in damage to the T & T line were directly attributed to adverse geologic factors along the route. The railroad's greatest menace was the unpredictable Amargosa River which, at times, was known to change from a dry wash into a raging torrent within minutes of a heavy downpour. The 12 mile stretch through the Amargosa Gorge was the most expensive to build and to maintain.

The Tourist Trade

For a short period of time, Borax Consolidated, Limited (BCL), the parent company of PCB, entered into the tourist business. Tourists traveling to Death Valley could ride on the T & T to Death Valley Junction and the DVRR to Ryan. Touring cars provided first-class transportation throughout Death Valley. Hotel accommodations were available at the Furnace Creek Inn, which was built by BCL and opened on February 1, 1927. Other accommodations included the remodeled Amargosa Hotel which was originally the civic center complex at Death Valley Junction. (The Amargosa Hotel building is presently the Amargosa Opera House). At Ryan, miners dormitories were converted into the Death Valley View Hotel. BCL's venture in the tourist industry was short lived.

The End of an Era

During the years 1927 and 1928, PCB began shifting its mining operations to the newly discovered Kramer borate deposit in the Mojave Desert, near the present day community of Boron in Kern County, Ca. The Kramer deposit consists of a large ore body of borax with kernite and other associated minerals. Early estimates of ore reserves at Kramer were on the order of hundreds of millions of tons of relatively high-grade borax.

The ore from the Kramer deposit was easier to mine, mill and to ship. As a mineral compound, borax hardness is lower and its solubility is higher than that of colemanite. These factors make borax a superior raw material in the mining, crushing and dissolving processes. Milling costs were far less for processing borax ore from Kramer than with the colemanite ore from the Death Valley region. In the milling process at Kramer, treating the raw borax to make refined borax required less energy than converting colemanite, a calcium borate mineral, into refined borax, a sodium borate product.



Death Valley Railroad, engine #1, 1914. © W. H. Smitheram.



Train wreck on the T & T, south of Tecopa at Acme Siding, 1915. © U.S. Borax Inc.

The Kramer deposit was adjacent to the main line of the Santa Fe Railroad, a factor that resulted in huge savings in transportation costs for shipping borax products. The new mill was also closer to energy sources such as fuel oil that often came by rail from refineries near Los Angeles and Bakersfield.

Simple economics dictated the fate of mining at Ryan. In June, 1927, all mining operations near Ryan ceased even though ore reserves were never depleted. This was the beginning of the end to the T & T. In 1931 the DVRR was officially abandoned. The T & T continued to haul supplies, equipment and ore on the main line for numerous mines and communities along the route.

In March, 1938, the T & T was severely damaged by floods from heavy rains. By December, 1938, an application to cease operations was officially registered with the Interstate Commerce Commission. On June 14, 1940, all operations on the T & T ceased. By 1942, the War Department requisitioned the line and all its scrap iron. On July 18, 1942, contractors began removing rails and associated equipment at Beatty and worked southward, using the line one last time to haul the scrap iron. Ludlow was reached on July 25, 1943, closing a final chapter to the history of this great railroad. The Nevada Short Line had lasted over 30 years, far longer than Clark's Las Vegas & Tonopah Railroad (which had been abandoned in 1918).

Remnants of the Past

You can still see traces of the T & T from Ludlow, California to Goldfield, Nevada. These features include the eroded segments of the railroad bed, concrete foundations around railroad sidings as well as bridge abutments and culverts at most major drainage crossings. The amount of erosion now visible along the old railroad bed can offer insight into the hardships encountered by the T & T during its active years.

The railroad passed by the present site of Zzyzx on the west edge of Soda (dry) Lake. The railroad siding at Soda was a short distance from what is now Zzyzx. The railroad bed can still be seen adjacent to the east edge of the property at Zzyzx.

California State Highway 127 parallels and crosses the original route of the T & T as it heads north from Baker, through Tecopa, Shoshone and beyond Death Valley Junction.

The railroad bed is also visible west of Nevada State Highway 373 and near Highway 95 from Lathrop Wells, through Beatty and on to Goldfield. Remnants of the DVRR are also present between Death Valley Junction and Ryan, along the south side of California State Highway 190.

On a calm day in the desert, some say they can still hear a train whistle along the old route!

Conclusion

The story of the Tonopah & Tidewater Railroad is only one chapter in the history of borate mining in the Death Valley region. The construction of the railroad was the direct result of Borax Smith's determination to develop a mineral deposit in a remote area of the Amargosa Desert. His biggest challenges were the geologic obstacles imposed by nature itself. The railroad enabled Pacific Coast Borax Company to overcome tremendous logistical problems

associated with the mining and milling of colemanite and the transporting of refined borax. The discovery of the Kramer borate deposit was an important geologic factor that influenced the course of mining at Ryan and resulted in the demise of the T & T. During its active years, the T & T became the lifeline for the remote mining camps and settlements along its route. It brought "civilization" and a means of income for those living near the railroad in isolated regions of the deserts of California and Nevada.

Notes

This article first appeared in "The Changing Face of the East Mojave Desert," R.E. Reynolds, ed., 1991. It has been revised and expanded for this volume.

¹ The Pacific Coast Borax Company evolved into the present day U.S. Borax Inc., a 129 year old corporation. Smith's first mining operation after establishing his new company began at Borate within Mule Canyon in the Calico Mountains of San Bernardino County.

² In 1909, Old Dinah was purchased by J. R. Lane of Calico. After repairing the boiler, Old Dinah was used to haul gold ore and freight for the Keane Wonder mine on the west edge of the Funeral Mountains of Death Valley. In November of 1909, after several months of operations, the boiler again blew out and was abandoned in Daylight Pass, a few miles northwest from the Keane Wonder Mine. In 1932, the tractor was moved to its final resting place at the main entrance to Furnace Creek Ranch in Death Valley. To this day, the ruptured steam boiler is still attached to the tractor.

³ In this area of California, southeast of Death Valley, the Garlock Fault and the mountains along this structural trend form a dividing line between the Mojave Desert to the south and the Amargosa Desert to the north.

References

- Chappell, Gordon, "By Rail to the Rim of Death Valley - Construction of the Death Valley Railroad", *Journal of the West*, January, 1992.
- Dana, James D. & Dana, Edward S., *The System of Mineralogy*, Vol. II, seventh edition, Wiley & Sons, 1966.
- Faye, Ted, *Death Valley Memories* (video), Flashpoint Films, CA, 1994.
- Faye, Ted, *The Great Desert Railroad Race* (video), Gold Creek Films, 2001.

- Faye, Ted, *The Twenty Mule Team of Death Valley* (video), Gold Creek Films, 2000.
- Gower, Harry P., *Fifty Years in Death Valley – Memoirs of a Borax Man*, Publication #9, Death Valley '49ers, 1969.
- Greene, Linda W., *Historic Resource Study - A History of Mining in Death Valley National Monument*, Vol. I, Part 2, National Park Service, 1981.
- Hildebrand, George H., *Borax Pioneer - Francis Marion Smith*, Howell-North Books, 1982.
- Lingenfelter, Richard E., *Death Valley & the Amargosa – A Land of Illusion*, University of California Press, 1986.
- Marcus, Jerry, "Rio Tinto Borax and U.S. Borax Inc. – The 20 Mule Team That Hasn't Quit", *Engineering and Mining Journal*, October, 1997.
- McAllister, J. F., "Geologic Map and Sections of the Amargosa Valley Borate Area", Map I-782, U. S. Geological Survey, 1973.
- McAllister, J. F., "Geology of the Furnace Creek Borate Area – Inyo County, California", Map Sheet 14, California Division of Mines & Geology, 1970.
- Myrick, David F., *Railroads of Nevada and Eastern California*, Vol. 2, *The Southern Roads*, Berkeley, Howell-North Books, 1962 and 1963.
- Palmer, T. S., *Place names of the Death Valley Region in California and Nevada*, 1891, reprinted by The Sagebrush Press, 1980.
- Reynolds, Robert E., "A Walk Through Borate - Rediscovering a Borax Mining Town in the Calico Hills", *San Bernardino Museum Assoc. Quarterly*, Vol. 46 #1, 1999.
- Smitheram, William H., "Memories, Minerals, Fossils and Dust - Memories of Old Borate", *San Bernardino County Museum Assoc.*, Vol. 44 #1, Winter, 1997.
- Spears, John R., *Illustrated Sketches of Death Valley and Other Borax Deserts of the Pacific Coast*, Rand, McNally & Co., 1892, reprinted by The Sagebrush Press, 1977.
- Travis, N. J. & Cocks, E. J., *The Tincal Trail – A History of Borax*, Great Britain, Pitman Press, 1984.
- Walker, Mike, *Railroad Atlas of North America – California & Nevada*, Steam Powered Publishing, 1994.

Geology and Minerals in the Area of Pisgah Volcanic Cone

Larry W. Monroe, Bureau of Land Management, 2601 Barstow Road, Barstow CA 92312

And Moses went up from the plains of Moab unto the mountains of Nebo to the top of Pisgah ... (Deuteronomy 34:1)

Although the California version of Pisgah is not in the mountains of Nebo it is not far east of the Nebo occupied by the Marine Corps Logistics Base. Some 32 miles east of Barstow, just south of Highway I-40, Pisgah cone and associated flows have long been used by various universities as a geology field study area. The excellent preservation of the cone and lava flows allow students to enhance their classroom studies by actually observing the details of the volcanic cone, lava tubes, and both aa (ah ah) and pahoehoe (ropey) lava flows.

Pisgah represents a series of magmatic events that occurred during the Pleistocene epoch which includes Amboy, Pipkin and some of the cones at Cima. The Pisgah lava field extends northwest from the volcanic center eleven miles onto Troy Dry Lake (playa) and six miles south onto Lavic Dry Lake. A rather broad range of proposed dates have been published for the age of Pisgah and only recently (April 2000) has a reliable

date been determined. The U. S. Geological Survey using argon dating (⁴⁰Ar/³⁹Ar) established an age of 24,000 ± 4,000 years before present (ybp). This radiometric dating was from samples recovered from the cone. Paleomagnetic data from samples of several of the basalt flows confirmed this date (23,000 ybp ± 3,000)(Champion, 2000).

Wise (1969) studied the lava fields associated with this cone, identifying five flow units with three distinct relative ages. These flows emanated from different vents around the existing cone which represents a late stage of this volcanic activity. Wise defined these lavas as basanite (not to be confused with the basanite mineral produced at the Mountain Pass mine) and alkali-olivine basalts. The mineralogy of each successive flow contained more silica and less potassium than the preceding flow.

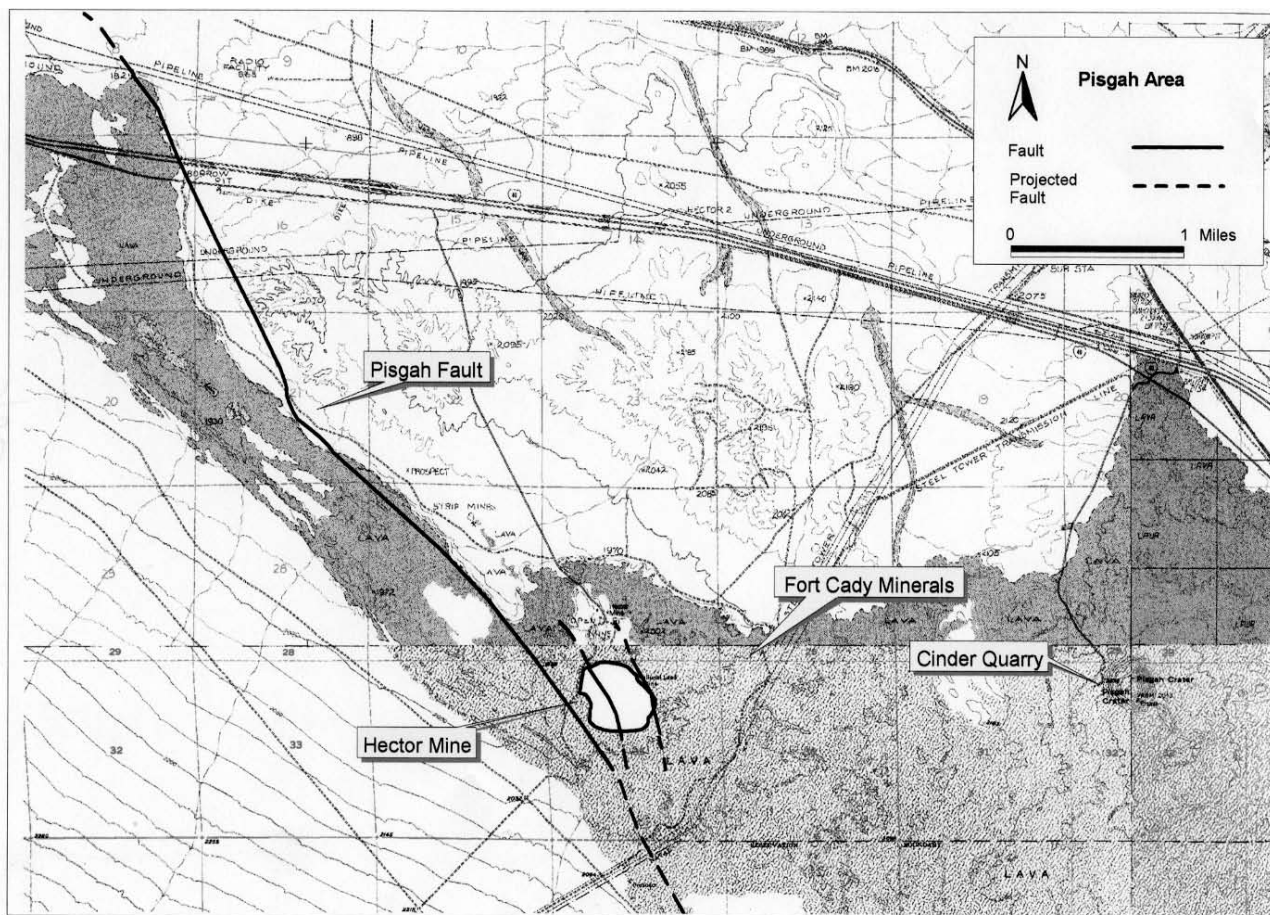


Figure 1

L.W. Monroe
Jan. 2002

U.S.G.S. Hector and Sunshine Peak
7.5' Quadrangles

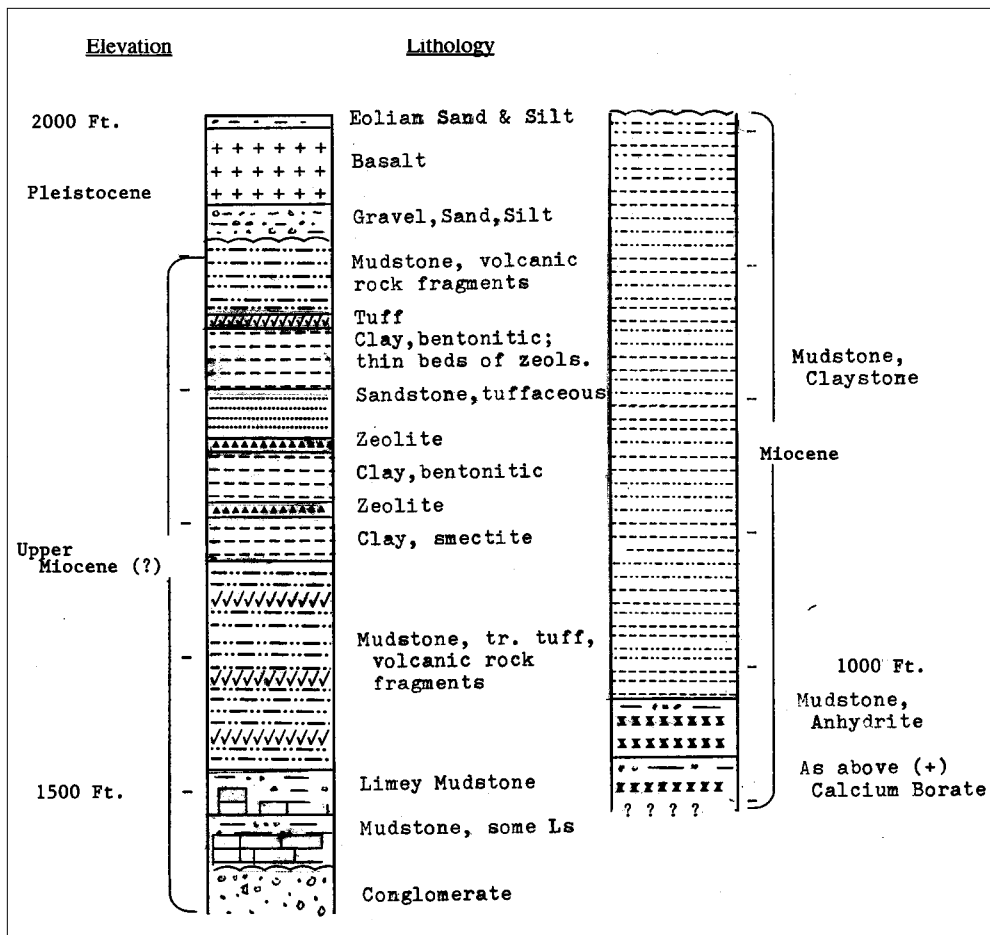


Figure 2. Generalized stratigraphic section, Pisgah area.

The mineralogy at Pisgah was also studied by Glazner et al. (1991) and Smith and Carmichael (1969). These authors established that this is an alkali and iron rich basalt poor in silica and impoverished in the rare earths when compared to other alkaline basalts.

The Mojave Desert is incised by a series of northwest trending strike-slip faults, some of which are evident in the area of Pisgah, the most prominent being the Pisgah fault (Fig. 1). The surface expression of this fault, represented by intermittent mounds and ridges of basalt about eight feet in height, can be seen along National Trails Highway (Old Route 66) 1.3 miles west of the Hector off-ramp. Mapped by Dibblee and others as right-lateral, this surface expression also shows a vertical component with the east block up-thrown. Exploration drilling by several mining companies has found over 700 feet of vertical displacement. The October 16, 1999 Hector Mine quake (7.1) reactivated a strand of this fault at the Hector Mine (Willette, 1999). There was also extensive fracturing of the ground surface east of the main fault near the mine during the 1992 Landers quake (7.3) (Willette, 1997).

Dibblee (1966) also mapped several parallel faults northwest of the Pisgah cone. In addition to movement reported along these mapped faults during the Hector Mine quake, fracturing was noted by the author on an unmapped fault in the cinder quarry at the west base of the Pisgah cone; vertical displacement was 2.5 inches (7 cm) with the down-thrown block on the west. Slope failure on the south and west flanks of the cone were also noted after this event.

Drilling in the area has encountered over 1000 feet of basin sediments including fine-grained clastics, tuffs and evaporites. At the base of the stratigraphic column (Fig. 2), there is an interval of mudstones and evaporites, laminated anhydrite, celestite, calcium gypsum, and howlite along with thin bedded tuffs. Within this section is the calcium borate, colemanite. These deposits have been assigned a Miocene age by several investigators and are commensurate with the Miocene borates found throughout the Mojave Desert. Above this interval is a 300–400 foot section of mudstones and claystones. Based on geophysical logs, they occur as alternating beds approximately 10–15 feet in thickness.

Sweet (1980) proposed a Pliocene date for an andesite (not shown on Fig. 2) and associated weathered conglomerate just above the Miocene lacustrine sediments. Based on work

by Jefferson (1985), Glazner (1980), and Stinson (1988) as well as others, I show this conglomerate and overlying sediments as Upper Miocene (?). The section above the conglomerate is dominated by mudstones and brown, bentonitic clays, with hectorite clay locally at the Hector Mine. The hectorite, a magnesium, lithium smectite, is associated with a north trending travertine ridge (Sweet, 1980 and Willette, 1995¹). These authors have proposed the origin of hectorite as alteration of lake bed tuffs by hydrothermal activity, and high magnesium-rich lake waters within a lagoon of a shallow lake. The travertine ridge is evidence of a buildup of calcium carbonate from nearby hot springs. Within these sediments are numerous thin beds of tuffs not greater than two feet (60 cm) in thickness. Some of these bedded tuffs at the Hector Mine have been altered to zeolite (an alteration of tuff deposited in alkaline lake waters).

Mining in the area has occurred at least since the 1930s when a bentonite clay was discovered. Initially established as an underground mine, the clay was sold to the drilling industry. At that time it was recognized that there was also an unusual clay present and this white, waxy, smectite clay, later assigned the name hectorite, was hand-cobbed. After a consolidation of leases and mining claims, open pit mining began in 1944 and the underground operations were abandoned in the 1960s. Current mining consists of blasting roughly 40 feet of basalt overburden and stripping 60 feet of gravels and clays (Fig. 2) to reach the ore body. Hectorite is selectively mined and processed separately from the more common clays. It is utilized in numerous products, such as paints, paper and cosmetics.

The adjacent Fort Cady Minerals Corporation operation is significant from several aspects. They have developed an in-situ extraction method for the recovery of calcium borate (colemanite) from depths of over 1200 feet. In this process a solution is injected into the formation, dissolving the borate which is then brought to the surface through extraction wells. Among numerous uses for borates are manufacture of glass, cleaning compounds, and gasoline additives.

On the flanks of the cone, cinders were mined for use as railroad ballast. This mine has been inactive for a number of years but structures and the processing machinery are still in place.

Conclusions

The association of borates in Miocene basin sediments throughout the Mojave Desert, the presence of Pleistocene Lake Manix and the now-dated Pisgah volcanic cone show that this area has been a depositional basin at least since the Miocene time.

Acknowledgments

I thank Robert E. Reynolds for reviewing the manuscript, and Shelly Jackson for assistance in drafting Figure 1.

Notes

Appreciation is expressed to Elementis (Rheox), Inc. and Fort Cady Minerals, Inc. for permission to publish some data from their exploration and mining operations.

¹For a detailed description of the Hector Mine deposits see Willette, 1995.

References

- Champion, Duane, U.S. Geological Survey, personal communication April, 2000.
- Dibblee, T.W. Jr. and Bassett, A.M., 1966, Geologic Map of the Cady Mountains Quadrangle, San Bernardino County, Calif., U.S. Geological Survey, Miscellaneous Geologic Investigations Map I-467.
- _____, 1966, Geologic Map of the Lavic Quadrangle, San Bernardino County, Calif. U.S. Geological Survey, Miscellaneous Geologic Investigations Map I-472.
- Hart, Earl W., 1987, Pisgah, Bullion, and Related Faults San Bernardino County, California, Calif. Div. of Mines and Geology, Fault Evaluation Report FER-188.
- Glazner, Allen F., Farmer, G.L., Hughes, W.T., Wooden, J.L., and Pickthorn, W., 1991, Contamination of Basaltic Magma by Mafic Crust at Amboy and Pisgah Craters, Mojave Desert California, *Journal of Geophysical Research*, v. 96, No. 88, pp. 13,673-691.
- _____, 1980, Geology of the Sleeping Beauty Area, Southeastern Cady Mountains, in *Geology and Mineral Wealth of the California Desert*, Fife D.L. and Brown, A.R. eds., South Coast Geological Soc., pp.249-255.
- Jefferson, George T., 1985, Stratigraphy and Geologic History of the Pleistocene Lake Manix Formation, Central Mojave Desert, California, in *Geologic Investigations Along Interstate 15 Cajon Pass to Manix Lake, California*, Robert E. Reynolds ed. pp 157-165.
- Smith, A.L. and Carmichael, I.S.E., Quaternary Trachybasalts From Southeastern California, *The American Mineralogist*, v. 54, May-June 1969, pp. 909-923.
- Stinson, Melvin C., 1988, Zeolites in California, Calif. Div. of Mines and Geology Bulletin 208.
- Sweet, W.E. Jr., 1980, The Geology and Genesis of Hectorite, Hector California, in *Geology and Mineral Wealth of the Calif. Desert*, Fife, D.L. and Brown, A.R., eds., South Coast Geological Soc., pp 279-283.
- Willette, Richard, 1995, Geology of the Hector Mine Deposit in Tabillo, M. and Dupras, D.L. eds., 29th Forum on the Geol. of Industrial Minerals: Proceedings; Calif. Dept. of Conservation, Div. of Mines and Geology, Special Pub. 110, pp 189-194.
- _____, 1997 and 1999, Hector Mine superintendent, personal communication.
- Wise, W.S., 1969, Origin of Basaltic Magmas in the Mojave Desert Area, California, *Contribution to Mineralogy and Petrology*, v.23, pp. 53-64.

The Sulfur Hole, Calico District, San Bernardino County, California

Joseph F. Cooper, Jr., 430 Van Ness Avenue, Santa Cruz, California 95060; **Gail E. Dunning**, 773 Durshire Way, Sunnyvale, California 94087-4709; **Ted A. Hadley**, 907 Anaconda Way, Sunnyvale, California 94087-3053; **William P. Moller**, 627 Grove Lane, Santa Barbara, California 93105; **Robert E. Reynolds**, LSA Associates, Riverside, California 92507

Discovered by local borax miners in the 1880s as a possible source of agricultural sulfur, the Sulfur Hole has produced an attractive suite of well-crystallized, colorful hydrous sulfates including coquimbite, halotrichite, krausite, metavoltine, potassium alum, quenstedtite, römerite and voltaite. Associated minerals include botryogen, copiapite, anhydrite, gypsum, melanterite, marcasite, and sulfur.

Introduction

The Sulfur Hole has long been known by California collectors as a source of rare hydrous iron-potassium-aluminum sulfate minerals. These minerals occur in a columnar pipe within a fault zone that precipitated iron-bearing acidic sulfate fluids in a reducing carbonate-poor environment. Fine crystallized specimens of coquimbite, krausite, metavoltine, quenstedtite and voltaite have been collected here and the potassium iron sulfate krausite was first described as a new mineral from this locality. Potassium alum, also new to this locality, has been recently found as small brilliant octahedral crystals.

While the Sulfur Hole locality is well known to collectors, its remote location and lack of identifying landmarks have hindered study. The site is located on the south wall of Mule Canyon in a shallow unobtrusive cleft with only a faint trail leading to it. The area is north of the old borax claims near the site of Borate in the Calico Hills and about 4 miles northeast of the town of Yermo, San Bernardino County, SE $\frac{1}{4}$ of SE $\frac{1}{4}$ of Section 18, T. 10N, R. 2E, San Bernardino Base and Meridian (34° 57' N, 116° 49' W). The cleft containing the Sulfur Hole is not readily apparent and the sulfates are not normally exposed at the surface to mark the locality. To collect requires digging down to the sulfate body through accumulated debris.

Area History

The first mining interest in the area began in the 1860s with the discovery of rich silver ores in the Calico hills. Calico quickly became a major silver producer and remained so for over 20 years. As the silver rush faded and the mines went into decline, prospectors searched the nearby lower hills for other profitable mineral deposits.

The colemanite deposits at Borate in the Calico Hills were discovered in 1883, and while these deposits were neither as large or as rich as the famed Death Valley borax deposits, they were able to successfully compete with them because of the primitive transportation system from Death Valley. Because of their proximity to the railroad shipping point at Dagget, the colemanite ores of Borate could be profitably worked. When the railroad reached Death Valley, the colemanite ores at Borate became marginal and, as the easily mined ore had been removed, production at Borate declined.

After the end of World War I, interest in the area was rekindled and William F. Foshag of the

National Museum examined the area as part of his study of the colemanite deposits of California. The borax deposits were worked by local prospectors who told Foshag of the "Sulfur Hole" nearby. Foshag visited the locality and described the unusual mineralogy of the area, including the new potassium iron sulfate, krausite (Foshag, 1931).

Geology

The Calico Mountains are a rugged landscape of steep slopes supporting sparse vegetation with volcanic flows creating bold outcrops of hard, resistant material. They are composed of a series of Miocene sedimentary beds that are underlain by andesites and rhyolite tuffs. These sedimentary rocks have been entirely removed in the western portion of the area and the exposed multicolored volcanic rocks gave the district its name, Calico, after the multicolored fabric. The eastern portion of the district is covered by remnants of the sediments that are composed of a series of sandstones, shales, marls and algal limestones that rest on the basement volcanic rocks. These sediments were originally deposited in a fresh water lake environment.

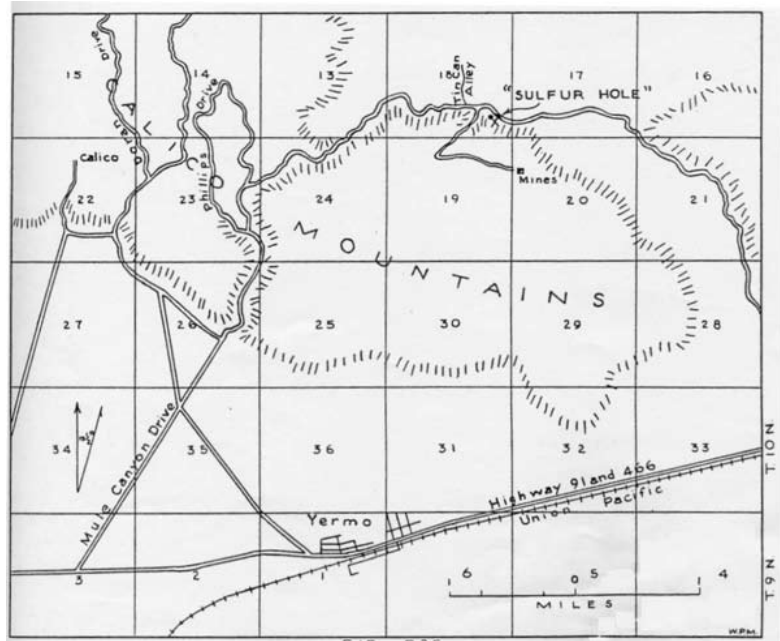


Figure 1. Map showing the location of the Sulfur Hole in the Calico Mountains, San Bernardino County, California. (After Moller, 1963a).

Deposits formed containing nodules of colemanite associated with ulexite, celestite and strontianite. Lower in the series the sediments have been partially silicified and a series of chert and shale beds have been produced. The difference in metamorphism is apparently due to the porosity of the individual beds. Foshag (1922) found no apparent connection between the lower, more silicic beds and the upper borate-bearing limestones and marls. The relationship between the deposition of the sulfates in the shales and the colemanite bodies found in the marly limestones is not known.

The volcanic, volcanoclastic to sedimentary series in the Calico Mountains has been discussed in detail (Dibblee 1970, Erwin and Gardner 1940, McCulloh 1965). Recent work (Reynolds and Woodburne 2001) indicates that the deposition sequence included a massive stromatolite layer, three brown, platy limestones, and a persistent bed of borax and strontium minerals. The section at Borate correlates to the section in the Mud Hills which corresponds to 17–16 Ma, with the borate and strontium minerals being no younger than 15.5 Ma. The section at Borate is overlain by gravity slides of siliceous andesitic breccia that dates to 17 Ma (B. Wilson pers. comm. to RER, 2001). Fossils in the sedimentary section of the Calico Mountains also suggest an earlier Barstovian Land Mammal Age (LMA) from the early middle Miocene. A large three-toed horse, “*Merychippus*,” is present (Dibblee 1970) and tracks of early proboscideans, restricted to younger than 16.3 Ma in western North America, have been found in Little Borate Canyon (Reynolds and Woodburne 2001).

Resting conformably upon the agglomerates are arkosic sandstone, argillaceous shales and hard, banded cherts. They are particularly apparent at the Sulfur Hole where the rocks surrounding the zone of sulfate deposition are chert members. Immediately above the chert are beds of dense arkosic sandstone and shale overlain by light yellow tuff and a little thinly bedded shale.

The Miocene sediments with silica and borates have been folded compressively along a west-northwest axis. This compression folding took place in response to rising andesite domes in the northern Calico Mountains and in response to gravity slide deposits that slid southward over the unconformity on top of the compressed Miocene sediments.

Ground water percolation that produced the various sulfate minerals has been controlled along two local fracture zones. The initial movement was along a fracture zone perpendicular to the strike of the sediments and vertical to the bedding planes. The surface exposure of this fault is partially covered, but it may be observed approximately 70 meters east of the Sulfur Hole, where bedding changes abruptly from nearly perpendicular, as exhibited at the hole, to approximately horizontal with only a moderate dip southward. The second generation of deformation was a fault parallel to the bedding planes that produced a vertical displacement of unknown magnitude. Small fracture zones and drag folds may be observed in the vicinity of the Sulfur Hole.

The sulfates at the Sulfur Hole were formed as a result of low temperature aqueous acidic sulfate-bearing solutions that percolated through the hot volcanic rocks and attacked existing iron sulfides. These solutions were rich in ferrous and ferric iron and also contained leached magnesium, potassium, sodium and aluminum from the underlying rock formations. The existing fault produced a fracture system that allowed the upward migration of these heated, highly acidic iron-rich solutions.

Changes in temperature, pressure and pH allowed the formation of the various sulfate minerals.

Description of the Sulfur Hole

The sulfates occur in pod-like masses up to several meters across in area of fractured shale that is cemented by white granular coquimbite. It is interesting to note that the sulfates in this deposit show a zoning pattern and that the material the authors found show a similar pattern to that mentioned by Foshag (1931) in his original paper.

Foshag estimated the original thickness of the exposed sulfates to be less than 3 meters and noted that the minerals were roughly zoned, with massive coquimbite occupying the footwall and grading into sugary granular coquimbite, while the hanging wall was composed of a mixed group of iron sulfates that became more acidic as the bottom edge of the deposit was neared.

The major portion of the sulfate mass is composed of granular white coquimbite and this may make up to half of the pod volume. The coquimbite varies in texture from a dense white fine-grained material near the footwall that grades into a more coarse grained sugary material near the center of the pod. The fine-grained coquimbite frequently shows shrinkage cracks and these are often lined with yellow-green to gray-green krausite crystals associated with occasional patches of golden yellow metavoltine.

The most interesting of these zones for the collector was the transition zone between the coquimbite and acid iron sulfate zone where colorful well-crystallized specimens typically occurred. This transition zone varied considerably in thickness and was entirely absent in some areas. Specimens commonly were contained in a base of granular sugary-white coquimbite that often contained large crystals of purple coquimbite, green krausite, reddish-brown römerite, golden yellow metavoltine and white fibrous halotrichite. Many of the rarer minerals were formed in this zone in cavities between the römerite and coquimbite crystals.

The acid iron sulfate zone near the footwall was also variable in thickness and was composed mainly of a mixture of melanterite, halotrichite, voltaite and römerite. The most abundant mineral in this zone is römerite and granular friable masses of rough römerite crystals over 10 cm thick were found. Melanterite and halotrichite veinlets commonly cut these römerite masses and occurred as white to pale green fibrous veinlets.

Table 1. Minerals from the Sulfur Hole, San Bernardino County, California

Anhydrite	CaSO_4
Botryogen	$\text{MgFe}(\text{SO}_4)_2(\text{OH})\cdot 7\text{H}_2\text{O}$
Copiapite	$\text{FeFe}_4(\text{SO}_4)_6(\text{OH})_2\cdot 20\text{H}_2\text{O}$
Coquimbite	$\text{Fe}_2(\text{SO}_4)_3\cdot 9\text{H}_2\text{O}$
Gypsum	$\text{CaSO}_4\cdot 2\text{H}_2\text{O}$
Halotrichite	$\text{FeAl}_{12}(\text{SO}_4)_4\cdot 22\text{H}_2\text{O}$
Krausite	$\text{KFe}(\text{SO}_4)_2\cdot \text{H}_2\text{O}$
Marcasite	FeS_2
Melanterite	$\text{FeSO}_4\cdot 7\text{H}_2\text{O}$
Metavoltine	$\text{K}_2\text{Na}_6\text{FeFe}_6(\text{SO}_4)_{12}\cdot 18\text{H}_2\text{O}$
Potassium Alum	$\text{KAl}(\text{SO}_4)_2\cdot 12\text{H}_2\text{O}$
Quenstadtite	$\text{Fe}_2(\text{SO}_4)_3\cdot 10\text{H}_2\text{O}$
Römerite	$\text{FeFe}_2(\text{SO}_4)_4\cdot 14\text{H}_2\text{O}$
Sulfur	S
Voltaite	$\text{K}_2\text{Fe}_3\text{Fe}_4(\text{SO}_4)_{12}\cdot 18\text{H}_2\text{O}$

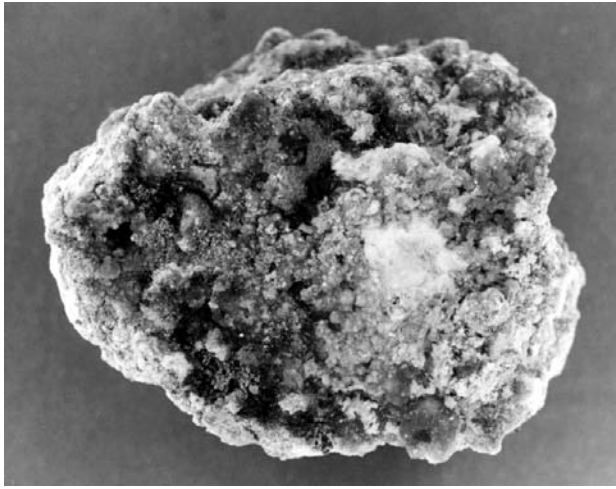


Figure 2. Hand sample, 5 x 7 cm, from the transition zone showing typical sulfate assemblage (purple coquimbite, brown römerite, gray-green krausite, and sugary-white coquimbite).

Pockets were not common in this zone but voids occurred in the coarsely crystalline römerite. They often contained other acid sulfates and voltaite occurred in this area both as massive material and well-crystallized masses of black cubic crystals.

At the base of the acid sulfate zone a thin discontinuous layer of loose friable sandy shale fragments was found. It was impossible to determine the extent of this layer but its absence of fines indicated that it was extremely porous. Sulfates were rare in this layer and composed mainly of minute feathery crystalline aggregates of melanterite and gypsum. Embedded in this layer were small masses of potash alum. Much of this material was massive but occasional pockets showed well-formed brilliant octahedral crystals.

Minerals

Alunite(?) $K_2Al_6(SO_4)_4(OH)_{12}$

Alunite was reported by Foshag (1922) as being relatively abundant at the Sulfur Hole, occurring as white granular masses near the hanging wall. Material resembling that described by Foshag was collected by the senior authors and was found to contain only iron and sulfate. A microscopic examination revealed only granular aggregates composed of minute bipyramidal crystals of coquimbite. Alunite was not found during the present study. XRD of samples previously reported to be alunite by Moller (1963a,b) proved to be coquimbite. To date no alunite has been identified from any samples collected at the Sulfur Hole.

Anhydrite $CaSO_4$

Foshag (1931) reported anhydrite associated with gypsum in the upper section of the Sulfur Hole. It probably formed as a dehydration product of gypsum.

Botryogen $MgFe^{3+}(SO_4)_2(OH) \cdot 7H_2O$

Rare brick-red minute botryoidal groups of botryogen occur on top of sugary coquimbite. Only a few samples were found to contain botryogen and it is probably the least abundant mineral present. It was identified by its color, radiating structure and EDS spectrum.

Copiapite $Fe^{2+}Fe^{3+}_4(SO_4)_6(OH)_2 \cdot 20H_2O$

Copiapite occurs in the aureole surrounding the sulfate body and is locally abundant within the sulfate mass. It is a yellowish-green to yellow brown color and occurs as small patches in cavities of the coquimbite in the transition zone and is often as-

sociated with römerite. Copiapite is commonly associated with seams of gypsum and occurs as thin yellow coatings on it.

Coquimbite $Fe^{2+}Fe^{3+}_4(SO_4)_3 \cdot 9H_2O$

Coquimbite is the most abundant mineral present in the Sulfur Hole and probably makes up almost eighty percent of the sulfates present. It forms the major portion of the vein filling material and occurs as colorless to pale lilac granular masses up to a foot thick. Microscopic examination of this granular material reveals it is composed principally of minute colorless bipyramidal crystals associated with scattered small anhedral masses of coquimbite. The most common crystal forms present are the pyramidal form $\{1011\}$ associated with a secondary prism $\{1010\}$ face. The crystals occasionally show the development of $\{0001\}$ and $\{1120\}$ faces but these are not common.

Near the transition zone larger coquimbite crystals start to occur and purple masses of equant crystals up to 2 cm across are relatively common. Most of the larger crystals are blocky in outline but occasional crystals that show the typical hexagonal bipyramid are also found. Although the larger crystals often show a blocky form and resemble overgrowths, paracoquimbite has not been identified from the site. Specimens of sulfate rock from the transition zone can be quite attractive and colorful

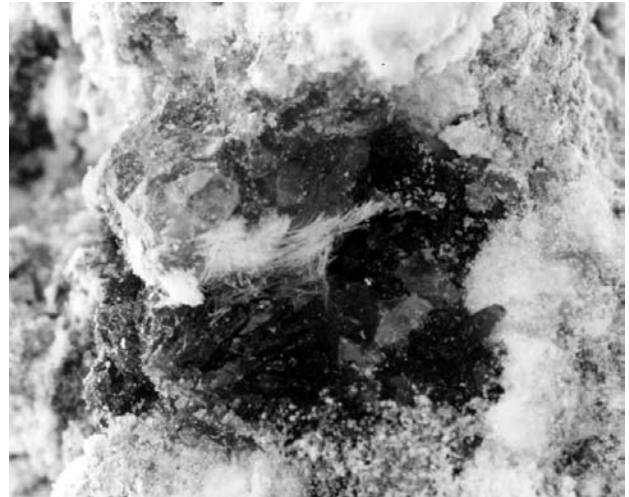


Figure 3. Purple coquimbite crystals associated with halotrichite (acicular white), römerite (dark brown) embedded in sugary-white coquimbite. 2 cm.



Figure 4. Typical blocky purple coquimbite crystals, to 6.8 mm, associated with brown römerite in fine-grained coquimbite.



Figure 5. Bipyramidal coquimbite crystal associated with krausite on massive coquimbite. 1.7 mm.

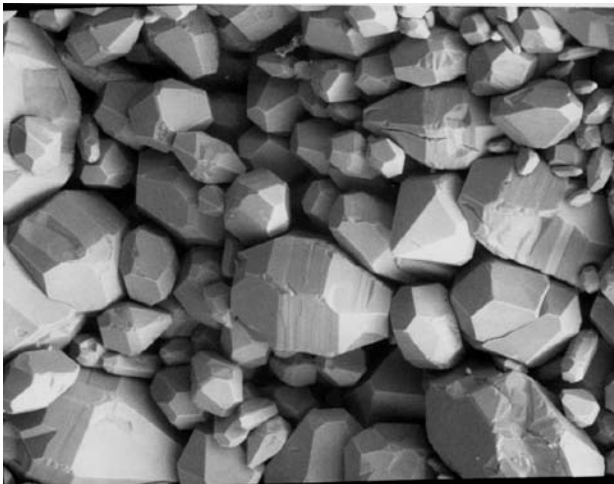


Figure 6. SEM photo of sugary-white coquimbite showing the bipyramidal habit of the individual crystals. 10 – 100 microns.

with the large purple coquimbite crystals, bright yellow metavoltine, green krausite crystals and red brown römerite crystals embedded in a white granular coquimbite groundmass.

Fibroferrite(?) $\text{Fe}^{3+}(\text{SO}_4)(\text{OH}) \cdot 5\text{H}_2\text{O}$

Fibroferrite was reported as occurring at the locality by Foshag (1922). The fibroferrite reported by Moller (1963a) was re-examined by XRD and found to be halotrichite admixed with copiapite. To date no fibroferrite has been identified from the samples collected at the Sulfur Hole.

Gypsum $\text{CaSO}_4 \cdot 2\text{H}_2\text{O}$

Gypsum occurs as isolated masses and veins of satin spar gypsum in the edge of the high iron sulfate zone near the footwall associated with copiapite. The gypsum is colorless to white, fibrous and can be up to 3 cm thick. They are often encrusted by massive yellow copiapite and fracture faces are often corroded. The gypsum shows a pale yellow fluorescence and often shows a yellow phosphorescence under short wave ultraviolet light.

Halotrichite $\text{Fe}^{2+}\text{Al}_2(\text{SO}_4)_4 \cdot 22\text{H}_2\text{O}$

Halotrichite is relatively common in the more acid rock near the footwall where it forms white fibrous veins associated with melanterite. The veins cut coarsely crystalline granular masses

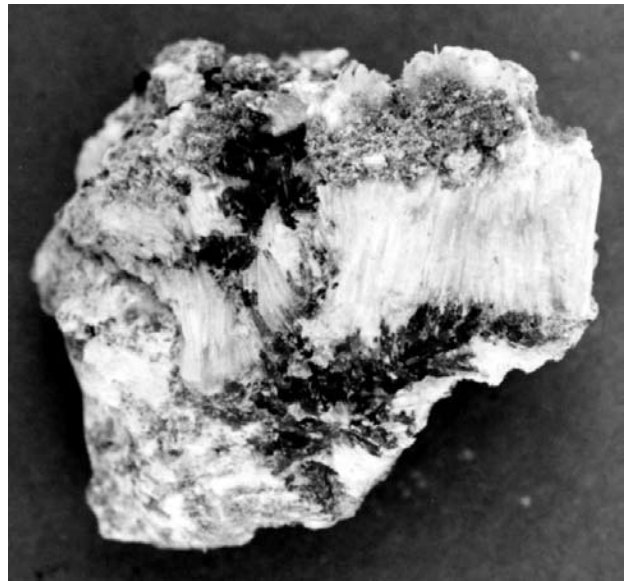


Figure 7. Sample of sulfates to 5 cm showing fibrous halotrichite vein with brown römerite .

of römerite and are commonly intergrown with melanterite. Occasionally it is found as delicate tufts of acicular crystals in cavities associated with römerite and voltaite crystals. Halotrichite veins often grade into massive apple green melanterite and intergrowths of fibrous halotrichite and melanterite are occasionally found.

Jarosite(?) $\text{K}_2\text{Fe}_6(\text{SO}_4)_4(\text{OH})_{12}$

Jarosite was reported by Foshag (1922) at the Sulfur Hole occurring as yellow coatings of minute crystals. Material resembling that described by Foshag was collected by the authors and was found to contain iron, potassium and sulfate and a microscopic examination revealed minute yellow crystals of metavoltine. To date no jarosite has been identified from the samples collected at the Sulfur Hole.

Krausite $\text{KFe}^{3+}(\text{SO}_4)_2 \cdot \text{H}_2\text{O}$

Krausite is relatively abundant in the transition zone and

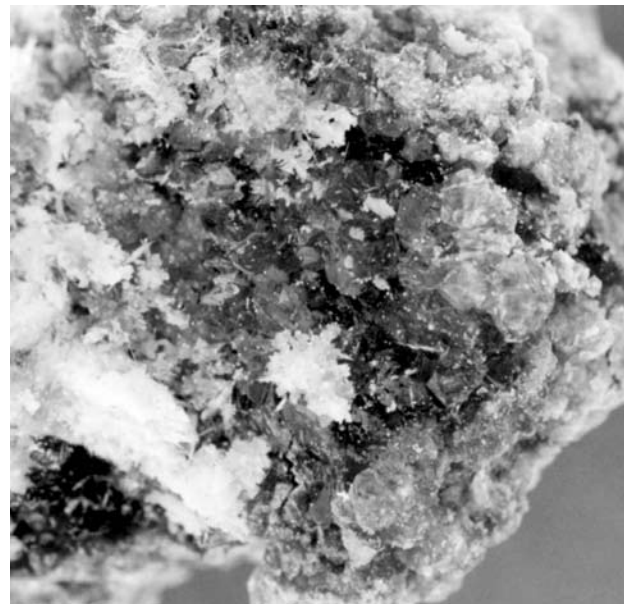


Figure 8. Sample showing dark green krausite crystals to 4 cm (center) surrounded by purple coquimbite, golden metavoltine, white acicular halotrichite on fine-grained coquimbite.

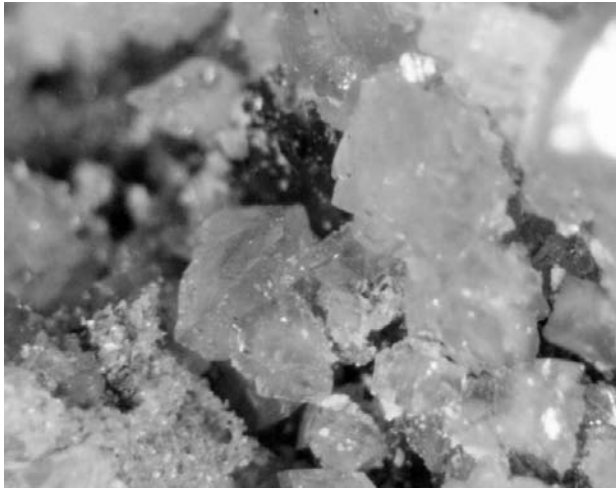


Figure 9. Blocky kausite crystals to 8.4 mm associated with golden metavoltine.

in the granular coquimbite near it. It occurs as groups of pale green to yellow green short equant crystals in shrinkage cracks and discrete masses embayed by coquimbite. It often covers areas as much as several cm across and almost always occurs as small monoclinic crystals with the terminating faces showing giving it an almost octagonal shape. In the transition zone crystals may be associated with lilac coquimbite and reddish brown römerite. The largest crystals of this mineral occur in the transition zone and single crystals of kausite up to 7 mm across have been found embedded in granular white coquimbite. The larger crystal faces are not brilliant as the smaller crystals and often appear to have been etched. This is the type locality for kausite described by Foshag (1931).

Marcasite FeS_2

Marcasite has been noted as small patches and grains on the rock that encloses the sulfate mass near the footwall. It generally shows a greenish-yellow color and a botryoidal surface. No marcasite has been noted in the sulfate mass and only a few specimens were found.

Melanterite $\text{FeSO}_4 \cdot 7\text{H}_2\text{O}$

Melanterite is only found in the mass of acidic iron sulfates that formed near the footwall. Melanterite occurs as small irregular grains and as veins of fibrous crystals that range in color from light green to white and is commonly intergrown with halotrichite. The green color disappears as the specimens dehydrate. Veins of fibrous melanterite up to 1 cm thick and a meter long have been found cutting the römerite and voltaite and were presumably among the last minerals to form.

Metavoltine $\text{K}_2\text{Na}_6\text{Fe}^{2+}\text{Fe}^{3+}_6(\text{SO}_4)_{12}\text{O}_2 \cdot 18\text{H}_2\text{O}$

Metavoltine is locally abundant at the Sulfur Hole and has been found as areas of scale-like bright golden yellow crystals that have the (010) form dominant. This material is most abundant in thin shrinkage cracks in the granular coquimbite and is most abundant near the upper portion of the coquimbite body in the more fine-grained material. While kausite is often closely associated with the metavoltine, the shrinkage cracks containing metavoltine generally show only this mineral and it is presumed to have been one of the last minerals to form.

Potassium Alum $\text{KAl}(\text{SO}_4)_2 \cdot 12\text{H}_2\text{O}$

Potassium alum was noted as occurring in a thin black, extremely porous friable layer at the base of the footwall of the Sulfur Hole. A few small rounded nodules that contained small cavities lined with brilliant octahedral crystals were found. This



Figure 10. Hand sample, 7 x 9 cm, showing golden metavoltine vein in fine-grained coquimbite.

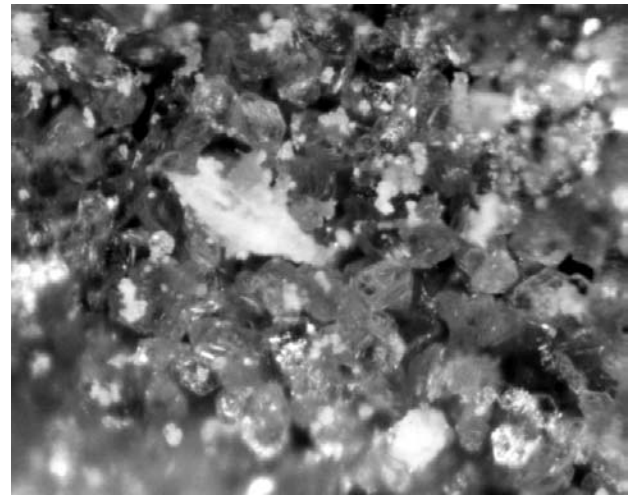


Figure 11. Metavoltine crystals showing hexagonal outline. Field of view 1.5 mm.



Figure 12. SEM photo of metavoltine crystals to 50 microns showing the stacked hexagonal plates.

material proved to be a potassium aluminum sulfate with only minute amounts of iron present. Potassium alum has not been previously reported from this locality.

Quenstadtite $\text{Fe}^{3+}_2(\text{SO}_4)_3 \cdot 10\text{H}_2\text{O}$

Quenstadtite was first identified from the Sulfur Hole by Weber and Graal (1975) and must be considered one of the

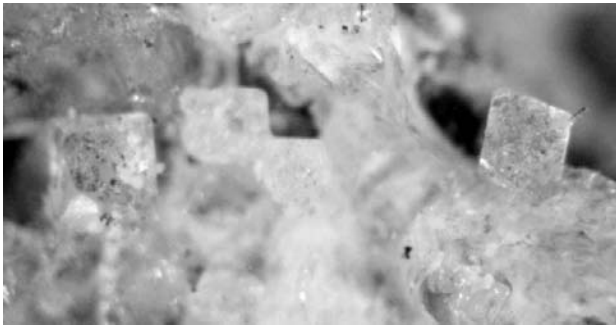


Figure 13. Clear octahedrons of potassium alum. Field of view 4 mm.

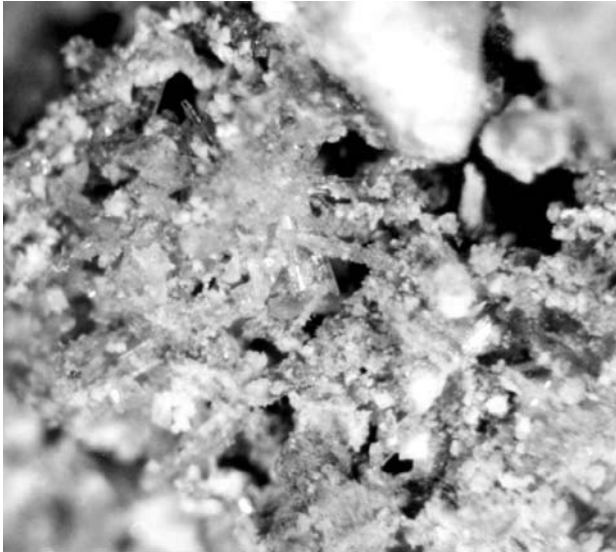


Figure 14. Typical surface showing clear to light pink, jack-straw crystals of quenstedtite. Width 4 mm.

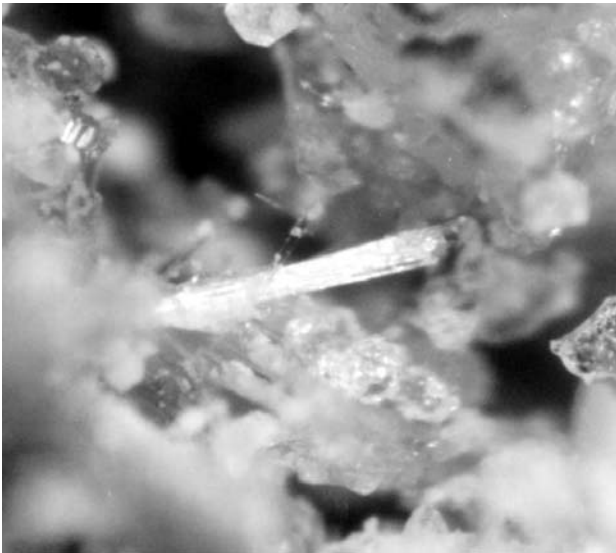


Figure 15. Enlargement of Figure 14 showing the acicular habit of quenstedtite associated with golden metavoltine and clear, blocky krausite. Crystal length 0.5 mm.

rarest of the minerals found here. It has been found only on the acid sulfates deposited near the footwall. Quenstadtite occurs as jackstraw groups of minute colorless to pale pink triclinic crystals and usually occurs as monomineralic groups of crystals in cavities of römerite.

Römerite $\text{Fe}^{2+}\text{Fe}^{3+}_2(\text{SO}_4)_4 \cdot 14\text{H}_2\text{O}$

Römerite is relatively abundant in the area of the footwall and large masses of friable reddish brown crystals can be found. The römerite is often cut by veins of green melanterite and white fibrous halotrichite that contains small cubic crystals of black voltaite. Römerite rarely forms good crystals but is most often found as granular masses of elongate anhedral crystals.

Sulfur S

Sulfur is not common in the mineral assemblage at the Sulfur Hole and occurs as thin pale yellow crusts associated with white granular coquimbite and krausite. It appears to have been one of the last minerals formed and is known from a few specimens. It occurs as pale yellow granular masses coating other sulfate minerals.

Voltaite $\text{K}_2\text{Fe}^{2+}_5\text{Fe}^{3+}_4(\text{SO}_4)_{12} \cdot 18\text{H}_2\text{O}$

Voltaite is relatively common close to the footwall of the Sulfur Hole where more acidic conditions exist. It often occurs in association with römerite and melanterite as black patches and well-formed cubic crystals. These crystals may reach 5 mm across and normally are brilliant cubes with no modifying faces. The römerite–melanterite–voltaite sulfate complex is the least stable of the sulfate assemblages and often forms a crumbly mass. It is interesting to note that the cube is the dominant

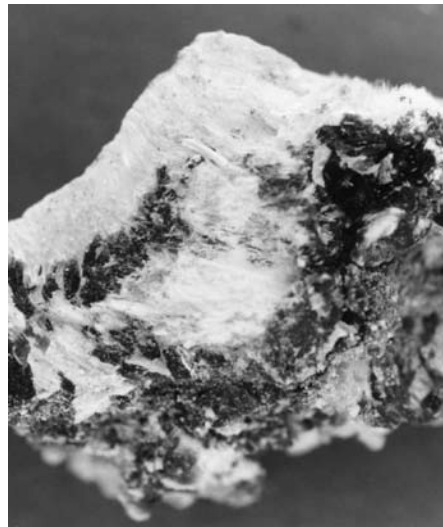


Figure 16. Sample of dark brown römerite associated with white fibrous halotrichite. Width 3 cm.

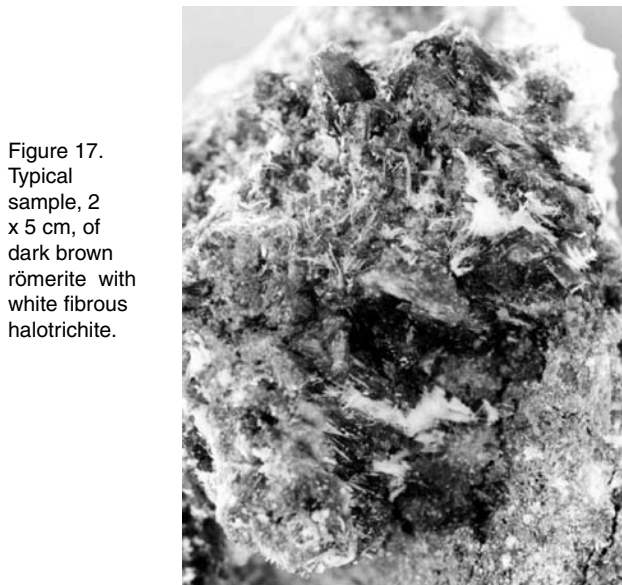


Figure 17. Typical sample, 2 x 5 cm, of dark brown römerite with white fibrous halotrichite.

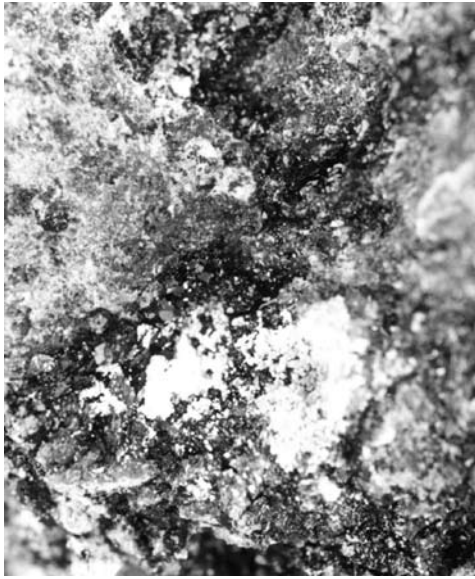


Figure 18. Typical specimen of voltaite showing black cubic outline associated with brown r merite and halotrichite. Width 1 cm.



Figure 20. Camp scene at the Sulfur Hole on November 25, 1961, showing the collecting locality at the dark area in the center of the photo.

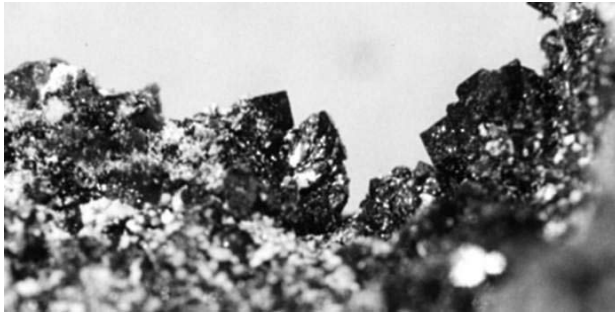


Figure 19. Voltaite specimen showing 2 mm cubic crystal outline (center top) associated with brown r merite (left).

form at this locality while the octahedron often forms in acid sulfate assemblages from post mine sulfate deposition.

Collecting

At present no restrictions are placed on entry to the area and it appears to be under the control of the Bureau of Land Management. Collecting at the Sulfur Hole is mainly a question of finding the locality and digging out the accumulated debris. This will produce a hole several feet deep and often requires removing slabs of the shale beds that have fallen into the sulfate body over the years. At best it is dry and dusty work but if you are lucky enough to find a pocket of sulfates the work is definitely worth the effort.

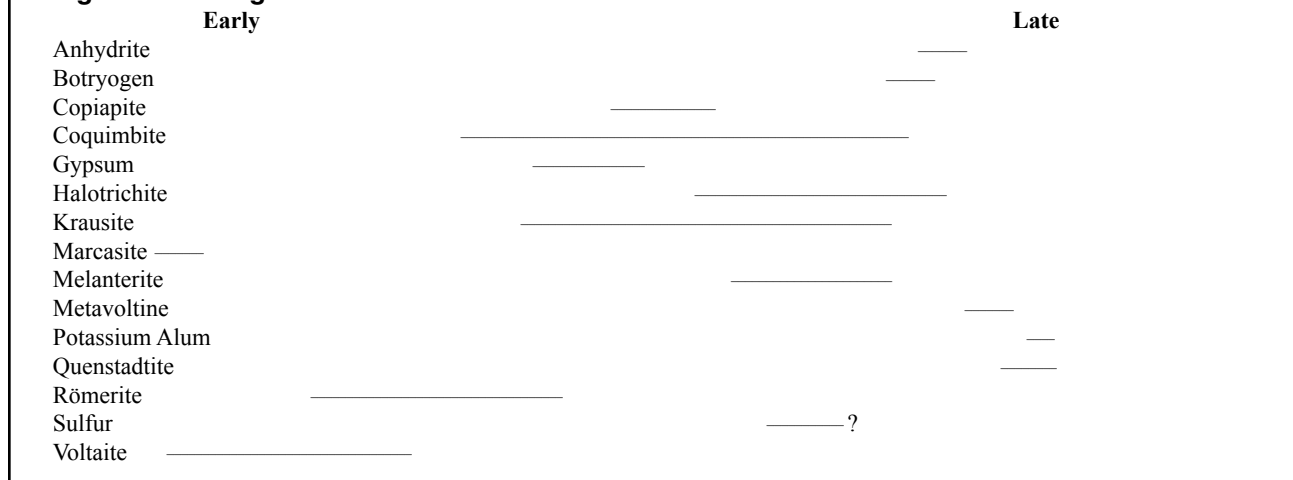
The Sulfur Hole does strange things to people. On our second visit (JFC & GED) we had driven for over 400 miles that day, arrived at dusk and had a hasty dinner after setting up camp. After dark we walked up to the locality, ostensibly to leave our tools for tomorrow. We started digging and shortly found a thin vein of massive coquimbite that we followed down to a good pocket of mixed sulfates, which produced many fine transition zone specimens of coquimbite, krausite r merite and the other sulfates the locality is famous for. We finished up about 4 A.M., covered with sulfate dust and in possession of some of the nicest coquimbite and krausite specimens we had ever seen from the locality.

Preservation of specimens

The sulfates at this locality appear to be relatively stable with the exception of the acid sulfate mineral assemblage that occurs near the footwall. Specimens collected by (JFC) almost forty years ago and stored in plastic boxes show little deterioration. While this may be true of most specimens from the Sulfur Hole, some of the minerals are sensitive to humidity and will hydrate and deteriorate unless care is taken to store them carefully. Exposure to either low or high humidity will allow the minerals found in the more acid footwall zone (r merite, voltaite, melanterite) to literally dissolve in their own water of crystallization or crumble into a fine grained powder. In extreme cases storing the specimens with desiccants has proved successful and coating the surface with acrylic resins has also proved successful, although doing so will change the luster of the crystal faces. Under normal conditions, storage in a sealed plastic box will suffice but the survivability of the acid footwall minerals are best guaranteed in a sealed jar.



Figure 21. Gail Dunning (left) and Dwight Weber examining specimens of sulfate minerals collected at the Sulfur Hole, December 20, 1959.

Figure 22. Paragenetic timeline for the formation of the sulfate minerals at the Sulfur Hole.

Associated minerals in the area

The old borax mines in the area contain several minerals of interest. Colemanite formed friable masses and crystal lined geodes were relatively common. The geodes reached several feet in diameter and often were lined with well-formed colemanite crystals up to several inches across. The colemanite is often associated with colorless to pale blue celestite prisms and occurs on a groundmass of pale yellow strontianite and makes attractive specimens. The prospects also produce well-crystallized gypsum specimens that show a characteristic flattened form. These specimens frequently show a pale yellow fluorescence under short wave ultraviolet light and often phosphoresce white. Bassanite forms small rounded masses in the mudstones in the area. Specimens of this material often show a radiating structure and are highly prized, as the nucleating agent for the concretion was often a fossil insect.

Paragenesis

While no direct paragenesis of the sulfates present is possible, the zoned nature, associations and chemistry of the deposit allows an apparent paragenetic relationship to be suggested. Examination of specimens has supported this hypothesis, however there is considerable species overlap. The more acid species were among the earlier sulfates to form while the less acid coquimbite assemblage formed later in the system's history. The apparent relationship of the minerals to each other is shown in Figure 21.

Discussion

Foshag's original description of the Sulfur Hole included alunite, fibroferrite and jarosite as the minerals occurring at the locality. Alunite was considered to be abundant and fibroferrite and jarosite were an important part of the mineral suite as described by him. The authors were unable to find specimens of these minerals in the material collected by them although many of the samples resembled the descriptions of these minerals given by Foshag. Botryogen, copiapite, gypsum, halotrichite, krausite, marcasite, melanterite, metavoltine, potassium alum, quenstadtite, römerite, sulfur and voltaite were verified by either XRD (WPM) or EDS (GED) methods and their occurrence at the Sulfur Hole has been confirmed. Material previously identified as alunite, fibroferrite and jarosite were restudied and found to be fine grained coquimbite, halotrichite stained

by copiapite and the yellow crystals of jarosite are metavoltine respectively. Foshag (1931), in his original description of the locality, does not describe the methods used to identify these minerals and merely mentions them as being present. No authentic samples of these three minerals from the Sulfur Hole are known to exist. In light of the present investigation, the existence of alunite, fibroferrite and jarosite at the Sulfur Hole must be considered questionable.

References

- Dibblee, T.W. Jr (1970) Geologic map of the Daggett quadrangle, San Bernardino County, California. U.S. Geological Survey Misc. Geologic Invest. Map I-461.
- Erwin, H. D., and Gardner, D. L. (1940) Notes on the geology of a portion of the Calico Mountains, San Bernardino County, California. *California Journal of Mines and Geology*, **36**, 295-298.
- Foshag, W.F. (1922) Calico Hills, San Bernardino County, California. *American Mineralogist*, **7**, 208-209.
- Foshag, W.F. (1931) Krausite, a new sulfate from California. *American Mineralogist*, **16**, 352-341.
- McCulloh, T.H. (1965) Geologic map of the Nebo and Yermo quadrangles, San Bernardino County, California. U.S. Geological Survey open-file report, scale 1:24,000.
- Moller, W.P. (1963a) "Sulfur Hole", Part 1, *The Mineralogist*, **31**, No. 3, 12-16.
- Moller, W.P. (1963b) "Sulfur Hole," Part 2, *The Mineralogist*, **31**, No. 4, 10-16.
- Reynolds, R.E. and Woodburne, M.O., 2001. Marker bed correlations between the Mud Hills, Calico Mountains, and Daggett Ridge, central Mojave Desert, California [abs]. GSA Cordilleran Section, 97th Annual Meeting, Los Angeles.
- Schuiling, Ty (1999) A Miocene hot spring exhalite in the southern Calico Mountains, IN Tracks Along the Mojave, R.E. and J. Reynolds (eds). San Bernardino County Museum Association Quarterly, **46**(3), 89-94.
- Weber, D., and Graal, R. A. (1975) Quenstadtite from California. *Mineralogical Record*, **6**, 106.

Fossil Creodont and Carnivore Footprints from California, Nevada, and Wyoming

William A.S. Sarjeant, Department of Geological Sciences, University of Saskatchewan, Saskatoon, SK S7N 5E2, Canada

Robert E. Reynolds, LSA Associates, Inc., Riverside, CA 92507

Michele M. Kissell-Jones, Collections Coordinator, Las Vegas Natural History Museum, Las Vegas, NV 89101

Though fossil mammalian tracks of other kinds had been reported much earlier from the Cenozoic strata of the United States, the first record of tracks of carnivorous mammals did not appear till 1937, when C. Stuart Johnston illustrated carnivore footprints from a Middle Pliocene volcanic ash layer from Hemphill County, western Texas. The footprints included those of both canoids and feloids, the former being considered those of the bone-crushing dog *Osteoborus cyonoides* and the latter of the sabertooth *Machairodus catocopsis*.

Subsequently George G. Simpson (1941) described the bones and footprints of Pleistocene jaguars from the Craighead Caverns of Tennessee and H.H. Nininger (1941) reported feloid tracks from the Verde Formation of Arizona, at that time poorly dated but later shown to be Plio/Pleistocene (Czaplewski, 1990). In that same year, H. Donald Curry (1941) reported discovering tracks of "at least eight kinds of carnivore" in sediments of similar age in Death Valley, California, but his finds were never to be properly documented. G.M. Robertson and George F. Sternberg (1942) recorded Pliocene feloid tracks from Graham County, Kansas, but were unable to decide on a likely trackmaker. The fullest account of Neogene tracks to date has been by Paul J. Scriver and David J. Bottjer (1986) from the Copper Canyon Formation of Death Valley; they described and illustrated five types of carnivore footprints, placing them into the ichnogenus *Bestiopedia* and considering some to have been made by the felid *Pseudaelurus*, others perhaps by a 'bear dog' or an ursid. An additional inventory of the Copper Canyon locality was conducted in 1999 (Santucci and Nyborg, 1999).

The earliest Miocene records are contained in two papers by Raymond M. Alf (1959, 1966), respectively reporting footprint assemblages from the Avawatz and Barstow Formations of California. His material, now housed in the Raymond M. Alf Museum in the Webb School, Claremont, California, is a principal theme of this paper.

The first report of Oligocene footprints of carnivores was by Philip R. Bjork (1976) from the Brule Formation of South Dakota. These were of small size and considered to be made by the canoid *Hesperocyon*.

The impressions of a manus and a pes from the Devil's Graveyard Formation of Texas by Sarjeant and Wilson (1988) were the first carnivore footprints to be reported from the Eocene. They were placed in a new ichnogenus and species, *Dischidodactylus stevensi*, and considered to be either the footprints of the large "insectivore" *Simidectes* or of a creodont, perhaps *Hyaenodon*. When Sarjeant and Langston (1994) described an extensive footprint assemblage from the later Eocene (Chadronian) of west Texas, they recognized and named six new ichnospecies that were interpreted as being footprints of predators. *Zanclonychopus cinicalcator* was thought to represent footprints of a hyaenodontid creodont, *Tetrastioibopus phoros* and *Falcatipes floriformis* were believed to represent miacids and *Phacelopus therates* a mustelid, while *Axiaciapes ferox* and *A. curvidactylus* were considered to be footprints of

amphicyonids.

This account reviews the footprints of carnivorous mammals from Tertiary strata in the western United States. It completes the study begun in earlier papers by Sarjeant and Reynolds (1999, 2001), respectively treating with camel and horse and with bird footprints.

CLASS MAMMALIA

ORDER CREODONTA

Ichnogenus *Quiritipes* nov.

Diagnosis. Semidigitigrade to semiplantigrade mammalian footprints of ovoidal to lanceolate outline and small to moderate size. Pes somewhat larger than manus. Four digits are imprinted; all are acuminate (though not acute), without claws. Digits III and IV are of similar length and have almost parallel axes, though in the pes their distal extremities converge somewhat. Digits II and V are shorter (pedal digit II markedly so) and directed forward, but slightly to pronouncedly outward. Digital pads are not normally distinguishable. A space separates the digital impressions from metacarpal pads and metatarsal pads; these latter are most deeply impressed, and triangular, in their anterior portion. Trackway narrow, stride and pace varying according to gait but quite long; the pedal imprints are commonly superimposed upon the manual imprints.

Derivation of Name. Latin, *quiritis*, a Sabine spear; *pes*, foot: with reference to the spearhead shape, not only of the individual digits but also of the whole imprints.

Type Ichnospecies. *Quiritipes impendens* Sarjeant, Reynolds, and Kissell-Jones, herein. Eocene (Wasatchian), Wyoming.

Remarks. No description of footprints comparable to this very simple type has been discovered in the literature. The lack of claw impressions suggests a feloid, but the relatively elongate, almost lanceolate shape of the imprints, and the markedly larger pes differentiate this ichnogenus from *Felipeda* Panin and Avram 1962, as emended herein. These Eocene tracks are probably made by a creodont carnivore since felids are not found in the North American fossil record until the Oligocene (Savage and Russel, 1983).

Quiritipes impendens ichnosp. nov.

Plates 1–3; Text-figures 1–5

Diagnosis. Semidigitigrade to (rarely) plantigrade mammalian footprints. Manus elongate ovoidal to sublancoelate, pes typically lanceolate, in outline. Pes around 30% larger than manus and somewhat broader. Four digits are imprinted, all being acuminate (though not acute) and lacking claws. Digit IV projects further forward than digit III but is of similar length; digits II and V are shorter, with manual digit II shortest of all. A space separates the bases of digital impressions from those of metacarpal pads and metatarsal pads; those impressions are triangular in their anterior portion, but exhibit lateral outbulges aligned with the bases of digits II and IV.

Derivation of Name. Latin, *impendere*, v. to overlap; with reference to the overlapping of manual by pedal impressions.

Type Material. Holotype: the succession of footprints in portion VI of the “Creodont Trackway” display (V.94207/154), R.M. Alf Museum, Webb Schools, Claremont, California (Plate 1; Plate 2, figure a; Text-figures 2, 4). Paratype: isolated pedal imprint V.94207/267, same locality and lodgement. Figured specimens: A) pedal imprint on portion IV of “Creodont Trackway” display (plantigrade pedal imprint, with metatarsal pads fully impressed: Plate 1; Plate 2, figure b centre; Text-figure 4); B) V.94207/152 (semidigitigrade manual impression: Text-figure 5). Same horizon and lodgement.

Horizon and Locality. Muddy Creek Formation (Eocene: Wasatchian), Baggs, Carbon County, Wyoming.

Dimensions. Holotype (right manus) maximum length ca. 70 mm, breadth 43 mm. Length of digits: II, 21.5 mm; III, 38 mm; IV, 38 mm; V, 27 mm. Paratype (right pes): maximum length ca. 80 mm, breadth 47 mm. Lengths of digits: ii, 33 mm; III, 38 mm; IV, 38 mm; V, 34 mm. Figured specimen: A) maximum length ca. 50 mm, breadth 54 mm. Length of digits: II, 22 mm; III, 30 mm; IV, 30 mm; V, 27 mm. Figured specimen: B) maximum length ca. 93 mm, breadth 52 mm. Length of digits: II, 27 mm; III, 37 mm; IV, 37 mm; V, 30 mm. Stride estimated at 50 cm; pace not measurable.

Divarication of Digits. See Text-figure 3; however, as stressed below, the outer digits appear to be quite flexible.

Remarks. This ichnofossil morphotype, though represented by abundant material in the collections of the R.M. Alf Museum, presented particular problems in interpretation. The principal slabs displaying footprint casts are contained in a showcase labelled “Creodont Trackway” (Plate 1, upper). However, a cursory inspection showed that the nine slabs which compose the display may not have been assembled in their original relative position. The senior author attempted an alternate reconstruction of the trackway pattern (Text-figure 1), utilizing the bird track traversing slabs V, I and VIII as evidence of relative position. This reduces the number of mammal tracks from several (Plate 1) to just three. In absence of supplementary evidence, this assembly is almost arbitrary.

The second major problem in interpretation is that the mammal footprints display what Peabody (1959) defined as “primary overlap”. As a consequence of the trackmaker’s relatively short body length, the impressions of the pedes are very commonly superimposed upon those of the manus. In the two opposing series of footprints that are shown from lower left to upper right on Text-figure 1, no manual imprints are visible, though the shape of the pedal imprints is variably modified or deformed by the manual imprints beneath. Indeed, only one manual imprint in this display can be seen clearly; since it is associated on slab VI with two pedal imprints (albeit of lesser quality), that slab was chosen as holotype (Plate 2, figure a, at right; Text-figures 1, 3). To better illustrate the form of the pes, a paratype on a separate small slab was selected (Plate 3, figure a; Text-figures 2, 3).

Examples of primary overlap of pes upon manus are seen in Plate 1, figure c (specimen V.94207/152) and 3, figure e (slab I, V.94207/154), while Plate 3, figure b shows a case of track overlap from two opposing directions (specimen V.94207/152). The unusual depth of impression of a part of the pedal imprint—very often, the metatarsal pads—may be noted. This may result from superposition of the metatarsal pads upon the metacarpal pads of the manus, since it is not apparent in specimens where the pedal digits lie behind those of the manus.

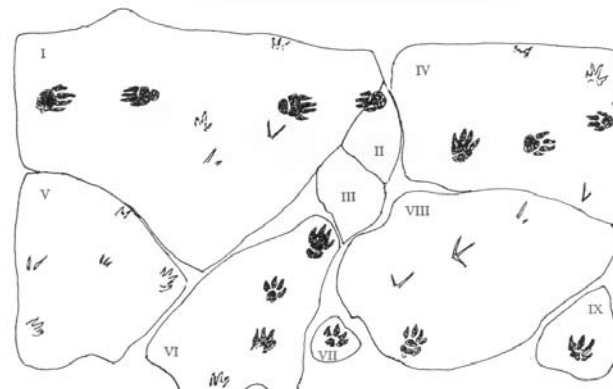


PLATE 1. The “Creodont trackway” exhibit in the Raymond M. Alf Museum. Upper: photograph of display. Lower: interpretative drawing, to show the component slabs.

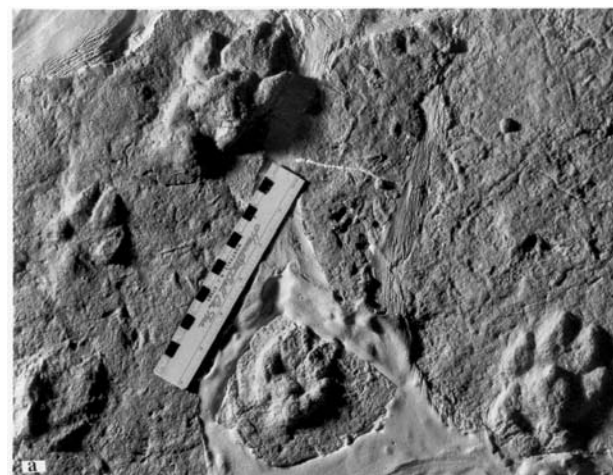


PLATE 2. The “Creodont trackway” exhibit. (a) Detail of slabs VI, VII and VIII, with the holotype track of *Quiritipes impendens* Sarjeant, Reynolds and Kissell-Jones, ichnogen. et sp. nov., at right; (b) detail of slab IV.

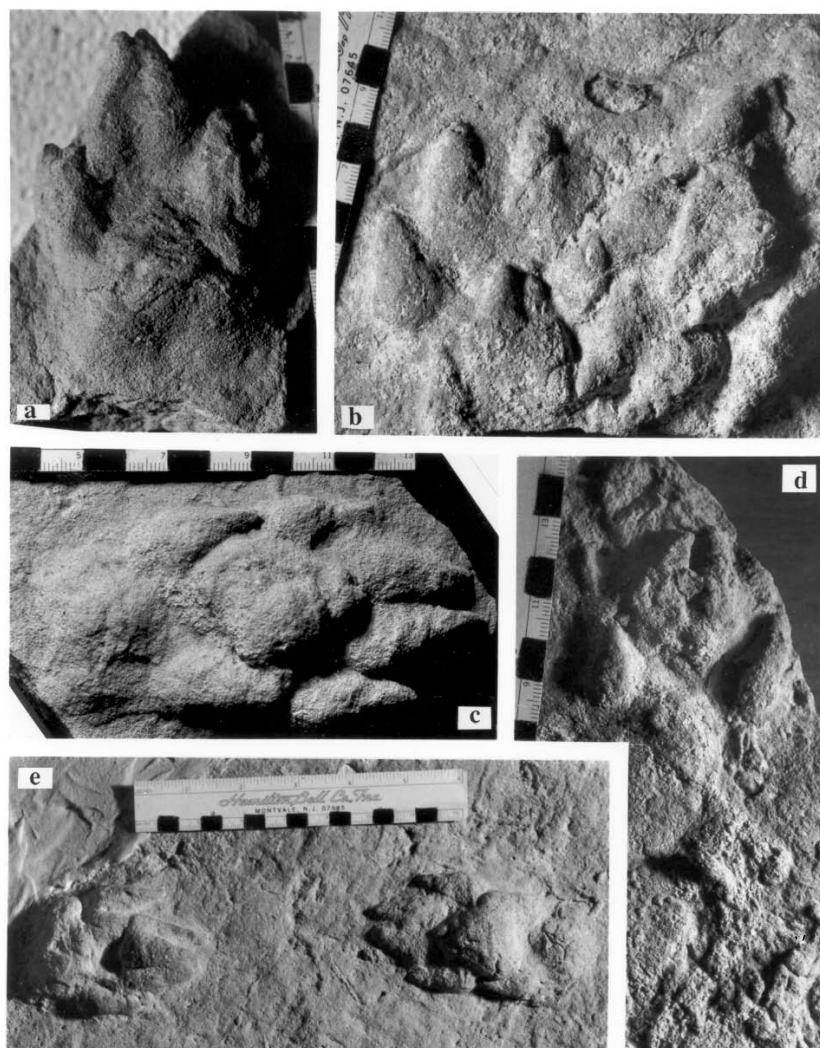


PLATE 3. *Quiritipes impendens* Sarjeant, Reynolds and Kissell-Jones, ichnogen. et sp. nov. (a) The paratype, a left pes (V.94207/267); (b) footprints superimposed from two contrary directions (V.94207/152); (c) right pes superimposed upon right manus (V.94207/153); (d) left pes (V.94207/132); (e) detail of showcase slab I.

Further complications are the variable degree to which the feet were imprinted and the flexibility of digits II and IV which, in some imprints, are seen to splay outward. Normally, the imprints are semiplantigrade, with the anterior portions only of metacarpal pads and metatarsal pads imprinted; however, some are semidigitigrade, others almost plantigrade. Figured specimen A is a plantigrade pedal imprint in which digits II and IV flex outward in some measure (Plate 3, figure e, at left; Text-figure 4); figured specimen B is a manual imprint of almost digitigrade character (Text-figure 5).

Further specimens in the collections of the R.M. Alf Museum, considered attributable to *Quiritipes impendens*, are V.94207/149, 264, 265, 266 and 268.

ORDER CARNIVORA
FAMILY AMPHICYONIDAE
Genus *Hirpexipes*, ichnogen. nov.

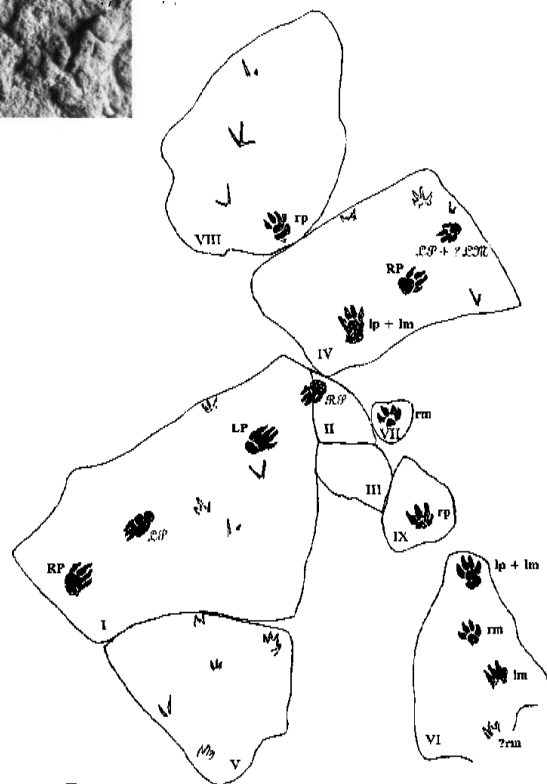
Diagnosis. Semidigitigrade to semiplantigrade mammalian footprints. Pes impressions markedly larger and more elongate than those of the manus. All digits exhibit long, sharp claws.

The manual digits each have three pads, though fusion of adjacent pads may occur. The tips of all digits are directed forward; however, digit IV shows slight, and digit V strong, initial outward curvature. The metacarpal pads is variably impressed, showing indistinct indications of the positions of the carpals. Four of the pedal digits show four pads, the other (I) only three; all digits are directed forwards, though again digit IV shows slight, and digit V strong, initial outer curvature. The metatarsal pads is variably impressed and may show indication of the positions of the tarsals. Trackway relatively narrow; stride and pace long.

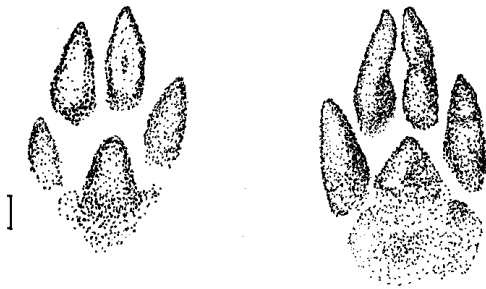
Derivation of Name. Latin, *hirpex*, rake; *pes*, foot: with reference to the long, flexible digits of the pes, so like the prongs of a leaf-rake.

Type Ichnospecies. *Hirpexipes alfi* Sarjeant, Reynolds and Kissell-Jones, herein. Miocene (Barstovian), California.

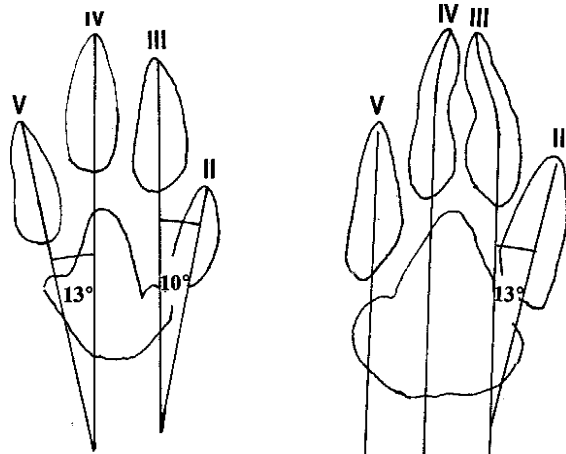
Remarks. These footprints exhibit the strong, sharp claws characteristic of predators. The large size and five digits of the print support the referral (Alf 1966) to *Amphicyon*. In the display in the Raymond M. Alf Museum, a replica of the skeleton of a Clarendonian *Amphicyon* is set upon the Barstovian footprint slab (see Plates 4 and 5), serving as an impressive demonstration of the credibility of Alf's conclusion.



TEXT-FIGURE 1. *Quiritipes impendens* Sarjeant, Reynolds and Kissell-Jones, ichnogen. et sp. nov. Reconstruction of the slabs composing the "Creodont trackway" display. (Bird footprints may also be seen at left and upper right).



TEXT-FIGURE 2. *Quiritipes impendens* Sarjeant, Reynolds and Kissell-Jones, ichnogen. et sp. nov. Left: cast of left manus (from holotype track). Right: cast of left pes (paratype). [Scale bar = 1 cm]



TEXT-FIGURE 3. *Quiritipes impendens* Sarjeant, Reynolds and Kissell-Jones, ichnogen. et sp. nov. Digits and interdigital angles of left manus (left) and left pes: reversed from holotype and paratype casts. [Scale bar = 1 cm]

However, for reasons set forth earlier (Sarjeant and Reynolds, 1999) we prefer to base ichnogenic names upon observed characters of the imprint or cast, not upon presumed affinity. Consequently, the ichnogenic name is chosen to refer to the unusually elongate, and probably flexible, pedal digits.

Hirpexipes alfi, ichnosp. nov.

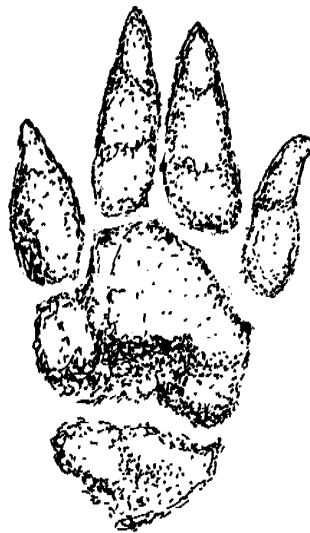
Plates 4–6; Text-figures 6–8

1966 Carnivore trackway. Alf, p. 258-261, figs. 1-2.

1995 Tracks of a large bear-dog. Lockley and Hunt, p. 268, fig. 6.21.

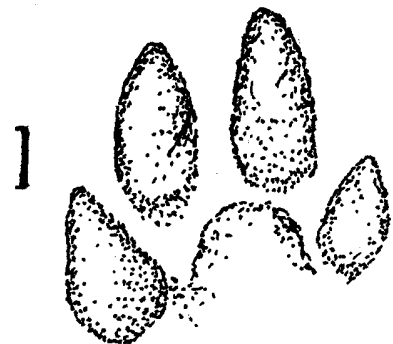
Diagnosis. Digitigrade to semidigitigrade mammalian tracks. Outline of four-digit manus a hemioval. Manual digit II is longest, digit III almost as long; digit IV is next in length, the pollex and digit V somewhat shorter. Digit V is quite strongly curved: all these digits show three digital pads and elongate, acute claws.

Pes spade-shaped: all digits are long and slender, with digit III longest and digit I shortest. Pedal digits II-IV exhibit four digital pads; digit III exhibits four pads, one of which may correspond to the cuboid metatarsal, while the hallux exhibits three pads, the proximal pad smallest. All pedal digits bear elongate claws: digits IV and V exhibit proximal flexure, but all digits are directed forward. Metacarpal pads and metatarsal pads variably impressed and showing some indication of the pattern of metacarpals and metatarsals.



TEXT-FIGURE 4. *Quiritipes impendens* Sarjeant, Reynolds and Kissell-Jones, ichnogen. et sp. nov. A plantigrade pedal impression, with outer digits flexed (specimen on slab I display). [Scale bar = 1 cm]

TEXT-FIGURE 5. *Quiritipes impendens* Sarjeant, Reynolds and Kissell-Jones, ichnogen. et sp. nov. An almost digitigrade manual impression (specimen V.94207/152). [Scale bar = 1 cm]



Trackway narrow, with pedal imprints slightly lateral to manual imprints. Stride and pace long.

Derivation of Name. Honouring Raymond M. Alf, who not only collected and first described the track, but was also instrumental in its display.

Type Material. Slab no. 100 (V94272/100). Lodged in the Raymond M. Alf Museum, Webb Schools, Claremont, California: a trackway with five pairs of footprints.

Horizon and Locality. Barstow Formation, Miocene (Barstovian), Owl Canyon, near Barstow, San Bernardino County, California. The stratigraphic position of the trackway below the Skyline Tuff (14.8 Ma, Woodburne 1991) suggests that the maker was *A. ingenis*.

Dimensions. Figured prints: Manus (Plate 6, figures a, c): overall length ca. 18 cm, width 13.2 cm. Length of digits: I, 8.2 cm; II, 10.8 cm; III, 10.0 cm; IV, 9.2 cm; V, 7.5 cm. Pes (Plate 6, figures b, d) overall length ca. 38 cm, width 18.2 cm. Length of digits: I, 20.8 cm; II, 25.0 cm; III, 26.4 cm; IV, 26.0 cm; V, 25.2 cm (20.4 cm if proximal pad—possibly the cuboid—is excluded). Stride 245 cm; pace 120 cm.

Remarks. The only footprints exhibiting any similarity to *H. alfi* were described from the Paleocene Paskapoo Formation near Red Deer, Alberta, Canada (Rutherford and Russell, 1928; Russell, 1930). In these also, the pes is much larger than the manus and exhibits rake-like digits; however, only four digits are evident and the size is somewhat smaller (pedal length ca. 15 cm), while the claws, though prominent, are rather blunt. Russell (1930, p. 220) considered these to be the footprints of a condylarth; however, Scrivner and Bottjer (1986, p. 327) suggested they might be those of a creodont. The earliest skeletal

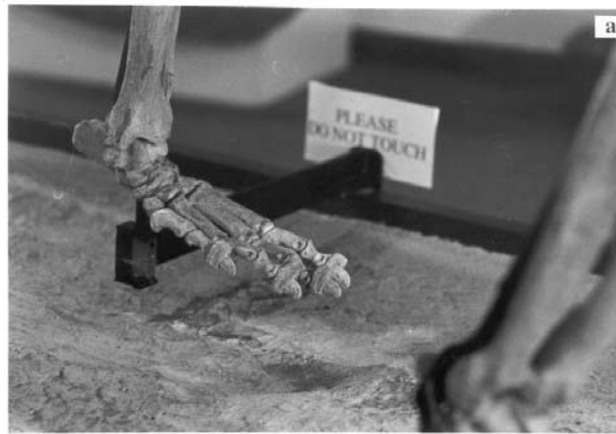


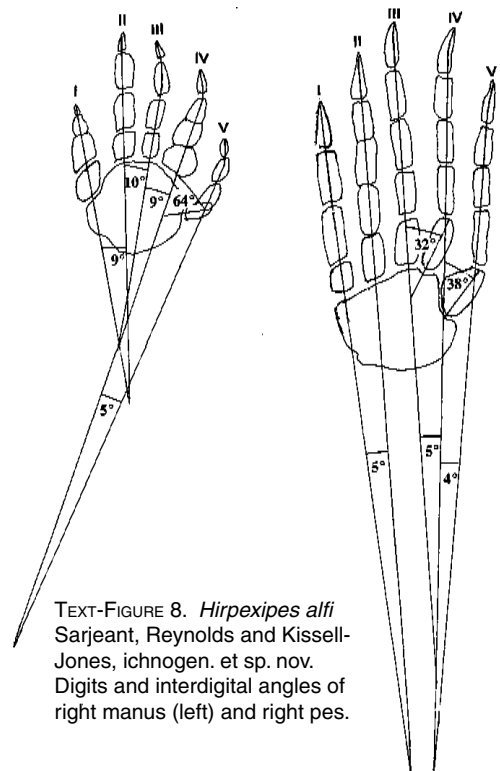
PLATE 5. Skeleton of *Amphicyon*: detail. (a) Left pes, with digits outstretches; (b) right pes, with digits flexed.

PLATE 4. Skeleton of *Amphicyon*, placed upon the footprint trackway (now the holotype of *Hirpexipes alfi*) in the Raymond M. Alf Museum. (a) Cast of right manus (the paratype, V.94164/277); (b) cast of right pes (the holotype, V.94164/232).



TEXT-FIGURE 6. *Hirpexipes alfi* Sarjeant, Reynolds and Kissell-Jones, ichnogen. et sp. nov. Mould of right manus on holotype slab. [Scale bar = 5 cm]

TEXT-FIGURE 7. *Hirpexipes alfi* Sarjeant, Reynolds and Kissell-Jones, ichnogen. et sp. nov. Mould of right pes on holotype slab. [Scale bar = 5 cm]



TEXT-FIGURE 8. *Hirpexipes alfi* Sarjeant, Reynolds and Kissell-Jones, ichnogen. et sp. nov. Digits and interdigital angles of right manus (left) and right pes.

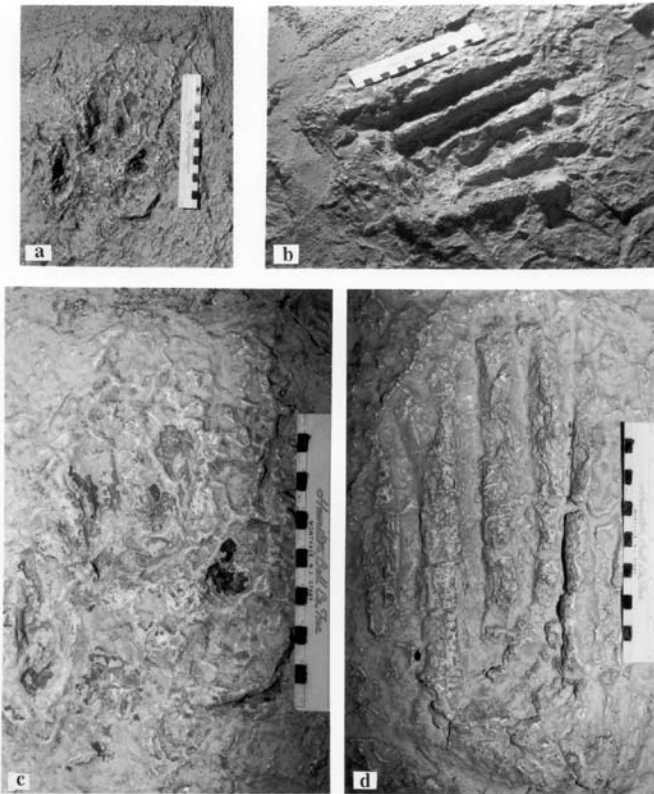


PLATE 6. *Hirpexipes alfi* Sarjeant, Reynolds and Kissell-Jones, ichnogen. et sp. nov. The holotype slab. (a, c) Right manus, at two different light angles and magnifications; (b, d) right pes, also at two different light angles and magnifications.

remains of the family Amphicyonidae are known from the latest Eocene/earliest Oligocene (Savage and Russell, 1983). Large amphicyons are known from middle Miocene (Barstovian/Clarendonian) time (Savage and Russell, 1983).

FAMILY URSIDAE

Ichnogenus nov. *Platykopos*

Diagnosis. Large plantigrade footprints with digits close to manual/pedal pad. Manus width similar to pes, pes being slightly narrower and elongate due to metatarsal pad. Five digits on manus and pes are clawed and digits II–V of equal length on quadrate manus with digit I offset. Digits I–V form a symmetrical arc around pes, digits I and V being shorter than II to IV.

Derivation of name. Greek, *platykos*, broad, and *pous*, foot, with reference to great width of the imprint.

Type Ichnospecies. *Platykopos ilycalcator* Sarjeant, Reynolds and Kissell-Jones, herein. Late Miocene (Late Hemphillian LMA), Nevada.

Platykopos ilycalcator, inchoespecies nov.

Plate 7, Text-figures 9–11

Diagnosis. Plantigrade footprints of large size, five digits on all feet, each bearing short, pointed claws. Pes breadth less than manus. Pes antero-posterior oval, including metatarsal pad. Manus rectangular without metacarpal pad, all digits closely appressed to manual/pedal pads. Manus digits II–V are approximately equal length from manus pad. Manus digit I posterior, arched anteriorly and narrower. Pedial digits closely appressed to pedal pad; all five are symmetrical about pad, with digit V somewhat shorter and digit I smallest. The phalangeal

pads are not distinct, consisting of two lobes; they are closely appressed to the manual/pedal pads.

Derivation of Name. Greek, *lys*, mud, dirt; *calcator*, one who treads something: thus, “mud-treader,” in reference to the occurrence of the footprints in the Muddy Creek Formation.

Type specimens: Holotype V.94163/277 (manual imprint), R.M. Alf Museum, Webb Schools, Claremont, California (Plate 7 Fig. a, Text-figures 10, 11). Paratype V.94164/232 (pedal imprint), same lodgement (Plate 7, fig. b, Text-figures 9, 11).

Horizon and Locality: Muddy Creek Formation (Lt. Miocene, latest Hemphillian LMA), Moapa, Clark County, Nevada.

Dimensions: Holotype: manual imprint, overall length 13.5 cm; overall breadth 10.7 cm. Length of digits (measured from claw tip to base of second phalangeal pad): I, ca. 3 cm; II, 5.2 cm; III, 6.5 cm; IV, 5.5 cm; V, 4.7 cm. Paratype: pedal imprint, overall length 13.5 cm (rear not clearly defined), overall breadth 13.7 cm. Approximate lengths of digits (measured from claw tip to base of second phalangeal pad): I, 4.5 cm; II–IV, 6.5 cm; V, 5 cm.

Divarication of digits: see Text-figure 11.

Remarks: These latest Miocene prints from Nevada are distinguished by large size and the presence of five digits, allowing comparison and contrast to tracks referred to cre-

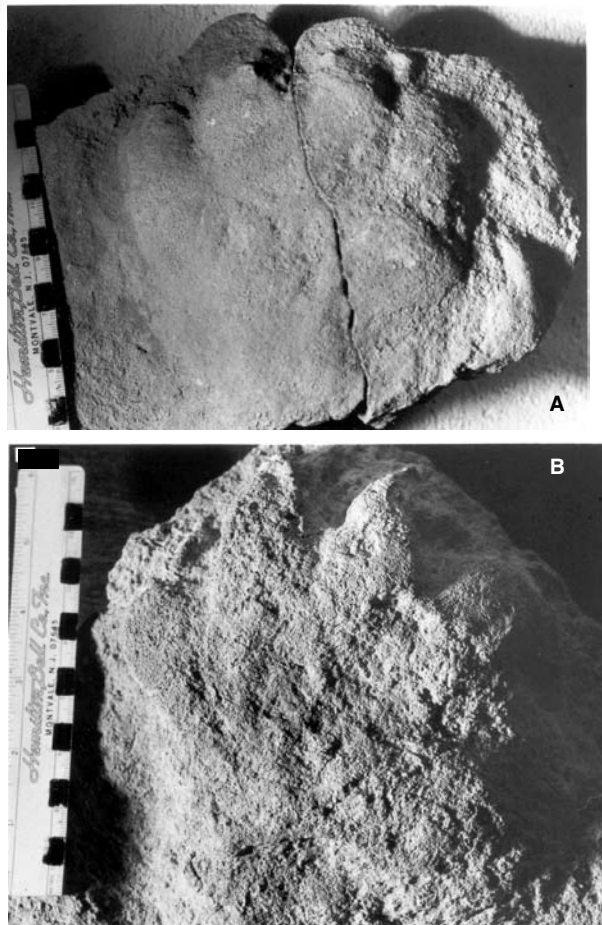
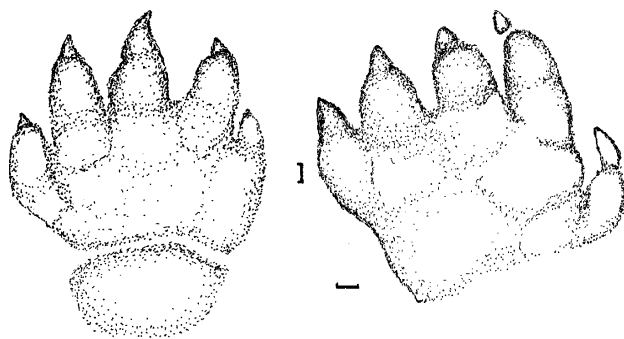
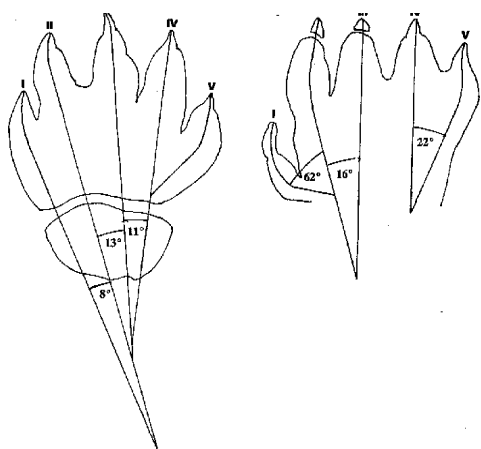


PLATE 7. *Platykopos ilycalcator* Sarjeant, Reynolds and Kissell-Jones, ichnogen. et sp. nov. (a) Cast of right manus (the holotype, V.94163/227); (b) cast of right pes (the paratype, V.94164/232).



TEXT-FIGURE 9 (left). *Platykopus ilycalcator* Sarjeant, Reynolds and Kissell-Jones, ichnosp. nov. Cast of right pes(paratype). [Scale bar = 1 cm]

TEXT-FIGURE 10 (right). *Platykopus ilycalcator* Sarjeant, Reynolds and Kissell-Jones, ichnosp. nov. Cast of right manus(holotype). [Scale bar = 1 cm]



TEXT-FIGURE 11. *Platykopus ilycalcator* Sarjeant, Reynolds and Kissell-Jones, ichnosp. nov. Digits and interdigital angles of right pes(left) and right manus: reversed from holotype and paratype casts.

donts and to amphicyonids (*Hirpexipes*, herein). *Platykopus* prints are twice the width of *Zanclonychopus* (Late Eocene, Sarjeant and Langston, 1994) but digits have only two pads anterior to the manual/pedal pads. Manual pads are short while pedal pads are long when *Platykopus* is compared to *Zanclonychopus*. Digits I in both manus/pes of *Zanclonychopus* are offset posteriorly as in Digit I manus of *Platykopus*. *Platykopus* manus is smaller and pes is much smaller than *Hirpexipes*. Digits of *Platykopus* are very short compared to *Hirpexipes* where digits with three or four pads are more than twice as long as the manual/pedal pads. A metatarsal pad is present in the ursid, *Platykopus*, but absent in the amphicyonid *Hirpexipes*.

The latest Miocene new ichnogenus and species is considered to represent the footprints of a large ursid, the first seen recorded by the authors.

FAMILY FELIDAE

Ichnogenus *Pycnodactylopus* ichnogen. nov.

Diagnosis. Semidigitigrade mammalian footprints of moderate size and broadly ovoidal outline. Four short digits on all feet, lacking claws. Phalangeal impressions rather stout (especially so in the presumed pes), their width being two-thirds of their length. Digits II to IV are of pyriform to scutiform out-

line, exhibiting two digital pads (though the division between the pads may not be clear) digit V is reduced (especially in the presumed manus) and with pad undivided. Proximally the phalangeal impressions are set closely about metacarpal pads and metatarsal pads, with which they may be in actual contact. Trackway relatively narrow.

Derivation of Name. Greek, *pyknos*, thick; *daktylos*, finger; *pous*, foot: with reference to the thickness of the digits.

Type Ichnospecies. *Pycnodactylopus achras* Sarjeant, Reynolds and Kissell-Jones, herein. Avawatz Formation (Miocene; Clarendonian), California.

Remarks. This ichnogenus is distinguished from *Felipeda* Panin and Avram 1962, as emended herein, by the variable form of the phalangeal impressions and the close proximity of their bases to metacarpal pads and metatarsal pads. During the Miocene Barstovian LMA the only felid genus in North America was *Pseudaelurus* (Savage and Russell, 1983). By the Clarendonian LMA, *Nimravides*, *Barbourofelis*, and *Sansanosmilus* were also present in North American faunas. The presence of four digits suggests the trackmaker was either a canid or a felid. The lack of both bilateral symmetry and impressions of claws implies felid rather than canid prints.

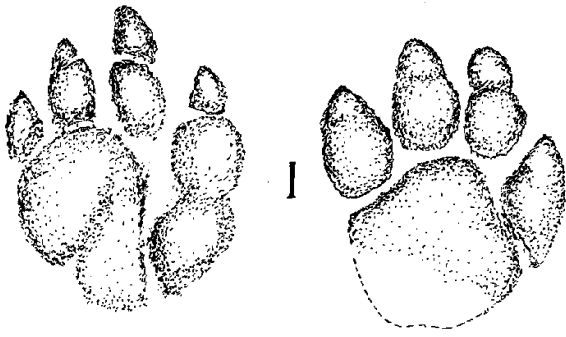
Pycnodactylopus achras, ichnosp. nov.

Plate 8; Text-figures 12-13

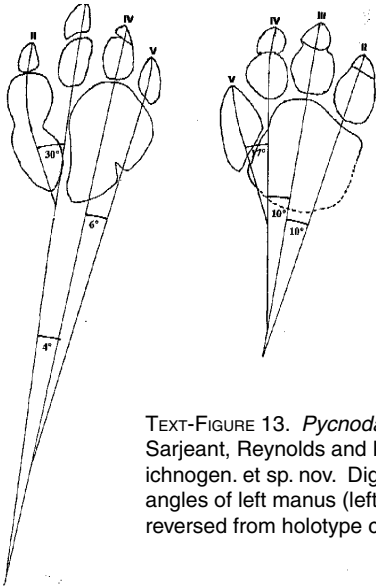
Diagnosis. Tetradactyl mammalian footprints, semiplantigrade and broadly ovoidal, with width around seven-ninths of length. Digital impressions broad, obtuse and lacking claws. In the presumed manus, digit III is longest, digit II next in length and digit IV shorter; these each show two phalangeal pads, the inner pad much thicker than the outer (up to two-thirds the digital length). These digits point forward and are of pyriform outline. Digit V is shortest and has a rounded triangular outline. The digits of the presumed pes are of more uniform



PLATE 8. *Pycnodactylopus achras* Sarjeant, Reynolds and Kissell-Jones, ichnogen. et sp. nov. (Holotype, V.94164/232).



TEXT-FIGURE 12. *Pycnodactylopus achras* Sarjeant, Reynolds and Kissell-Jones, ichnogen. et sp. nov. The holotype. Right: presumed left manus; left: presumed right pes. [Scale bar = 1 cm]



TEXT-FIGURE 13. *Pycnodactylopus achras* Sarjeant, Reynolds and Kissell-Jones, ichnogen. et sp. nov. Digits and interdigital angles of left manus (left) and right pes: reversed from holotype casts.

length, with digits II-IV pyriform and composed of two pads (division not always clear) and digit V of one; the latter digit is somewhat set back, larger than manual digit V but of similar shape. Pedal digits III-IV point forward, II and V somewhat outward. The digital bases are set close to the metacarpal pads and metatarsal pads; the metacarpal pads may give indication of metacarpal structure.

Derivation of Name. Greek *achras*, a wild pear; with reference to the pyriform digits.

Holotype. Specimen V.94021/205, Raymond M. Alf Museum, Webb Schools, Claremont, California.

Type Horizon and Locality. Avawatz South, Avawatz Formation (Miocene; Clarendonian), San Bernardino County, California.

Dimensions. Presumed left manus: overall length 90 mm, overall breadth 70 mm. Length of digits: II, 35 mm; III, 37 mm; IV, 25 mm; V, 16 mm. Presumed right pes: overall length ca. 85 mm (rear missing); overall breadth 70 mm. Length of digits: II, 30 mm; III, 32 mm; IV, 31 mm; V, 30 mm. Width of trackway 180 mm.

Divarication of Digits. See Text-figure 13.

Remarks. Though only two footprints were available for study, they are extremely clear. Since we found in the literature no reports of similar footprints, we consider that they fully merit taxonomic differentiation.

- Ichnogenus *Felipeda* Panin and Avram, 1962, emend. nov.
 1962 *Felipeda* Panin and Avram, p. 461
 1965 *Bestiopeda* Vialov, p. 112
 1966 *Bestiopeda* Vialov, p. 128
 1986 *Bestiopeda* subgen. *Felipeda* Scrivner and Bottjer, p. 299
 1987 *Pumaeichnium* Aramayo and Bianco, p. 534
 1994 *Bestiopeda* Vialov emend. Sarjeant and Langston, p. 27

Original Diagnosis (generico-specific). "Impressed footprint of a felid having a breadth of 52 mm. Length not so easy to determine, since the foot was not completely impressed. One may observe the oval imprints of four digital pads, [spatially] divided from the heel.... Digits 2 and 3 are set close together and occupy a more anterior position than digits 1 and 4. Between the first digit and the heel is a distance of circa 6 mm. Between digits 4 and 3, the distance is approximately 4 mm. Digit 1 is at the same distance as 2, at only 2-3 mm. The dimensions of these impressions vary around 17 x 12 mm. No impressions of claws were observed, since these must have been retractile." (Panin and Avram, 1962, p. 461, new transl.)

Emended Diagnosis. Plantigrade to semi-plantigrade footprints exhibiting four digits (II to V), each with a spheroidal to ovoidal or elongate digital pad. The pads form a semicircle in front of, or about the front portion of, the metatarsal pads. Digital pad III is often the most anterior and there never appears to be lateral symmetry on an AP line between digital pads III and IV. Digital pads may be of equal or similar size or may show limited dimensional variation. Impressions of claw tips may be present, but are usually absent.

Type Ichnospecies. *Felipeda lynxi* Panin and Avram, 1962. Miocene (Vindobonian), Romania.

Other Included Species.

Felipeda bestia (Vialov, 1966) Sarjeant, Reynolds and Kissell-Jones, comb. nov. (= *Bestiopeda bestia* Vialov, 1966, p. 128-192, pl. 36, fig. 1). Miocene (Burdigalian), Ukraine.

Felipeda biancoi (Aramayo and Bianco, 1987) Sarjeant, Reynolds and Kissell-Jones, comb. nov. (= *Pumaeichnium biancoi* Aramayo and Bianco, 1987, p. 534, fig. 2a-b). Late Pleistocene, Argentina.

Felipeda felis Panin, 1965, p. 148-149, pl. 6, figs. 15-17. Miocene, Romania.

Felipeda maxima (Kordos, 1985) Sarjeant, Reynolds and Kissell-Jones, comb. nov. (= *Bestiopeda maxima* Kordos, 1985, p. 281-282, 3367; illus. by Abel, 1935, fig. 144). Lower Miocene, Hungary.

Felipeda sanguinolenta (Vialov, 1966) Sarjeant, Reynolds and Kissell-Jones, comb. nov. (= *Bestiopeda sanguinolenta* Vialov, 1966, p. 129, pl. 36, figs. 3-6, text-fig. 43). Miocene (Burdigalian), Ukraine.

Felipeda milleri (Remeika, 1999) Sarjeant, Reynolds and Kissell-Jones, comb. nov. (= *Pumaeichnium milleri*, Remeika, p. 42). Pleistocene (Irvingtonian), California.

Remarks. It is evident that, when Vialov set up his ichnogenus *Bestiopeda* (1966, p. 112)—an ichnogenus designed to include all fossil carnivore footprints—he did so in ignorance of the senior name *Felipeda*. The situation was further complicated by two further actions. Firstly, Scrivner and Bottjer (1986, p. 299-301), in recognizing five types of carnivore tracks from California, improperly treated *Felipeda* as a subgenus of *Bestiopeda*. Secondly, Sarjeant and Langston (1994, p. 27), when emending the ichnogenus *Bestiopeda*, implicitly accepted the procedure of Scrivner and Bottjer (*op. cit.*), not realizing

that *Felipeda* had been proposed as an ichnogenic name. That error is here corrected, the phraseology of the emended diagnosis proposed for *Bestiopedia* by Sarjeant and Langston (*op.cit.*) being essentially utilized anew as an emended diagnosis for *Felipeda*. The generic name *Pumaeichnium* Aramayo and Bianco, 1987, treated by Sarjeant and Langston (*ibid.*) as a junior synonym of *Bestiopedia* following their emendation, is accordingly treated here as a junior synonym of *Felipeda*. *Carnivoripeda* Kordos, 1985, differs from *Felipeda* in showing impressions of five, not four, digits.

The three ichnospecies attributed to *Bestiopedia* by Vialov (1966) present problems, because of the over-brevity of their diagnoses and inadequacies in illustration. The diagnosis of *Bestiopedia bestia* reads thus:

Four-digit trackway approximately 60 mm long, with ovally extended, strongly tapering digits. (Vialov, 1966, p. 128, new transl.)

Nothing is said about the span of the digits, their size or their degree of contact with the impressions of metacarpal pads and metatarsal pads. The single photograph (Vialov, 1966, pl. 36, fig. 1) is unhelpful and there is no text-figure.

His second ichnospecies, *B. sanguinolenta*, receives a slightly longer diagnosis:

Four-digit trackway, approximately 65 mm wide and 75-85 mm long; the digits somewhat separated, divided by an intervening distance; the middle digits extend noticeably forwards; the trackways of the hind paws—much narrower, ovally extended, but those of the front [paws] are broadly rounded. (*ibid.*, p. 129, new transl.)

In this case the illustration is ampler, comprising five photographs (*ibid.*, pl. 36, figs. 3-6, text-fig. 43) and a drawing illustrating the track pattern (*ibid.*, text-fig. 46).

The third ichnospecies named by Vialov is *B. gracilis*. This is only briefly characterized:

Small, four-digit footprints, 35 mm long; digits having the appearance of fans, with traces of claws. (Vialov, 1966, p. 134, new transl.)

It is illustrated by one photograph and one drawing (*ibid.*, pl. 36, fig. 2, text-fig. 47). Since both a photograph and a drawing of a dog footprint are presented for comparison, it is clear that Vialov considered these to be footprints of canoids. Accordingly, while two of Vialov's species are reassigned above to *Felipeda*, this third species is assigned below to the emended

ichnogenus *Canipeda* Panin and Avram, 1962. A similar new assignment is given also to *Bestiopedia amphicyonides* Thenius, 1967, whose name makes evident its author's view of its affinity.

Felipeda scrivneri ichnosp. nov

Plate 9, figure a, b

Text-figures 14-16

1966 Cat footprint. Alf, fig. 4

?1967 Mittelgrosser Felidentype. Thenius, p. 367-368, pl. 1, figs. 1-2, pl. 4, fig. 3

1986 *Bestiopedia (Felipeda)* sp. A. Scrivner and Bottjer, p. 299-300, fig. 4A

Diagnosis. Tetractyl mammal tracks, plantigrade, with four digital impressions forming an arc of about 75° span in front of the impressions of metacarpal pads and metatarsal pads. Digital impressions III and IV are separated by a broad gap from metacarpal pads and metatarsal pads, II by a narrower gap, while V is in contact and corresponds to an indentation on the outer side of the metacarpal pads or metatarsal pads. The digital impressions are all broadly ovoidal and of quite uniform size. They are undivided; claw impressions are lacking. Metacarpal pads and metatarsal pads are roughly hemispherical but modified by a prominent central, and slight lateral, outbulges.

Derivation of Name. In tribute to Paul J. Scrivner, joint author of an important study of Californian Neogene footprints.

Holotype. Specimen V.94285/242, Raymond M. Alf Museum, Webb Schools, Claremont, California (Plate 9, figure a; Text-figure 14-15), now returned to the National Park Service, Death Valley, California. Paratype: V.94276/105 (Plate 9, figure b; Text-figure 15), Raymond M. Alf Museum, Webb Schools, Claremont, California.

Type Horizon and Locality. Holotype: Miocene (Hemphillian LMA), Death Valley, California. Figured specimens: Miocene (Barstovian LMA), Barstow, San Bernardino County, California.

Dimensions. Holotype (left manus) V.94285/242: overall length 106 mm, overall breadth 96 mm. Length of digits: II, 34 mm; III, 36 mm; IV, 34 mm; V, 34 mm. Pace 440 mm: stride not measurable. Paratype: V.94276/105 (left manus?): overall length 71 mm, overall breadth 62 mm. Length of digits: II, 13 mm; III, 15 mm; IV, 16 mm; V, 16 mm.

Divarication of Digits. See Text-figure 16.



PLATE 9
(a) *Felipeda scrivneri*
Sarjeant,
Reynolds and
Kissell-Jones
ichnosp. nov.
The holotype,
V.94285/242.

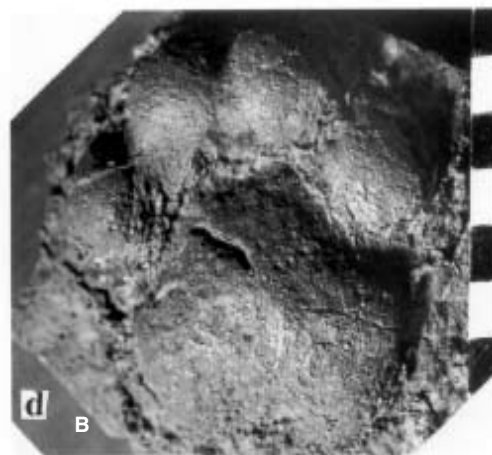
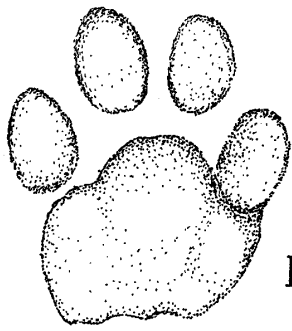
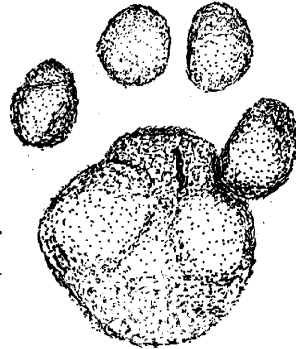


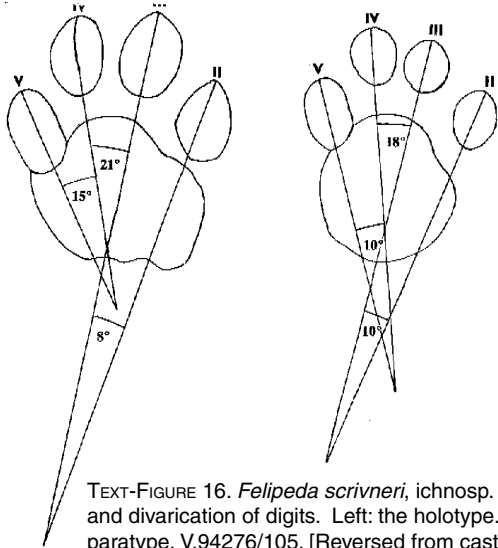
PLATE 9 (b) *Felipeda scrivneri* Sarjeant, Reynolds and Kissell-Jones, ichnosp. nov. The paratype, V.94276/105.



TEXT-FIGURE 14. *Felipeda scrivneri*, ichnosp. nov. The holotype: cast of left manus. [Scale bar = 1 cm]



TEXT-FIGURE 15. *Felipeda scrivneri*, ichnosp. nov. The paratype specimen V.94276/105, cast of presumed left manus of a younger individual. [Scale bar = 1 cm].



TEXT-FIGURE 16. *Felipeda scrivneri*, ichnosp. nov. Digits and divarication of digits. Left: the holotype. Right: the paratype, V.94276/105. [Reversed from casts].

Remarks. A footprint figured by Alf (1966), from Barstow; constitutes the first record of this morphotype from the Miocene. The R.M. Alf Museum collections contain quite a number of specimens of this morphotype but, except for the holotype (where there is a second, poorer impression on the same slab), all are isolated, so their recognition as manus or pes is difficult. The specimen illustrated by Alf (1966), unfortunately, was not confidently identified by us and is not reillustrated here.

The footprints naturally increased in size with age and growth, changing slightly in form. However, the changes in proportions and divarication of digits are only minor (see Text-figure 15). Consequently the paratype (Plate 9, figure b) can be placed into this ichnospecies without hesitation.

Felipeda scrivneri shows close accord with the description and illustration of Scrivner and Bottjer's *Bestiopedina* (*Felipeda*) sp. A. It differs from all named ichnospecies of this genus in digital shape and span and in the fact that digit V is in contact with metacarpal pads and metatarsal pads. It differs from *F. bottjeri* also in being less elongate and in not having being

found in association with claw impressions. The Austrian Pliocene footprints reported by Thenius (1967), of a "medium-sized felid", are quite similar to *F. bottjeri*, but the digital pads appear more elongate: their dimensions and the digital span were not indicated. Thenius's "small felid type" (1967, pl. 2, fig. 3) may have been made by a young individual of the same species. The feloid footprints from Mexico described by Dugès (1894) are quite similar to *F. bottjeri*, but differ in that digit V is less close to metacarpal pads or metatarsal pads. *Felipeda maxima* (Kordos, 1985) differs in its greater size and the greater proportionate length of digit III. The Pliocene carnivore tracks attributed by Johnston (1937) to *Machairodus catocopsis* have larger digital pads of more variable shape. The jaguar footprints described by Simpson (1941) from a Tennessee cave are similar to *F. scrivneri* but have more elongate digital pads.

The trackmaker of *F. scrivneri* was certainly a large feloid, perhaps a species of *Pseudaelurus*, as suggested by both Alf (1966) and Scrivner and Bottjer (1986). In sediments of Barstovian age, *Pseudaelurus* was the only felid genus present to leave tracks, but four or more other genera were present in Clarendonian and Hemphillian time.

Felipeda bottjeri, ichnosp. nov.

Plate 10; Text-figures 17-18

1986 *Bestiopedina* sp. D Scrivner and Bottjer, p. 300, fig. 4D

1993 Huella de *Pseudaelurus*. Lockley, Anton and Nieves, p. 59, unnumb. fig.

Diagnosis. Tetradactyl mammal tracks, plantigrade, with four digital impressions. These form an arc of about 60° span in front of the impressions of metacarpal pads and metatarsal pads, with which they are not in contact. The gap separating digits III and IV from the metacarpal and metatarsal pads is about twice that separating II and V from the metacarpal and metatarsal pads; these latter are broadly ovoidal to almost circular, without conspicuous indentations. Claw impressions may be present either on manus or pes, or may be lacking.

Derivation of Name. In tribute to David J. Bottjer, joint author of an important study of Californian Neogene footprints.

Holotype. Specimen V.94276/103, Raymond M. Alf Museum, Webb Schools, Claremont, California (Plate 10, figure a; Text-figure 17, left). Paratype (presumed right manus): V.94276/104, same lodgement (Plate 10, figure d; Text-figure 17, right). Figured specimens: V.94281/275 (Plate 10, figure c-d) and V.94276/181 (pl. 10, fig. f).

Type Horizon and Locality. Miocene (Barstovian), Barstow, San Bernardino County, California.

Dimensions. Holotype (presumed right pes): overall length 75 mm, overall breadth 58 mm. Length of digits: II, 20 mm; III, 21 mm; IV, 20 mm; V, 19 mm. Paratype: overall length 74 mm, overall breadth 62 mm. Length of digits, exclusive of claws: II, 21 mm; III, 24 mm; IV, 20 mm; V, 22 mm; with claws: II, 25 mm; III, 30 mm; IV, 24 mm; V, 25 mm. Figured specimens: V.94231/275. Overall length 80 mm, overall breadth 67 mm. Length of digits: II, 20 mm; III, 22 mm; IV, 22 mm; V, 21 mm. V.94276/102: Overall length 68 mm, overall breadth 58 mm. Length of digits: II not measureable (damaged); III, 18 mm; IV, 18 mm; V, 17 mm.

Divarication of Digits. See Text-figure 18.

Remarks. Though specimens of *Felipeda bottjeri* are quite numerous in the Raymond M. Alf Museum collections—around twenty specimens—all are single prints. Consequently, though it is presumed that the pes is likely to be less large than the manus, the discrimination of pedal from manual imprints is

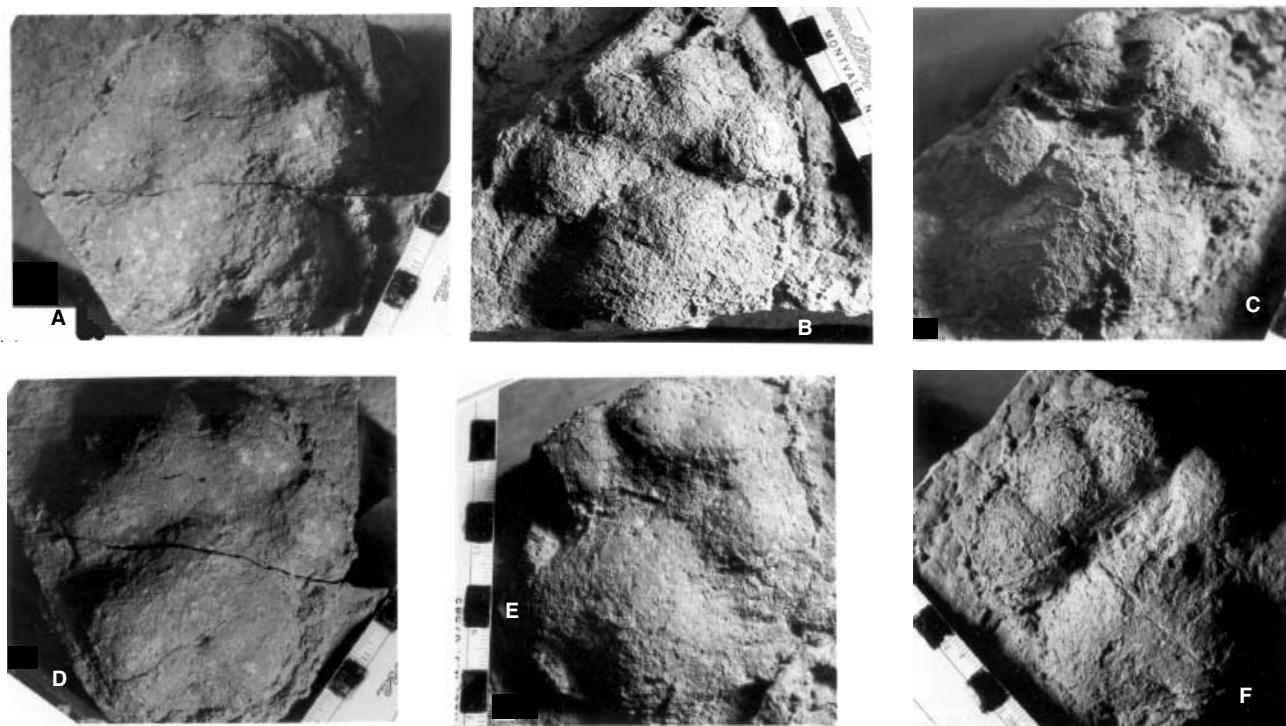


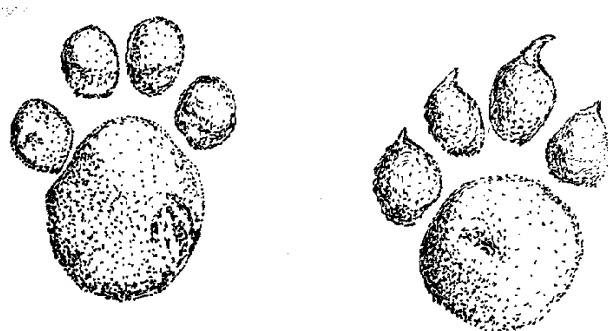
PLATE 10. *Felipeda bottjeri* Sarjeant, Reynolds and Kissell-Jones, ichnosp. nov. (a) Specimen V.94281/275; (b) the paratype, V.94276/104; (c) the holotype, V.94283/103; (d) specimen V.94281/275; (e) specimen V.94276/102; (f) specimen V.94283/182.

questionable. The claws were clearly retractile and are only sometimes impressed; for this reason, a holotype without claw impressions was selected.

Felipeda bottjeri differs from *F. scrivneri* in its more elongate shape and lesser digital span, also in the more variable digital shape and their degree of separation from metacarpal pads and metatarsal pads. It differs from the illustrations of *F. felis* Panin, 1965—the text is unhelpful—in that the latter exhibits digital pads with more acute distal extremities.

These footprints appear to correspond with those described as *Bestiopedia* sp. D from the Hemphillian of Death Valley (Scrivner and Bottjer 1986), though their illustration (fig. 4D) does not permit complete confidence. *F. bottjeri* accords quite well with the *Pseudaelurus* footprint figured by Lockley *et al.* (1993), in a general paper on Spanish Tertiary footprints. In the Hemphillian LMA of North America, the true genus *Felis* appears, along with five other genera of Felidae and the last record of the genus *Pseudaelurus*.

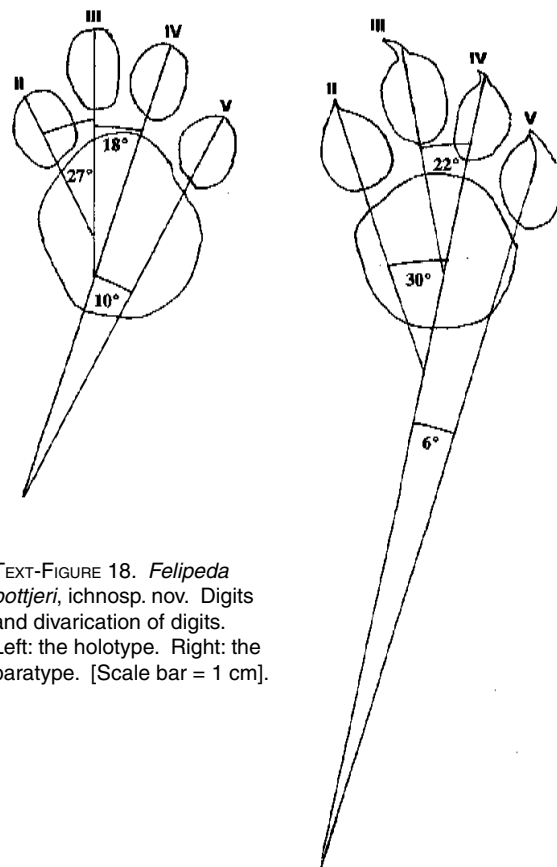
FAMILY CANIDAE



TEXT-FIGURE 17. *Felipeda bottjeri*, ichnosp. nov. Left: the holotype, cast of presumed right pes. Right: the paratype, cast of presumed right manus, with claws impressed. [Scale bar = 1 cm].

Ichnogenus *Canipeda* Panin and Avram 1962, emend. nov.
 1962 *Canipeda*. Panin and Avram, p. 461-462.
 1999 *Chelipus* Remeika, p. 46.

Original Diagnosis (generico-specific). “Total length of



TEXT-FIGURE 18. *Felipeda bottjeri*, ichnosp. nov. Digits and divarication of digits. Left: the holotype. Right: the paratype. [Scale bar = 1 cm].

the footprint is 61 mm, its maximum breadth 32 mm. It shows impressions of four digital pads, oval, closely spaced, having dimensions in the range 13-14 mm digital length and 8-9 mm digital breadth. The total length and breadth from metacarpal pads tip to heel is 27 mm. Between heel and digits 2 and 3 is a distance of 8-9 mm. One may perceive that the digits have strong claws, non-retractile, having a length of 8-11 mm.” (Panin and Avram, 1962, p. 461, new transl.)

Emended Diagnosis. Semidigitigrade footprints exhibiting four digits (II to V), each with an ovoidal to elongate digital pad. The digital pads form an arc in front of the metatarsal pads and the digital pads are arranged in a bilaterally symmetrical pattern along the anterior/posterior axis. Digital pads may be of equal or similar size or may show limited dimensional variation. Impression of claws are consistently present and typically separated by a gap from the digital pads.

Type Ichnospecies. *Canipeda longigriffa* Panin and Avram, 1962, p. 461-462, pl. 2, fig. 16. Miocene (Vindobonian), Romania.

Other Included Ichnospecies.

Canipeda amphicyonides (Thenius, 1967) Sarjeant, Reynolds and Kissell-Jones, comb. nov. (= *Bestiopedia amphicyonides* Thenius, 1967, p. 368-372, pl. 2, fig. 1; pl. 3, fig. 1; text-figs. 1-2). Pliocene, Austria.

Canipeda gracilis (Vialov, 1966) Sarjeant, Reynolds and Kissell-Jones, comb. nov. (= *Bestiopedia gracilis* Vialov, 1966, p. 134, pl. 36, fig. 2, text-fig. 47). Miocene (Burdigalian), Ukraine.

Canipeda therates (Remeika, 1999), Sarjeant, Reynolds and Kissell-Jones, comb. nov. (= *Chelipus therates* Remeika, 1999 p. 42-43, fig. 8), early Pleistocene, Anza-Borrego Desert, California.

Remarks. The diagnosis of Panin and Avram, with its inclusion of such precise measurements, was essentially limited to a single specimen. It is here expanded to incorporate other canoid footprint types. Of similar ichnogenera, the genus *Tetraostobopus* Sarjeant and Langston, 1994 differs in that digit V is lateral to the metatarsal pads, while in *Falcatipes* Sarjeant and Langston, 1994, the claws curve inward.

Canoid footprints have been much less commonly reported world-wide than feloid footprints. None of the tracks previously reported from western North America are those of canoids. R.M. Alf's collections contain a single imprint which he identified as a “dog footprint”: but he did not publish any record of this. It is described below.

Canipeda sp. A

Plate 11; Text-figures 19–20

Description. A relatively small mammal footprint, semi-plantigrade and of broadly ovoidal outline. Each digit bears a single pad, essentially ovoidal but slightly truncate proximally. The digital pads form a 60° arc about the front of the metatarsal pads; the clawmarks are distinct, acute and inwardly directed. Anterior part only of metatarsal pads impressed.

Figured Specimen. V.94283/183 (presumed left manus), Raymond M. Alf Museum, Webb Schools, Claremont, California.

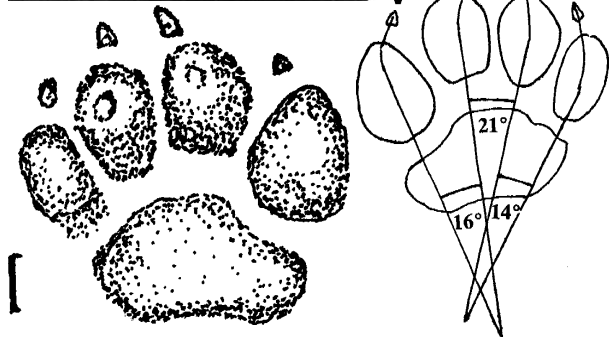
Horizon and Locality. Barstow Formation (Miocene: Barstovian), Barstow, San Bernardino County, California.

Dimensions. Overall length 57 mm, overall breadth 57 mm. Length of digits, with claws: II, 27 mm; III, 27 mm; IV, 28 mm; V, 30 mm; without claws: II, 20 mm; III, 21 mm; IV, 20 mm; V, 23 mm.



PLATE 11. *Canipeda* sp. A, specimen V.94283/183.

TEXT-FIGURE 19. *Canipeda* sp. A Digits and interdigital angles. [Reversed from casts].



TEXT-FIGURE 20. *Canipeda* sp. A Specimen V.94283/183. [Scale bar = 1 cm].

Divarication of Digits. See Text-figure 20.

Remarks. This footprint, though proportionately broader, is otherwise quite comparable to that of the living African civet, *Civettictis civetta* (see Walker, 1996), which likewise sports claws that converge inward. The most common small canoid recovered as a body fossil from the Barstow Formation is the generic group referred to as “*Tomarctus*” (Savage and Russe

Canipeda sp. B

Plate 12; Text-figures 21–22

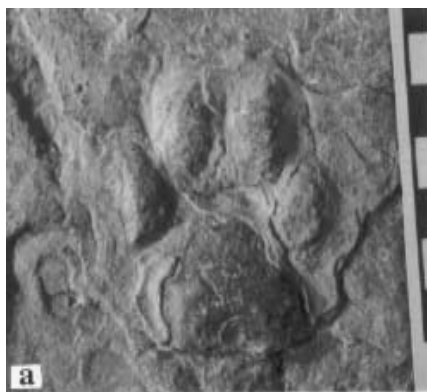
Description. A relatively small tetradactyl mammal footprint, plantigrade and of ovoidal outline overall. Each digit bears a single pad, of elongate ovoidal outline. At the apex of each pad, the impression of a claw tip may be seen. Digits II-IV are directed forward, digit V slightly outward. Span of digits narrow (33°). A broad gap separates the digital pads from metacarpal pads (or metatarsal pads); the latter is tri-lobed like a club (in the card-player's sense) and gives indication of metacarpal/metatarsal position.

Figured Specimen. UNLV-HS-2(1), University of Nevada, Las Vegas, Nevada.

Horizon and Locality. Thumb Member, Horse Spring Formation (Miocene, Barstovian LMA), near Lake Mead National Recreation Area, southern Nevada, UNLV-HS-2.

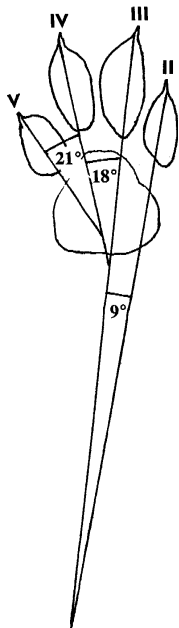
Dimensions. Overall length: 59 mm, overall breadth 41 mm. Length of digits: with claws, II, 18 mm; III, 26 mm; IV,

PLATE 12.
Canipeda sp. B



TEXT-FIGURE 21. *Canipeda* sp. B
[Scale bar = 1 cm].

TEXT-FIGURE 22. *Canipeda* sp. B
D digits and interdigital angles.
[Reversed from casts].



28 mm; V, 22 mm; without claws, II, 16 mm; III, 18 mm; IV, 23 mm; V, 18 mm.

Divarication of Digits. See Text-figure 22.

Remarks. This single cast of a right foot may be manus or pes with claw tips impressed, as in a canoid. In size and proportions, this footprint is very like that of the coyote and African jackals (Rezendes, 1999; Walker, 1996, p. 53, 55). In contrast to *Canipeda* sp. A, this print is narrower, the digits are smaller and their length is more variable. "*Tomarctus*" is known from the Barstovian LMA sediments from southwestern North America.

Summary

The North American Tertiary fossil record of meat-eating mammals starts with miacid carnivores in the early Paleozoic. By late Paleocene and Eocene, members of the order Creodonta became abundant and diverse, including the Hyaenodontidae and Oxyaenidae. The creodonts apparently failed to compete with the Carnivora and the last North American hyaenodont became extinct in the late Oligocene. The primitive foot structure of the hyaeno-

donts, plantigrade feet which retained five digits, persisted until that time. Carnivora started with primitive plantigrade feet.

By the latest Eocene, the modern families of Carnivora are recognized in North America. Miacidae, Amphicyonidae, Ursidae, Procyonidae, and Mustelidae retained five digits with a plantigrade or semi-plantigrade stance. The more derived Felidae and Canidae developed a semi-digitigrade stance on four digits. Canidae generally appear to have more bilateral symmetry than the Felidae, perhaps due to locomotor adaptations.

Early Tertiary creodonts and carnivores had primitive foot characteristics and are not easily distinguishable except on the basis of size, gracility, or robustness. In the late Tertiary, prints with five digits have been referred to Mustelidae, Procyonidae, Ursidae and, if of exceptional size, Amphicyonidae. Late Tertiary prints with four digital impressions are referred to feloids if they are approximately equi-dimensional and do not have pronounced bilateral symmetry. If the Late Tertiary prints are ovate-elongate, bilaterally symmetrical, with impressed claws, they are referred to canoids.

Acknowledgements

The work of the first author was begun in January 1995 during sabbatical leave from his duties at the University of Saskatchewan and with the support of a sabbatical travel grant. He is very much indebted to Dr. Donald Lofgren, Director of the Raymond M. Alf Museum, Webb Schools, Claremont, California, for help during his visit and subsequently, and to Don's colleague Judy Mercer for help during the visit and for providing data at later stages of this research. Lofgren and Natalia Wigmann are also thanked for their careful attention to locality numbers of Alf Museum specimens. The collaboration of Sarjeant and Reynolds began during the first author's visit to Redlands and has continued amicably since; this third project, in which Kissell-Jones has joined, concludes their joint work.

The first author is very much indebted to his research assistant, Mrs. Linda Dietz, for help in production of the manuscript. We are both indebted Mr. Alexander Dietz and Dr. Patrick B. Cashman (Krydor, Saskatchewan) for translating Russian taxonomic passages.

Our thanks are offered also to Mary Aruta and Peggy Eby, San Bernardino County Museum, for processing specimens from field to catalogued repository. Thanks, too, to Don

Table I. Age distribution of Creodont and Carnivore Ichnotaxa.

Taxa referenced, this paper	PALEOCENE	EOCENE	OLIGOCENE					PLIOCENE	PLEISTOCENE
			Arikarean	Hemingfordian	Barstovian	Clarendonian	Hemphillian		
			MIOCENE						
<i>Quiritipes impendens</i>		•							
<i>Hirpexipes alfi</i>					•				
<i>Platykopus ilycalator</i>							•		
<i>Pycnodactylopus achras</i>						•			
<i>Felipeda scrivneri</i>							•		
<i>Felipeda bottjeri</i>							•		
<i>Canipeda</i> sp. A					•				
<i>Canipeda</i> sp. B					•				

Lofgren of the Alf Museum for his thoughtful review of the manuscript, and to Jennifer Reynolds for patient editing and manuscript preparation.

Most photographs were taken, and most drawings made, by the first author. We accept joint responsibility for all opinions expressed, whether correct (as we trust) or erroneous!

References Cited

- Alf, Raymond M., 1959. Mammal footprints from the Avawatz Formation, California. *Bulletin of the Southern California Academy of Sciences*, vol. 58, pt. 1, pp. 1-7, pls. 1-4.
- Alf, Raymond M., 1966. Mammal trackways from the Barstow Formation, California. *Bulletin of the Southern California Academy of Sciences*, vol. 65, no. 4, pp. 258-64, figs. 1-4.
- Aramayo, Silvia A. & Bianco, Teresa M. de., 1987. Hallazgo de una icnofauna continental (Pleistoceno Tardío) en la Localidad de Pehuen-Có (partido de Coronel Rosales), Provincia de Buenos Aires, Argentina. Parte II. Carnívora, Artiodactyla y Aves. IV Congreso Latinoamericano de Paleontología, Bolivia 1987, vol. 1, pp. 532-547, figs. 1-12.
- Bjork, P.R., 1976. Mammalian tracks from the Brule Formation of South Dakota. *Proceedings of the South Dakota Academy of Sciences*, vol. 55, pp. 154-158.
- Curry, H. Donald, 1941. Mammalian and avian ichnites in Death Valley. *Bulletin of the Geological Society of America*, vol. 52, Abstr. p. 1979.
- Czaplewski, N.J., 1990. The Verde Local Fauna: small vertebrate fossils from the Verde Formation, Arizona. *San Bernardino County Museum Association Quarterly*, vol. 37, no. 3, p. 39.
- Dugès, Alfredo, 1894. *Felis fossilis* de San Juan de Los Lagos. *Naturaleza*, vol. 2, pp. 421-423.
- Johnston, C. Stuart, 1937. Tracks from the Pliocene of west Texas. *American Midland Naturalist*, vol. 18, no. 1, pp. 147-152, pls. 1-3.
- Kordos, L., 1985. Lábnymok az ipolytarnóci alsó-miocén korú homokköben. *Geologica Hungarica*, ser. Palaeontologica, vol. 46 (1983), pp. 259-415.
- Lockley, Martin G., Antón, Mauricio and Nieves, José M., 1993. CIENCIA: ¿Quién paso por aquí hace 20 millones de años? *Blanco Negro*, vol. 102, pp. 56-65.
- Lockley, Martin G. and Hunt, Adrian P., 1995. *Dinosaur tracks and other fossil footprints of the western United States*. New York: Columbia University Press, xx+338 pp.
- Nininger, H. H. 1941. Hunting prehistoric lion tracks in Africa. *Plateau*, 14(2):21-27, 1 fig.
- Panin, N., 1965. Coexistence de traces de pas de vertébrés et des mécanoglyphes dans la molasse Miocène des Carpates Orientales. *Revue Roumaine de Géologie, Géophysique et Géographie*, ser. Géologie, vol. 9, pp. 141-163.
- Panin, N. and Avram, E., 1962. Noe urme de vertebrate in Mioconul Subcarpatilor Romine ti. *Studii Cercetari de Geologie*, vol. 9, pp. 455-484.
- Peabody, Frank E. 1959. Trackways of living and fossil salamanders. *Univ. Calif. Publ in Zool.*, 63(1): 1-72. Pls. 1-11, 9 figs in text.
- Remeika, Paul, 1999. Identification, stratigraphy, and age of Neogene vertebrate footprints from the Vallecito-Fish Creek Basin, Anza-Borrego Desert State Park, California. *San Bernardino County Museum Association Quarterly*, vol. 46, no. 2, p. 37-46
- Rezendes, Paul, 1999. *Tracking and the Art of Seeing*. Willowdale, Ontario: Firefly Books, 336 p.
- Robertson, George M. and Sternberg, George F. 1942. Fossil mammal tracks in Graham County, Kansas. *Transactions Kansas Academy of Science*, vol. 45, p. 258-261, figs. 1-5.
- Russell, Loris S., 1930. Early Tertiary mammal tracks from Alberta. *Transactions of the Royal Canadian Institute*, vol. 17, pp. 217-221.
- Rutherford, Ralph L. and Russell, Loris S. 1928. The mammal tracks from the Paskapoo beds of Alberta. *Amer. Jour Sci.*, 15:262-264.
- Santucci, V.L. and Nyborg, T.G., 1999. Paleontologic resource management, systematic recording, and preservation of vertebrate tracks within Death Valley National Park, California. *San Bernardino County Museum Association Quarterly*, vol. 46, no. 2, p. 21-26.
- Sarjeant, William A.S. and Langston, Wann, Jr., 1994. Vertebrate footprints and invertebrate traces from the Chadronian (Late Eocene) of Trans-Pecos Texas. *Texas Memorial Museum Bulletin*, no. 36, 86 pp., 25 pls., 52 text-figs.
- Sarjeant, William A.S. and Reynolds, R.E., 1999. Camel and horse footprints from the Miocene of California. *San Bernardino County Museum Association Quarterly*, vol. 46, no. 2, p. 3-20.
- Sarjeant, William A.S. and Reynolds, R.E., 2001. Bird footprints from the Miocene of California, IN *The Changing Face of the East Mojave Desert*, R.E. Reynolds, editor. California State University Desert Studies Consortium, p. 21-40.
- Sarjeant, William A.S. and Wilson, J.A., 1988. Late Eocene (Duchesnean) mammal footprints from the Skyline Channels of Trans-Pecos Texas. *Texas Journal of Science*, vol. 40, pp. 439-446.
- Savage, D.E. and Russell, D.E., 1983. Mammalian paleofaunas of the world. Reading, Addison-Wesley, 432 p.
- Scrivner, Paul J., and Bottjer, David, 1986. Neogene avian and mammalian tracks from Death Valley National Monument, California: their context, classification and preservation. *Palaeogeography, Palaeoclimatology, Palaeoecology*, vol. 57, pp. 285-331, figs. 1-16.
- Simpson, George G., 1941. Discovery of jaguar bones and footprints in a cave in Tennessee. *SAmerican Museum Novitates*, no. 1131, pp. 1-12.
- Thenius, E. 1967. Säugetierfährten aus dem Rohrbacher Konglomerat (Pliozän) von Niederösterreich. *Ann. naturhist. Mus. Wien*, 71, p. 363-379, figs. 1-3, pls. I-IV.
- Vialov, O.S., 1966. Sledy zhiznedeiatel'nosti organizmow i ikh paleontologicheskoe znachenie. [Activity traces of organisms and their palaeontological meaning]. *Institut Geologie i Geocimii gwayac iskopaemuse Akademya Nauk Ukrainskoi USSR*. pp. 5-214, pls. 1-53, figs. 1-51, tabs 1-4.
- Walker, Clive, 1996. *Signs of the Wild*. 5th edition. Cape Town, South Africa: Struik Publishers, 213 pp.
- Woodburne, M.O., 1991. The Cajon Valley, IN *Inland Southern California: the last 70 million years*, M.O. Woodburne, R.E. Reynolds and D.P. Whistler, eds. *San Bernardino County Museum Association Quarterly*, vol. 38, nos. 3, 4, p. 49-51.

Preliminary Report on the Stratigraphic Setting and Microstructure of Avian Eggshell Fragments from the Calico Mountains: Barstow Formation, Mojave Desert, California

V. Leroy Leggitt, *Department of Natural Sciences, Loma Linda University, Loma Linda, CA 92350*

Abstract

This is the first report of avian eggshell from the Middle Miocene Barstow Formation. The eggshell occurs in a widespread limestone marker unit at the base of the middle member of the Barstow Formation in the Calico Mountains. The limestone marker can be correlated with the type section of the Barstow Formation in the Mud Hills (about 17 km northwest of the Calico Mountains). Facies changes in the limestone marker are frequently observed. These variations include lacustrine layered limestone, beach flat pebble conglomerate, spring-deposited tufa mounds, tufa coated branches and microbial bioherms up to 2 m in diameter. These facies suggest a nearshore paleoenvironment. The eggshell is not associated with any vertebrate bones or embryos at the study site.

The eggshell was studied by light microscopy (LM), by polarized light microscopy (PLM), and by scanning electron microscopy (SEM). The resultant micrographs were compared with published reports of modern and fossil "ornithoid", "crocodilliod", "testudoid" and "geckoid" eggshell.

The Calico Mountains fossil eggshell shows the following microstructure zones (from internal to external): 1) an organic core, 2) a zone of radial calcite plates, 3) a zone of tabular crystallite plates, 4) a zone of squamatic aggregates and 5) an external zone of vertical crystals. Macrostructure zones (from internal to external) are: 1) wedges of the mammillary layer (diverging outward from the central core), grading into 2) long vertical columns of the prismatic layer. These findings are consistent with modern neognathous eggshell.

The absence of associated vertebrate bones or embryos provided few clues to the origin of the Barstow Formation eggshell. This SEM study suggests that the eggshell is of avian origin.

Introduction

The purposes of this paper are: 1) to determine the origin of eggshell fragments found in the Calico Mountains and 2) to place these eggshell fragments in their stratigraphic setting. The study sites are shown in Figure 1. Site A is in the Mud Hills, site B is at Hill 3370 and site C is in the Calico Mountains.

Barstow Formation sediments are exposed in disjunct outcrops across the central Mojave Desert. Exposures are found in the Gravel Hills, Mud Hills, Calico Mountains, Yermo Hills and Alvord Mountains (Woodburne et al., 1990). The Barstow Formation is unconformable with the underlying Miocene Pickhandle Formation, and with overlying Pliocene basalt and Quaternary alluvium (MacFadden et al., 1990). At the type section in the Mud Hills, the Middle Miocene Barstow Formation consists of 1000 m of fluvial and lacustrine sediments with intercalated water-laid air-fall tuffs. Some of the more distinctive tuff beds are used as time-synchronous marker units for correlation and to divide the formation into three members. This paper follows the lead of Woodburne et al. (1990) in recognizing: 1) the Owl Conglomerate Member, 2) the middle member and 3) the upper member of the Barstow Formation. The Barstow Formation is folded into a broad east-west trending syncline that is cut by several northwest trending right lateral faults.

Significant marker tuff units that occur close to Barstow Formation member boundaries have been assigned isotopic ages (Woodburne et al., 1990; MacFadden et al., 1990). For example, the Red Tuff occurs near the base of the Owl Conglomerate

Member and has been isotopically dated at 19.3+/-0.02 Ma, the Rak Tuff occurs near the base of the middle member and has been isotopically dated at 16.3+/-0.3 Ma, the Skyline Tuff (of Sheppard and Gude, 1969) occurs near the base of the upper member. About 18 m above the Skyline Tuff is the Dated Tuff (of Sheppard and Gude, 1969) that has been isotopically dated at 14.8+/-0.1 Ma. These time-synchronous marker units are most useful for correlation among Barstow Formation outcrops in the Mud Hills.

In other Barstow Formation outcrops (especially in the Calico Mountains), these tuff marker units are difficult to identify with certainty. In response to this problem, Reynolds (2000, 2001) proposed several time-transgressive marker units that seem to adequately correlate Barstow Formation sediments in the Mud Hills with those in the Calico Mountains. In ascending stratigraphic order, these units are: 1) the MSL (massive stromatolite limestone), 2) the BPL (a series of three brown platy limestone units) and 3) the SBH (strontium-borax horizon). Leggitt (2000) reported three-dimensional silicified fossils (arachnid, water beetle larvae and ostracods) from concretions in the Mud Hills that correlate with the concretions that contain three-dimensional arthropods from the Calico Mountains (Palmer and Basset, 1954; Palmer, 1957, 1960; Park, 1995). The unique mode of preservation of these fossils enables them to be used for correlation between the Mud Hills and the Calico Mountains (Fig. 2). The arthropod marker unit occurs just below Reynold's SBH marker.

Despite abundant reports on the fauna, flora and ichnofos-

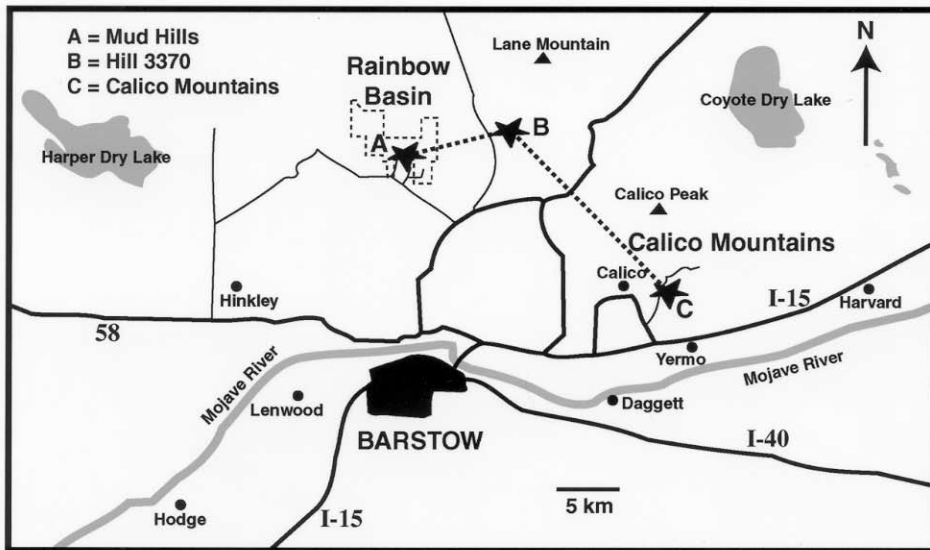


Fig. 1 Location map. Black stars and letters (A, B, C) mark the location of the measured sections (see Fig. 2). The heavy dotted line indicates the correlation line.

sils of the Barstow Formation, little is known about the sauropsids (birds and reptiles). Merriam (1919), Miller (1952, 1966) and Lindsey (1972) and have reported avian and reptilian fossils from several sites in the Mud Hills.

Merriam (1919) reported common land tortoise fragments and several partial plastrons and carapaces of the tortoise, *Testudo mohavense*. Merriam (1919) reported fragmentary remains of birds that included pieces of three bones (tarsometatarsus, femur and tibiotarsus) from two collecting sites. Although the bones are fragmentary, they may be referable to *Buteo*, a buteonid hawk. Miller (1952, 1966) described 14 avian bones from 6 orders of birds: Ciconiiformes, Anseriformes, Falconiformes, Galliformes, Podicipediformes, and Charadriiformes. Lindsey (1972) reported avian remains from 6 collecting sites, and reptilian remains from 7 collecting sites, but he did not describe the fossils. Lindsey's collecting sites were from the middle and upper members of the Barstow Formation in the Mud Hills.

Other traces of birds have been reported from the Barstow Formation. These fossils include: 1) tracks (Alf, 1966; Woodburne et al., 1990; Reynolds, 1998), 2) feathers (Pierce, 1959; Leggitt, 2000) and 3) an interior mold of an egg (Reynolds, 1998). The tracks were reported by Alf (1966) as "several prints of a bird" and by Reynolds (1998) as "three ichnomorphs". These tracks were likely found in the Mud Hills. The feathers were reported by Pierce (1959) as "three impressions, and two crystallized feathers" (from the Calico Mountains concretions) and by Leggitt (2000) as "a silicified feather fragment" (from the Mud Hills concretions). Reynolds (1998) reported "the interior mold of a duck-size egg" from the Calico Mountains. This egg fossil is likely referable to the flamingos but lacks preserved eggshell (Reynolds, 1998).

Methods

The eggshell fragments were inadvertently discovered while cutting hand samples of a limestone marker unit (Reynold's MSL) for other research purposes. Standard thin-sections and SEM mounts were prepared for microscope analysis. Although

several eggshell fragments were found, this paper reports micrographs (SEM, PLM) from a single eggshell fragment. A single fragment was analyzed in order to eliminate the possibility of mixing sauropsid eggshell types. As a consequence, it is possible that the other fragments are not avian.

Radial cross-sections of the eggshell fragment were studied in order to view and describe the basic shell unit of the fossil eggshell. The microstructure of the eggshell fragment was compared with published descriptions of sauropsid eggshell (Mikhailov, 1997) in order to determine if the Calico Mountains eggshell was "ornithoid", "crocodilloid", "testudoid" or "geckoid" (Fig. 3). Furthermore, the Calico Mountains eggshell was compared with modern "ornithoid", "crocodilloid" and "testudoid" eggshell (Fig. 4).

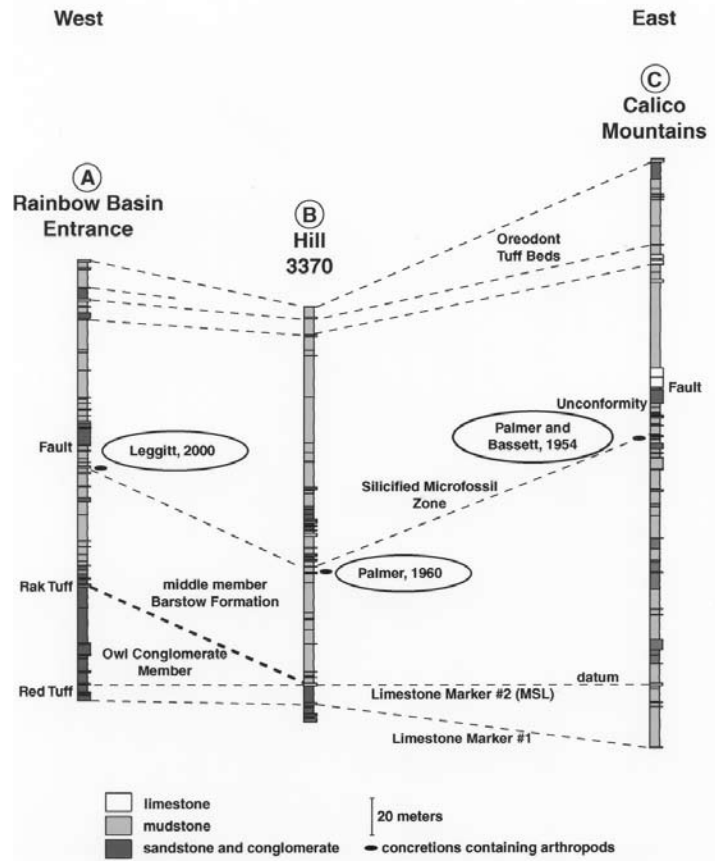


Fig. 2 Correlation of measured sections. These are partial sections of Barstow Formation rocks in the study area (between the limestone markers and the Oreodont Tuff beds). Limestone marker unit #2 is the datum. References are to the first description of concretions containing three-dimensional microfossils (arthropods etc.) at the indicated section. Horizontal distance between sections is not to scale.

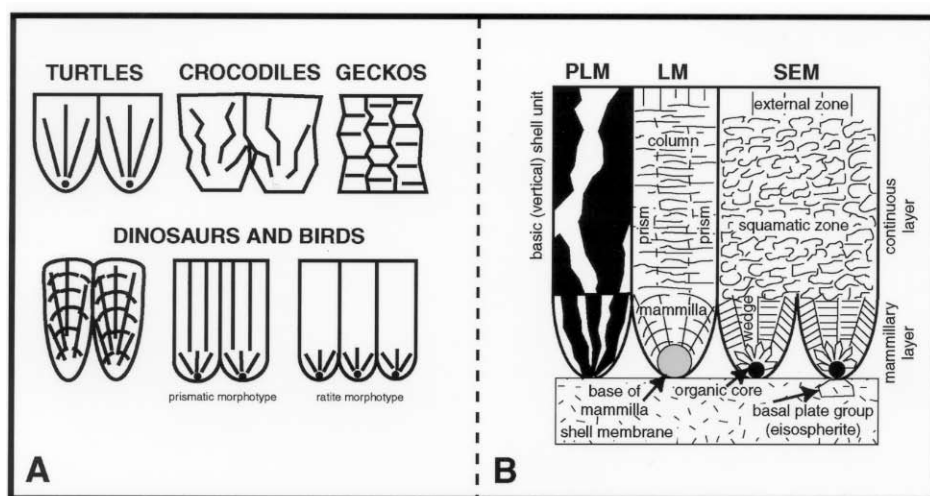


Fig. 3 A. Sauropsid eggshell basic shell units. Turtles; the entire shell unit is made of aragonite crystals that radiate outward from an organic core. Crocodiles; the entire shell unit is composed of a large wedge of calcite crystals that diverge outward. There is no organic core. Geckos; the shell unit does not contain radiating crystal structure. There is no organic core. Dinosaurs and birds; the basic shell unit shows two main layers: 1) an internal mamillary layer, and 2) an external prismatic or continuous layer. The mamillary layer has an organic core, and there may be an external layer of vertical calcite crystals that is external to the continuous layer. B. Avian basic shell unit terminology. PLM = polarized light microscopy, LM = light microscopy, SEM = scanning electron microscopy. All drawings show the internal surface of the eggshell toward the bottom of the page. Modified from Mikhailov (1997).

Standard stratigraphic sections (Fig. 2) were measured in the Calico Mountains, Mud Hills and Hill 3370 (located half way between the Calico Mountains and the Mud Hills). The section in the Mud Hills was measured on the south limb of the Barstow Syncline at the entrance road to Rainbow Basin. The section in the Calico Mountains was measured on the west side of Mule Canyon. Both Hill 3370 and Mule Canyon sections are on the north limb of the Barstow Syncline.

Description of the Eggshell Fragments

The eggshell fragments are 0.5 mm thick. The fragment studied is 1.5 cm long and slightly convex toward the external surface of the eggshell (note the white arrow in Fig. 5E). The fragments are dark black in color and contrast with the gray limestone matrix. All the eggshell fragments occur in two hand samples from limestone marker unit #2 (Reynold's MSL) in the Calico Mountains. The fragments may represent a highly localized fossil concentration (perhaps derived from a single egg) because samples from adjacent areas of limestone marker unit #2 revealed no other eggshell fragments.

Polarized light microscopy (Fig. 5F) shows a basic shell unit that is identical with Mikhailov's (1997) description of "ornithoid" eggshell (Fig. 3A,B). The ratio of the thickness of the continuous layer (CL) to the thickness of the mamillary layer (ML) is 2:1, and the external layer is about 1/3 the thickness of the mamillary layer. The basic shell unit is as wide as the thickness (height) of the mamillary layer. The internal surface of the eggshell is tightly scalloped and reflects the tightly packed mamilla that is characteristic of the "ornithoid" basic shell unit. A single basic shell unit is outlined in Fig. 5F. The black dotted

line outlines a single mamilla, the dotted white lines show the basic shell unit upwards into the continuous layer and the external layer. At the base (apex) of the mamilla (Fig. 5F-1,5) there is a dark organic core surrounded by a circular zone of radial calcite plates. In Figure 5F-5 this complex is circled with a black dotted line. Extending upward from this circular zone of radial calcite plates is a wedge shaped zone of calcite crystals that terminate at the ML/CL junction. Above this junction in the continuous layer, the calcite crystals are more perpendicular to the external surface of the eggshell. The

external surface of the eggshell is smooth and slightly curved. Pores cannot be seen in the studied sections.

Scanning electron microscopy (Fig. 6) shows a basic shell unit that is identical with Mikhailov's (1997) description of "ornithoid" eggshell (Fig. 3A,B). The CL to ML ratio is 2.2:1 and the external layer is 1/3 the thickness of the ML. The mamilla with organic core, radial calcite plates and radiating tabular calcite crystals is clearly visible (Fig. 6A-D). The continuous layer shows vertical fracturing that can be described as columnar or prismatic. The external layer is visible as vertically aligned flat calcite crystals (Fig. 6F). These features are characteristic of a prismatic morphotype (Fig. 3A).

Comparison of the fossil eggshell (Figs. 5,6) with modern sauropsid eggshell (Fig. 4) shows that the Calico Mountains eggshell most resembles avian (chicken) eggshell (with a prismatic morphotype). The Calico Mountains eggshell is distinguished from crocodylian and testudoid eggshell because the fossil eggshell has distinct mamillary, and continuous layers. The Calico Mountains eggshell is more like chicken eggshell than ostrich eggshell because the continuous layer of the fossil eggshell is composed of prisims and columns (ostrich eggshell is more homogenous in the continuous layer).

Correlation and Stratigraphy

The eggshell fragments occur in the top 10 cm of a 1 m thick limestone unit (Fig. 2, limestone marker #2) that outcrops in the Calico Mountains, at Hill 3370 and in the Mud Hills (Fig 5A,B). Several criteria are used to distinguish this unit: 1) 1-2 m thick ledge-forming gray limestone, 2) abundant chert nodules, 3) wavy layering, 4) abundant flat pebble conglomerate, 5) microbial tufa bioherms (large layered mounds up to 2 m thick), 6) tufa coated branches (in coarse grained rocks at the inferred lake margin), 7) spring-deposited tufa mounds (isolated, in coarse grained rocks at the inferred lake margin), 8) mudcracks and 9) a 10-20 cm thick external coating of tufa that weathers with a characteristic vertical tube pattern (Fig. 5E).

In the Mud Hills, on the south limb of the Barstow Syncline (in the coarse grained Owl Conglomerate Member) limestone marker #2 occurs as isolated patches of thick gray limestone (Fig. 5A), or more commonly as lake margin tufa coated branches, or spring-deposited tufa mounds. The thick gray lacustrine limestone is easily physically correlated with the tufa coated branches and the isolated spring-deposited tufa. The

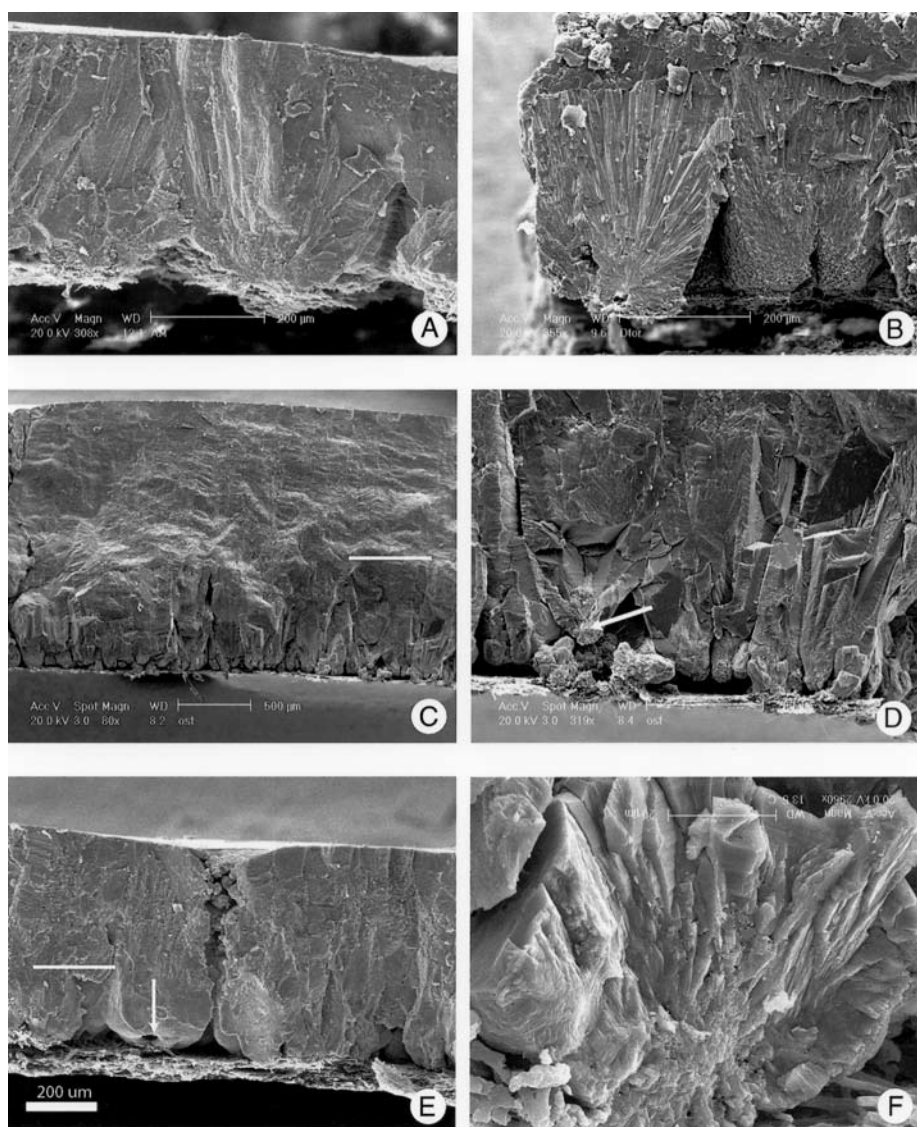


Fig. 4 SEM micrographs of some sauropsid eggshell in radial cross-section. A. American alligator (*Alligator mississippiensis*) eggshell illustrating the “crocodilloid” basic shell unit. Note the loosely packed basic shell units and the wide wedges of tabular calcite crystals that make up the basic shell unit. There is no organic core. B. Desert tortoise (*Gopherus agassizii*) eggshell illustrating the “testudoid” basic shell unit. Note the long aragonite crystals that make up the entire shell unit. An organic core is present. C. Ostrich (*Struthio camelus*) eggshell (ratite morphotype) illustrating one type of “ornithoid” basic shell unit. The white bar shows the division between the lower mamillary layer, and the upper continuous layer. D. Mamillary layer of ostrich eggshell. The arrow points to the organic core. Note the tabular calcite crystals that are stacked outward and upward to form the mamilla. E. Chicken (*Gallus gallus*) eggshell (prismatic morphotype) illustrating the second type of “ornithoid” basic shell unit. The white bar shows the division between the lower mamillary layer and the upper prismatic layer. The white arrow points to the organic core at the apex of the mamilla. F. Cross-section through a mamilla (chicken). Note the tabular calcite crystals that are stacked outward and upward to form the mamilla.

spring-deposited tufa mounds were recently studied by several authors (Rasbury et al., 1999; Becker et al., 2001). Limestone marker # 2 occurs about 4 m above the Red Tuff.

At Hill 3370, on the north limb of the Barstow Syncline (at the base of the middle member of the Barstow Formation) limestone marker #2 occurs as a 10 cm thick brown limestone ledge that contains bioherms or mounds up to 1.5 m tall. Chert and tufa coated twigs and branches are common. The unit is capped with a 10-20 cm thick tufa that weathers with a characteristic vertical tube pattern. The small tubes are 1-3 mm in diameter. The Red Tuff is not easily distinguishable at Hill 3370, and likely is located lower in the section within the underlying Pickhandle Formation.

In the Calico Mountains, on the north limb of the Barstow Syncline (in the fine-grained middle member of the Barstow Formation) limestone marker #2 occurs as a 1-2 m thick ledge of gray limestone and chert. Wavy lamination, flat pebble conglomerate, and biohermal thickenings of the unit are common. Tufa coated branches are rare in limestone marker #2 in the Mule Canyon area, although occasionally limestone marker #2 thins and contains large accumulations of tufa coated branches. The unit is capped with a 10-20 cm thick tufa that weathers with a characteristic vertical tube pattern. The small tubes are

1-3 mm in diameter. The Red Tuff is not easily distinguishable in the Calico Mountains, although it may be associated with limestone marker #1.

Limestone marker #1 is recognized by applying similar criteria: 1) 1 m thick reddish or gray ledge-forming lacustrine limestone (Fig. 5AB), 2) abundant chert zones, 3) wavy layering, 4) microbial bioherm thickenings, 5) accumulations of tufa coated branches and 6) mudcracks. At Hill 3370 this unit is clearly a transgressive unit (deepening upward sequence). The unit is coarse grained at the base, followed by tufa encrusted branches, followed by 30 cm of mudcracked limestone, followed by 30 cm of laminated limestone (with no mudcracks). Limestone marker #1 is recognized in the Mud Hills, at Hill 3370 and in the Calico Mountains.

This pair of transgressive microbial limestone marker units (limestone marker #1 and limestone marker #2) make an excellent tool for correlation between these disjunct outcrops of the Barstow Formation (Fig. 2). These transgressive, nearshore, microbial limestone units are unique lithologies in the Barstow Formation.

One of the strongest arguments for correlation between the Mud Hills and the Calico Mountains is the recent discovery of silicified three-dimensional microfossils in Rainbow Basin

(Leggitt, 2000). Figure 5C shows the fine detail of the new microfossils and illustrates the fact that they are exactly comparable with microfossils from the Calico Mountains (Fig. 5D). The unusual preservation of these fossils in three-dimensional silica argues for a unique mode of preservation and for special paleolimnologic conditions (that can be considered an unparalleled event). This type of fossil preservation has not been reported outside the Barstow Formation. Correlation using these microfossils is a type of event stratigraphy that can be considered time-synchronous (Fig. 2). The silicified microfossils occur in the Mud Hills (Leggitt, 2000), at Hill 3370 (Palmer, 1960), and in the Calico Mountains (Palmer and Bassett, 1954).

When stratigraphic sections are correlated using the pair of limestone markers and the silicified microfossil zone, it becomes apparent that three altered tuff beds in the Calico Mountains are equivalent to the Oreodont Tuff beds in the Mud Hills and at Hill 3370. This is the first report that recognizes the Oreodont Tuff in the Calico Mountains.

Reynolds (2000, 2001), recognized correlation between the Mud Hills and the Calico Mountains using at least three markers: 1) MSL (massive stromatolitic limestone), 2) BPL (brown platy limestone units) and 3) SBH (strontium-borax horizon).

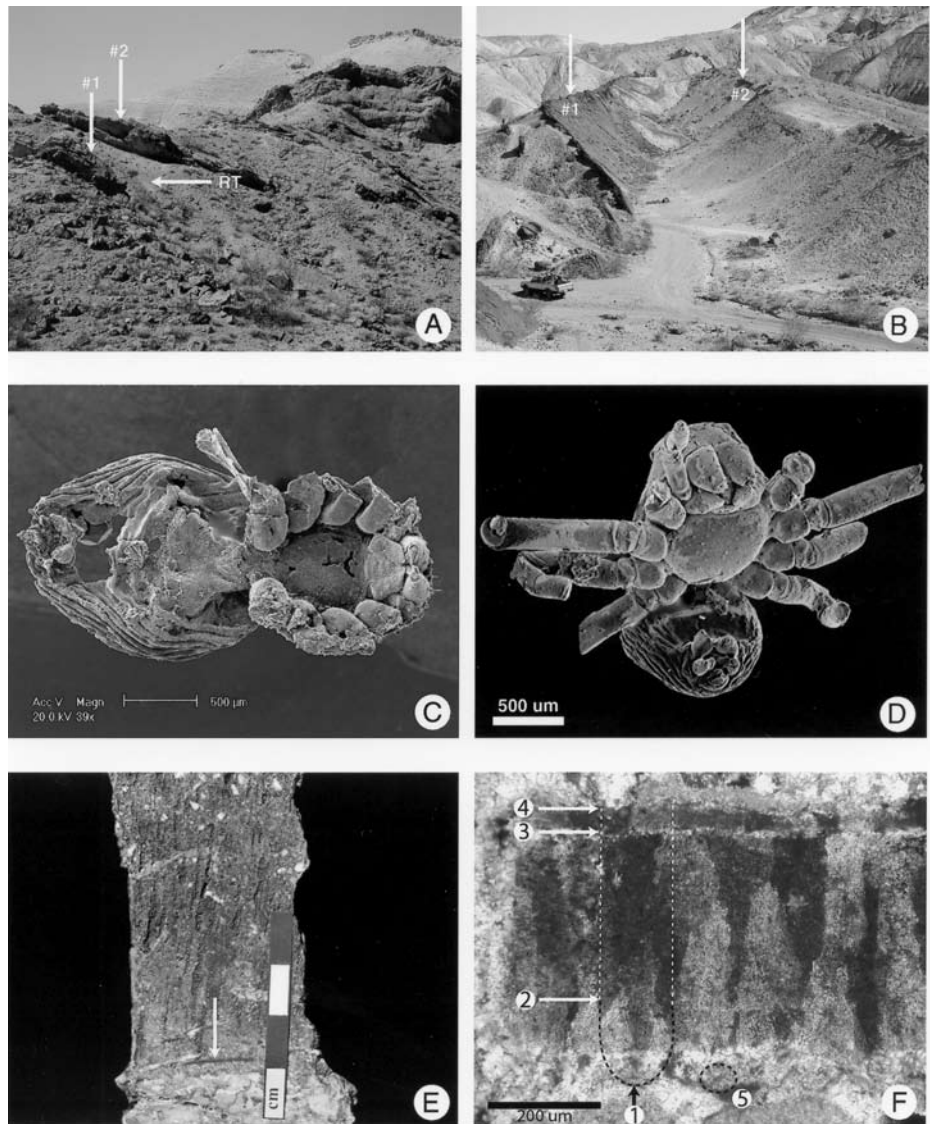
The MSL is equivalent to limestone marker #2 in this paper. The BPL occurs between limestone marker #2 and the silicified microfossil zone. The SBH occurs 1-2 m above the silicified microfossil zone. I have not included the BPL in my correlation because I did not conduct detailed field observations of the individual limestone units (although units similar to the BPL are present in my measured sections). I have not included the SBH in my correlation because I could not accurately identify the strontium-borax horizons in the Rainbow Basin section or in the Hill 3370 section (although mining prospects are evident).

Discussion and Paleoenvironment of the Eggshell

The Calico Mountains fossil eggshell shows the following microstructure zones (from internal to external): 1) an organic core, 2) a zone of radial calcite plates, 3) a zone of tabular crystallite plates, 4) a zone of squamatic aggregates and 5) an external zone of vertical crystals. Macrostructure zones (from internal to external) are: 1) wedges of the mammillary layer (diverging outward from the central core), grading into 2) long vertical columns of the prismatic layer. These findings are consistent with modern neognathous eggshell. The eggshell is

Fig. 5 Marker units and some views of the Calico Mountains eggshell.

A. Limestone marker beds #1 and #2 in the Mud Hills (at the entrance road to Rainbow Basin). The Red Tuff (horizontal arrow and white RT) is located just below limestone marker #2. Each marker bed is 1 m thick. B. Limestone marker beds #1 and #2 in the Calico Mountains (Mule Canyon). C. A three-dimensional arachnid from a concretion in Rainbow Basin. D. A three-dimensional arachnid from a concretion in the Calico Mountains. The unique mode of preservation of these fossils suggests correlation between the Mud Hills and the Calico Mountains. E. Slab from limestone marker #2. The white arrow points to an eggshell fragment. F. Thin-section (radial cross-section) showing the microstructure of the Calico Mountains eggshell. PLM. 1) Base of a mamilla (and internal eggshell surface). The dotted black line encompasses a single mamilla. The dotted white lines surround the columnar portion of the basic shell unit. 2) Junction between the mamillary layer and the continuous layer. 3) Junction between the continuous layer and the external layer. 4) External surface of the eggshell. 5) The dotted black line encircles a central organic core, and a zone of radial calcite plates (above the circled area, a zone of tabular calcite crystals completes the structure of the mamilla).



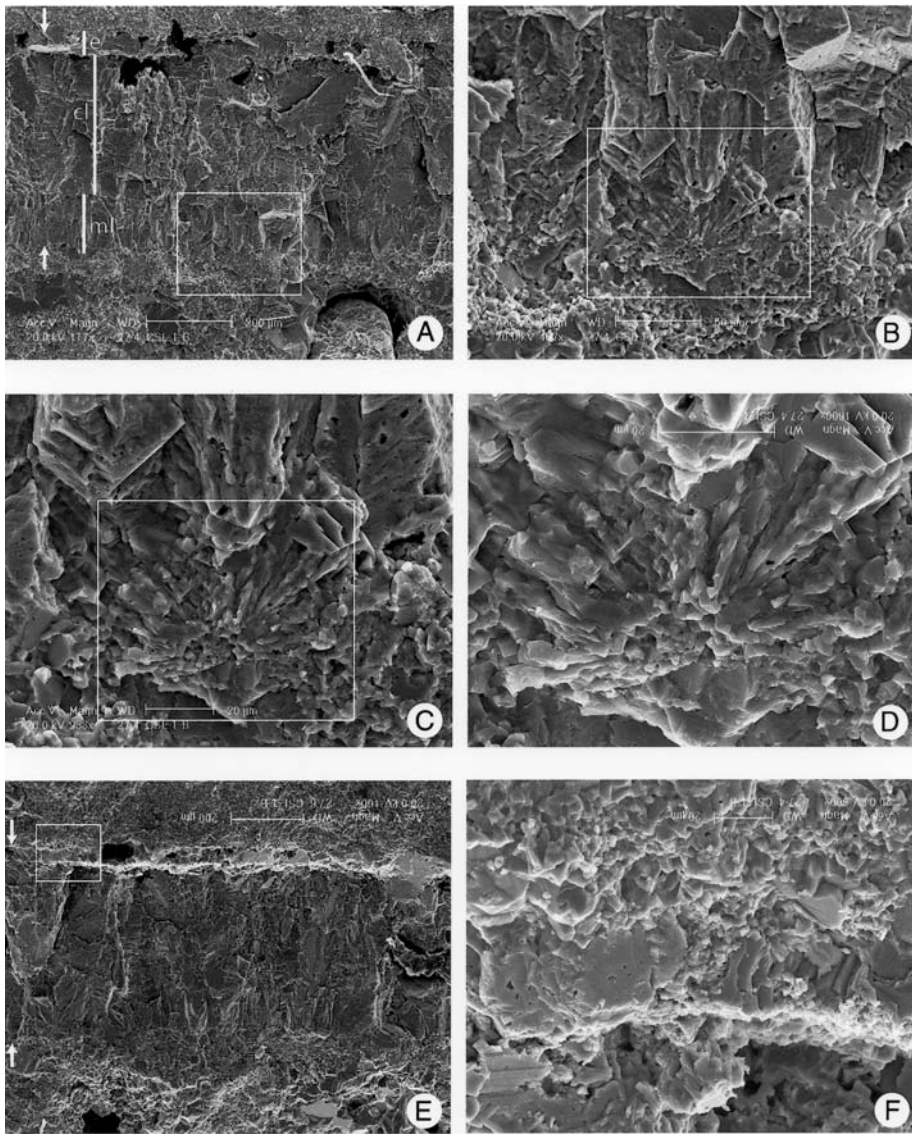


Fig. 6 SEM views of the Calico Mountains eggshell. A. Radial cross-section of the eggshell fragment. The small white arrows indicate the internal and external edges of the fragment. The vertical white bars indicate the main divisions of the eggshell: ml = mamillary layer, cl = continuous layer (or columnar layer), e = external layer. The white box is the area shown in the next micrograph. B. Close-up view of the mamillary layer. The white box is the area shown in the next micrograph. C. Close-up view of the apex (or base) of the mamilla. The organic core and a zone of radial calcite plates are visible. The white box is the area shown in the next micrograph. D. Close-up view of the organic core and the zone of radial calcite plates. E. Radial cross-section of the eggshell fragment. The small white arrows indicate the internal and external edges of the fragment. The white box is the area shown in the next micrograph. F. Close-up view of the vertical calcite crystals in the external zone of the eggshell.

considered “ornithoid” with a prismatic morphotype.

The pair of limestone marker units was likely deposited in response to successive rapid influxes of Ca-rich water into the relatively saline-alkaline lake waters of a closed basin. The Ca-rich water may have been derived from springs in the Owl Canyon area (Becker et al., 2001), from hydrothermal springs in the Calico Mountains (Park, 1995) or from rainwater runoff. The limestone units preserve transgressive features such as drowned forests and cycles of mudflat-derived, flat pebble conglomerate followed by layered limestone of deeper water origin. The Ca-rich littoral zone of the expanding lake was a good environment for microbial mediated precipitation of tufa and microbial mounds. Oxygen isotopes ($d^{18}O = -6.37$ to -6.87‰) reported by Becker et al. (2001) from spring-deposited tufa mounds in Owl Canyon seem to indicate deposition of calcite in mixed lake waters intermediate between fresh water and saline-alkaline water.

Authigenic zeolites were reported from the Calico Mountains concretions and surrounding sediments (Park, 1995), and the Skyline Tuff in the Mud Hills (Shepard and Gude, 1969). The presence of authigenic zeolites is a good indication of saline-alkaline lake water. If the Miocene lake water was as saline-alkaline as modern Mono Lake, calcite would precipitate

immediately upon introduction of Ca-rich water (Becker et al., 2001). The eggshell is a secondary indication of the nearshore processes, or an indication of fluctuating water depth (decreasing water depth might allow nesting on subaerially exposed carbonate mudflats). Preservation of the original structure of the eggshell is also an indication of the alkalinity of the lake water because acidic conditions would dissolve the eggshell calcite.

The Calico Mountains eggshell may be roughly equivalent in isotopic age to the Red Tuff in Rainbow Basin (19.3 Ma). The limestone marker units outcrop at the base of the Owl Conglomerate Member in Rainbow Basin (in close proximity to the Red Tuff), but outcrop near the top of the Owl Conglomerate Member in Owl Canyon (in the same stratigraphic position as seen at Hill 3370). In Owl Canyon the limestone marker units appear more correlative with the Rak Tuff (16.3 Ma) at the top of the Owl Conglomerate Member. There are several possible explanations for this problem: 1) faulting, 2) miscorrelation or 3) the Owl Conglomerate Member was deposited rapidly at the lake margin (resulting in duplication of the limestone marker units). U-Pb dates on spring-deposited tufa mounds in Owl Canyon (at the top of the Owl Conglomerate Member) have an isotopic age of 14.76 ± 0.43 Ma (Rasbury et al., 1999). These

authors offer an explanation for this discrepancy that is beyond the scope of this eggshell paper.

Conclusions

1) The Barstow Formation eggshell is comparable to modern neognathous eggshell. This is strong evidence that the eggshell is of avian origin.

2) Two transgressive microbial limestone marker units are recognized in the Mud Hills, at Hill 3370 and in the Calico Mountains. In fine-grained lacustrine facies of the middle member of the Barstow Formation (at Hill 3370, and in the Calico Mountains), the limestone marker units are thickly layered, cherty limestones with microbial biohermal thickenings. In the coarse-grained lake margin facies of the Owl Conglomerate Member of the Barstow Formation, the limestone marker units are discontinuous and grade into tufa coated branches and spring-deposited tufa mounds.

3) The avian eggshell fragments support the idea that limestone marker #2 was deposited near the shoreline (or the water level dropped enough to allow nesting on the surface of the exposed carbonate mudflat). Flat pebble conglomerate associated with the eggshell is also indicative of periodic subaerial exposure of limestone marker #2.

4) Oreodont tuff beds (time-synchronous marker beds) are recognized in the Calico Mountains. This interpretation is based on stratigraphy and correlation between the Mud Hills and the Calico Mountains and is strongly supported by the pair of limestone marker units and the silicified microfossil zone.

Acknowledgements

Field discussions with Bob Reynolds, Paul Buchheim, Bob Cushman, Kevin Nick, Roberto Biaggi, Ben Clausen, Stan Awramik and unnamed students from my field mapping classes were critical to the success of this paper. Kent Beamon from the Los Angeles County Museum provided the alligator and desert tortoise eggshell for SEM analysis. Mark Loewen should be credited with the thin section that was used in this analysis. The SEM micrographs were done at the University of California, Riverside. Funding for this project was provided by a research grant from Loma Linda University, Department of Natural Sciences.

References

- Alf, R.M., 1966. Mammal trackways from the Barstow Formation, California. *Bulletin So. Calif. Academy of Sciences*, 65(4): 258-264.
- Becker, M.L., Cole, J.M., Rasbury, E.T., Pedone, V.A., Montanez, I.P., Hanson, G.N., 2001. Cyclic variations of uranium concentrations and oxygen isotopes in tufa from the Middle Miocene Barstow Formation, Mojave Desert, California. *Geology*, 29(2): 139-142.
- Leggitt, V.L., 2000. Three-dimensional microfossils from Rainbow Basin: Barstow Formation, Mojave Desert, California. *Geological Society of America Abstracts with Programs*, 32(7): A-15.
- Lindsay, E.H., 1972. Small mammal fossils from the Barstow Formation, California. *California University Publications in Geological Sciences*, 93:1-104.
- MacFadden, B.J., Swisher, C.C., Opdyke, N.D., Woodburne, M.O., 1990. Paleomagnetism, geochronology, and possible tectonic rotation of the middle Miocene Barstow Formation, Mojave Desert, California. *Geological Society of America Bulletin*, 102(4): 478-493.
- Mikhailov, K.E., 1997. Fossil and recent eggshell in amniotic vertebrates: fine structure, comparative morphology and classification. *The Paleontological Association Special Papers in Paleontology* No. 56: 1-80.
- Miller, L., 1952. The avifauna of the Barstow Miocene of California. *Condor*, 54: 296-301.
- Miller, L., 1966. An addition to the bird fauna of the Barstow Miocene. *Condor* 68(4): 397.
- Miriam, J.C., 1919. Tertiary mammalian faunas of the Mojave Desert. *California University Publications in Geological Sciences*, 11: 437-485.
- Palmer, A.R., 1957. Miocene arthropods from the Mojave Desert, California. *U.S. Geological Survey Professional Paper*, 294-G: 237-280.
- Palmer, A.R., 1960. Miocene copepods from the Mojave desert, California. *Journal of Paleontology*, 34: 447-452.
- Palmer, A.R., Basset, A.M., 1954. Nonmarine Miocene arthropods from California. *Science* 120: 228-229.
- Park, L.E., 1995. Geochemical and paleoenvironmental analysis of lacustrine arthropod-bearing concretions of the Barstow Formation, Southern California. *Palaaios*, 10: 44-57.
- Pierce, W.D., 1959. Fossil arthropods of California. No. 22. A progress report on the nodule studies. *Bulletin So. Calif. Academy of Sciences*, 58(2): 72-79.
- Rasbury, E.T., Hemming, S.R., Montanez, I.P., Pedone, V.A., Cole, J.M., Hanson, G.N., Becker, M.L., Klas-Mendelson, M., 1999. Ar-Ar and U-Pb age constraints on the medial Miocene Barstow Formation, Mojave, California. *Geological Society of America Abstracts with Programs*, 31(7): A-233.
- Reynolds, R.E., 1998. Flamingo egg from the Miocene sediments of the Calico Mountains, San Bernardino County, California. *San Bernardino County Museum Association Quarterly*, 45(1,2): 106.
- Reynolds, R.E., 2000. Marker units suggest correlation between the Calico Mountains and the Mud Hills, Central Mojave Desert, California. *San Bernardino County Museum Association Quarterly* 47(2): 21-24.
- Reynolds, R.E., 2001. Marker bed correlations between the Mud Hills, Calico Mts., and Daggett Ridge, Central Mojave Desert, California. *The Geological Society of America Abstracts with Programs, Cordilleran Section, GSA and Pacific Section*, 33(3): A-70.
- Sheppard, R.A., Gude, A.J., 1969. Diagenesis of tuffs in the Barstow Formation, Mud Hills, San Bernardino County, California. *U.S. Geological Survey Professional Paper* 634: 1-35.
- Woodburne, M.O., Tedford, R.H., Swisher, C.C., 1990. Lithostratigraphy, biostratigraphy, and geochronology of the Barstow Formation, Mojave Desert, southern California. *Geological Society of America Bulletin*, 102: 459-477.

Carbonate Phytoherm Mounds in the Middle Miocene Barstow Formation, Mud Hills, California

Vicki Pedone and Carmen Caceres, Dept of Geological Sciences, California State University, Northridge, CA 91330-8266

Abstract

A 5-m-thick limestone unit at the base of the Middle Member of the Barstow Formation in the Mud Hills formed during a temporary cutoff of clastic deposition that could be related to synsedimentary faulting. The most prominent lithology of the limestone unit is phytoherm biolithite, i.e., a constructional mound developed by calcification of macrophytes. The phytoherms are elliptical to circular in area, with diameters of ranging from 3 m to 5 m, and maximum thickness ranging from 1 m to 3 m. Successive growth layers that drape over the tops of the mounds demonstrate that the phytoherms formed positive constructional features on the lake floor. The temporary shutoff of siliciclastic sediment into this area allowed lush plant growth to develop along the shallow lake margin. The plants underwent calcification as they grew to form the phytoherms. Currents fragmented the delicate, coated fronds and deposited the bioclastic material on the lake floor between the mounds. Moderate levels of Mn in pristine depositional components indicate lake waters were only weakly oxic, most likely the result of high productivity in the shallow nearshore environment. Burial by coarse-grained clastic sediment ended limestone formation.

Introduction

The objective of this study is to reconstruct the depositional and diagenetic history of an unusual lacustrine limestone unit in the Miocene Barstow Formation in the Mojave Desert. The study will synthesize field, petrographic, cathodoluminescence, electron microprobe, and stable isotope data. The results will provide new information on the relationship between tectonics and limestone deposition in the basin, the formation of phytoherms, the geochemistry of lake waters, and the timing and source of diagenetic fluids. This paper reports the initial findings of the field and petrographic study.

The limestone occurs on the north limb of the Barstow syncline at the base of the Middle Member of the Barstow Formation, directly overlying the Owl Conglomerate Member. The boundary between the members has been dated on

the south limb of the syncline, using K-Ar analyses of biotite separates from the Rak Tuff (Woodburne et al., 1990). The ~5-m-thick limestone unit occurs only on the steep north side of the asymmetric detachment basin, where there are common normal faults thought to be contemporaneous with the early stages of deposition of the Barstow Formation (Ingersoll et al. 1996). Deposition of the limestone in a sequence dominated by conglomerate and pebbly sandstone indicates a temporary cutoff of clastic deposition, which could be related to synsedimentary faulting.

Lithology

The most prominent lithology of the limestone unit is phytoherm biolithite, which developed by calcification of macrophytes. The phytoherms are elliptical to circular in area, 3 to 5 m in diameter, and 1 m to 3 m thick. They are laterally discontinuous and formed localized growths along the lake margin. Successive growth layers drape over the tops and demonstrate that the phytoherms formed positive constructional features on the lake floor (Fig. 1). In cross section, they have a mushroom shape, formed as the phytoherms expanded in area as they grew, downlapping biosparite and biointrasparite units that were syndepositional with the older layers. The phytoherms also interfinger with and are finally onlapped by these carbonate grainstones.

The phytoherms formed by calcification of a delicate, shrub-like plant. Stems range in diameter from 0.3 to 1.0 mm and occur in clumps (Fig. 2). Spiky ornamentation is preserved around the molds of most stems (Fig. 3). Calcification consists of alternating layers of bladed calcite cement and micrite. Ostracodes were commonly trapped in framework porosity, but siliciclastic grains are absent. As concentric coatings on individual stems were added, they coalesced to form a rigid, current-resistant biolithite. Framework porosity, now partly to com-



Figure 1. Phytoherm mound. GSA Scale card in center.

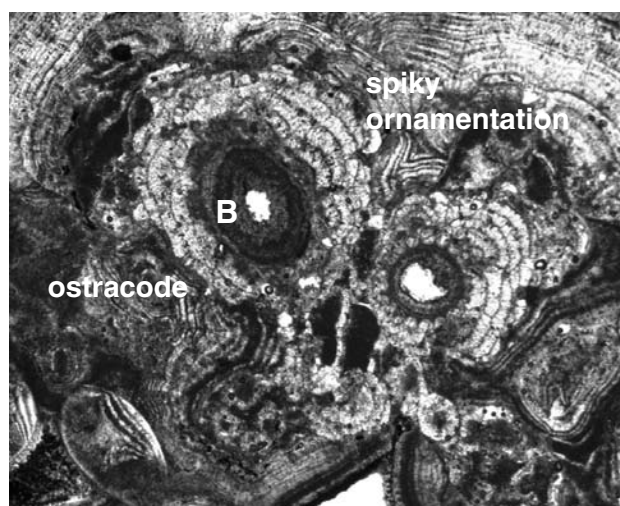


Figure 2. Concentrically coated molds of stems in phytoherm. Scale bar is 1 mm. Labels are explained in text.

pletely filled by sparry calcite and/or chalcedony, formed 20% to 50% of the rock. Beds of biosparite onlap the phytoherms. Grains are fragments of calcified stems (Fig. 3). In both the biolithite and the biosparite, alternating prismatic calcite and iron oxide form early cements. Final porosity is occluded by blocky calcite. Siliciclastic grains are absent in former pore spaces.

Electron-microprobe analyses

The abundances of Ca, Mg, Mn, Fe, and Sr were measured by electron microprobe in selected fabric components of the phytoherm biolithite and biosparite. Two samples of biolithite, one from the center and one from the margin of a mound, and one sample of biosparite were used in the study. The analyzed components, from oldest to youngest, include: 1) clear, concentric cement immediately adjacent to stem molds in biolithite (A in Fig. 2), 2) micrite in banded concentric fabric (B in Fig. 2), 3) clear, finely crystalline calcite in banded concentric fabric (B in Fig. 2), 4) finely laminated clear calcite of outer rind (C in Fig. 2), 5) prismatic early cement (P in Fig. 3), and 6) blocky, sparry calcite overlying prismatic cement (S in Fig. 3).

All of the constructional components of the biolithite (A, B, and C) higher Mg and Sr and lower Mn abundances than the overlying prismatic and blocky cements (Fig. 4). Interestingly, the Sr abundances in the micrite bands of fabric B are significantly lower than the clear calcite bands with which they alternate. The constructional components, A, B, and C, formed from the lake water. The exquisite detail of fabric in the rock suggests that the calcite, which contains only ~1 mole % $MgCO_3$, is pristine and has not undergone recrystallization. The elemental geochemistry of the primary components indicates two important features of the lake chemistry. Firstly, the Sr abundance is unusually high for calcite. The calculated Sr/Ca of the lake water is 0.220, using an average Sr abundance of 2462 ppm and K_d^{Sr} calcite = 0.028. This ratio is one to two orders-of-magnitude higher than mean seawater (0.015) and meteoric water (0.004). The cause of the puzzling difference in Sr abundance between the micrite and clear calcite that form alternating coatings in the biolithite is uncertain. The abundances of Sr, Mn, and Fe are similar; only the Sr abundances are distinctly different. The difference is unlikely due to diagenetic loss of Sr because both Sr and Mg have distribution coefficients less than one and typically behave similarly during recrystallization. Equally, it is unlikely the result of oscillating water chemistry

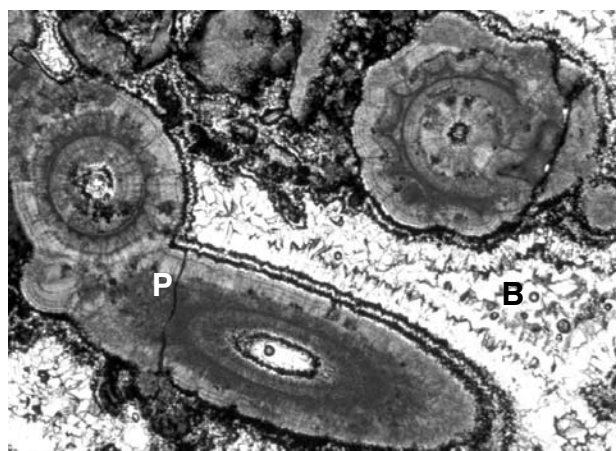


Figure 3. Fragments of calcified stems in biosparite are cemented by alternating generations of iron oxides and prismatic dogtooth calcite (P). Final pore space is occluded by sparry calcite (B). Scale bar is 1 mm.

during original formation because other elemental abundances would be likely to be different too. Possibly, the micrite was biologically mediated, and the microorganism(s) involved discriminated against Sr.

The second feature of lake chemistry indicated by the geochemistry of the limestone concerns its redox state. Only Mn^{2+} in the aqueous state is incorporated into calcite. In order to facilitate the incorporation of Eh-sensitive Mn in the primary constructional components (mean Mn abundance of 1400 ppm), the waters must have been only weakly oxic. High organic productivity in the shallow lake margin likely was responsible for low-levels of dissolved oxygen in the waters. Significantly higher values of both Mn and Fe in the prismatic and blocky

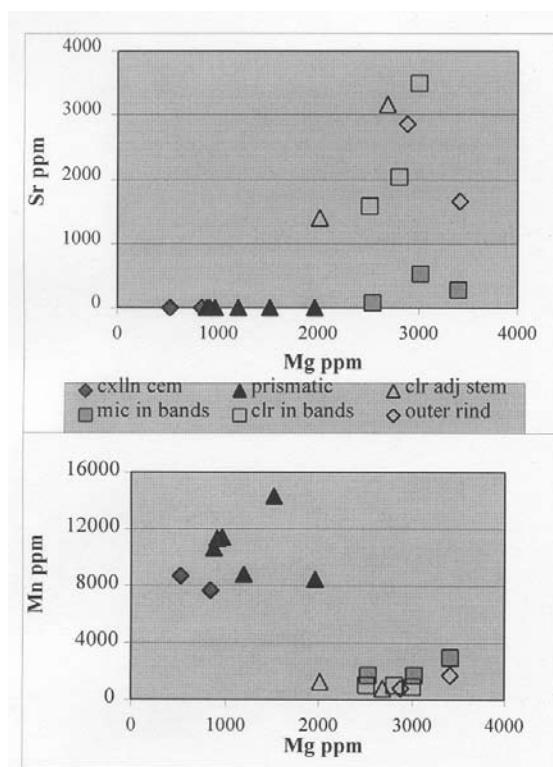


Figure 4. Element-element plots for limestone.

calcite, compared to the primary components, indicate that later diagenetic fluids were strongly reducing. The low Sr and Mg abundances in the cements suggest that the diagenetic fluids might have been meteoric groundwater.

Discussion and Conclusions

The limestone unit is under- and overlain by sandstone and conglomerate deposited in a fan-delta environment. Absence of detrital siliciclastic grains in the limestone unit indicates a complete shutoff of clastic sediment into this area, which allowed lush plant growth to develop along the shallow lake margin. Currents fragmented the delicate, coated fronds and deposited the bioclastic material on the lake floor between the mounds. High Sr and Mn abundances in primary constructional components indicate that the lake water were only weakly oxic and had an usually high Sr/Ca ratio. Highly productivity in the shallow nearshore lake margin resulted in low levels of dissolved oxygen. Later diagenetic fluids were probably strongly reduced meteoric waters. Burial by coarse-grained clastic sediment ended limestone formation. The most likely cause of the temporary diversion of clastic sediment is synsedimentary normal faulting in the source area.

References Cited

- Ingersoll, R. V., Devaney, K. A., Geslin, J. K., Cavazza, W., Diamond, D. S., Heins, W. A., Jagiello, K. J., Marsaglia, K., M., Paylor, E. D. II, and Short, P. F., 1996, The Mud Hills, Mojave Desert, California: Structure, stratigraphy, and sedimentology of a rapidly extended terrane, in Beratan, K. K., ed., *Reconstructing the History of Basin and Range Extension Using Sedimentology and Stratigraphy*: Boulder, Colorado, Geological Society of America Special Paper 303, p. 61-84.
- Woodburne, M. O., Tedford, R. H., and Swisher III, C. C., 1990, Lithostratigraphy, biostratigraphy, and geochronology of the Barstow Formation, Mojave Desert, southern California: *Geological Society of America Bulletin*, v. 102, p. 459-477

Mineralogical Survey of the Mount General Area

Robert M. Housley, *Mineralogical Society of Southern California*, rhousley@its.caltech.edu

Robert E. Reynolds, *LSA Associates, Inc.*, Riverside, California 92507 bob.reynolds@lsa-assoc.com

Abstract

The Southern California Chapter of Friends of Mineralogy recently inventoried the Mount General area in the central Mojave Desert, west-northwest of Barstow, San Bernardino County, California. The small workings and dumps suggest that mineral collecting potential is limited, even though the variety and quality of the minerals themselves is good. The mineralogy of prospects differ from west to east in the district. The inventory in the western portion recorded sulfides, barite abundant as gangue, sulfate and carbonate oxides, and lead molybdate (wulfenite) on arsenate/phosphate matrix. Secondary iron oxides, chalcedony and silicates of zinc and copper are present. In the eastern portion of the district, all the lead sulfides have been oxidized to vanadinite, the lead vanadate, and lead vanadates of copper and zinc. Barite is rare, and secondary oxides include limonite, chrysocolla and “embolite.”

Background

The Southern California Chapter of the Friends of Mineralogy (SCFM) has a continuing program to document notable mineral occurrences in southern California. The recent focus of the inventory has been on the mineral-rich Mojave Desert Province. During 2001, volunteers focused the survey on the Mount General area northwest of Barstow. Geographically, Mount General is located about 5 miles west of Mount Waterman (Waterman Gold Mine, 1880s) and about 11 miles west of the Calico Silver District (1880s). Although Mount General contains no large or famous mines, it was probably initially prospected about the same time and is covered with numerous prospect pits and small workings. Its history is scarce, although one mine, the Pedry, is briefly discussed (Wright et al, 1953; Bowen, 1954). Additional geologic mapping is helpful for interpreting the area (Bortugno and Spittler, 1986; Dibblee, 1960; Kiser, 1981). The most recent and comprehensive study (Bezore and Shumway, 1994) assigned numbers to the prospects and mines, which will be referred to in this report; for example, the Pedry Mine is location BS-28.

Geology

The area from Mount Waterman west to Mount General is divisible into rock units of Miocene age that overlie Paleozoic sedimentary and Jurassic volcanic rocks that have been metamorphosed. The Paleozoic and Mesozoic metamorphic rocks are cut by Early Miocene granodiorite plutons and diorite dikes. These two units of dissimilar age are deformed by the overlying Waterman Hills Detachment Fault (WHDF), the upper plate of which contains Early Miocene volcanic rocks correlated with the Pickhandle Formation (Glazner and others, 1989; Bezore and Shumway, 1994). Mount General consists of Miocene Pickhandle volcanic rocks that are in low-angle fault contact with underlying pre-Tertiary metamorphic rocks that have been intruded by early Miocene plutons and dikes (Bezore and Shumway, 1994). In many places the Pickhandle volcanics in the upper plate of the WHDF contain short discontinuous veins of barite with secondary silica and limonite ranging from a less than an inch up to three feet in thickness. A short adit on the lower northwest slope explores a two foot thick barite, silica, limonite vein. Two shafts and an adit in the southern part of the mountain also explore brecciated barite. The mineralogical assemblage at these locations is simple, and no other secondary minerals were reported, or were seen during our examination.

Western Workings

SCFM interest in Mount General was sparked when Walter Margerum discovered colorful micro specimens of prismatic orange wulfenite on green malachite and blue chrysocolla at the north shaft of the Pedry Mine. Although small to microscopic in size, “micro-specimens” or micromounts usually have the most perfectly formed crystals, interesting associations of minerals, and, with the right equipment, are very photogenic.

The Pedry Mine itself consists of six patented claims that encompass a mile long brecciated quartz vein supporting a low, northwest-striking ridge on the north side of Mount General. The ore minerals mentioned by Wright include sulfides of lead, zinc, copper and iron: galena, which oxidized to anglesite, and cerussite, and sphalerite, chalcopyrite, and pyrite. Primary gangue minerals on this vein are barite and calcite, all coated with chalcedony and limonite.

The main workings of the Pedry Mine consist of two

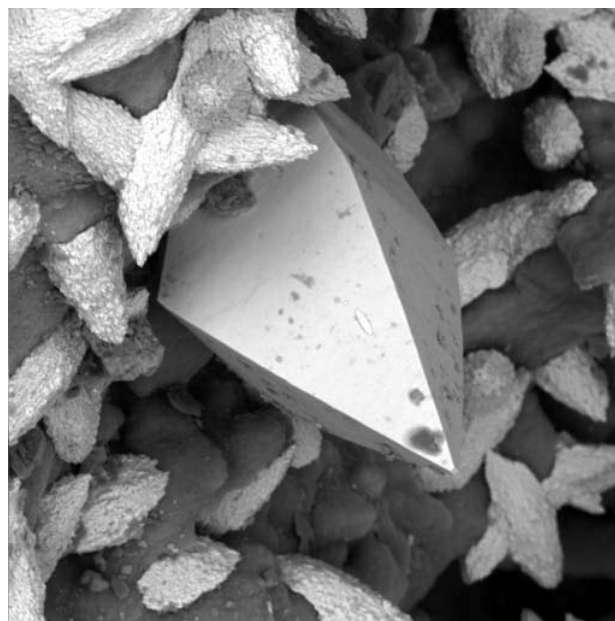


Figure 1. Scanning backscattered electron image of Pedry Mine wulfenite. Smaller poorly formed crystals are mimetite/pyromorphite. The field of view is 140 micrometers.

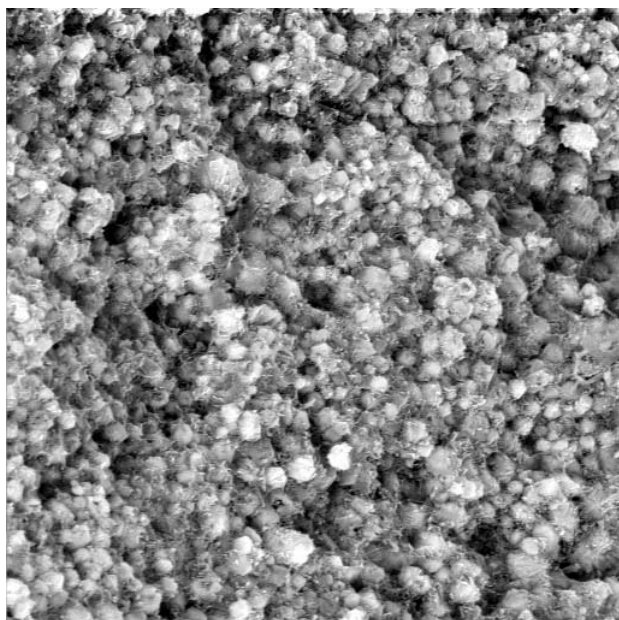


Figure 2. Pedry Mine plumbojarosite is generally poorly crystallized. Field of view 14 micrometers.

inclined shafts near opposite ends of the vein and a series of shallow pits and trenches along its length. The north shaft is about 200 feet deep and has short drifts at several levels. Exploration here produced “micros” of pale blue hemimorphite and prismatic wulfenite with malachite and chrysocolla. Under scanning electron microscope (SEM) examination, some samples of wulfenite proved to be on a gray coating of mimitite/pyromorphite over brown earthy submicrometer grains of plumbojarosite. The gray drusy material is a solid solution between the arsenate mimitite and the phosphate pyromorphite. These are illustrated in Figures 1 and 2.

The Pedry Mine was under lease in 1949 and work was concentrated on the 270 feet deep southern shaft (Wright, 1953) with short drifts at approximately 50 foot intervals with a 40 foot crosscut to a parallel vein at 100 feet. A shipment of concentrates in 1952 returned 26% lead and almost 9 ounces per ton of silver. At that time a headframe, hoist, and loading bin were in place (Bowen, 1954). This shaft is now filled with rubbish and the original dump has been bulldozed. What remains of the dump produced crystals of cerussite and barite (to 5 mm), and earthy plumbojarosite.

On the east side of Mount General is a small prospect pit studied by Professor David R. Jessey of California Polytechnic University, Pomona. Galena occurs in massive barite at this site. Barite crystals to one inch on green drusy quartz were obtained from the 150 foot vein exposure and tailings. The barite shows zoning and flat faces are frequently coated with drusy quartz. In some cases the barite has been totally replaced with quartz, producing attractive pseudomorphs.

Eastern Workings

Two miles southeast of Mount General is unnamed working BS-34, noted for vanadinite (Bezore and Shumway, 1994), and referred to as the A. O. Prospect since it was first called to SCFM attention by Al Ordway. This prospect has yielded colorful micros of vanadinite and descloizite. Mineralization seems to follow the marble/gneiss contacts correlated with the

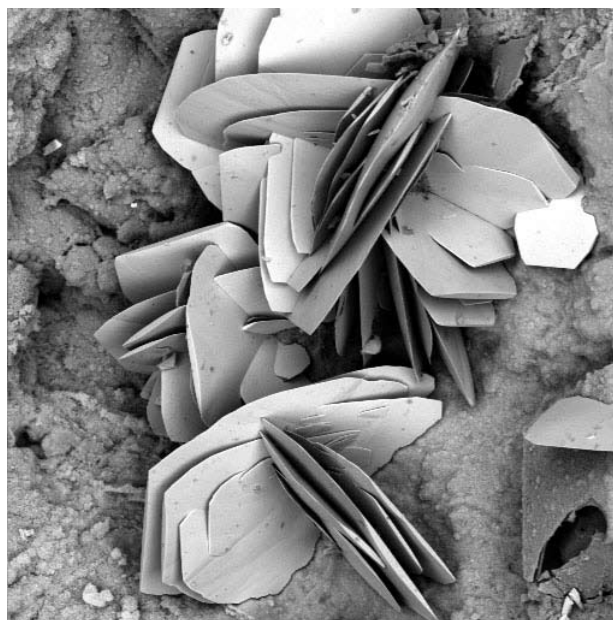


Figure 3. Backscattered electron image of descloizite from the A. O. Prospect. Field of view 350 micrometers.

Waterman gneiss (Bezore and Shumway 1994). The dolomitic marble contains graphite flakes to several millimeters here and in the vicinity of many of the eastern prospects.

The A. O. Prospect was initially explored by a shallow adit, and subsequent work was with a bulldozer and backhoe. A large excavation below the adit level exposes the concentration of vanadinite/descloizite area. These minerals occur in dark porous silica in both walls of the adit, particularly on the south wall. The mineralized zone is about 4 feet thick with a total depth below the original surface of 30 feet.

Cavities within the mylonitic gneiss (Bezore and Shumway, 1994) are the result of carbonate dissolution near the contact and now contain secondary silica. No cerussite or anglesite has been observed and no sulfides remain, but the silica contains iron hydroxide, indicating their former presence. All available lead has been incorporated into lead vanadate minerals.

The A. O. vanadinite varies in aspect from stubby prisms to long needles colored white, yellow and through bluish shades to black. Oddly, it is never orange or red. The rosettes of descloizite are greenish yellow. Vanadinite crystals on balls of yellow descloizite are especially attractive. Vanadinite shows well on clear drusy quartz pseudomorphs after hemimorphite. A typical descloizite group is shown in Figure 3.

The vanadate mineralization appears to have cyclic repetitions. Specimens commonly show descloizite on fresh vanadinite previously deposited on descloizite pseudomorphs after vanadinite. Copper minerals are almost absent from the main pit and no mottramite has been found. All zinc here has also been incorporated in the vanadates, and silica shells suggest the former presence of hemimorphite.

Apparently the ore removed in generating the pit where these minerals occur was shipped to a smelter since no vanadinite has been found on the dump. However, specimens of descloizite on calcite can be found on the dump. Occasional pieces contain chrysocolla with mottramite, embolite (chlorargyrite/bromargyrite), and rhombic pseudomorphs after a carbonate mineral. Specimens of mottramite on calcite also occur in a trench east of the pit. A chlorargyrite/bromargyrite crystal is

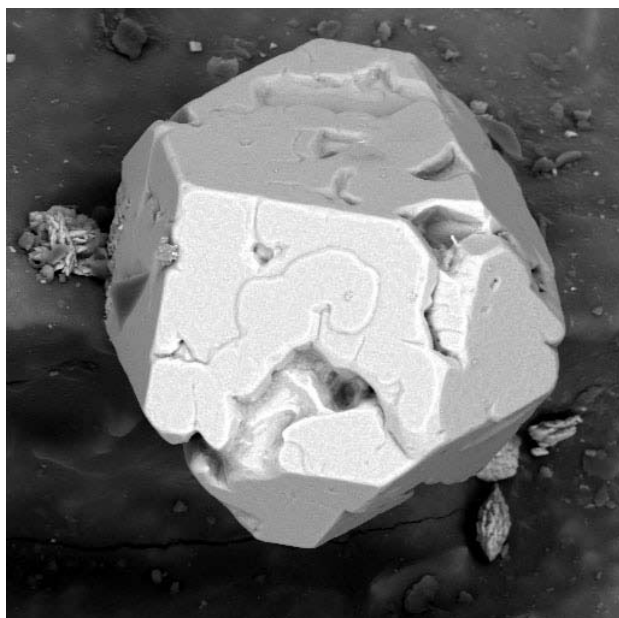


Figure 4. Chlorargyrite/bromargyrite from the A. O. Prospect dump. Field of view 70 micrometers.

- Kiser, N. L., 1981, Stratigraphy, Structure and Metamorphism in the Hinkley Hills, Barstow, California; Unpublished map for the C. D. M. G., Scale 1:12,000.
- Wright, L. A., R. M Stewart, T. E. Gay, and G. C. Hazenbush (1953) Mines and Mineral Deposits of San Bernardino County, California. Annual Report of the State Mineralogist 49.

shown in Figure 4. A single specimen from the dump yielded fresh hemimorphite and a trace of cerussite.

One quarter mile east is working BS-38, which yielded mottramite, possibly after vanadinite, on calcite, and celestine with malachite. As at the A. O. Prospect, the overprint of 1950s exploration is also evident in the eastern localities. The original dumps and surrounding areas have been cut with bulldozer and backhoe. In a wash south of locality BS-38, bulldozer trenches apparently unrelated to earlier work expose copper stained silica that contains malachite and mottramite, and traces of barite.

Conclusion

The contrast between mineralization of the eastern areas and the Pedry Mine area 4 miles west is worth noting. Like the veins on Mount General, the Pedry vein is massive quartz with abundant barite. There are no vanadium oxides in the secondary minerals. To the east, around sites BS-34 and BS-38, the mineralized gneiss contains no quartz veins and very little barite. All the lead present has been converted to vanadates!

Acknowledgements

The authors wish to thank Walter Margerum, Garth Bricker, Paul Malone, and Jennifer Rohl for assistance.

References

- Bezore, Stephen P. and Dinah O. Shumway, 1994. Mineral lands Classification of a part of Southwestern San Bernardino County, California. California Department of Conservation, Division of Mines and Geology. O. F. R. 94-04, 62p. and appendices.
- Bortugno, E. J. and T. E. Spittler, 1986. Geologic Map of the San Bernardino Quadrangle, California Division of Mines and Geology, Map No. 3A, Scale 1:250,000.
- Bowen, Oliver E., Jr., 1954. Geology and Mineral Deposits of the Barstow Quadrangle, San Bernardino County, California, California Division of Mines and Geology, Bulletin 165, 208p.
- Dibblee, T. W., Jr., 1960, Geologic Map of the Barstow Quadrangle, San Bernardino county, California: U. S. Geological Survey Mineral investigations field Studies Map MF-233, Scale 1:62,500.

The Bodfish Layered Basic Intrusive

Gregg Wilkerson, U.S. Bureau of Land Management, 3801 Pegasus Dr., Bakersfield, CA 93308

Abstract

The Bodfish Gabbro is a complex mafic and ultramafic rock unit in the Tehachapi Mountains south of Lake Isabella. This complex contains outcrops of dunite, peridotite, magnetite and norite. The western part of the Bodfish Gabbro, adjacent to the Breckenridge-Kern River fault, has outcrops of layered basic intrusive (LBI) consisting mainly of magnetite. The LBI portions of the Bodfish Gabbro are in fault contact with younger granitic rocks and older metamorphic rocks. The Bodfish LBI is a rarely exposed remnant of the ancestral roots of the Southern California Batholith.

Igneous Stratigraphy of the Sierra Nevada

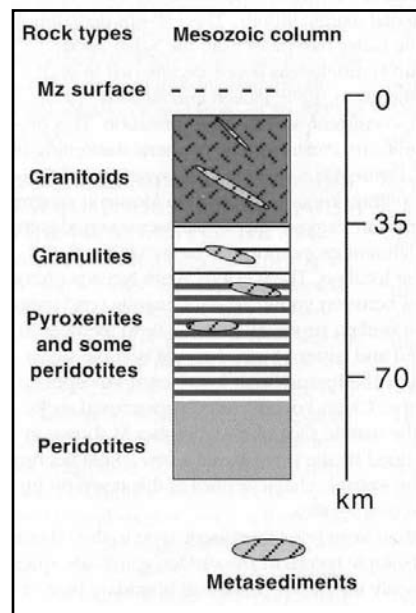
Ducea (2001) summarizes the igneous stratigraphy of the Southern California Batholith (SCB). An idealized stratigraphic column is reproduced in Figure 1 of this report. The SCB has been tilted to the northwest. This tilting, combined with erosion, has exposed the structurally deepest parts of the SCB in the Tehachapi Mountains. Exposures of mafic and ultramafic rocks of the SCB are more common south of latitude 36° (Ross, 1987). The differentiated granitoids are at the top and the undifferentiated ultramafic rocks at the bottom in this idealized stratigraphic reconstruction.

Mafic and Ultramafic Rocks of the Southern Sierra Nevada

Generally, there are two families of mafic/ultramafic rocks in the SCB, those that cut through granitoids and those that are in fault contact with them. The former are clearly younger, being Cenozoic or late Mesozoic. The fault-bounded mafic/ultramafics may be older.

There were two bursts of magmatism in the SCB, one in the Late Cretaceous (100-85 my, 78% of the granitoids) and the other in the Jurassic (160-150 m.y; Ducea, 2001). These episodes must have produced corresponding ultramafic bodies in the lower parts of those plutons. The remnants of these deep-seated mafic/ultramafic units are now widely distributed throughout the Tehachapi

Figure 1. Igneous Stratigraphy of the Sierra Nevada. Reproduced from Ducea, 2001.



and San Emigdio Mountains (Figure 2). Late-stage mafic magmatism in the SCB is recorded by lamprophyre dikes that cut almost all of the granitoids (Figure 3).

Xenoliths in the granitoids and in the San Joaquin volcanic field provide clues to the composition and age of mafic/ultramafic rocks underlying the granitoids (Ducea, 2001). Many of the xenoliths in the granitoids of the Tehachapi Mountains are structurally controlled, especially within the Bear

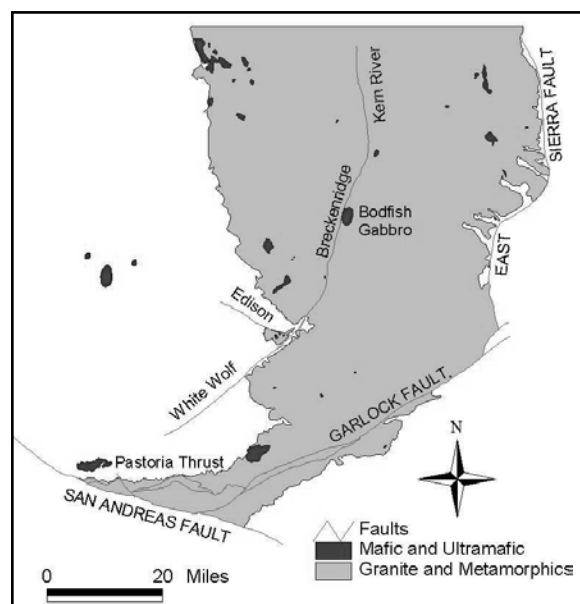


Figure 2. Mafic and ultramafic rocks of the Southern Sierra Nevada. Adapted from Ross, 1995.



Figure 3. Lamprophyre dike near Borel Power Plant, Lake Isabella, California. Photo by Gregg Wilkerson.

Valley Tonalite (Ross, 1987). Early petrographers called these features “Autoliths” (Pabst, 1928) and Collins (1988) interpreted them as relics of regional hydrothermal differentiation.

Bodfish Gabbro

Reconnaissance mapping of the Bodfish Gabbro indicates that it can be subdivided into several separate mapable divisions based on mineralogy, magnetism and texture. The formation is cut by a number of faults that complicate structural reconstruction. A general layered sequence can be observed with dunite at the base, in the northwest. There is a 100 meter thick magnetite zone along the western edge of the Bodfish Gabbro that transitions up-section into lighter colored norite to the east.

The Bodfish Gabbro represents a LBI, the lowest parts of a Jurassic or Mesozoic pluton. It has many characteristics that are similar to those of the Bushveld (Hutchinson, 1988) and Stillwater Complexes (Jackson, 1968).

References

- Collins, L., 1988, Hydrothermal Differentiation and Myremekite – A Clue to Many Geological Puzzles, Theophrastus Publications, 33 J. Theologou Street, Zographou, Athens, Greece, 382p.
- Ducea, M., 2001, The California Arc: Thick granitic batholiths, eclogitic residues, lithospheric-scale thrusting and magmatic flare-ups, *GSA Today*, 11:11:2-10.
- Ducea, M. and J. Saleeby, 1998, The age and origin of a thick mafic-ultramafic root from beneath the Sierra Nevada, *Contributions to Mineralogy and Petrology*, 133:169-185.
- Hutchinson, C.S., 1982, *Economic Deposits and Their Tectonic Setting*, John Wiley and Sons, p. 104-
- Jackson, E.D., 1968, The chromite deposits of the Stillwater Complex, Montana, in *Ore Deposits of the United States*, John D. Ridge, editor, p. 1495-1510.
- Mukhopadhyay, B., 1989, Petrology and geochemistry of mafic and ultramafic xenoliths from the Sierra Nevada batholith, Part 1, Ph.D. thesis, Dallas Texas, University of Texas, 215 p.
- Pabst, A., 1928, Observations on inclusions in the granitic rocks of the Sierra Nevada: University of California Publications, Bulletin of Department of Geological Sciences, 17:325-386.
- Ross, 1987, Mafic plutons of the Southern Sierra Nevada. U.S. Geological Survey, Open File Report 87-275, 42p.
- Ross, 1995, Reconnaissance Geologic Map of the Southern Sierra Nevada, Kern, Tulare, and Inyo Counties, California, U.S. Geological Survey, Miscellaneous Investigations Map I-2295.

The Goler Formation of California

Don Lofgren, *Raymond Alf Museum, 1175 Baseline, Claremont, CA 91711*

Malcolm McKenna, *American Museum of Natural History, New York*

The Goler Formation is the only Paleocene aged rock unit in California that has yielded mammals and other non-marine vertebrates. The Paleocene Epoch was a time of great diversification for mammals and California's record of this diversification comes entirely from the Goler Formation. Recent collecting efforts have greatly increased the size of the sample of vertebrates from the Goler Formation and preliminary study of these fossils has significantly changed our perception of the Paleocene mammalian fauna of California.

The Goler Formation was named and studied by Dibblee (1952). Later, Cox (1982; 1987) completed a detailed geologic analysis of the formation. They established that the Goler Formation is over 3 kilometers thick and is comprised of mostly clastic sediments deposited mainly by fluvial processes. However, the uppermost part of the formation has yielded marine fossils that indicate deposition of sediment at ocean depths of up to several hundred feet (Cox and Edwards 1984; Cox and Diggles 1986; McDougall 1987). The Goler Formation is unconformably overlain by Miocene volcanoclastic sediments and andesitic-basaltic lavas representing the Cudahy Camp and Dove Springs formations of the Ricardo Group.

At first, the Goler Formation was thought to be Eocene in age based on fossil plants (Axelrod 1949). In 1950, R. Tedford and R. Schultz found a turtle shell and mammal tooth near Black Mountain and these specimens were taken to C. Stock at Caltech. Unfortunately, later in 1950, before they could be stud-

ied, Stock died, and these fossils were discarded. But in 1952, Tedford with M. McKenna found an alligator tooth at another site (Laudate Discovery Site) higher in the section and thorough prospecting of this locality in 1954 yielded a mammal jaw. The mammal jaw belonged to a member of the condylarth family Peripitychidae (McKenna 1955), herbivorous mammals restricted to Paleocene rocks elsewhere in North America. A Paleocene age for the Laudate Discovery Site showed that the previously proposed Eocene age of the formation was incorrect.

Subsequently, from 1955 to 1990, a series of trips to the Goler Formation was initiated by McKenna. Because the formation is mostly barren of vertebrate fossils, success was modest and only about a dozen specimens were found, but these fossils did corroborate the Paleocene age (McKenna 1960; West 1970). In the early 1980s marine fossils were found near the top of the formation (Cox and Edwards 1984), above the occurrences of Paleocene mammals. These strata were dated as early Eocene (Cox and Diggles 1986; McDougall 1987) or late Paleocene (Cox and Edwards 1984; Reid and Cox 1989) based on their invertebrate fauna.

In 1993 McKenna and D. Lofgren began a detailed biostratigraphic study of the formation. They recovered a few mammal teeth at the Laudate Discovery Site. But in 1997 a major discovery was made as H. Hutchison found a toothless mammal jaw at a new locality (Edentulous Jaw Site) one mile east of the Laudate Discovery Site. The Edentulous Jaw Site looked very promising because mudstone containing the fossils could be screen-washed. Soon thereafter, small screen-washing samples were processed from both of these sites and each sample yielded a few mammal teeth. Spurred on by this initial success, the scope of screen-washing efforts was expanded and 9 tons of sediment from the Edentulous Jaw Site and 3 tons from the Laudate Discovery Site were processed over a period of three years. This was very labor-intensive work as sediment was first screen-washed in the field, using water from a small local reservoir, and then dried. A large group of volunteers assisted in these screen-washing efforts. The dried matrix was then taken to a lab where it was screen-washed again, then soaked in limonene and acetic acid to break up any remaining clumps of sediment, and then screen-washed a third time. The small percentage of remaining matrix was floated in a high-density liquid whose density was adjusted to be between that of the fossils and the remaining sediment. The fossils and heavy minerals sank while the rest floated and was discarded. The matrix was then scanned through microscopes and any specimens found were removed for study.

Through the screen-washing efforts hundreds of specimens of vertebrates were recovered including 150 mammal teeth. The mammal fossils were immediately exciting because many kinds were represented, notably California's oldest known primates and marsupials, as well as various multituberculates and ungulates (Lofgren et al. 1999). Primates and marsupials are known from California's Eocene rocks, but these Goler ones were earlier, like the primates *Plesiadapis*, *Ignacius*, and *Paromomys*, and the marsupial *Peradectes*.

In November 1999, the two localities producing mammalian specimens were joined by a third as B. Baum found a new site (Land of Oz) lower in the section and about one mile southwest

Goler Formation		
Member 4	4d	Includes mudstone (marine) sub-unit
	4c	Conglomerate unit of Black Hills
	4b	Upper Sandstone and siltstone
	3 2 4a	Conglomerate and sandstone unit of Sheep Spring
Member 3	1	Lower sandstone and siltstone
Member 2		
Member 1		

Figure 1. Chart outlining subdivisions of the Goler Formation and approximate stratigraphic positions of: (3) Laudate Discovery Site; (4) Edentulous Jaw Site; (2) Land Of Oz locality; and (1) Tedford-Schultz site. Modified from Cox (1987: fig. 2).



Figure 2 (above left). Volunteers filling buckets of matrix for screen-washing at the Edentulous Jaw Site.



Figure 3 (above right). Screen-washing operation in the field using a local sheep tank as a water source.

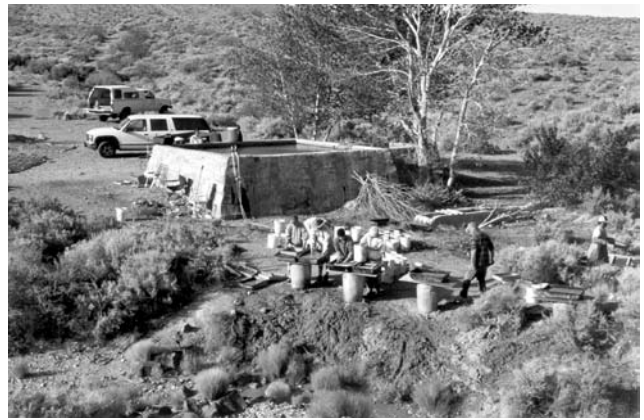
Figure 4 (left). Wood boxes lined with fine wire mesh in cement tubs of water are employed to screen-wash sediment gathered from the Edentulous Jaw Site.

of the Laudate Discovery Site. The Land of Oz produced a few mammalian specimens, including jaw fragments and a partial palate but has yet to be screen-washed. Thus, the Goler Formation presently has yielded mammals from three main sites but the entire extent of the formation is only partly sampled.

Detailed mapping of the Goler Formation was completed by Cox (1982) in which he described four members: the mammal-yielding sites are located in Member 4a-b (figure 1; sites 2-4). Member 4d yielded the late Paleocene-early Eocene marine fossils. The site where Tedford and Schultz found a mammal tooth in 1950 is situated high in Member 3 (figure 1; site 1). This specimen, if not lost, might have helped constrain the age of Member 3. Unfortunately, after decades of prospecting, no other mammalian fossils have been found in Member 3 and members 1 and 2 have not yielded fossils of any type.

The mammals themselves from Member 4a-b provide the best method for dating that part of the Goler Formation because mammalian paleontologists from North America have developed a series of biochronologic units to subdivide the Cenozoic, termed North American Land Mammal Ages. These units are based on assemblages of fossil mammals, each interpreted to denote a particular interval of geologic time (see Wood et al. 1941; Woodburne 1987). The mammal ages that span the Paleocene are, in ascending chronologic order, Puercan, Torrejonian, Tiffanian, and Clarkforkian. Comparison of the mammalian faunas from the three Goler sites to assemblages that characterize these Paleocene mammal ages further constrain the age of Member 4a-b.

For faunal lists provided, identifications are considered prelimi-



nary.

Laudate Discovery Site (RAM loc. V94014, V94133); uppermost Member 4a.

Order Multituberculata: cf. *Microcosmodon* sp., cf. *Neoliotomus* sp., *Ptilodus* sp., *Neoplagiaulax* sp., ?*Mesodma* sp.

Order Cete: *Dissacus* sp.

Order Primates: *Paromomys* sp., *Plesiadapis* sp.

?Order Procreodi: *Mimotricentes tedfordi* n. sp. (McKenna and Lofgren in press)

Order Condylarthra: *Conacodon* new species, *Phenacodus* sp.

Edentulous Jaw Site (RAM loc. V98012); lower part of Member 4b.

Order Multituberculata: *Neoplagiaulax* sp., *Mesodma* sp.

Order Didelphimorphia (of Cohort Marsupialia): *Peradectes* sp.

Order Primates: *Ignacius* sp., *Plesiadapis* sp.

Land of Oz (RAM loc. V20001); mid-lower part of Member 4a.

Order Multituberculata: Large multituberculate (?*Neoliotomus* sp.)

?Order Procreodi: Unidentified arctocyonid

Order Condylarthra: *Phenacodus* sp., hyopsodontid, phenacodontid

Early in the study of the Goler mammalian fauna, based on admittedly sparse data, McKenna (1960) and McKenna et al. (1987) argued that the Laudate Discovery Site was probably late Torrejonian or early Tiffanian in age. With the success of recent screen-washing efforts, many more taxa have been identified, making correlation of Goler assemblages more precise. The three Goler assemblages have some key taxa in common and thus, in

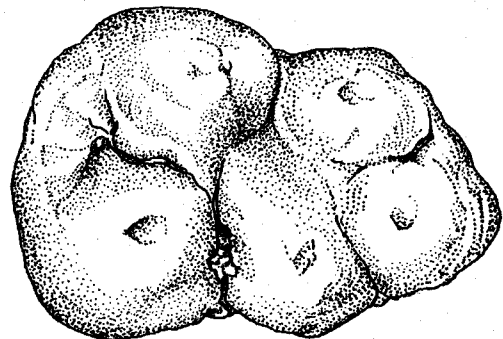


Figure 5. Lower third molar of *Phenacodus* found at the Laudate Discovery Site. Tooth length is 13 mm; drawn by Kathy Sanders.

a general sense, appear to be similar in age. Most Goler genera have a long geologic range with a zone of overlap spanning the mid-Torrejonian through the mid-Tiffanian, or middle Paleocene. However, *Plesiadapis*, *Neoliotomus*, and *Phenacodus* have known ranges that provide greater temporal resolution. *Plesiadapis* has not been reported to occur in rocks older than Tiffanian, the oldest known record of *Neoliotomus* is mid-Tiffanian, and *Phenacodus* is very common in Tiffanian rocks (Archibald et al. 1987; Lofgren et al. in press) and was not known from the late Torrejonian until recently (see Higgins 2000). Thus, presence of *Phenacodus*, *Neoliotomus*?, and especially *Plesiadapis* at the three Goler mammal sites indicates a Tiffanian age for Member 4a-b. Preliminary analysis of 7 isolated teeth referred to *Plesiadapis*, indicates that one species is present. The Goler species is similar in size and morphology to *P. anceps* and *P. rex*. Gingerich (1976) proposed a lineage zone subdivision of the Tiffanian Mammal Age based on non-overlapping species of *Plesiadapis* from superposed sites in Wyoming and Montana. Using this scheme, the presence of *Plesiadapis anceps* would denote the second oldest Tiffanian lineage zone or Ti2, and *Plesiadapis rex* the third oldest lineage zone or Ti3. If this zonation can be extended to California, the three mammal sites in the Goler Formation approximately correlate to lineage zone Ti2 or Ti3, indicating a middle Paleocene age, or about 60 ma.

Specimens of primates, marsupials, multituberculates, condylarths, and other mammalian groups from the Goler Formation constitute the oldest records of Mammalia and other vertebrates known from California. The nearest sites of comparable age are located in Wyoming and Colorado. Thus, the Goler Formation provides a unique opportunity for study of the vertebrate fauna from the West Coast of North America that existed 60 million years ago.

References Cited

- Archibald, J. D., Clemens, W. A., Gingerich, P. D., Krause, D. W., Lindsay, E. H. and K. D. Rose, 1987. First North American Land Mammal Ages of the Cenozoic Era: p. 24-76, in Woodburne, M. O. ed., Cenozoic Mammals of North America, Univ. Calif. Press, Berkeley.
- Axelrod, D. I., 1949. Eocene and Oligocene formations in the western Great Basin: Geol. Sci. Amer. Bull., v. 60 (12, pt. 2), p. 1935-6.
- Cox, B. F., 1982. Stratigraphy, sedimentology, and structure of the Goler Formation (Paleocene), El Paso, Mountains, California: implications for Paleogene tectonism on the Garlock Fault Zone: unpub. PhD dissertation, Univ. Calif. Riverside.
- Cox, B. F., 1987. Stratigraphy, Depositional Environments, and Paleotectonics of the Paleocene and Eocene Goler Formation, El Paso Mountains, California—Geologic Summary and Roadlog: p. 1-29, in Cox, B.F., ed., Basin Analysis and Paleontology of the Paleocene and Eocene Goler Formation, El Paso Mountains, California. SEPM Pacific Section.
- Cox, B. F. and M. F. Diggles, 1986. Geologic map of the El Paso Mountains Wilderness Study Area, Kern County, California: U.S. Geol. Survey Misc. Field Studies Map, MF-1827, plus 13 p.
- Cox, B. F. and L. F. Edwards, 198. Possible marginal-marine deposits in the Goler Formation (Paleocene), El Paso Mountains, California: Eos, v. 65 (45), p. 1084.
- Dibblee, T. W., Jr., 1952 Geology of the Saltdale Quadrangle, California: Calif. Div. Mines Bull., v. 160, p. 7-43.
- Gingerich, P. D., 1976 Cranial anatomy and evolution of early Tertiary Plesiadapidae (Mammalia, Primates). Univ. Mich. Papers Paleo. V. 15, p. 1-141.
- Higgins, P., 2000 Re-evaluation of the boundary between the Torrejonian and Tiffanian North American Land Mammal "Ages" with description of a new fauna from the Hanna basin, south-central Wyoming. Unpub. PhD dissertation, Univ. Wyoming, Laramie.
- Lofgren, D. L., Lillegraven, J. A., Clemens, W. A., Gingerich, P. D. and T. E. Williamson, in press. Paleocene Biochronology of North America: The Puercan through Clarkforkian Land Mammal Ages: in Woodburne, M. O. ed., Late Cretaceous and Cenozoic Mammals of North America. Univ. Calif. Press, Berkeley.
- Lofgren, D. L., McKenna, M. C. and S. L. Walsh, 1999 New Records of Torrejonian-Tiffanian Mammals from the Paleocene-Eocene Goler Formation, California, Journal of Vertebrate Paleontology, v. 19(3), p. 60A.
- McDougall, K., 1987 Foraminiferal Biostratigraphy and Paleocology of Marine Deposits, Goler Formation, California: p. 43-67, in Cox, B. F., ed., Basin Analysis and Paleontology of the Paleocene and Eocene Goler Formation, El Paso Mountains, California. SEPM Pacific Section.
- McKenna, M. C., 1955 Paleocene mammal, Goler Formation, Mojave Desert, California: American Assoc. Petrol. Geol. Bull., v. 39(4), p. 512-515.
- McKenna, M. C., 1960 A continental Paleocene vertebrate fauna from California: American Mus. Novitates, no. 2024, p. 1-20.
- McKenna, M. C., Hutchison, J. H. and J. H. Hartman 1987 Paleocene vertebrates and nonmarine mollusca from the Goler Formation, California: p. 31-41, in Cox, B.F. ed., Basin Analysis and Paleontology of the Paleocene and Eocene Goler formation, El Paso Mountains, California. SEPM Pacific Section.
- McKenna, M.C. and D. L. Lofgren, in press *Mimotricentes tedfordi*, a new arctocyonid from the Paleocene of California. American Museum Novitates.
- Reid S. A. and B. F. Cox, 1989 Early Eocene uplift of the southernmost San Joaquin Basin, California. Amer. Assoc. Petrol. Geol. Bull. v. 73, p. 549-550.
- West, R. M., 1970 *Tetraclaenodon puercensis* (Mammalia: Phenacodontidae), Goler Formation, Paleocene of California, and distribution of the genus. Jour. Paleo., v. 44(5), p. 851-857.
- Wood, H. E., R. W. Chaney, J. Clark, E. H. Colbert, G. L. Jepsen, J. B. Reeside, Jr., and C. Stock, 1941 Nomenclature and correlation of the North American continental Tertiary. Bull. Geol. Soc. Amer. V. 52, p. 1-48.
- Woodburne, M. O., 1987 Mammal ages, stages, and zones: p. 18-23, in Cenozoic Mammals of North America, in Woodburne, M. O. ed., Cenozoic Mammals of North America. Univ. Calif. Press, Berkeley.

Ag-Cu-Pb-Bi Sulfosalts New to Darwin, Inyo County, California

Gail E. Dunning, 773 Durshire Way, Sunnyvale, California 94087-4709

Yves Moëlo, Institut des Matériaux, Laboratoire de Chimie des Solides, UMR 110, (CNRS - Université de Nantes), B.P. 32229, 44322 Nantes Cedex 03, France

Andrew C. Roberts, Geological Survey of Canada, 601 Booth Street, Ottawa, Ontario K1A 0E8

Joseph F. Cooper, Jr., 430 Van Ness Avenue, Santa Cruz, California 95060

Abstract

Several rare Ag-Cu-Pb-Bi sulfosalts occur sparingly in dump material from three small mines in the Darwin mining district. These sulfosalts include cupropavonite, friedrichite, gustavite, heyrovskyite, junosite, krupkaite, pavonite and vikingite.

Introduction

The Darwin mining district, Inyo County, California, located at 36° 17' N., 117° 35' W., has long been known for its deposits of lead-silver-zinc ore, including several rare sulfosalts; in addition, ores of tungsten, antimony, copper and gold have been produced. Complete descriptions of the Darwin Quadrangle geology and ore-related deposits are given by Hall and MacKevett (1958), Czamanske and Hall (1975), Hall (1962,1971), and Hall *et al.* (1971).

The sulfosalts described in this study were identified following a quantitative electron microprobe and X-ray powder-diffraction examination of specimens collected during the winters of 1961 and 1962 from the dumps of the abandoned St. Charles, Lucky Lucy and Silver Spoon mines. These sulfosalts include cupropavonite, friedrichite, gustavite, heyrovskyite, junosite, krupkaite, pavonite and vikingite and are represented by the $\text{Cu}_2\text{S-Ag}_2\text{S-PbS-Bi}_2(\text{S,Se})_3$ system with no discernible Sb or As substitution. The complexity of the sulfosalt mineralogy at Darwin, noted first by Czamanske and Hall (1975), is confirmed by the discovery of these additional rare sulfosalts.

Geological Setting

The geology of the Darwin area has been described by Hall and MacKevett (1958) and Hall (1962). Lead-zinc-copper ores occur in a sequence of upper Paleozoic sedimentary rocks ranging in age from early Ordovician to Permian. These sedimentary rocks were intruded by a biotite-hornblende quartz monzonite stock of Jurassic (?) age and were altered to calc-silicate minerals. Ore deposits are correlated with the lower member of the Keeler Canyon formation, which is of Pennsylvanian and Permian age. Overturned bedding in the meta-sedimentary rocks strikes N. 30° W. and dips 50° SW, with many faults cutting these rocks at steep angles.

Most of the ore mined in the Darwin district is massive and occurs in veins, bedded deposits and steep, irregular replacement-type bodies. The sulfide ore consisted of galena, sphalerite and pyrite, with lesser amounts of bismuthinite, chalcopyrite, pyrrhotite, arsenopyrite, stibnite, tetrahedrite and rare Ag-Cu-Pb-Bi sulfosalts, some of which contain appreciable Se substituted for S. Oxidation of the sulfide ore has produced massive cerussite in addition to lesser amounts of malachite, azurite, aurichalcite, chrysocolla, smithsonite, hemi-morphite and hydrozincite.

Mine and Specimen Descriptions

St. Charles mine

The St. Charles tungsten mine is located near the head of a narrow, steep canyon 18 km east of Darwin at an elevation of about 1500 meters. Rocks in the mine area are interbedded calc-hornfels and pure limestone beds that are in part recrystallized to marble and altered to tactite. This tactite is composed of andradite and calcite with minor pyrite, fluorite and vesuvianite. The mine workings include an incline shaft and two adits that have exposed veins of scheelite associated with small amounts of sphalerite and pyrite.

The single discovery specimen recovered from the dump measured about 3 x 5 cm and was composed of a thin sulfosalt vein, as determined by EDS, replacing calcite in tactite. The steel gray sulfosalt vein has a feathery habit with a metallic luster. When broken, the sulfosalt possesses a conchoidal

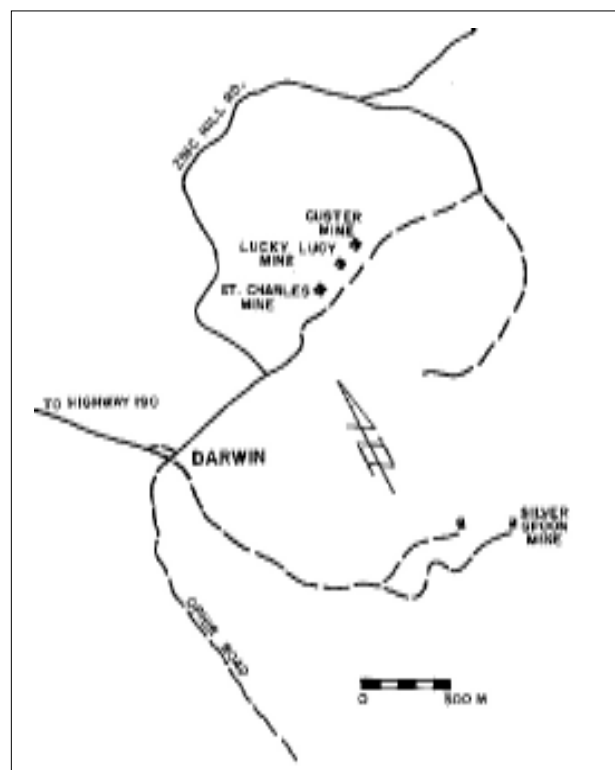


Figure 1. Location map for the Darwin mining district, Inyo County, California.



Figure 2. Thin vein containing a mixture of friedrichite and gustavite in calcite from the St. Charles mine. BSE image.

fracture. Megascopically, several small, flat crystal sections were visible along the sulfosalt margin with the calcite and are heavily striated along the direction of elongation. This specimen contained less than three grams of sulfosalt material, most of which is now contained in two polished sections and several small specimens. Extensive searching of the dump area failed to yield additional sulfosalt-containing material.

Lucky Lucy mine

The Lucky Lucy mine is located about 100 meters to the east of the St. Charles mine along the north side of the same steep canyon. Rocks in the area are consistent with those of the St. Charles mine except that most are heavily iron stained and silicified. The mine consists of a single surface pit about 4 meters deep that extends into the steep canyon slope. Oxidation of the primary minerals (chalcopyrite, sphalerite, pyrite) has produced several secondary Cu and Zn-bearing minerals, which include brochantite, serpierite, rosasite, aurichalcite, hemimorphite, bismutite and iron oxides. The serpierite and brochantite are very attractive and typically occur as delicate, well-formed acicular crystals attached to cavity and fracture surfaces in the silicified tactite.

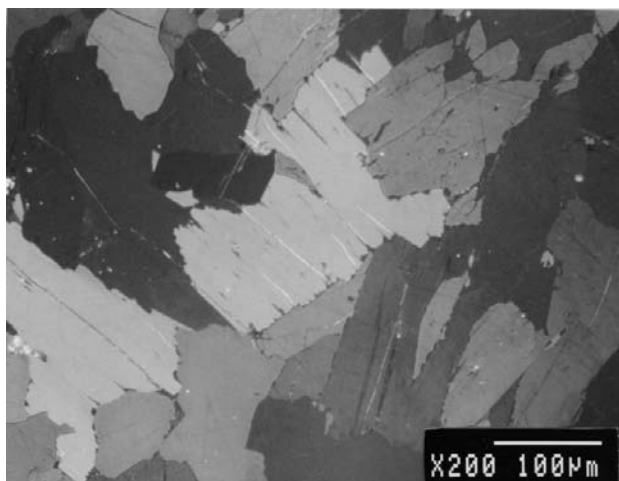


Figure 4. Typical mixture of gustavite and friedrichite (St. Charles mine) under polarized light. 200X.

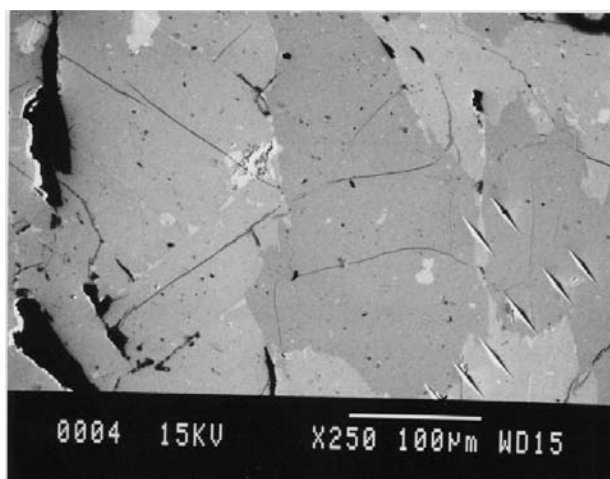


Figure 3. Polished section showing dark friedrichite grains in gustavite. Lighter phase is Ag-rich galena. St. Charles mine. BSE image.

Two sulfosalt-bearing specimens, each about 4 x 6 cm, were recovered from the small dump and constitute the entire material known. Megascopically, the first specimen consisted of small, irregular, elongate masses of a dark gray sulfosalt with a conchoidal fracture in a coarse calcite-rich tactite. No evidence of crystallization was observed. The specimen contained less than one gram of material that is contained a single polished section and several very small specimens.

The second specimen was similar to the first but contained a dark gray sulfosalt vein with a definite fibrous habit and partially altered to a yellowish-green, fine-grained copper-stained bismutite. Further searching of the limited dump area during subsequent years failed to yield additional specimens.

Silver Spoon mine

The Silver Spoon mine is located about 2 km south of Darwin along the southwest flank of the Darwin Hills and is developed by a single inclined shaft about 25 meters deep. Rocks exposed in the mine area consist of fine-grained wollastonite-bearing limestone that has been partially replaced by tactite.

Specimens from the mine dump show disseminated masses of a silvery sulfosalt that occur as replacement bands in the limestone. The sulfosalt appears as minute flattened grains

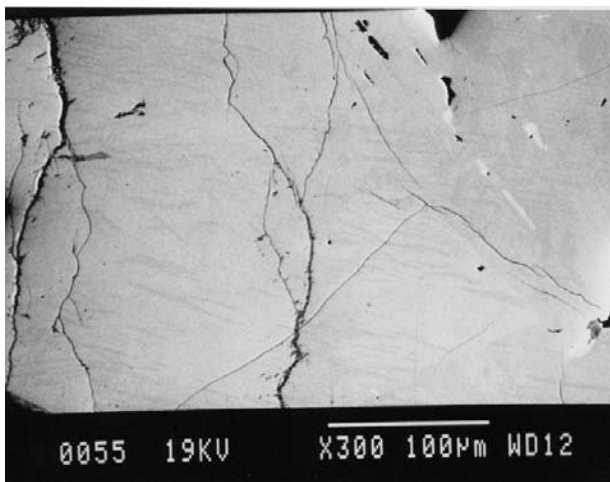


Figure 5. Polished section of Lucky Lucy mine specimen showing mixture of thin, parallel grains of vikingite and heyrovskyite. 200X.

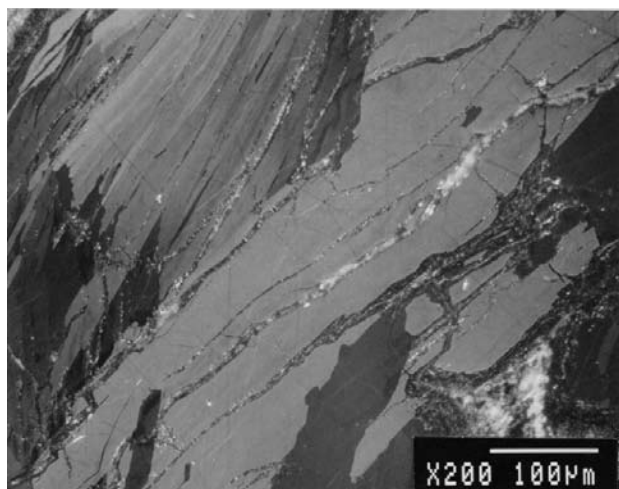


Figure 6. Polished section of Lucky Lucy mine specimen showing isolated thin grains of junosite (light gray) in pavonite. 200X.

that are somewhat tarnished yellowish-blue upon exposure. When specimens are treated with warm, dilute acetic acid, the individual sulfosalt grains show rough crystalline outlines. No secondary alteration or weathering products were observed.

Mineralogy

Initially, a small, unaltered portion of each specimen was examined by energy-dispersive spectrometry (EDS) which indicated significant levels of Ag, Cu, Pb, Bi, Se and S. Following this initial examination, a small representative unaltered portion from each specimen was submitted for routine X-ray powder-diffraction identification. The resulting patterns contained diffraction lines that were not readily identified with any known mineral, which can often be characteristic of a complex mixture of several phases. To resolve this problem, polished sections were carefully prepared, using standard methods, from the remaining portions of the bulk specimens for optical, electron microprobe and X-ray powder-diffraction study.

Optical microscopy, using bright field and polarized light, resulted in the detection of several phases in the polished sections, including bright inclusions within the sulfosalt matrix and along some grain boundaries of one of the primary matrix phases. All the matrix phases observed are moderately to

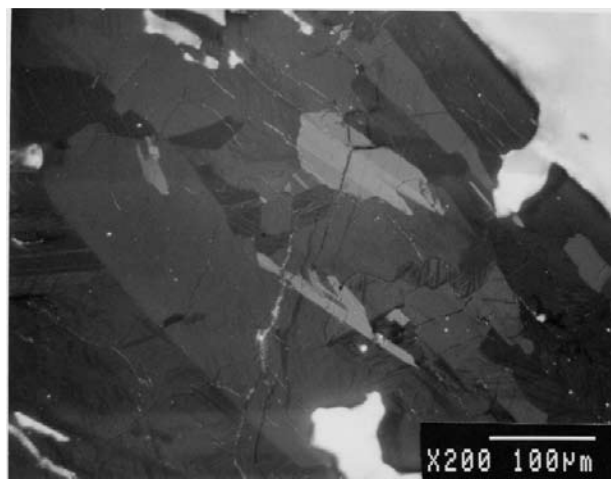


Figure 7. Polished section of Silver Spoon mine specimen showing mixture of junosite (light massive phase) and krupkaite (dark massive phase) with isolated bright grains of Se-rich tetradymite. BSE image.

strongly anisotropic under cross nicols. Backscattered electron (BSE) imaging and EDS of these polished sections also confirmed that more phases were present within these specimens than originally suspected.

To further characterize these phases, the polished sulfosalt sections were analyzed by electron-probe microanalysis using a CAMECA SX-50 microprobe (BRGM-CNRS-University common laboratory, Orléans; programming by O. Rouer, CNRS). Operating conditions were 20 kV, 20 nA, 10 s/spot counting time; standards (element, emission line) used were Cu (Cu Ka), FeS₂ (S Ka), PbS (Pb Ma), Bi (Bi Ma), Se (Se La), Cd (Cd La), Ag (Ag La), Te (Te La); undetected were Fe, Sb, As, Mn, Hg, Sn at less than 0.01%. The electron microprobe analyses (Table 1) resulted in the probable identification of cupropavonite, friedrichite, gustavite, heyrovskyite, junosite, krupkaite, pavonite and vikingite. All these sulfosalts are members of well known homologous series, according to the modular classification of Makovicky (1989).

Following the microprobe analyses, small amounts of material were extracted from the polished sections using photomicrographs and microhardness indents as guides and subjected to X-ray powder-diffraction using modified 57.3 mm

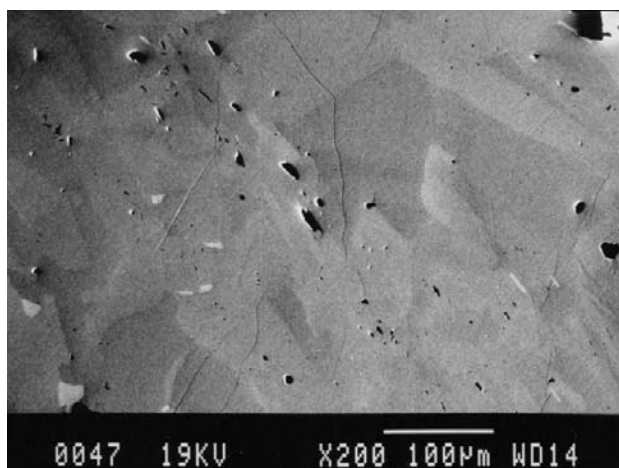


Figure 8. Isolated elongated grains of junosite exposed by etching from limestone (Silver Spoon mine). SEM image.



Figure 9. Typical combination of junosite and krupkaite grains exposed by etching from limestone. SEM image.

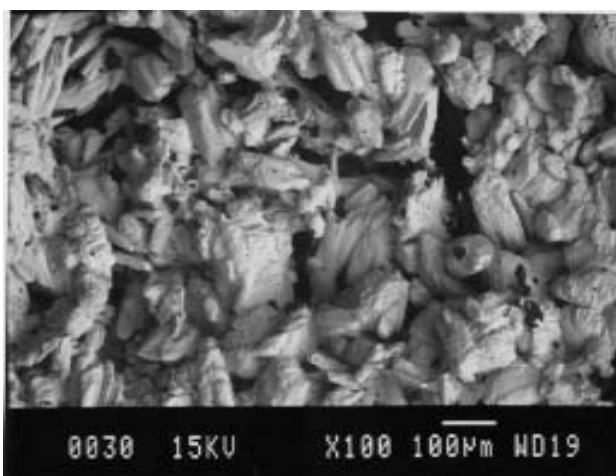


Figure 10. Polished section of Silver Spoon specimen showing elongated juninite grains in krupkaite under polarized light. 200X.

Debye-Scherrer powder cameras with Ni-filtered Cu radiation. Friedrichite, gustavite, krupkaite, juninite, pavonite and vikingite were confirmed. Heyrovskyite, cupropavonite, juninite and gustavite from the Lucky Lucy mine could not be confirmed by X-ray powder-diffraction because of their minute grain size. Specific descriptions of these eight sulfosalts and their associations are presented below.

Bismuthinite-Aikinite series

Friedrichite $Pb_5Cu_5Bi_7S_{18}$

Friedrichite was originally found in the "Sedl" region, Habach Valley, Salzburg, Austria (Chen *et al.*, 1978). At Darwin the mineral occurs associated with gustavite in the specimen from the St. Charles mine. In polished section, both friedrichite and gustavite grains are visible under BSE imaging, with friedrichite being slightly darker. Under cross nicols, both minerals can be distinguished by their polarization colors. The friedrichite grains are irregular (200 x 300 microns) and compose about 25% of the polished section area. The average of four microprobe analyses gives the formula $Cu_{4.95}Pb_{5.15}Bi_{6.95}(S_{17.88}Se_{0.12})_{S=18}$. Also observed in the polished section are small grains of galena, chalcocopyrite and sphalerite.

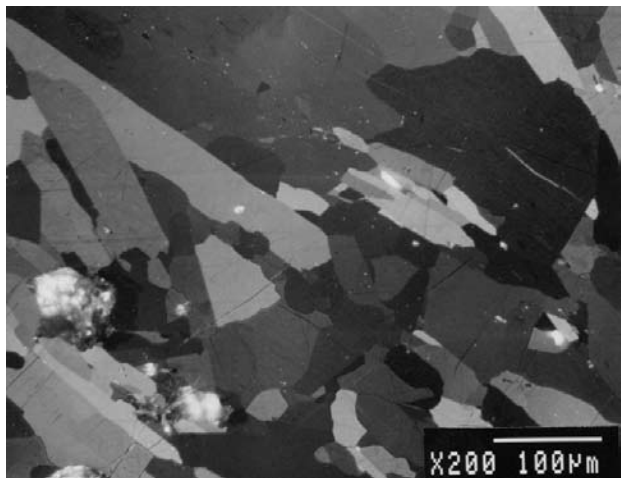


Figure 11. Pavanite matrix showing thin exsolution lamellae of cupropavonite (Lucky Lucy mine). BSE image. 300X.

Krupkaite $CuPbBi_3S_6$

Krupkaite was described from Krupka, northeast Bohemia, Czech Republic (Žák *et al.*, 1974; Mumme, 1975a). At the Silver Spoon mine it occurs as minute grains associated with juninite and inclusions of Se-rich tetradymite and pyrite as a vein constituent of the limestone-tactite rock. In polished section the krupkaite can be distinguished from the juninite by its polarization colors. The two minerals also can be distinguished by the difference in the Cu-(Pb,Bi) ratio using BSE imaging. The average of two microprobe analyses gives the formula $Cu_{0.99}Pb_{1.02}Bi_{3.00}(S_{5.60}Se_{0.40})_{S=6}$.

Lillianite series

Gustavite $Pb_3Bi_2S_6$ to $AgPbBi_3S_6$

Gustavite, originally found with beryllite in the cryolite deposit at Ivigtut, southwest Greenland (Karup-Møller, 1970) occurs as rare grains associated with heyrovskyite and vikingite in the second specimen from the Lucky Lucy mine. Microprobe analysis of a single grain gives $Ag_{0.67}Pb_{1.81}Bi_{2.69}(S_{5.45}Se_{0.50}Te_{0.05})_{S=6}$ and places this gustavite at Gus₆₅ between the solid solution compositional range of $Pb_3Bi_2S_6$ to $AgPbBi_3S_6$ and illustrates the coupled substitution of $Ag^+ + Bi^{3+} \rightarrow 2Pb^{2+}$ found in several of the sulfosalts series. Due to the small grain size, it was not confirmed by X-ray powder-diffraction.

Gustavite, containing appreciable copper, also occurs with friedrichite from the adjacent St. Charles mine. In polished section the grains are irregular and strongly anisotropic. Under BSE the gustavite and friedrichite can be distinguished. The average microprobe analysis of five spots gives $Cu_{0.12}Ag_{0.79}Pb_{1.39}Bi_{2.78}(S_{5.73}Se_{0.26}Te_{0.01})_{S=6}$. Also present is rare Ag-bearing galena seen as a thin exsolution (?) phase along some of the gustavite grains. Previously at Darwin, gustavite was reported as small exsolution inclusions in Ag-Bi-rich galena (Czamanske and Hall, 1975). Moëlo *et al.* (1987) discusses the Ag and Bi-rich chemistry of several members of the lillianite series, including gustavite, vikingite and heyrovskyite.

Heyrovskyite $Pb_6Bi_2S_9$ to $Ag_{2.5}PbBi_{4.5}S_9$

Heyrovskyite, originally described from Hürky, Czech Republic (Klominský *et al.*, 1971) occurs as elongated rare grains associated with gustavite and vikingite in the second specimen from the Lucky Lucy mine. These sulfosalts cannot be distinguished by either optical or BSE imaging. Microprobe analyses of a single grain gives $Cu_{0.08}Ag_{0.83}Pb_{4.38}Bi_{2.97}(S_{8.18}Se_{0.74}Te_{0.08})_{S=9}$. Relative to the Ag-free end member (Hey₁₀₀), its composition is close to Hey₆₅, between $Pb_6Bi_2S_9$ and $Ag_{2.5}PbBi_{4.5}S_9$.

Foord and Shawe (1989) give microprobe data for exsolved phases in galena from the Jackass mine, Darwin which they consider to be either eskimoite (?) or Ag-bearing heyrovskyite (?).

Vikingite $Pb_{18}Bi_8S_{30}$ to $Ag_7Pb_4Bi_{15}S_{30}$

Vikingite, initially described from the cryolite deposits, Ivigtut, Greenland (Makovicky and Karup-Møller, 1977) occurs associated with heyrovskyite and gustavite in the second specimen from the Lucky Lucy mine. These minerals are not distinguishable by either optical or BSE imaging. The microprobe analysis of four grains gives $Cu_{0.13}Ag_{3.14}Pb_{11.92}Bi_{11.00}(S_{27.12}Se_{2.62}Te_{0.26})_{S=30}$ and places this vikingite at about Vik₄₃ between the compositional end members $Pb_{18}Bi_8S_{30}$ and $Ag_7Pb_4Bi_{15}S_{30}$. Vikingite from Ivigtut corresponds to Vik₆₀-Vik₆₇.

Junoite series

Junoite $\text{Pb}_3\text{Cu}_2\text{Bi}_8(\text{S,Se})_{16}$

Junoite was first described from the Juno mine, Tennant Creek, Australia (Mumme, 1975b). Later it was identified from the Kidd Creek mine, Timmins, Ontario (Pringle and Thorpe, 1980) and the Linka mine, Lander County, Nevada (Williams, 1988).

At Darwin it occurs as elongated grains with krupkaite and inclusions of Se-rich tetradymite in limestone-tactite rock at the Silver Spoon mine. When this rock is treated with dilute acetic acid, abundant grains with striations parallel to the elongated direction are observed. The junoite can be distinguished from krupkaite by its polarization colors and BSE imaging effect. Microprobe analysis of two grains gives $\text{Cu}_{1.95}\text{Ag}_{0.16}\text{Pb}_{2.67}\text{Bi}_{8.08}(\text{S}_{13.97}\text{Se}_{1.95}\text{Te}_{0.08})_{\text{S}=16}$.

Junoite also occurs rarely as elongated grains in the first specimen from the Lucky Lucy mine associated with Cu-rich pavonite, cupropavonite and Se-rich tetradymite. Microprobe of two grains gives $\text{Cu}_{1.95}\text{Ag}_{0.22}\text{Pb}_{2.56}\text{Bi}_{8.22}(\text{S}_{14.24}\text{Se}_{1.70}\text{Te}_{0.06})_{\text{S}=16}$.

Pavonite series

Pavonite $(\text{Ag,Cu})(\text{Bi,Pb})_3\text{S}_5$

Pavonite, originally named alaskaite (benjaminite) from the Porvenir mine, Cerro Bonete, Bolivia (Nuffield, 1954), occurs as the Cu-Se-rich variety associated with exsolved cupropavonite, junoite and Se-rich tetradymite in the first specimen from the Lucky Lucy mine. The pavonite constitutes most of the specimen. It is moderately anisotropic and the grains are generally elongated parallel to the vein direction. Microprobe analysis of two grains gives $\text{Cu}_{0.43}\text{Ag}_{0.67}\text{Pb}_{0.33}\text{Bi}_{2.74}(\text{S}_{4.34}\text{Se}_{0.64}\text{Te}_{0.02})_{\text{S}=5}$.

Cupropavonite $\text{Cu}_{0.9}\text{Ag}_{0.5}\text{Bi}_{2.5}\text{Pb}_{0.6}\text{S}_5$

Cupropavonite was first noted from the Alaska mine, Colorado (Karup-Møller and Makovicky, 1979) as exsolved lamellae in pavonite associated with interstitial gustavite.

Two of the nine microprobe analyses of the pavonite-rich specimen from the Lucky Lucy mine gave Cu/(Cu+Ag) atom ratios of 0.52 and 0.56, indicating the possibility that cupropavonite exists as an exsolved phase within the pavonite. The seven other microprobe analyses gave Cu/(Cu+Ag) atom ratios from 0.31 to 0.46, which places them in the pavonite region of the pavonite-cupropavonite compositional range.

An optical examination of the microprobed area containing high copper revealed abundant, exsolution lamellae within the pavonite grains. The strong anisotropy and habit of these lamellae are comparable with the exsolved lamellae observed in the Cu-rich pavonite from the Alaska mine, Colorado cited by Karup-Møller and Makovicky (1979). SEM/BSE imaging of the pavonite grains revealed that the lamellae observed optically all are indeed Cu-rich with respect to the host pavonite grains. These lamellae average 5 microns x 50 microns and are oriented parallel along the crystallographic planes of the pavonite. The X-ray powder-diffraction of the area rich in Cu was of a mixture of pavonite (confirmed) and cupropavonite (suspected). The calculated microprobe analysis gives $\text{Cu}_{0.72}\text{Ag}_{0.67}\text{Pb}_{0.36}\text{Bi}_{2.63}(\text{S}_{4.34}\text{Se}_{0.63}\text{Te}_{0.03})_{\text{S}=5}$, which probably consists of a mixture of pavonite and cupropavonite.

Unclassified sulfosalt analyses

Two unclassified microprobe analyses were obtained from one St. Charles mine specimen (UN-1 and UN-2 in Tables 1 and

2). They resemble gustavite, but with an abnormally high Cu content (2.4 wt. %) for UN-1, and a significant Se enrichment in UN-2. Without correlated X-ray data, one cannot definitively assume their identification as gustavite varieties.

Metacinnabar HgS

Metacinnabar occurs as a rare constituent of a very fine-grained mineral mixture at the end of the specimen from the St. Charles mine that is rich in friedrichite and Cu-rich gustavite. This is the first recorded occurrence of a mercury mineral in the Darwin ores. Also associated in this mixture is a Cu-Cd sulfide that has formed very thin replacement veins along the gustavite grain boundaries.

Tetradymite $\text{Bi}_2\text{Te}_2(\text{S,Se})$

Se-rich tetradymite occurs as minute inclusions in the sulfosalt assemblage of the Silver Spoon and Lucky Lucy mines. It is easily recognized by its high reflectivity, good polish, EDS spectrum and microprobe analyses. This mineral previously has been reported by Czamanske and Hall (1975) from the Thompson mine, Darwin as inclusions in galena.

Discussion

Czamanske and Hall (1975) recognized four different assemblages of sulfide minerals in the Darwin district, two of which are galena-rich. These latter assemblages consist of fine-grained galena-rich ore that contains abundant Ag, Bi and Se (Te) and minor associated pyrite. They reported an exsolved Ag-bearing phase in galena with associated matildite that was considered to be heyrovskite. Foord and Shawe (1989) gave micro-probe data for these exsolved phases in galena that they considered to be either eskimoite (?) or a Ag-bearing heyrovskite (?).

Pb-sulfosalts previously reported from the Darwin mines were generally considered as minor exsolution products from main galena (Czamanske & Hall, 1975). Those reported herein from the St. Charles, Lucky Lucy and Silver Spoon mines appear to be the result of a complex galena-free Pb-Bi-Cu-Ag co-precipitation event related to the relative high temperature W mineralization. The specimens, which we have examined, consist of a complex intergrowth of members of the lillianite, bismuthinite-aikinite, pavonite and the junoite series, associated with very minor galena and tetradymite.

Galena and associated sulfosalts at Darwin were interpreted to have crystallized at a temperature greater than 350°C (Czamanske & Hall, 1975), while Mumme (1975b) suggests a temperature below 600°C. The Sb:Bi ratio is an indication of formation temperature. Low values are indicative of relatively high temperature and considerable depth. Galena from the Jackass mine, Darwin has a Sb:Bi ratio of <0.07 (Foord & Shawe, 1989). EDS results for the several sulfosalts examined in our study show no discernible Sb at the 0.1 wt.% analytical level. Microprobe analyses of tetradymite specimens from the Lucky Lucy and Silver Spoon mines show an Sb range from 0.02 to 0.22 wt.%.

This new mineralogical data of our study correlates with some of the results obtained by Czamanske & Hall (1975) on the Darwin district, and by Foord *et al.* (1988), who discussed the relationship between coexisting galena, (Bi, Ag)-enriched galena, and sulfosalts. At the Lucky Lucy mine, the gustavite-vikingite-(Ag,Bi)-rich heyrovskite trend (or Gus₆₅-Vik₄₇-Hey₆₅ trend) is very close to the Type I – Type II – Type III sulfosalts (+ galena) trend of Czamanske & Hall (1975). This trend has

Table 1. Average microprobe analysis (wt. %) of Darwin sulfosalts (this study).

Mineral (#)	Mine	Cu	Ag	Cd	Pb	Bi	Te	Se	S	Total
Friedrichite (4)	St. Charles	9.16	n.d.	n.d.	31.12	42.39	n.d.	0.54	16.61	99.84
Gustavite (5)	St. Charles	0.62	7.24	0.03	24.58	49.68	0.09	1.8	15.64	99.68
Krupkaite (2)	Silver Spoon	5.68	n.d.	n.d.	19.16	56.78	n.d.	2.80	16.29	100.69
Junoite (2)	Silver Spoon	4.28	0.50	n.d.	18.54	56.14	0.32	5.12	14.92	99.67
Junoite (2)	Lucky Lucy	4.08	0.78	0.01	17.49	57.06	0.25	4.46	15.22	99.31
Heyrovskyite (1)	Lucky Lucy	0.17	4.77	0.0	46.90	31.47	0.36	3.13	13.52	100.33
Vikingite (4)	Lucky Lucy	0.10	5.58	0.03	40.38	37.24	0.36	3.32	14.16	101.13
Gustavite (1)	Lucky Lucy	0.08	6.03	0.0	30.21	45.73	0.45	3.33	14.69	100.51
Pavonite (7)	Lucky Lucy	2.92	7.76	0.10	7.25	61.83	0.37	5.37	14.85	100.44
Cupropavonite (2)	Lucky Lucy	4.93	7.05	0.10	8.02	58.94	0.35	5.38	14.96	99.71
Unclassified (1)	St. Charles	2.42	7.23	0.14	24.27	48.57	0.13	1.79	15.78	100.33
Unclassified (1)	St. Charles	1.01	8.10	0.0	18.74	52.60	0.09	2.98	15.22	98.83

(#) = number of microprobe analyses.

also been described from the following deposits: the Treasure mine, Colorado (Karup-Møller, 1977); the Montaneme W-Sn deposit, Spain, (Gouanvic & Babkine, 1985); the La Roche-Baluc, France (Moëlo *et al.* 1987); the Corrie Buie lead veins, Scotland (Patrick, 1984); the Round Mountain and Manhattan gold districts, Nevada (Foord *et al.* 1988) and in the mineralized veins in the Oberprinzgau region, Austria (Paar *et al.* 1980).

Increasing the Ag-Cu-Bi content relative to Pb gives the gustavite-friedrichite association at the St. Charles mine. Ag-Pb impoverishment gives the krupkaite-junoite association at the Silver Spoon mine.

Se partitioning between Bi-sulfosalts is an interesting aspect our study. In the sulfosalts of the pavonite series, which always have a high Bi/Pb ratio, Mumme (1990) indicates no limit in

Table 2. Average chemical formulas for Darwin sulfosalts (this study).

Mineral	Mine	Chemical formula
Friedrichite	St. Charles	$\text{Cu}_{4.85}\text{Pb}_{6.15}\text{Bi}_{6.96}(\text{S}_{17.88}\text{Se}_{0.12})_{\Sigma=18}$
Gustavite	St. Charles	$\text{Cu}_{0.12}\text{Ag}_{0.79}\text{Pb}_{1.39}\text{Bi}_{2.78}(\text{S}_{6.75}\text{Se}_{0.28}\text{Te}_{0.01})_{\Sigma=8}$
Krupkaite	Silver Spoon	$\text{Cu}_{0.99}\text{Pb}_{1.02}\text{Bi}_{3.00}(\text{S}_{6.80}\text{Se}_{0.40})_{\Sigma=8}$
Junoite	Silver Spoon	$\text{Cu}_{1.95}\text{Ag}_{0.16}\text{Pb}_{2.67}\text{Bi}_{9.08}(\text{S}_{13.97}\text{Se}_{1.95}\text{Te}_{0.08})_{\Sigma=18}$
Junoite	Lucky Lucy	$\text{Cu}_{1.95}\text{Ag}_{0.22}\text{Pb}_{2.58}\text{Bi}_{9.22}(\text{S}_{14.24}\text{Se}_{1.70}\text{Te}_{0.08})_{\Sigma=18}$
Heyrovskyite	Lucky Lucy	$\text{Cu}_{0.08}\text{Ag}_{0.83}\text{Pb}_{4.36}\text{Bi}_{2.97}(\text{S}_{8.19}\text{Se}_{0.74}\text{Te}_{0.08})_{\Sigma=9}$
Vikingite	Lucky Lucy	$\text{Cu}_{0.13}\text{Ag}_{3.14}\text{Pb}_{11.92}\text{Bi}_{11.09}(\text{S}_{27.12}\text{Se}_{2.62}\text{Te}_{0.26})_{\Sigma=30}$
Gustavite	Lucky Lucy	$\text{Ag}_{0.67}\text{Pb}_{1.81}\text{Bi}_{2.68}(\text{S}_{3.45}\text{Se}_{0.50}\text{Te}_{0.05})_{\Sigma=8}$
Pavonite	Lucky Lucy	$\text{Cu}_{0.49}\text{Ag}_{0.67}\text{Pb}_{0.33}\text{Bi}_{2.74}(\text{S}_{4.34}\text{Se}_{0.64}\text{Te}_{0.02})_{\Sigma=5}$
Cupropavonite	Lucky Lucy	$\text{Cu}_{0.72}\text{Ag}_{0.67}\text{Pb}_{0.35}\text{Bi}_{2.63}(\text{S}_{4.34}\text{Se}_{0.65}\text{Te}_{0.03})_{\Sigma=5}$
Unclassified	St. Charles	$\text{Cu}_{0.44}\text{Ag}_{0.78}\text{Pb}_{1.37}\text{Bi}_{2.70}(\text{S}_{6.75}\text{Se}_{0.28}\text{Te}_{0.01})_{\Sigma=8}$
Unclassified	St. Charles	$\text{Cu}_{0.20}\text{Ag}_{0.89}\text{Pb}_{1.06}\text{Bi}_{2.94}(\text{S}_{5.55}\text{Se}_{0.44}\text{Te}_{0.01})_{\Sigma=8}$

Minerals in bold verified by X-ray powder diffraction.

the Se-for-S substitution in such a crystal structure type. This explains the highest Se content encountered in the pavonite-cupropavonite inter-growth from Lucky Lucy mine. For a lower Bi/Pb ratio, corresponding to junoite and krupkaite, the equilibrium association between these two sulfosalts at the Silver Spoon mine is original and clearly confirms the stabilizing effect of Se for junoite (Se content twice that of krupkaite). Reversibly, the Se-for-S substitution in krupkaite may be considered as a maximum value. On the other hand, the association of junoite and pavonite-cupropavonite at the Lucky Lucy mine represents another phase equilibrium, but with only a weak Se-partitioning in favor of the pavonite-type phase.

Mumme (1975b) reports that junoite was not found during

studies of the $\text{Bi}_2(\text{S},\text{Se})_3\text{-Pb}(\text{S},\text{Se})\text{-Cu}_2(\text{S},\text{Se})$ compositions carried out above 600°C. He suggests that selenium is an essential component of the junoite crystal structure, ordering out during the conditions of relatively slow cooling found in natural systems.

Minerals of the gustavite series have the lowest Bi/Pb ratio, but the limit of the Se-for-S substitution is unknown. Our data shows up to 3.3 wt.% Se, but Czamanske & Hall (1975) indicate up to 10 wt.% Se for the sulfosalt assemblage (probable (Ag, Bi)-rich heyrovskyite) at Darwin, and Large & Mumme (1975) about 7 wt.% Se for pure heyrovskyite at the Juno mine, Australia.

In such a complex district as Darwin, from deposit to deposit, or even within a given deposit, small variations in the ratio between various associated elements (Pb, Bi, Ag, Cu, Se) is sufficient to induce the formation of distinct (and various) Bi-sulfosalts. In the future, one may hope that the collection and examination of new samples at the Darwin district will permit the discovery of other rare sulfosalts.

Acknowledgments

The authors sincerely thank Drs. A. J. Criddle, T. T. Chen, J. Jambor, J. H. G. LaFlamme, and J. Cabri for reviews of this paper.

References

- CHEN, T. T., KIRCHNER, E., and PAAR, W. (1978) Friedrichite, $\text{Cu}_3\text{Pb}_5\text{Bi}_7\text{S}_{18}$, a new member of the aikinite-bismuthinite series. *Canadian Mineralogist*, **16**, 127-130.
- CZAMANSKE, G. K., and HALL, W. E. (1975) The Ag-Bi-Pb-Sb-S-Se-Te mineralogy of the Darwin lead-silver-zinc deposit, southern California. *Economic Geology*, **70**, 1092-1110.
- FOORD, E. E., SHAW, D. R., and CONKLIN, N. M. (1988) Coexisting galena, PbS_{88} and sulfosalts: evidence for multiple episodes of mineralization in the Round Mountain and Manhattan gold districts, Nevada. *Canadian Mineralogist*, **26**, 355-376.

- FOORD, E. E., and SHAW, D. R. (1989) The Pb-Bi-Ag-Cu-(Hg) chemistry of galena and some associated sulfosalts: a review and some new data from Colorado, California and Pennsylvania. *Canadian Mineralogist*, **27**, 363-382.
- GOUANVIC, Y. and BABKINE, J. (1985) Métallogénie du gisement à tungstène-étain de Monteneme (N.W. Galice, Espagne). *Mineralium Deposita*, **20**, 8-15.
- HALL, W. E., and MACKEVETT, E. M. (1958) Economic geology of the Darwin Quadrangle, Inyo County, California. *California Division of Mines Special Report*, **51**, 73 p.
- HALL, W. E. (1962) Geology and ore deposits of the Darwin Quadrangle, Inyo County, California. *U. S. Geological Survey Professional Paper*, **368**, 87p.
- HALL, W. E. (1971) Minor-element contents of the sulfide minerals, Darwin lead-silver-zinc mine, Inyo County, California. *Society of Mining Geologists, Japan, Special Issue 2*, 119-126.
- HALL, W. E., ROSE, H. J., JR., and SIMON, F. O. (1971) Fractionation of minor elements between galena and sphalerite, Darwin lead-silver-zinc mine, Inyo County, California and its significance in geothermometry. *Economic Geology*, **66**, 602-606.
- KARUP-MØLLER, S. (1970) Gustavite, a new sulfosalt from Greenland. *Canadian Mineralogist*, **10**, 173-190.
- KARUP-MØLLER, S. (1977) Mineralogy of some Ag-(Cu)-Pb-Bi sulphide associations. *Bulletin Geological Society Denmark*, **26**, 41-68.
- KARUP-MØLLER, S., and MAKOVICKY, E. (1979) On pavonite, cupropavonite, benjaminite, and "oversubstituted" gustavite. *Bulletin de la Société française Minéralogie et Cristallographie*, **102**, 351-367.
- KLOMÍNSKÝ, J., RIEDER, M., KIEFT, C., and MRAZ, L. (1971) Heyrovskyite, $6(\text{Pb}_{0.86}\text{Bi}_{0.08})(\text{Ag,Cu})_{0.04}\text{S}\cdot\text{Bi}_2\text{S}_3$ from Hürky, Czechoslovakia, a new mineral of genetic interest. *Mineralium Deposita*, **6**, 133-147.
- LARGE, R.R. and MUMME, W.G. (1975) Junoite, "wittite" and related seleniferous bismuth sulfosalts from Juno Mine, Northern Territory, Australia. *Economic Geology*, **70**, 369-383.
- MAKOVICKY, E., and KARUP-MØLLER, S. (1977) Chemistry and crystallography of the lillianite homologous series II. Definition of new minerals: eskimoite, vikingite, ourayite, and treasureite. Re-definition of schirmerite and new data on the lillianite-gustavite solid-solution series. *Neues Jahrbuch für Mineralogie Abhandlungen*, **131**, 56-82.
- MAKOVICKY, E. (1989) Modular classification of sulphosalts—current status: Definition and Application of homologous series. *Neues Jahrbuch für Mineralogie Abhandlungen*, **160**, 269-297.
- MOËLO, Y., MARCOUX, E., MAKOVICKY, E., KARUP-MØLLER, S., AND LEGENDRE, O. (1987) Homologues de la lillianite (gustavite, vikingite, heyrovskyite riche en Ag et Bi...) de l'indice à W-As-(Pb, Bi, Ag) de La Roche-Baluc (Loire-Atlantique, France). *Bulletin de Minéralogie*, **110**, 43-64.
- MUMME, W. G. (1975a) The crystal structure of krupkaite, $\text{CuPbBi}_3\text{S}_6$, from the Juno mine at Tennant Creek, Northern Territory, Australia. *American Mineralogist*, **60**, 300-308.
- MUMME, W. G. (1975b) Junoite, $\text{Cu}_2\text{PbBi}_3(\text{S,Se})_6$, a new sulfosalt from Tennant Creek, Australia: its crystal structure and relationship with other bismuth sulfosalts. *American Mineralogist*, **60**, 548-558.
- MUMME, W.G. (1990) A note on the occurrence, composition and crystal structures of pavonite homologous series members ^4P , ^6P , and ^8P . *Neues Jahrbuch für Mineralogie, Monatshefte*, 193-204.
- NUFFIELD, E. W. (1954) Studies of mineral sulphosalts: XVIII-pavonite, a new mineral. *American Mineralogist*, **39**, 409-415.
- PAAR, W.H., CHEN, T.T. and MEIXNER, H. (1980) Pb-Bi-(Cu)-sulfosalts in Paleozoic gneisses and schists from Oberpinzgau, Salzburg Province, Austria. *Tschermaks Mineralogische und Petrographische Mitteilungen*, **27**, 1-16.
- PATTRICK, R. A. D. (1984) Sulphide mineralogy of the Tomnadashan copper deposit and the Corrie Buie lead veins, south Loch Tayside, Scotland. *Mineralogical Magazine*, **48**, 85-91.
- PRINGLE, G. J., and THORPE, R. I. (1980) Bohdanowiczite, junoite and laitakarite from the Kidd Creek mine, Timmins, Ontario. *Canadian Mineralogist*, **18**, 353-360.
- WILLIAMS, S. A. (1988) Pottsite, a new vanadate from Lander County, Nevada. *Mineralogical Magazine*, **52**, 389-390.
- ŽÁK, L., SYNECEK, V., and HYBLER, J. (1974) Krupkaite, $\text{CuPbBi}_3\text{S}_6$, a new mineral of the bismuthinite-aikinite group. *Neues Jahrbuch für Mineralogie, Monatshefte*, 533-541.

Abstracts from the 2002 Desert Symposium

China Ranch and Chinese in the Mojave Desert

Brian Brown, *P.O. Box 61, Shoshone, CA 92384-0061*

China Ranch, located near the south end of Death Valley, has always been a point of interest in the Mojave Desert because of the generous flow of water and as one of the few places historically where farming was possible before the modern era of machinery. The story of how the property got its name has been considered largely anecdotal, as no real verification of the popular local tale has ever been revealed.

Recent discoveries in the archives of the borax company as well as misplaced county documents have shed some light on the story, but have also raised more questions about the presence of the mysterious Chinese farmer who gave the property the one name that has stuck. The presence and contribution of Chinese workers in the early mining efforts in the Mojave was significant, through little is recorded.

Edmund Jaeger and the Poorwill Mystery

James M Bryant, *Curator of Natural History, Riverside Municipal Museum, 3580 Mission Inn Avenue, Riverside, CA 92501*

Sixty-five years ago this April, naturalist Edmund Jaeger made his momentous discovery regarding the behavioral biology of one of the most common yet seldom seen birds of the Southwestern deserts: the Common Poorwill (*Phalaenoptilus nuttallii*). In a rare instance of a scientific investigation being recorded in real time, Jaeger and Loyd Mason Smith (at that time Director of the Palm Springs Desert Museum) teamed up to create a 16mm film of the Poorwill Project. Recently, the negative of the film was donated to the Riverside Municipal Museum. For this presentation, the film, entitled "The Poorwill Mystery" will be shown in a restored, video transfer version.

Geology of the Cowhole Mountains, Mojave Desert, California

Horacio Ferriz, *Water for the World Project, California State University Stanislaus, Turlock CA 95382, USA. hferriz@geology.csustan.edu*

The Cowhole Mountains are an east-tilted remnant of the Jurassic volcanic arc that once formed the crest of the Sierra Nevada/Peninsular Ranges magmatic arc. In the Middle Jurassic, the eolian Aztec Sandstone accumulated in two grabens and mantled the intervening horst. These structures cut Paleozoic limestones and were bound by syndepositional faults. The grabens appear to have developed perpendicular to a larger structure (probably a regional rift), whose bounding listric faults tilted the accumulating sandstone sequence to the west, as shown by the fact that east dip in one of the grabens increases from 30° at the base of the sandstone section to 65° at its top. Busby-Spera et al. (1987) reported a 173 ± 4 -Ma date for an andesite flow breccia interbedded with the Aztec sandstone, and a 170 ± 2 -Ma date for the basal ignimbrite of an overlying volcanic series (Cowhole volcanics), thus confirming the middle Jurassic age of the Aztec Sandstone in this part of the Mojave Desert. Westward tilting continued during extrusion and accumulation of the Cowhole volcanics, which were fed by magma chambers similar to the

ones that formed the plutons now found in the Sierra Nevada and the Peninsular Ranges. Silicic volcanic rocks that buried the grabens and intervening horst include ignimbrites, volcanoclastic rocks, and flow breccias, emplaced in a proximal but extra-caldera setting. Coeval plutons and sills were intruded at shallow levels into the Paleozoic limestones, the Aztec Sandstone, and even the volcanic sequence. Local magmatism ended with intrusion of a bimodal dike swarm that may be correlative with the Independence dike swarm—dated at 148 million years. The most recent stage of tectonic deformation is probably associated with Cenozoic Basin-and-Range extension, and resulted in tilting of the whole Cowhole block 90° to the east, so the plan view of the range is a well-exposed cross-section of the Jurassic structures and formations.

Busby-Spera, C.J., Schermer, E.R., Mattinson, J.M., 1987, Lower Mesozoic extensional continental arc, Arizona and California: A depocenter for craton-derived quartz arenites: Geological Society of America Abstracts with Programs, v. 19, no. 7, p.607.

Nona Proctor Rosenberg: Her Life on the Tonopah and Tidewater Railroad

Robin Flinchum, *Shoshone, CA 92384*

At the junction of the Union Pacific and T&T Railroads, in a little town called Crucero, a willowy young woman named Nona Proctor spent her every spare moment daydreaming and reading books in the shelter of a mesquite-circled sand dune. Early in the 1920's, the railroad was still king of the west and Nona's father worked at the Crucero station. From her vantage point at the top of the dune, known as The Lookout to her family, Nona could advise her mother when Dad was on his way home and supper would hit the table as he walked in the door.

The Proctors were a family of desert pioneers—they had come to Crucero in a covered wagon, with the children walking most of the way, from California's Coachella Valley in 1917. By the time Nona graduated from high school, the desert, and the railroad, were in her blood. When she fell in love with Harry Rosenberg, foreman of the T&T Railroad bridge gang, in 1926, it made sense that her married life would begin in a boxcar traveling up and down the track, parking on a side rail wherever repairs were needed. Nona and Harry eventually added two boys to their family and began raising them in the unrestricted, unconventional atmosphere of a desert railroad.

Nona's experience of the T&T was entirely different than that of the men in her life—her focus was domestic and her interactions with the people she met up and down the line were either social, or motivated by the fulfillment of some household need. In this way, her story shows us a side of the T&T that isn't often portrayed in the popular history.

Using Nona's unpublished diaries and letters, as well as letters from and interviews with her sisters and her son, Harry Rosenberg, Jr., I will present the story of Nona Proctor Rosenberg. For background information about the T&T I will rely on published sources, as well as the advice and insight of a few of the railroad's aficionados who have been extremely helpful in answering questions.

Tracks Through Time: The Fossil Animal Track Replication Project

Bob Hilburn, 270 E. Virginia Way, PO Box 1282, Barstow, CA 92311; Robert Reynolds, LSA Associates, Riverside CA 92507

The objective of the "Tracks Through Time" program of the Mojave River Valley Museum (MRVM) under Bureau of Land Management (BLM) permit is to locate and inventory fossil tracks in the Mojave Desert, and to preserve them through replication as opposed to excavation and removal. The experience of trackway replication at outcrops and the production of trackway casts in the lab of the Desert Discovery Center (BLM and MRVM) is educational for all avocational students. In addition to exhibit replicas, an outdoor, hands-on exhibit of tracks of Paleozoic, Mesozoic and Cenozoic animals is in progress.

Replication techniques are non-destructive; preparation includes cleaning the surface with brushes and water, and applying a soap-based sealer to protect the rock. The second application is a paraffin based mold release agent that will degrade in sunlight and wash away with soap and/or rainfall. Silicon rubber is applied, hardens, and is reinforced with fiber mesh. Removal of the silicon rubber mold allows replication in the Desert Discovery Center lab with various casting mediums. Casts completed include Jurassic dinosaurs and mammal-like reptiles, prints of five Miocene mammals and one arthropod, and four Ice Age mammal tracks.

A New Gomphothere from the Mid-Pliocene Ancestral Colorado River Deltaic Deposits in Anza-Borrego Desert State Park®, California

George T. Jefferson and George E. McDaniel Jr., Colorado Desert District Stout Research Center, Borrego Springs, CA 92004

The Colorado Desert District of the Department of Parks and Recreation recently established an interagency contract with the Department of Geological Sciences, University of California Riverside, to study and GPS map the significant mid-Pliocene fossil wood deposits in Anza-Borrego Desert State Park® (ABDSP). During initial reconnaissance survey work, 5 June 2001, the remains of a previously unrecognized gomphothere were recovered in upper Deguynos Canyon within the Vallecito/Fish Creek Basin (Arroyo Tapiado 7.5 minute USGS quadrangle).

Upper Deguynos Canyon is incised within the Diablo formation of Palm Spring group (Winker and Kidwell, 1996), which consists of ancestral Colorado River nonmarine deltaic deposits. Local sediments consist of very pale yellowish gray to grayish yellow (5Y7/2 to 5Y8/4), well sorted, fine to medium-grained, massively bedded sandstone. The site, ABDSP2233, is on strike from the paleomagnetic section of Opdyke et al. (1977), and lies within "collecting zone" (see Cassiliano, 1996) number 26, providing an approximate age of 3.6 Ma. Although large, 0.25 to 1.0 m-diameter, permineralized tree logs (including deciduous hardwoods, oaks, avocado and palm) (Remeika and Fleming, 1995) occur in the same beds, vertebrate remains in this part of the section are very rare. Fragments of the specimen, weathered 10-20 cm-sized chunks of cortical and medullar bone, were found on the surface scattered over 15 m-diameter area, and apparently had been weathering on site for a considerable time. The bone is fully permineralized with dark brown cryptocrystalline calcite.

The specimen, ABDSP2233/V6409, consists of premaxillary, dentary and other, unidentifiable cranial fragments. Pre-maxillae fragments include the distal alveolar area for the right and left I2/. The radius of curvature of the alveoli measure 57.9 mm, providing an estimated diameter of 116 mm for the upper second incisors. Portions of the anterior (distal end) mandibular symphyseal process with alveoli for both I/2 are preserved. The radius of curvature of the alveoli, right 33.0 mm and left 41.7 mm, yield an approximate estimated diameter of 75 mm for the lower second incisors. Both the left and right posterior dentary with alveoli for posterior root of M/3 were recovered along with fragments of both ascending rami.

Gomphotherium is a short-legged, hippopotamus-sized Gomphothere. Mandibular tusks occur in both *Gomphotherium* and *Rhynchotherium*. The anterior mandibular symphyseal process of both are much shorter and smaller in diameter than the upper tusks. The anterior symphyseal process of *Gomphotherium* is straight and long, extending forward so the distal end of the smaller mandibular tusk extends nearly to the end of the longer upper tusk. In contrast, this process in *Rhynchotherium* is short and sharply downturned (Kurten and Anderson, 1980). The distal alveolar area of specimen ABDSPV6409 has no curvature. The calculated diameter of the lower tusk in ABDSPV6409 compares favorably with specimens of *Gomphotherium* from Black Hawk Ranch in the collection of the Paleontology Museum, University of California, Berkeley.

According to Woodburne (1987), *Gomphotherium* first appears in North America during the Barstovian North American Land Mammal Age (NALMA), and was widespread in the Hemphillian NALMA. *Gomphotherium* survived in southwestern North America into the late Hemphillian NALMA, while *Rhynchotherium* became widespread. With an approximate age of 3.6 Ma, ABDSPV6409 extends the temporal range of the *Gomphotherium* to middle Blancan NALMA.

References

- Cassiliano, M.L. 1999. Biostratigraphy of Blancan and Irvingtonian mammals in the Fish Creek-Vallecito Creek section, southern California, and a review of the Blancan-Irvingtonian boundary. *Journal of Vertebrate Paleontology* 19(1):169-186.
- Kurten, B., and E. Anderson 1980. Pleistocene mammals of North America. Columbia University Press 442 p.
- Opdyke, N.D., E.H. Lindsay, N.M. Johnson, and T. Downs 1977. The paleomagnetism and magnetic polarity stratigraphy of the mammal-bearing section of Anza-Borrego State Park, California. *Quaternary Research* 7:316-329.
- Remeika, P., and R.F. Fleming 1995. Cretaceous plynoflora and Neogene angiosperm woods from Anza-Borrego Desert State Park, California: implications for Pliocene climate of the Colorado Plateau and age of the Grand Canyon. In *Paleontology and Geology of the Western Salton Trough Detachment, Anza-Borrego Desert State Park, California*, edited by P. Remeika and A. Sturz, Field Trip Guidebook and Volume for the 1995 San Diego Association of Geologists Field Trip to Anza-Borrego Desert State Park, Volume 1:64-81.
- Winker, C.D., and S.M. Kidwell 1996. Stratigraphy of a marine rift basin: Neogene of the western Salton Trough, California. *American Association of Petroleum Geologists, Pacific Section Conference Guidebook* 1996, GB 73, 80:295-336.
- Woodburne, M.O. 1987. *Cenozoic mammals of North America*. University of California Press 335 p.

Ivanpah Playa Dry for a Long Time: Paleoclimate and Sedimentation based on Identification of the Lava Creek B Ash Bed, Ivanpah Playa, Southeastern California

J. R. Knott, *Department of Geological Sciences, California State University, Fullerton, Fullerton, CA 92834-6850*; **G. W. Nason**, *Molycorp, Inc., Mountain Pass Mine, 67750 Bailey Road, Mountain Pass, CA 92366*; **A. M. Sarna-Wojcicki**, *US Geological Survey, 345 Middlefield Road MS-977, Menlo Park, CA*; **J. N. Carter**, *TRC Environmental Solutions, 21 Technology Drive, Irvine, CA 92618*

Comparison of sedimentary facies and sedimentation rates beneath playas of the western United States provides an opportunity to compare Late Neogene to Quaternary paleoclimate and sedimentation rates across broad regions. In this study, several borings were drilled along the western margin of the Ivanpah Playa, which on the margin of the Colorado River drainage basin in the Mojave Desert. Sediments are tan to brown sands, silts and clays with only traces of gypsum and a marked absence of green muds. These facies are consistent with a playa depositional environment with no evidence of a perennial lake. At depths of 21, 33 and 32 meters (69.0, 109.5 and 104.0 feet) below the ground surface in three borings we found a gray ash. Based on the glass shard composition, we have correlated this ash bed with the Lava Creek B ash bed, which erupted from the Yellowstone caldera ~660,000 years ago. The table below compares the depth to the Lava Creek B in Ivanpah and other basins in the western US.

Basin	River System	660,000 yr datum	Determined by:
Silver	Mojave	396-462 m bgs	Sedimentation rate (Brown et al., 1980)
Owens	Owens	234 m bgs	Borehole data (Smith and Pratt, 1957)
Searles		170 m bgs	Borehole data (Smith, 1984)
Bonneville		90-175 bgs	Borehole data (Williams, 1994)
Ivanpah	Colorado	21-33 m bgs	Borehole data (This study)

As the table illustrates, the 660,000-year-old datum in the Ivanpah playa is relatively shallow compared to other basins in the western US. These other basins also show evidence of perennial lakes at various times in the last 660,000 years as well, which would reduce deflation. Our preliminary conclusions are that the Ivanpah region has experienced lower sedimentation rates that are the result of a combination of deflation and limited weathering and fluvial transport. This suggests that Ivanpah playa has experienced lower effective precipitation rates during the late Quaternary than other basins in the western US.

New discoveries at Kokoweef Peak

Ralph Lewis, *Crystal Cave Mining Co., 2413 Southeastern #295, Las Vegas, NV 889104*

Searching for truth about the Mojave Desert's "River-of-Gold" legend requires more than reading treasure stories. New insights require field work ... and communication! To create a visual "paper-tour" of curiously related new discoveries, two 4' x 8' panels of photos and aerial-maps were assembled to show the author's most recent discoveries of heavy set-stone markers on the private property at Kokoweef Peak. These panels illustrate the existence of inconspicuous, precisely engineered,

triangular and perpendicular patterns, recreated by plotting these set-stone markers' locations on high-resolution aerial photographs. Out of a possible 50 stones used, at least twelve markers have been documented which are over 200 pounds! I'm making the new panels available to see if these desert-rock patterns will "spark" anyone's knowledge about little-known "desert surveying techniques" or links toward two legends within the Mojave Desert. The markers are set with incredible precision for long-distance accuracy. But I'm stumped as to as to the "who, what when and why" of their existence. The author believes they relate to both the legend of "The Lost (hidden) Dorr Mine" and the Mojave Desert's "Underground River-of-Gold."

Gila Monsters (*Heloderma suspectum cinctum*) in California: the Influence of Paleoeologic and Bioclimatologic Factors on Distribution and Rarity

Jeff Lovich, *U.S. Geological Survey, Western Ecological Research Center, 7801 Folsom Boulevard, Suite 101, Sacramento, California 95826, jeffrey_lovich@usgs.gov*; **Kent Beaman**, *Natural History Museum of Los Angeles County, Section of Herpetology, 900 Exposition Boulevard, Los Angeles, California 90007, kbeaman@nhm.org*

The Gila monster (*Heloderma suspectum*) is widely distributed in the Mojave and the Sonoran Deserts in the southwestern United States and northwestern Mexico, but rare in California. The current range was profoundly shaped by changes in landform and climate during geological time as reflected by a much wider distribution of helodermatids during the Paleocene. During the last 142 years, over 20 sightings have occurred in four California counties, at no less than eight locations. Habitat appears to be characterized by rugged foothill areas with rocky, deeply incised topography, in many cases, close to large and relatively high mountain ranges. Most localities are in association with riparian areas, including the lower Colorado River and range from near sea level to over 1,200 m. All records except one (Mojave River) occur east of about 116° longitude. Records documented with photographs or museum specimens generally show color patterns diagnostic of the geographically expected subspecies *H. s. cinctum*. The distribution of the species in the state suggests an invasion of the Mojave Desert during the last interglacial via the Colorado River corridor into the high mountain ranges of the northeastern Mojave. We explored the hypothesis that climate patterns shaped the current distribution of the Gila monster in California. Precipitation is decidedly bi-phasic east of 116° longitude, with over 24 percent falling in the warm season and the remainder falling in the winter. Warm season precipitation records for recording stations closest to Gila monster localities are almost identical for those in western Arizona where the species is more common. The hypothesis that Gila monsters are relictual species isolated in Mojave Desert "sky islands" was rejected because all records, except one, occur east of 116° longitude, despite the presence of habitats west of 116° that appear to be suitable, but lack significantly bi-phasic rainfall. Summer precipitation may be important in the foraging ecology of the species. Gila monsters were probably already rare in California long before the arrival of Europeans due to changes in climate and landform that delimited the marginal location of the state in the range of this species. The pattern of rarity exhibited in California, relatively limited geographic range, small population size, and tolerance for a narrower range of habitats, present unique challenges to conservation.

Fortunately, most of the habitat for this species in California is protected or relatively free from human disturbance. The rarity of the Gila monster in California is profoundly defined by its evolutionary history and places the species on tenuous footing for survival. Continued survival will require protecting the species from additional causes of rarity attributed to humans.

Rare Plants of Short Canyon in Kern County, California

Maria A. Lum, LSA Associates, Inc. 1650 Spruce Street Riverside, CA 92507, maria.lum@lsa-assoc.com; **Terri Middlemiss**, KernCrest Chapter of the California Audubon Society P.O. Box 984 Ridgecrest, CA 93556, catbird4@earthlink.net

Short Canyon is known for its diverse assemblage of plant species. The canyon is one of several along the western front of the southern Sierra Nevada Mountains. The southern terminus of the Sierra Nevada bounds the western edge of the Indian Wells Valley. The abrupt topographic changes in this canyon induce shifts in plant communities and species distribution, and the geographic location of Short Canyon has an effect upon the occurrence of these rare plant species. The region, Indian Wells Valley, is situated in between several geographic and natural provinces which influence species distribution and diversity. In addition to the Sierra Nevada Province, the Basin Ranges Province is located to the north and northeast, and the Mojave Desert Province is located to the south and southeast.

A few plant species on the California Native Plant Society (CNPS) "watch list" are reported to occur in Short Canyon. Species on the CNPS watch list are either rare or common with potential for extinction or threatened by extinction within part of all of its range. The species may be California endemics or may also occur in other western states.

Following is a list of rare plants observed in Short Canyon during botanical surveys (M. A. Henry, Maturango Museum 1970 to 1994). All of these plants have limited distribution within the state of California.

Liliaceae (*Muilla coronata*) little muilla
Campanulaceae (*Nemocladius gracilis*) slender nemacladus
Crassulaceae (*Dudleya calycicola*) limestone live-forever
Onagraceae (*Camissonia kernensis kernensis*) Kern evening primrose
Papaveraceae (*Canbya candida*) pygmy poppy
Rubiaceae (*Galium munzii*) brown-flowered bedstraw

These plant species have different distribution ranges, growing conditions, and plant community associations. Some of these species are California endemics found within the Central Valley, in cismontane southern California, or the desert provinces. Other species can be found throughout the Great Basin and the western Mojave Desert Provinces. The various plant species establish on rocky outcrops, canyon slopes, shady canyon bottoms, or sandy flats. Substrates include granitic, sand, clay, carbonate, and limestone. Plant communities in which these species occur in, outside of Short Canyon, range from coniferous forest, pinyon-juniper woodland, Joshua tree woodland, chaparral, coastal sagebrush, shadscale scrub, Great Basin desert scrub, and Mojavean desert scrub to valley grassland.

References

California Native Plant Society. 2001. Inventory of rare and endangered plants of California, 6th ed. Rare Plant Scientific Advisory Committee, David P. Tibor, Convening Editor. CNPS. Sacramento.
Henry, M. A. 1995. A checklist of plants of Short Canyon. Maturango Museum, Ridgecrest, CA.

Hickman, J. C. 1993. The Jepson Manual: higher plants of California. University of California Press, Los Angeles.
Munz, P. A. 1974. A flora of southern California. University of California. Los Angeles.
Schoenherr, A. A. 1995. A natural history of California. University of California Press, Los Angeles.

Overview of the Surficial Geology of Dove Spring Area, Kern County, California

David M. Miller, U.S. Geological Survey, 345 Middlefield Rd, Menlo Park, CA 94025

The Dove Spring Off-Highway Vehicle Open Area, in the western California desert near Red Rock Canyon State Park, is situated in and adjacent to a canyon cut into a broad incised pediment. The U.S. Geological Survey has begun a study for Bureau of Land Management to develop baseline data sets for the area and develop a monitoring protocol for this area of badlands and steep canyon walls. Initial surficial geologic mapping in the area has delineated several new relationships in this area near the junction of two major tectonic features—the Sierra Nevada frontal fault and the Garlock fault system—that provides new information on the depositional and erosional history of the area.

The canyon in which Dove Spring lies was incised into a broad, gently SE-sloping pediment. This pediment was cut into granite of the Sierra Nevada block, which is faulted against Tertiary and Quaternary (?) sediments of the Ricardo Group that dip NW and were shed first from the area south of the Garlock fault and later from the Sierra Nevada (Whistler, 1987). The fault bounding these rock units, a part of the Sierra Nevada frontal fault system, consists of several anastomosing segments that place the youngest part of the Ricardo Group sediment against granite. The fault does not demonstrably cut Holocene sediments, may cut late Pleistocene sediment, and demonstrably cuts middle (?) Pleistocene sediment. Evidently, the Holocene activity along the Sierra Nevada frontal fault system farther north in Owens Valley is not represented on this segment of the fault system.

The pediment has been incised by several deeply entrenched streams that form canyons as deep as 35 m. Middle (?) Pleistocene sediment deposited in the paleo Dove Spring Canyon is reddish and derived from Sierra Nevada granite. It hosts two to five strongly developed argillic horizons, most near its top; the multiple argillic horizons indicate one to several hundred thousand years of soil development during sequential filling episodes of the paleo-canyon. This deposit is overlain by a thin alluvial veneer that has many characteristics of late Pleistocene deposits throughout the Mojave Desert: flat surface, strong argillic horizon, and stage II to III calcic horizon textural development. After late Pleistocene deposition, the present canyon was cut into the paleo-canyon. Inset deposits in terraces within the present canyon have characteristic soil horizons and surface topographic features indicating that they range from terminal Pleistocene (5-7 m above the active wash) to mid Holocene (2 m above the active wash), to decadal flooded surfaces and the active wash floor. An uncalibrated C¹⁴ age of 10,730 ± 110 yr BP was reported by Whistler (1990) for the oldest inset terrace, which in several locations contains organic-rich strata and fossils indicating wetland development.

It has been suggested that the upper part of the Ricardo Group represents basinal sedimentation driven by uplift of the Sierra Nevada. If so, the youngest NW-dipping strata of the Ricardo group, questionably Pleistocene in age (Dibblee, 1952), indicate activity of the Sierra Nevada frontal fault until that

time. Subsequent to the deposition of the Ricardo, pediments apparently rapidly developed and were incised and filled during middle (?) Pleistocene time. Last demonstrable faulting placed this canyon-filling deposit against granite, but the pediments and canyons appear to have been stable features during and after this last faulting. Latest Pleistocene wetlands in the now largely dry wash of Dove Spring canyon attest to post-late glacial maximum wet conditions, compared to those of today, as is seen in several parts of the northern Mojave Desert.

Geomorphic Elements of the San Bernardino Mountains along the San Andreas Fault: Landform Evolution and Evidence for Episodic Uplift

Robert E. Mortimer, *Wyo. Reg. Prof. Geol. #1721*

The San Andreas Fault separates the front of the San Bernardino Mountains from the alluvial valley floor to the south. This fault boundary is generally delineated by an abrupt topographic break as one crosses the fault, as well as by the basically linear trace of the fault at the foot of the mountains. The San Bernardino Mountains along the San Andreas, especially between Cajon Pass and Oak Glen, are a virtually unique segment of the fault for several reasons. The last great San Andreas Fault rupture, in 1857, ended at the general area where the fault becomes the bounding fault of the south face of the San Bernardino mountains. This segment is currently one of low seismic activity, yet the geomorphic features clearly show a long term character of major activity, creating obvious problems in assessing short term risk. Finally, this segment differs from most of the San Andreas Fault system in that this portion also marks a zone of complex intersections of numerous active faults, the most notable being the San Jacinto Fault. For these reasons, any information which clarifies the dynamic history of the fault zone may be of value.

This project approached these problems by looking for relict features of uplift or strike slip cycles which might have occurred across the mountain front. While erosion is obviously an active element of the area, block motion by slippage and rotation is the dominant process which has created the major topographic pattern across the mountain face. Numerous facets truncate ridges, and ridge offsets, mainly by down-dropped blocks, are indicative of mass wasting on a large scale. With this material sliding down towards the fault from the uplifting mountain front, this is probably a response to extension across the mountain front concurrent with the progressing uplift. This frontal zone of extension is implied by the combination of abundant block rotation and sliding with the general lack of this slumped material crossing the San Andreas Fault. Unless some extension has occurred along with the uplift, a significant amount of the material should have slid and crossed the adjacent fault. Further, several faults branch off the San Andreas into the area of inferred extension, and in several cases these form classic grabens. This implied extension lacks ready explanation by either classic wrench fault models or transpressive mechanisms recently proposed to explain the San Bernardino Mountains uplift.

Possibly the most interesting result so far in this study is the presence of what appear to be relict elements of benches which, despite the slumping and block motions, preserve what appear to be at least two stages where there was a long enough period for significant terraces and pediments to have formed. Along with these are several uplifted upper alluvial fan heads, which though dissected by subsequent erosion, are clearly recogniz-

able. The significant periods during which uplift was reduced or halted, may indicate that the uplift and strike-slip motion stop as strain is transferred to other faults for moderate periods of time, possibly being reflected in the seismic gap across the area at present.

Carbonate Phytoherm Mounds in the Middle Miocene Barstow Formation, Mud Hills, California

Vicki Pedone and Carmen Caceres, *Department of Geological Sciences, California State University Northridge, Northridge, CA 91330-8266*

A 5-m-thick limestone unit at the base of the Middle Member of the Barstow Formation in the Mud Hills formed during a temporary cutoff of clastic deposition that could be related to synsedimentary faulting. The lacustrine limestone unit occurs within a sequence otherwise dominated by conglomerate and pebbly sandstone and crops out only on the north side of the basin between the eastern end of the Mud Hills and Owl Canyon, where it is terminated by a fault. The steep north side of the asymmetric detachment basin contains common normal faults thought to be contemporaneous with the early stages of deposition of the Barstow Formation.

The most prominent lithology of the limestone unit is phytoherm biolithite, i.e., a constructional mound developed by calcification of macrophytes. The phytoherms are elliptical to circular in area, with diameters of ranging from 3 m to 5 m, and maximum thickness ranging from 1 m to 3 m. Successive growth layers that drape over the tops of the mounds demonstrate that the phytoherms formed positive constructional features on the lake floor. The internal molds of the stems, most commonly filled by calcite cement, occur in clumps and range in diameter from 0.3 to 1.0 mm. Calcification consists of alternating layers of bladed calcite cement and micrite. As concentric coatings on individual stems were added, they coalesced to form a rigid, current-resistant biolithite. Framework porosity, now partly to completely filled by sparry calcite and/or chalcidony, formed 20% to 50% of the rock. Between the mounds, biosparite and biointrasparite were deposited. These units overlap and interfinger with the mound margins.

A temporary shutoff of siliciclastic sediment into this area, most likely caused by synsedimentary faulting in the nearby source area, allowed lush plant growth to develop along the shallow lake margin. The plants underwent calcification as they grew to form the phytoherms. Currents fragmented the delicate, coated fronds and deposited the bioclastic material on the lake floor between the mounds.

A preliminary examination of the Pliocene camelids from Anza-Borrego Desert State Park®, California

Kesler A. Randall, *San Diego Natural History Museum, San Diego, CA 92112-1390, krandall@sndnhm.org*

Several camelid genera are recognized to have lived in North America during the Pliocene and Pleistocene. These genera are grouped within two separate monophyletic clades or tribes: the Lamini and the Camelini (Honey et. al, 1998; Harrison, 1979). Recognized genera for the tribe Lamini include: *Hemiauchenia*, *Blancocamelus*, *Camelops*, and *Palaeolama*. Recognized genera for the tribe Camelini include: *Procamelus*, *Megatylopus*, *Titanotylopus*, and *Gigantocamelus*. In addition, Whistler and Webb (1999) reported on a new stenomyline, a primitive camelid, from the Blancan of southern California. Although most

camelid genera can be distinguished by characters of the dentition, skull, mandibles, certain features of the distal limbs, most notably metapodial length/width ratios and shape of suspensory ligament scars on the first phalanx, may also be used for generic identification (Honey et al., 1988).

Numerous (1079) specimens of camelids have been collected in the Pliocene and Pleistocene terrestrial sediments in Anza-Borrego Desert State Park (ABDSP). This material has been identified to either *Hemiauchenia*, *Blancocamelus*, *Camelops*, *Titanotylopus*, *Paleolama*, *Gigantocamelus* or Camelidae indeterminate (Jefferson, 1999). An examination of geographic ranges of North American camelids indicates that all Plio-Pleistocene genera could have existed in southern California and thus may increase camelid diversity in the ABDSP. Although most material collected in ABDSP consists of partial isolated elements, uniqueness of camelid postcrania may enable generic level specimen identification. Further study will continue not only to improve camelid diversity in ABDSP but better substantiate geographic ranges and population distribution in North America for the Camelidae.

References Cited

- Jefferson, G.T. 1999. Anza-Borrego Desert State Park 622 Paleontological Resources Inventory and Management Recommendations. Unpublished Document, on File California Department of Parks and Recreation, Colorado Desert District Stout Research Center, 48 p.
- Harrison, J.A. 1979. Revision of the Camelinae (Artiodactyla, Tylopoda) and description of the new genus *Alforjas*. The University of Kansas Paleontological Contributions, 95:1-20.
- Honey, J.G., J.A. Harrison, D.R. Prothero, and M.S. Stevens 1998. Camelidae. In Evolution of Tertiary Mammals of North America Volume 1: Terrestrial Carnivores, Ungulates, and Ungulate like Mammals, edited by C.M. Janis, K.M. Scott and L.L. Jacobs, Cambridge University Press, Cambridge, pp. 439-462.
- Mckenna, M., and S.K. Bell 1997. Classification of Mammals Above the Species Level. Columbia University Press, New York, 631 p.
- Webb, S.D. 1965. The osteology of Camelops. Bulletin of the Los Angeles County Museum Science 1:1-54.
- Whistler, D.P. and Webb S. 1999. A new stenomyline camelid from the latest Blancan of the Tecopa Lake Beds, California. Journal of Vertebrate Paleontology 19:84A.

Bat Protection Strategy for Abandoned Mine Openings

Michael H. Rauschkolb, Principal Land Agent, U.S. Borax Inc., 26877 Tourney Road, Valencia, Ca 91355, mike.rauschkolb@borax.com

U.S. Borax has joined with Bat Conservation International to protect two populations of desert dwelling bats. Prior to closing mine openings on company property, biological consultants conducted pre-closure wildlife surveys. These surveys involved internal mine surveys and night vision monitoring of mine openings. Outside of the mine, echolocation signals were recorded onto a laptop computer using an Anabat detector and ZCAIM. Signals were detected of pallid bats (*Antrozous pallidus*), western pipistrelles (*Pipistrellus hesperus*), California myotis (*Myotis californicus*) and Townsend's big-eared bats (*Corynorhinus townsendii*).

The decision to place bat gates on particular openings was based on several factors including airflow, access, size and stability of the opening, visibility from roads and evidence of bat use. Three bat gates and a bat cupola have been installed at the Lila C mine. At Borax's Gerstley mine, two bat gates and three air grates provide safe access and continued good airflow, while

at the same time, permitting open pit mining to occur adjacent to the closed underground mine.

U.S. Borax developed an innovative method for installing secure and stable bat gates in areas of weak and faulted bedrock. The bedrock at both locations is structurally weak, consisting of clay, shale, volcanic ash and limestone, which are highly weathered and fractured. This situation made it almost impossible to securely anchor bat gates to the walls of the various openings. To eliminate this problem we placed six-foot diameter cement sewer pipe in front of each opening and installed the gates inside or at the end of these pipes. In a few cases where the mine opening was larger than the cement pipe, rock-filled steel mesh gabions were placed around the pipe to close the remainder of the opening. After sealing the bedrock/pipe interface, we backfilled around the pipe. These structures are much more stable than the bedrock and hopefully will be able withstand minor earthquakes and trespassers attempts to bypass the gates.

The Devil Peak Sloth Associated Fauna: A Progress Report

Richard L. Reynolds, Research Associate, George C. Page Museum, 5801 Wilshire Blvd., Los Angeles, CA

A late Rancholabrean vertebrate fauna was associated with the sloth (*Nothrotheriops shastensis*) found by the BLM in a vertical limestone fissure northwest of Stateline and south of Goodsprings, Nevada (elevation 3600'). This fauna was salvaged by the San Bernardino County Museum under BLM permit and has been under preparation, identification, and organization at the George C. Page Museum. This fossil resource will be deposited in the Nevada State Museum, Las Vegas for cataloging and curation. The large assemblage came from the silt zone entombing a 75% complete *Nothrotheriops shastense* in the lower 12 feet (of 33') of cavern fill. The base of the fissure was closed by canyon fill, and all subsequent material came in through the upper opening of the fissure. Except for the sloth that fit through the upper opening, the size of this fauna is characterized by animals no larger than eagles and marmots. All elements of larger animals were carried into the fissure by woodrats.

This undated fauna was deposited when canyon fill and pedogenic carbonate (caliche) filled the canyon to the elevation of the cave mouth. Deposition may represent a terminal phase of the Wisconsinan glacial period (12,000 ybp). Fauna recognized include: molluscs (6 species), turtles (1), lizards (?6-12), snakes (6-12), birds (?6-12), shrews (2), bats (?5), rabbits (2), squirrels (?3-5), gophers (1), pocket mice (?2-4), kangaroo rats (?2-4), deer mice (?2-4), woodrats (?3-5), carnivores (2), horses (?2), camels (?2), deer (1), and mountain sheep (1). Amphibians, voles, jumping mice, and antelope have been tentatively identified; so far no fish remains have been recognized.

Curatorial emphasis will be placed on stratigraphic organization of this significant collection of late Pleistocene mammals that indicate shifting, post-Pleistocene habitats in southern Nevada. The collection will be cataloged and deposited in a permanent fossil resource collection.

California Dinosaur Tracks: Inventory and Management

Robert E. Reynolds, LSA Associates, Inc., Riverside, CA 92507 and **Ted Weasma**, Mojave National Preserve, Barstow, California 92311

California's only dinosaur tracks are early? Jurassic in age and

are located in the Aztec Sandstone of the Mescal Range near Mountain Pass, in the eastern Mojave Desert. The Aztec crops out in the Mojave Block at Ord Mountain, the Soda Mountains, Cow Hole Mountains and in the Mescal Range. The western occurrences are metamorphosed, while the eastern outcrops are orthoquartzites that retain biologic and sedimentary structures. The tracks are unique in the state and early Jurassic track sites are rare in the western United States. Previous work identified trackways representing three bipedal coeleurosaurs assigned to ichnogenera *Anchisauripus*, *Grallator*, and an unnamed genus. In addition to coeleurosaurs, tracks and trackways of more than four quadrupedal ichnogenera are represented, and the track impressions of both quadrupeds and bipeds produce compression rings that suggest original slope of dune topography. Also preserved are sedimentary structures, cross-bedding, ripples, raindrops and trails and tracks left by arthropods(?).

The popularity of dinosaurs during the late 20th century prompted concern that no detailed inventory existed for California's only tracks. The inventory was undertaken in the fall of 2001 by volunteers from the Mojave River Valley Museum through its Desert Discovery Center "Tracks through Time" program, with authorization from the Bureau of Land Management and assistance from National Park Service, Mojave National Preserve and the Desert Managers Group. The inventory of the trackways was performed to establish base line reference data. These data will be analyzed to determine rates of attrition. The outcrop exposure was examined by teams to locate and flag, photograph digitally, record attitudes, and plot Universal Transverse Mercator (UTM) coordinates. All Global Positioning System (GPS) data were collected with a pack-mounted Trimble 12 channel Pathfinder Pro XRS Global unit and recorded with a TSC1-2MB controller with Real Time Radio Beacon correction. Data were downloaded using the Pathfinder software and exported to a Geographic Information System (GIS) as an ESRI Shapefile. Data were then imported into ESRI ArcGIS 8.1 software.

One hundred and sixteen track and structure localities were recorded, including outcrop panels and loose slabs. Of importance, the second of two occurrences of a small (juvenile) bipedal trackway paralleling an adult trackway was located. All loci were photographed and attitudes were taken of outcrops that reflected the local dune surface. Plots of the loci suggest that tracks occur in two arenaceous facies of the Aztec Sandstone. Baseline data are now available for further inventory and management of the trackway site. Research questions that can now be quantified include: what are the characteristics of the sedimentary facies in which tracks are preserved, and where they are not preserved; and whether there is significance to the direction of the tracks left by the track makers.

Marker Bed Correlations Between the Mud Hills, Calico Mountains, and Daggett Ridge, Central Mojave Desert, California

Robert E. Reynolds, *LSA Associates, 3403 10th St, Riverside, CA 92501, bob.reynolds@lsa_assoc.com* and **Michael O. Woodburne**, *University of California, Riverside, 1432 Geology Bldg, Riverside, CA 92521-0423*

The early Miocene depositional sequence of volcanic and lacustrine rocks in the central Mojave Desert can be divided into lower, middle, and upper intervals. The middle interval contains distinctive lithologic markers that unite sections recognized in

the Mud Hills, Calico Mountains, Lead Mountain, Harvard Hill and at Daggett Ridge. Their extent and depositional environment suggest an expanding lacustrine basin in Late Hemingfordian (late early Miocene) time, that, without reconstruction along late Tertiary strike slip faults, may have covered 777 Km² (300 square miles). From the lowest, the marker units include a granitic arkosic unit, green volcanoclastics, a stromatolitic limestone, brown platy limestones, and a horizon rich in strontium and borax minerals. The two former occur on the north margin of the basin while the latter three are recognized throughout the Miocene basin. Coarse clastic and volcanic lenses suggest proximity to highlands of specific lithology. Magnetic polarity data from the section in the Mud Hills that contains these markers suggests that lacustrine deposition in the broader Barstow Basin started around 17 mya and continued through 16.2 mya. Vertebrate faunas in sections to the south and east support this age range. The stratigraphic position of lacustrine siltstone suggests that the center of the broader basin migrated northwest through time. In the Mud Hills, lacustrine siltstone continued to be deposited until 13 mya. The portion of the basin that is now the Calico Mountains was deformed, eroded, and covered with gravity slides of volcanic debris. Throughout the eastern portion of the basin near Harvard, erosion has removed deposits, including the upper two marker units.

Review of the Proboscidean Datum Within the Barstow Formation, Mojave Desert, California.

Robert E. Reynolds, *LSA Associates, 3403 10th St, Riverside, CA 92501, bob.reynolds@lsa_assoc.com* and **Michael O. Woodburne**, *University of California, Riverside, 1432 Geology Bldg, Riverside, CA 92521-0423*

Proboscidea appear to have dispersed to North America in late Hemingfordian time, and are found associated with Nevada faunas dating to 16.2Ma. (Chron C5C.n1) and with Barstovian faunas in Florida that date around 15.8 Ma. (Chron C5B.r2). In contrast, the lowest stratigraphic datum (LSD) for bones and teeth of Proboscidea in the Barstow Formation is at or below the Dated Tuff (14.8 Ma, Chron C5B.n1). This is a difference of 1.4 million years between localities in California and Nevada. Recently, marker units in the Hemingfordian section of the Barstow Formation have been located that allow correlation with similar lithologic sequences in the Calico Mountains and at Daggett Ridge. These marker units include, from the lowest, granitic/arkosic detritus, green tuffs, a massive stromatolite layer, brown platy limestones, and a horizon rich in strontium and borate minerals. Occurrence of large footprints and trackways attributed to Proboscidea occur at Barstow, 100 feet stratigraphically above the Dated Tuff (14.8 Ma., Chron C5AD.r1). A second set of tracks is located 350 feet stratigraphically above the Oreodont Tuff (15.8 Ma., Chron C5B.r2). Recently, a Proboscidean trackway has been located at Borate, in the Calico Mountains, that is in the uppermost of the three brown, platy limestones. Based on provisional paleomagnetic data developed by L.B. Albright and E.H. Lindsay, the comparable ledge of limestone in the Mud Hills section is within Chron C5C.r1, and below the transition to C5C.n1, which dates to approximately 16.2 Ma. The occurrence of proboscidean tracks in a marker limestone of the Calico Mountains that likely dates to about 16.2 Ma. (Chron C5C.r1) suggests that the proboscidean datum in the Barstow Formation is in accord with the site in Nevada and relatively consistent with the 15.8 Ma. date from Florida.

New Mammalia from the El Golfo Local Fauna, Sonora, Mexico

Christopher A. Shaw, *George C. Page Museum, Los Angeles, CA 90036*; **Fred W. Croxen III**, *Western Arizona College, Yuma, AZ 85366*

Middle Pleistocene Colorado River Delta deposits exposed in the upper Gulf of California have yielded a diverse vertebrate fauna and associated flora. Late Quaternary doming along the Cerro Prieto Fault has allowed extensive dissection of ancient deltaic sediments in western Sonora, revealing thick fluvial units from which Irvingtonian-aged fossils have been recovered.

Field studies in the past eight years have added thousands of specimens to a relatively small sample of vertebrates collected between 1939 and 1985. New records of vertebrate species from El Golfo de Santa Clara include unexpected taxa in North American faunas, along with a new species of sheep and antelope.

Magnetic Stratigraphy of the Late Pliocene–Early Pleistocene Mammal-Bearing Deposits from Gypsum Ridge, San Bernardino County, California

Hugh M. Wagner, *Department of Paleontology, San Diego Natural History Museum, P.O. Box 121390, San Diego, CA 92112*; **Donald R. Prothero**, *Department of Geology, Occidental College, Los Angeles, CA 90041*

Paleontological collecting between 1997 and 1999 at Gypsum Ridge on the Marine Corps Air Ground Combat Center (MCAGCC), Twentynine Palms, San Bernardino County has yielded a significant vertebrate assemblage of early Irvingtonian age. The fauna is diverse containing invertebrates such as the slug *Deroceras* sp., an unidentified cyprinid fish, amphibians such as salamanders, frogs and toads, reptiles including the giant tortoise *Hesperotestudo*, snakes, shore birds and rails, and mammals including edentates, insectivores, rodents, lagomorphs, carnivores, perissodactyls and artiodactyls. The grade of evolution of the *Neotoma* (*Paraneotoma*) sp. coincident with the joint occurrences of *Erethizon* sp., *Pamalydonon harlani*, *Nothrotheriops texanus*, *Ondatra oahoaensis*, and *Sigmodon minor medius* in deposits of reversed polarity support an age of 2.1 to 1.9 Ma for the Gypsum Ridge local fauna. The composition of the Gypsum Ridge assemblage resembles faunas of late Blancan–early Irvingtonian age in the Fish Creek–Vallecito Creek assemblage.

Solving the Problems of Lake Mojave Cultural Stratigraphy: Work-in-progress

Claude N. Warren and **Joan S. Schneider**, *University of Nevada, Las Vegas, University of California, Riverside, and the Western Center for Archaeology & Paleontology*

Two major geoarchaeological problems at Lake Mojave were recognized by Warren and DeCosta (1964:206): (1) establishing the contemporaneity of artifact assemblages and former lake stands and (2) dating former lake stands. The data that were available before the present research was undertaken includes relatively precise dates for the major lake stands, a record of a series of relatively minor lakestands derived from cores taken from the playa, and demonstration that humans

occupied the shores of Lake Mojave during late-Pleistocene–early Holocene high lake stands. The current work is addressing problems of (1) developing a more fine-tuned chronology of environmental changes associated with changing lake levels and (2) acquiring data that will make it possible to integrate the archaeological data (Clovis, as well as Lake Mojave) with the chronology of changing lake levels and environment.

In 2001, test excavations on the northern shoreline at Benchmark Bay resulted in acquiring new chronological data from buried deposits. Independent data sets were derived from ASM radiocarbon dates on *Anodonta* sp. shell, obsidian hydration rim thickness, and optical-stimulated luminescence (OSL) dating of profile sediments. In addition, radiocarbon dates were obtained on matched pairs (*Anodonta* sp. and charcoal) of specimens from mussel-shell middens in an effort to obtain precise correction factors for shell dates in the Mojave River drainage system. A collaboration with Professor Lewis Owen and his students in the Department of Earth Sciences at the University of California, Riverside, produced a definitive stratigraphic study of the gravel spit exposure near Benchmark Bay, with new dates on *Anodonta* sp., tufa, and sediments in the various strata, as well as cosmogenic isotope dating of shoreline bedrock exposures thought to be associated with certain lakestands.

The substantial newly-acquired data are being studied and an integrated chronology is forthcoming. It is anticipated that the long-standing problems of early human presence at Lake Mojave may be resolved.